YALE MEDICAL LIBRARY
3 9002 08676 2730

QUANTITATION OF REGIONAL CHONDRO-OSSEOUS BLOOD FLOW IN THE MATURING CANINE TIBIA AND FEMUR AND ITS RELATIONSHIP TO TC-99m MDP UPTAKE

POLLY MCKINSTRY

YALE UNIVERSITY SCHOOL OF MEDICINE

1981

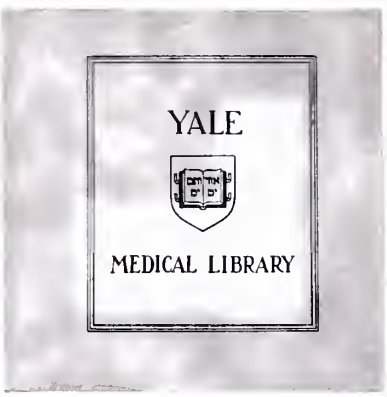
YALE
MEDICAL LIBRARY

Permission for photocopying or microfilming of "Quantitation of Chondro-osseous Blood Flow in the Maturing Canine Tibia and Femur and Its Relationship to ~~(Title of thesis)~~ Tc-99m MDP Uptake"

for the purpose of individual scholarly consultation or reference is hereby granted by the author. This permission is not to be interpreted as affecting publication of this work or otherwise placing it in the public domain, and the author reserves all rights of ownership guaranteed under common law protection of unpublished manuscripts.

Polly McKinstry

Signature of Author

2/26/81

Date

Digitized by the Internet Archive
in 2017 with funding from
Arcadia Fund

https://archive.org/details/quantitationofre00mcki

QUANTITATION OF REGIONAL CHONDRO-OSSEOUS BLOOD FLOW IN THE MATURING CANINE TIBIA AND FEMUR AND ITS RELATIONSHIP TO Tc-99m MDP UPTAKE

A Thesis Submitted to the Yale University School of Medicine in Partial Fulfillment of the Requirement for the Degree of Doctor of Medicine, 1981

POLLY MCKINSTRY
1981

Med. Lib.
T113
Y12
4098

ACKNOWLEDGEMENTS

I would like to most gratefully thank:

JAN SCHNITZER, who spent countless hours working with me on every aspect of this research, wrote the computer program, and was a constant source of advice, encouragement, and inspiration;

MARY JANE LABAREE for her generous and much appreciated assistance in the laboratory;

MARY CARROLL for patiently typing and retyping the many revisions of the manuscript;

JOHN A. OGDEN and TERRY R. LIGHT for their support, suggestions, funding, and editing;

and Spyros Condos, Laura Chandler, George Lister, Paul Hoffer, Marcy Haire, Chris Yonge, Gerry Conlogue, Gertrude Chaplin, Mary Bronson, Jim McKay and John Braslin for their technical support and suggestions.

ABSTRACT

Regional chondro-osseous blood flow was measured using radioactively labelled microspheres in the femurs and tibias of neonatal, skeletally immature and mature canines under physiological conditions in an effort to duplicate the potential patterns of flow during infancy, mid-childhood and adulthood. Each bone was cut into as many as 41 anatomically distinct sections. Developmental and regional comparisons in osseous blood flow were evaluated via the Student's T-test. A decrease in osseous blood flow with increasing chondro-osseous maturity was observed for both the whole bones as well as many regions within a given bone. The epiphyseal and metaphyseal regions nearest the growth plates had the highest flow. The growth plate was found to have a statistically significant flow rate. Furthermore, regional differences in osseous blood flow correlated well with known regional functions. Osseous blood flow tended to be greater in regions of greater metabolic activity associated with hematopoiesis and endochondral osteogenesis. Osseous blood flow values correlate well with regional predilections of various diseases such as acute hematogenous osteomyelitis and osseous metastases.

In the second part of the study, chondro-osseous blood flow patterns were compared to the uptake of intravenously injected Tc-99m MDP. The similarity of Tc-99m MDP and microsphere distribution indicates that blood flow plays an important, but not exclusive, role in the uptake of bone-seeking tracers. A measure of the relative affinity of Tc-99m MDP for bone is derived by dividing uptake by % blood flow. The affinity varies with the juxtaphyseal

region having the greatest, followed in decreasing order by: cortex, cartilage, trabecular bone of the metaphysis and secondary ossification center, and marrow. Within the spongiosa of bone, affinity generally increases as the proportion of osseous trabeculae relative to marrow increases. Tc-99m MDP uptake is disproportionately increased in areas of active bone growth and remodeling.

TABLE OF CONTENTS

Chapter		Page
	List of Figures	1
	List of Tables	3
	List of Graphs	5
	List of Abbreviations	7
I.	INTRODUCTION	9
II.	BACKGROUND	10
	A. Vascular Anatomy	10
	B. Development of the Osseous Circulation	19
	C. Functional Vascular Anatomy	34
	D. Quantitative Measurement of Bone Blood Flow	42
	E. Physiologic Control of Osseous Flow	69
	F. The Association Between Bone Blood Flow and Bone Growth	79
	G. Blood Supply and Age	83
	H. Osseous Blood Flow and Pathology	84
	1. Hematogenously Spread Bone Disease	84
	a. Acute Hematogenous Osteomyelitis	84
	b. Cancer Metastases	90
	2. Bone Disease from Decreased Osseous Blood Flow: Aseptic Necrosis	97
	3. Bone Diseases with Increased Osseous Blood Flow	104
	I. Bone Seeking Radionuclides and Bone Scanning	109
III.	MATERIALS AND METHODS	122
	A. Surgery	123
	B. Injection	123
	1. Tc-99m MDP	123
	2. Microspheres	124
	C. Processing of Bones	125
	1. Neonatal Bones	125
	2. Immature Bones	126
	3. Mature Bones	128

TABLE OF CONTENTS
(Cont.)

Chapter		Page
	D. Computation of Results	129
	E. Bone Region Recombination for Developmental Circulation Comparison	130
	F. Figures 12-18 (Bone Regions)	134
IV.	RESULTS	141
	A. Quantitative Osseous Circulation	143
	1. Technique	143
	2. Total Bone Flow	144
	3. Gross Tissue Flow	145
	4. Developmental Regional Osseous Flow: Neonatal vs. Immature vs. Mature	146
	5. Neonatal	148
	6. Immature Bones	148
	7. Immature vs. Mature; and Mature	153
	B. 99m Technetium-Methylene Diphosphonate Uptake	157
	1. Gross Tissues	157
	2. % Total 99m Technetium-Methylene Diphosphonate Uptake/% Total Weight	158
	3. % Total Blood Flow/% Total Weight	160
	4. % 99mTc-MDP Uptake/% Blood Flow	161
	C. Figures 19-25 (Dot Densiograms)	165
	D. Graph 1-60	172
	E. Tables 11-38	236
V.	DISCUSSION	272
	A. Microsphere Technique and Comparison to Previous Studies for Quantification of Regional Osseous Blood Flow	272
	B. The Association Between Chondro-osseous Blood Flow and Osteogenesis	273
	C. Neonatal Regional Chondro-osseous Flow	275
	D. Immature Regional Chondro-osseous Circulation	277
	E. Mature Regional Chondro-osseous Circulation	283
	F. Blood Supply and Age	286
	G. Osseous Blood Flow Related to Acute Hematogenous Osteomyelitis	288
	H. Skeletal Metastases	290
	I. Effects of Illness on One Immature Pup	291
	J. Factors Determining Uptake of Technetium-99m Methylene Diphosphate	292
	1. Tissues	293
	2. Mature Bone	294
	3. Immature Bone	295

TABLE OF CONTENTS
(Cont.)

Chapter		Page
	K. Clinical Applicability	298
VI.	REFERENCES	299

LIST OF FIGURES

FIGURE		PAGE
1.	Vascular Organization of a Long Bone in Longitudinal Section	11
2.	Hunter's Circulus Articuli Vasculosus	13
3.	Blood Supply of Bone Cortex in Cross-Section	18
4.	Vascular Connection Between Bone Cortex, Periosteum, and Attached Muscle	18
5.	Development of a Long Bone	20
6.	Three Types of Osseochondral Junctions	26
7.	Incorporation of Periosteal Vessels Into Cortical Haversian Canals	31
8.	Vascular Patterns in Bone Cortex	33
9.	Nutrient Vascular System With M-Side Vascular Loops	86
10.	Vertebral Vein System	94
11.	King's Model for Bone Uptake of ^{18}F and ^{47}Ca	117
12.	Immature Pup Bone Regions	134
13.	Mature Dog Bone Regions	135
14.	Neonatal Pup Bone Regions	136
15.	Bone Regions for Comparison of Immature VS. Mature Femur	137
16.	Bone Regions for Comparison of Immature VS. Mature Tibia	138
17.	Recombined Femoral Bone Regions for Three-Age Comparison	139
18.	Recombined Tibial Bone Regions for Three-Age Comparison	140
19.	Dot Densiogram: Osseous Blood Flow in Three Age Groups	165
20.	Dot Densiogram: Immature Bone Blood Flow	166
21.	Dot Densiogram: Mature Bone Blood Flow	167

LIST OF FIGURES
(Cont.)

FIGURE		PAGE
22.	Dot Densiogram: Immature Bone: %Tc-99m MDP/%Total Weight	168
23.	Dot Densiogram: Mature Bone: %Tc-99m MDP/%Total Weight	169
24.	Dot Densiogram: Immature Bone: Tc-99m MDP/Blood Flow	170
25.	Dot Densiogram: Mature Bone: Tc-99m MDP/Blood Flow	171

LIST OF TABLES

TABLE		PAGE
1	Osseous Blood Flow: Summary of the Literature	44-49
2	Summary of Average Values for Total Bone Flow	55
3	Reports of Vessel Diameter	64
4	Factors Associated with Increased Osseous Flow	72-73
5	Factors Associated with Decreased Osseous Flow	74-75
6	Cardiac Output and Metastases by Organ	92
7	Distribution of Skeletal Metastases	96
8	Bone-Seeking Nuclides	112
9	Properties of Bone-Seeking Radionuclides	113
10	Three-Age Comparison Region Recombinations	133
11	Osseous Tissue Flow By Age (Infant vs. Adolescent vs. Adult) cc/min/hg	236-237
12	Osseous Tissue Flow By Age (Infant vs. Adolescent vs. Adult) %TBF/%TW	238-239
13	Developmental Osseous Regional Flow (Infant vs. Adolescent vs. Adult) cc/min/hg	240-241
14	Developmental Osseous Regional Flow (Infant vs. Adolescent vs. Adult) %TBF/%TW	242-243
15	Infant Pup Osseous Regional Flow cc/min/hg	244
16	Infant Pup Osseous Regional Flow %TBF/%TW	245
17	Adolescent Pup Femoral Regional Flow cc/min/hg	246
18	Adolescent Pup Tibial Regional Flow cc/min/hg	247
19	Adolescent Pup Femoral Regional Flow %TBF/%TW	248
20	Adolescent Pup Tibial Regional Flow %TBF/%TW	249

LIST OF TABLES

(Cont.)

TABLE		PAGE
21	Adult vs. Adolescent Femoral Regional Flow cc/min/hg	250-251
22	Adult vs. Adolescent Tibial Regional Flow cc/min/hg	252
23	Adult vs. Adolescent Femoral Regional Flow %TBF/%TW	253-254
24	Adult vs. Adolescent Tibial Regional Flow cc/min/hg	255
25	Adult Dog Femoral Regional Flow cc/min/hg	256
26	Adult Dog Tibial Regional Flow cc/min/hg	257
27	Adult Dog Femoral Regional Flow %TBF/%TW	258
28	Adult Dog Tibial Regional Flow %TBF/%TW	259
29	^{99m}Tc-MDP Uptake in Bone Tissues %Tc-MDP/%TW	260-261
30	^{99m}Tc-MDP Uptake/Blood Flow in Bone Tissues	262-263
31	Adolescent Femoral Regional Uptake of ^{99m}Tc-MDP %Tc-MDP/%TW	264
32	Adolescent Tibial Regional Uptake of ^{99m}Tc-MDP %Tc-MDP/%TW	265
33	Adult Femoral Regional Uptake of ^{99m}Tc-MDP %Tc-MDP/%TW	266
34	Adult Tibial Regional Uptake of ^{99m}Tc-MDP %Tc-MDP/%TW	267
35	Adolescent Femoral Regional ^{99m}Tc-MDP Uptake/Blood Flow	268
36	Adolescent Tibial Regional ^{99m}Tc-MDP Uptake/Blood Flow	269
37	Adult Femoral Regional ^{99m}Tc-MDP Uptake/Blood Flow	270
38	Adult Tibial Regional ^{99m}Tc-MDP Uptake/Blood Flow	271

LIST OF GRAPHS

GRAPH

1. Infant vs. Adolescent vs. Adult Femoral Tissues, flow:cc/min/hg
2. Infant vs. Adolescent vs. Adult Tibial Tissues, flow:cc/min/hg
3. Infant vs. Adolescent vs. Adult Osseous Tissues, flow:cc/min/hg
4. Infant vs. Adolescent vs. Adult Femur, flow:cc/min/hg
5. Infant vs. Adolescent vs. Adult Tibia, flow:cc/min/hg
6. Infant vs. Adolescent vs. Adult Femur, %TBF/%TW
7. Infant vs. Adolescent vs. Adult Tibia, %TBF/%TW
8. Infant Pup Femur, flow:cc/min/hg
9. Infant Pup Tibia, flow:cc/min/hg
10. Infant Pup Femur, %TBF/%TW
11. Infant Pup Tibia, %TBF/%TW
12. Adolescent Pup Femur, flow:cc/min/hg
13. Adolescent Pup Tibia, flow:cc/min/hg
14. Adolescent Pup Femoral Cortex, flow:cc/min/hg
15. Adolescent Pup Tibial Cortex, flow:cc/min/hg
16. Adolescent Pup Femur, %TBF/%TW
17. Adolescent Pup Tibia, %TBF/%TW
18. Adolescent Pup Femoral Cortex, %TBF/%TW
19. Adolescent Pup Tibial Cortex, %TBF/%TW
20. Adolescent Pup (vs. Adult Dog) Femur, flow:cc/min/hg
21. Adult Dog (vs. Adolescent Pup) Femur, flow:cc/min/hg
22. Adolescent Pup (vs. Adult Dog) Tibia, flow:cc/min/hg
23. Adult Dog (vs. Adolescent Pup) Tibia, flow:cc/min/hg
24. A,B Adolescent Pup (vs. Adult Dog) Femur, %TBF/%TW
25. Adult Dog (vs. Adolescent Pup) Femur, %TBF/%TW
26. Adolescent Pup (vs. Adult Dog) Tibia, %TBF/%TW
27. Adult Dog (vs. Adolescent Pup) Tibia, %TBF/%TW
28. Adult Dog Femur, flow:cc/min/hg
29. A,B Adult Dog Tibia, flow:cc/min/hg
30. Adult Dog Femoral Cortex, flow:cc/min/hg
31. Adult Dog Tibial Cortex, flow:cc/min/hg
32. Adult Dog Femur, %TBF/%TW
33. Adult Dog Tibia, %TBF/%TW
34. Adult Dog Femoral Cortex, %TBF/%TW
35. Adult Dog Tibial Cortex, %TBF/%TW
36. Adolescent vs. Adult Femoral Tissues, %Tc-MDP/%TW
37. Adolescent vs. Adult Tibial Tissues, %Tc-MDP/%TW
38. Adolescent vs. Adult Osseous Tissues, %Tc-MDP/%TW

LIST OF GRAPHS
(Cont.)

39. Adolescent vs. Adult Femoral Tissues, %TBF/%TW
40. Adolescent vs. Adult Tibial Tissues, %TBF/%TW
41. Adolescent vs. Adult Osseous Tissues, %TBF/%TW
42. Adolescent vs. Adult Femoral Tissues, Tc-MDP/Blood flow
43. Adolescent vs. Adult Tibial Tissues, Tc-MDP/Blood flow
44. Adolescent vs. Adult Osseous Tissue, Tc-MDP/Blood flow
45. Adolescent Pup Femur, %Tc-MDP/%TW
46.A,B Adolescent Pup Femoral Cortex, %Tc-MDP/%TW
47. Adolescent Pup Tibia, %Tc-MDP/%TW
48.A,B Adolescent Pup Tibial Cortex, %Tc-MDP/%TW
49. Adult Dog Femur, %Tc-MDP/%TW+
50. Adult Dog Femoral Cortex, %Tc-MDP/%TW+
51. Adult Dog Tibia, %Tc-MDP/%TW+
52. Adult Dog Tibial Cortex, %Tc-MDP/%TW+
53. Adolescent Pup Femur, Tc-MDP/Blood flow
54. Adolescent Pup Femoral Cortex, Tc-MDP/Blood flow
55. Adolescent Pup Tibia, Tc-MDP/Blood flow
56. Adolescent Pup Tibial Cortex, Tc-MDP/Blood flow
57. Adult Dog Femur, Tc-MDP/Blood flow
58. Adult Dog Femoral Cortex, Tc-MDP/Blood flow
59. Adult Dog Tibia, Tc-MDP/Blood flow
60. Adult Dog Tibial Cortex, Tc-MDP/Blood flow

+ = T-tests not done

KEY TO ABBREVIATIONS FOR BONE REGIONS

b	between
C	Cartilage
Cx	Cortex
c	central
D.	Distal portion of total bone relative to the trunk (DF - Distal Femur) (DT - Distal Tibia)
DCx	Diaphyseal Cortex
DMar	Diaphyseal Marrow
DS	Diaphyseal Spongiosa
d	distal*
E	Epiphyseal
fib	fibrous portion
Fh	Femoral head
Fn	Femoral neck
GP	Growth Plate
Gt	Greater trochanter
i	inner
It	Intertrochanteric
Lt	Lesser trochanter
l	lateral (femoral condyle)
me	medial (femoral condyle)
m	middle*

*relative to the growth plate if metaphysis
relative to trunk if diaphysis

KEY TO ABBREVIATIONS FOR BONE REGIONS (CONT.)

M	Metaphyseal
o	outer
20	secondary ossification center
P.	Proximal portion of bone relative to the trunk (PF - Proximal Femur) (PT - Proximal Tibia)
p	proximal*
S	Spongiosa
Tub	Tibial Tuberosity

*relative to the growth plate if metaphyseal
relative to the trunk if diaphysis

I. INTRODUCTION

Bone is a highly vascular dynamic organ. The blood vessels of bone are in close contact with a total bone-crystal surface area of 200 acres in man (Newman and Newman, 1958). Osseous circulation is necessary for osteogenesis, bone growth and calcification, fracture repair, hematopoiesis, and for maintaining bone-blood equilibrium for minerals stored in the bone, including calcium, phosphorous, strontium, potassium, sodium, and hydrogen. In the role of maintaining mineral homeostasis, it is responsive enough to remove excess calcium from the blood at the rate of 100mgm% per minute (McLean, 1958).

Accurate blood flow quantitation is needed to evaluate the pathology of various bone diseases. Clinically, blood borne bone-seeking radionuclides, such as technetium diphosphonate show a different distribution in diseased bone than they do in normal bone. The link between osseous circulation and the functions of bone in health and disease has been the subject of an increasing number of scientific investigators. However, without an accurate method of measuring osseous flow, it is impossible to quantitatively relate bone flow growth, metabolism or the rate uptake bone-seeking radionuclides.

This study presents a valid method of quantitatively regional osseous flow within long bones. The technique is valuable in evaluating flow to some through the various stages of development under physiologic conditions.

In the background, a survey of past measurements of blood flow through normal bone is given. Measurements of altered osseous flow are reviewed to document and discern factors central to the physiological control of flow and bone blood flow in disease.

II. BACKGROUND

A. Vascular Anatomy

The vascular anatomy of bones has been studied by a variety of techniques. The larger vessesl may be perfused with plastic and preserved as the rest of the bone is preserved. India ink perfusion of capillaries, light and electron microscopy, and microangiography also provide useful information. In microangiography, the particulate size and injection site of the radio-opaque media may be varied to better visualize arteries, veins or capillaries. Studies of this type have shown that the bones of the dog, cat, rabbit, rat, and man are quite similar in the basic arrangement of their vasculature (Trueta, 1968).

The blood vessels of long bone can be categorized into (a) afferent vessels, (b) vascular lattice, and (c) efferent vessels. The afferent system is made of the principle nutrient artery, metaphyseal and epiphyseal arterioles, and periosteal arterioles. The vascular lattice consists of the medullary sinusoids, the cortical capillaries and the periosteal capillaries. The efferent vessels are the large emissary veins and the vena comitans of the principle nutrient artery, the interfascicular and intramuscular veins, and the periosteal veins.

(a) AFFERENT SYSTEM (Figure 1)

Nutrient Artery:

There is generally one principle nutrient artery per long bone, although two and even three can exist, as in the human femur and humerus, respectively. The canine femur and tibia each are supplied by a single nutrient artery. The artery centers the bone through an oblique canal and divides into ascending and descending branches. Each of these gives rise into multiple arterioles which diverge and subdivide in the peripheral zone of the marrow to become straight terminal twigs which

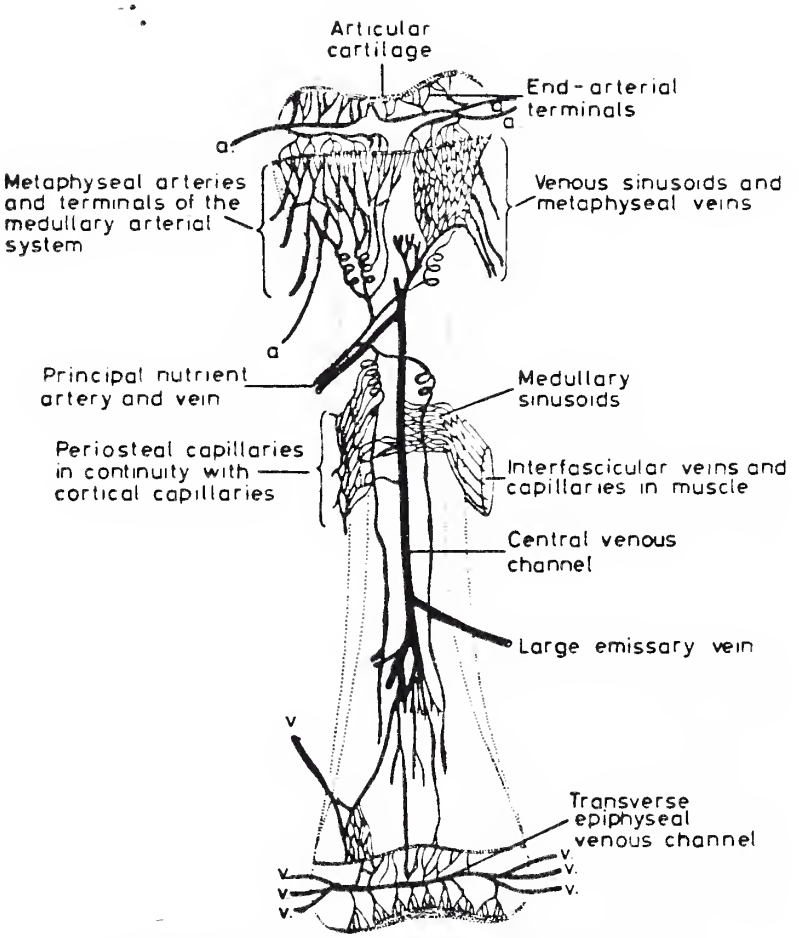
Articular cartilage
End-arterial terminals
Metaphyseal arteries and terminals of the medullary arterial system
Venous sinusoids and metaphyseal veins
Principal nutrient artery and vein
Medullary sinusoids
Periosteal capillaries in continuity with cortical capillaries
Interfascicular veins and capillaries in muscle
Central venous channel
Large emissary vein
Transverse epiphyseal venous channel

Figure 1 Vascular organization of a long bone in longitudinal section

(Brookes, 1972)

feed into capillary loops. Small branches to the cortex and marrow are given off the ascending and descending arterioles at multiple levels. The end arterioles normally supply distinct areas with little functional overlap (Brooks, 1972).

Epiphyseo-Metaphyseal Arterioles:

The epiphyseo-metaphyseal arterioles enter the bone through many nutrient foramina in the cortex of the metaphysis and epiphysis. These vessels arise from a vascular ring which encircle the end of the bone. Hunter's "circulus articuli vasculosus" (Figure 2, labeled CVA).

The metaphyseal vessels arise directly from the vascular ring. They enter the metaphysis and turn towards the epiphysis, arborizing, and perhaps anastomosing with the vessels of the nutrient system (Rhinelander, 1976). Brookes (1972) contends however, that the metaphyseal and diaphyseal blood systems are normally totally independent above the level of fine arterioles, and that there are few, if any, anastomosis before the precapillary level.

The epiphyseal arteries arise from the circulus articuli vasculosus indirectly, via vascular arcades. These arcades may be responsible for the lower intramedullary pressure of the epiphysis contrasted to that of the metaphysis (Stein et al, 1957). Within the cancellous bone of the epiphysis the epiphyseal vessels, anastomosing freely, converge on the center of the epiphysis and then radiate outwards forming arcades. These arcades of arches are similar to these of the intestinal mesentary and comprise three to four tiers in the human femoral condyles (Brookes, 1972). The terminal branches which pass adjacent to the articular cartilage are finer in caliber than the other epiphyseal arterioles. The branches feed into tortuous sinusoid loops, most of which are separated from the articular cartilage by several lamellae

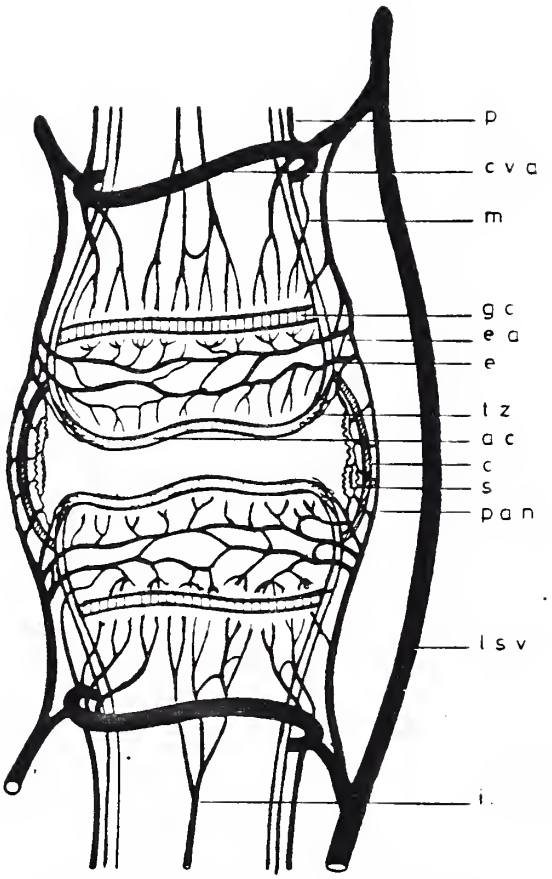

Figure 2. Diagram of the arterial arrangements in a joint and the connections of Hunter's vascular circle

p.	periosteal artery	a.c.	articular cartilage
c.v.a.	circulus vasculosus articuli	c.	fibrous capsule of joint
m.	metaphyseal artery	s.	subsynovial plexus
g.c.	growth cartilage	p.a.n.	periarticular plexus
e.a.	epiphyseal arterial arcades	l.s.v.	large systemic vessel
e.	epiphyseal artery	i.	intramedullary branches of the nutrient artery
t.z.	transitional zone		

(Brookes, 1972)

of bone; a few loops extend through the calcified cartilage layer to abut on cylinders of uncalcified cartilage. Some branches of the epiphyseal arteries pass directly to the adjacent "growth plate scar", which is actually the bone plate that lays parallel to the former physis. In the adolescent, the vessels turn 90 degrees to pierce the bone plate, then turn again to run parallel to the growth plate. These vessels give rise to perpendicular branches, each of which divides into two or three capillary loops. The loops perforate a thin layer of calcified cartilage and have terminal expansions which abut on germinal cartilage, each loop lying over four to ten cartilage columns (Stockwell, 1979). The venous side of the loop drains into veins which anastomose on the other side of the bone plate and then feed into the epiphyseal sinusoids. In the adult, the physis is no longer a partial barrier between epiphyseal and metaphyseal circulation. Small spiral epiphyseal arteries run from the physis to anastomose with the metaphyseal arteries (Trueta, 1957). Some authors contend that there are no epiphyseal/metaphyseal arterial anastomoses (Crelin, 1957), and hold that only capillary anastomoses exist (Brookes and Harrison, 1957). There is agreement that wide venous connections occur in the adult.

Periosteal Arteries:

The periosteum is composed of an inner osteogenic and outer fibrous layer, each of which has a vascular network. The fibrous layer, contains arteries, veins and capillaries, while the osteogenic layer contains only capillaries. This capillary network is continuous with the capillaries (or venules) of the cortex on one side and the vessels in the fibrous layer on the other side. The fibrous layer contains arteries with venae comitans which run down the length of the bone with

little change in caliber (Trueta, 1968). These arteries anastomose with themselves and branches from muscular arteries to form connected vascular circles at the ends of the long bone. These circles include Hunter's circulus articuli vasculosus and a smaller plexus located at the level of the epiphyseal plate. Both circles anastomose with the epiphyseal and metaphyseal vessels. While the arterioles of the fibrous layer do feed the osteogenic layer capillaries, it is rare to find a periosteal arteriole directly supplying the cortex of the shaft (Root, 1963). Rhinelander has observed that periosteal arterioles enter the diaphyseal cortex only along heavy fascial attachments. Such sites include the linea aspera of the femur and the insertions of interosseous membranes in the forearm or lower leg. Multiple arterioles enter here and arborize and anastomose with terminal branches of the medullary arterioles in the outer one-third of the cortex.

(b) VASCULAR LATTICE and EFFERENT SYSTEM

Diaphyseal and Metaphyseal Medulla

The arteries of the marrow originate from the nutrient artery and empty into capillaries both in the marrow and in the cortex. The marrow arteries are histologically similar to arteries found elsewhere in the body, complete with three tunicae (Brookes, 1972). The small arteries, however, make an abrupt transition into short arterioles and arterial capillaries, and then into sinusoids (Rhodin, 1974). There are no precapillary sphincters (Michelson, 1967). The vessel diameter which decreases to 5μm by the smallest arterioles, widens to 15μ in the early sinusoids (Brookes, 1972). The sinusoids are thin-walled and irregular in caliber ranging from 15 to 50μm (Trueta, 1968). The endothelium is

the discontinuous type found in organs where excessive exchange of cells or large particles occurs, namely the marrow, spleen and liver (Weiss and Greep, 1977). Discontinuous endothelium has thin walls, large gaps up to 1,000 Å in diameter, and a discontinuous or absent basement membrane. Most species have no basement membrane in their marrow sinusoids (Rhodin, 1974).

The sinusoids of the diaphysis are transversely oriented and peripherally are continuous with the endosteal capillaries of the cortical vascular system. The metaphyseal sinusoids run longitudinally, and are far more numerous than the arteries they accompany (Brookes, 1972). The increased diameter and number of sinusoids as opposed to arterioles results in a much greater cross-sectional area and a decreased blood flow rate in the sinusoids. The metaphyseal and diaphyseal sinusoids coalesce into collecting sinusoids, most of which converge on a large central venous sinus running down the full length of the diaphysis. The collecting sinusoids at the periphery of the metaphysis, however, drain into metaphyseal veins that exit from the bone. The central venous sinus is drained by the vena comitans of the principle nuteient artery and large emissary veins which exit the bone through cortical channels.

There are no lymph vessels described in the marrow. The sinusoids are thought to function dually as blood and lymph channels.

Cortex

The cortical vascular lattice is enclosed in a system of Haversian canals which run more or less parallel to the shaft of the bone and transverse Volkmann's canals. The canals range from 22 to 100μm in diameter (Bloom and Fawcett, 1975), averaging 50μm. These blood vessels are termed large capillaries by some, and venules by others. The number

and diameter of the vessels within the canals is a matter of debate. Branemark observed the rabbit cortex by vital microscopy and found the cortical vessels to be generally less than 15μm wide (Lunde, 1970). Brookes and Harrison (1957) studied the rabbit cortex via micro-angiography and found that the vessels were between 15-30μm in diameter, with the wider capillaries located near endosteal surface in continuity with the marrow sinusoids. Trueta (1968, 1974) believes that the vessels fill the entire canal. Trueta, however, perfused his specimens at pressures above those encountered under physiological conditions (Rhinelander, 1976) and may have abnormally dilated the distensible vessels.

Trueta also describes the frequent occurrence of two vessels per canal. Brookes (1972) agrees that this arrangement occurs in the primary osteons of young bone, but says that mature secondary osteons contain only one vessel. Bloom and Fawcett (1962) report that only about 2% of the Haversian canals contain two blood vessels. Rhinelander (1974) maintains that although there may be either one or two vessels per canal (in adult dogs), only one of them is functioning under normal, non-stressed conditions. However, in fracture repair and in pathological conditions where there is increased flow to an area of bone, both vessels may open.

The cortical capillaries are continuous with the sinusoids of the marrow on one side and with the capillary network of the osteogenic periosteum on the other side (Figures 3,4). The arterioles which feed into the cortical system are primarily those originating from the medullary circulation, along with a few fibrous periosteal arterioles that enter at fascial or ligamentous attachments. Cortical venous

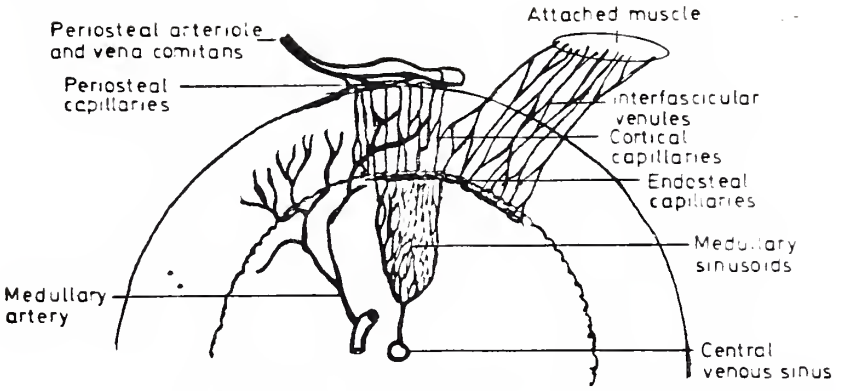

Figure 3. Blood supply of bone cortex in cross-section

(Brookes, 1972)

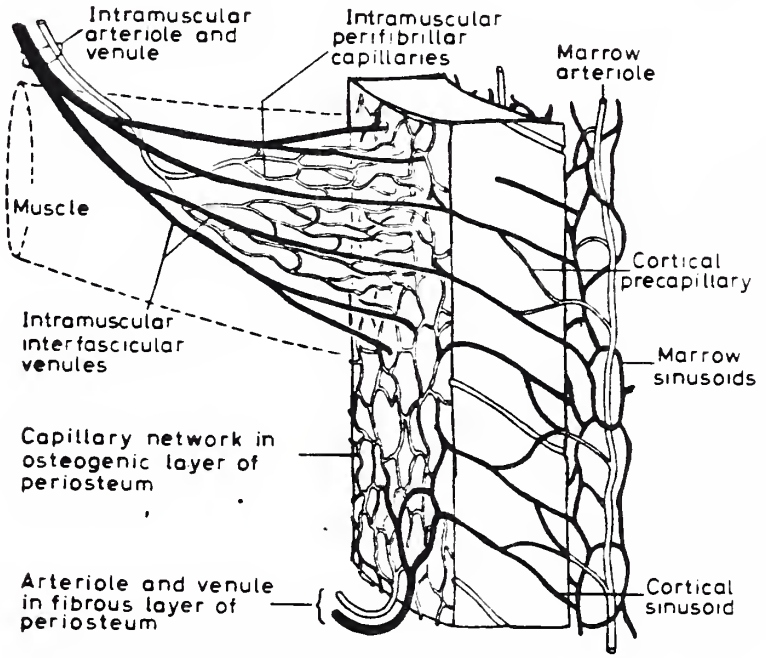

Figure 4. Vascular connection between bone cortex, periosteum and attached muscle

(Brookes, 1972)

channels are found traversing those areas of cortex to which muscle is directly attached. In these areas, the periosteum is greatly attenuated. The cortical venous channels are directly continuous with the interfascicular venules of the attached muscle.

The direction of flow within the cortical capillaries is a matter of controversy and will be discussed in the functional vascular anatomy section.

Epiphysis

The epiphysis, like the diaphysis, has a system of profuse sinusoids which radiate inwardly to coalesce a central venous sinus. This sinus in the epiphysis is transverse, while that of the shaft is vertical. The sinusoids of the epiphysis are more irregular in caliber and in distribution than those in the remainder of the bone. The transverse venous sinus is drained by epiphyseal veins.

B. Development of the Osseous Circulation

The sequence of the development of the osseous circulatory system and bone itself are interdependent. The human femur is discussed as an example of the developing long bone.

Prenatal (A-F, Figure 5)

Chondrification of the femoral anlage of condensed mesenchyme begins in the human embryo at 38 days (Trueta, 1968). At 46 days the adjacent surrounding mesenchyme condenses to form two-layered perichondrium, an inner chondrogenic layer and an outer fibroblastic connective tissue sheath. The inner perichondrium adds new chondrocytes to the shaft of the cartilage model while the model also undergoes interstitial growth. The chondrocytes in the center of the model hypertrophy and mature, vacuolating and producing much intercellular matrix. Membrane vessicles

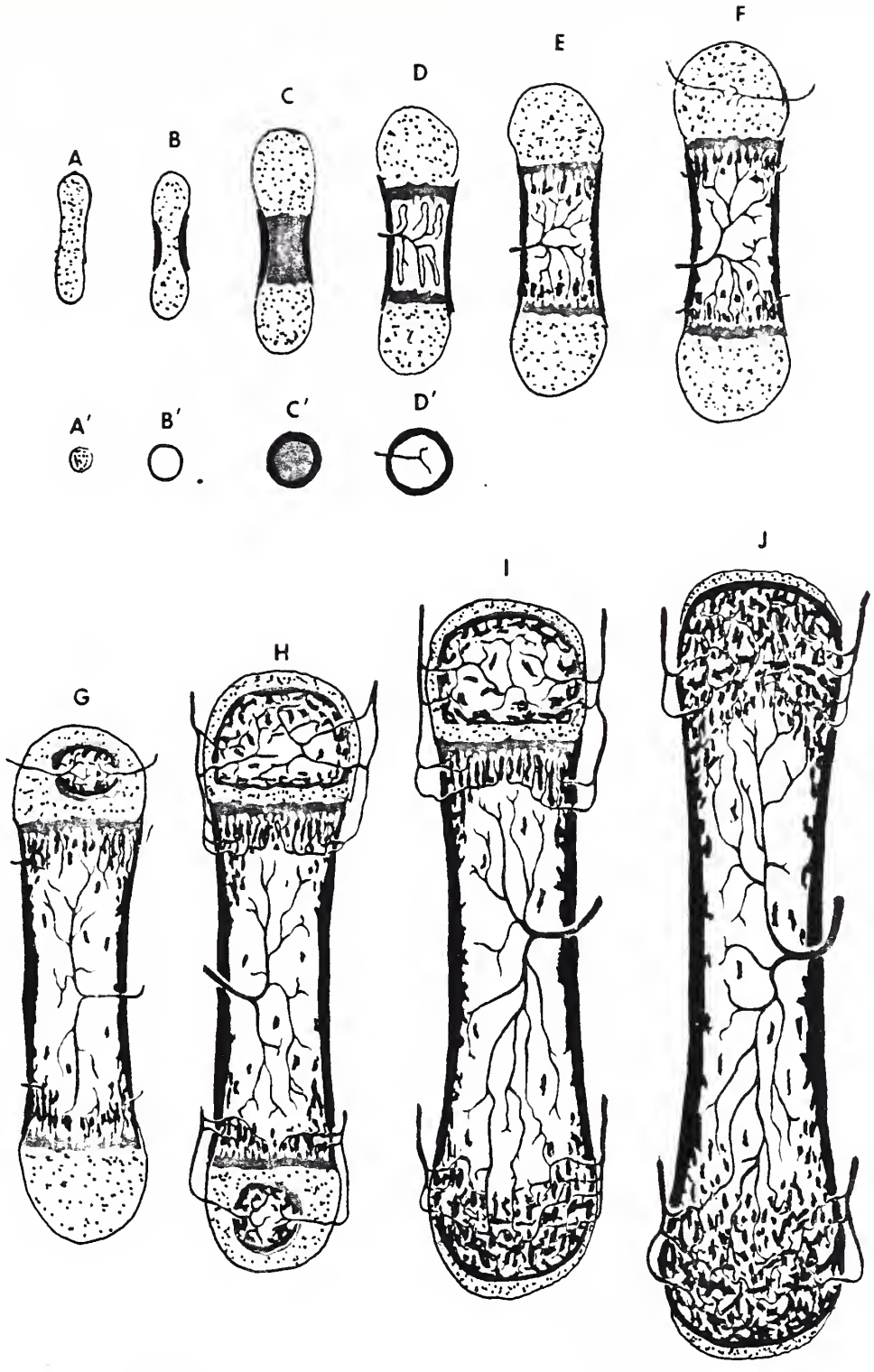

Figure 5
Development of a Long Bone

A, B, C, and D cross sections through the centers of A, B, C, and D--stippled, cartilage; grey, calcified cartilage; black, bone. A, cartilage model; B, periosteal bone collar appears before any calcification of cartilage; C, cartilage begins to calcify; D, vascular mesenchyme enters the calcified cartilage matrix and divides it into two zones of ossification (E); F, blood vessels and mesenchyme enter upper epiphyseal cartilage and the epiphyseal ossification center develops in it (G). A similar ossification center develops in lower epiphyseal cartilage (H). As the bone ceases to grow in length the lower epiphyseal plate disappears first (I) and then the upper epiphyseal plate (J). The bone marrow cavity then becomes continuous throughout the length of the bone, and the blood vessels of the diaphysis, metaphyses, and epiphyses intercommunicate. (Bloom and Fawcett, 1976).

containing alkaline phosphatase bud off the chondrocytes and induce precipitation of calcium phosphate (Felix and Fleish, 1976). These crystal nests enlarge and merge so that the intercellular matrix is soon uniformly calcified. The cartilage cells undergo degenerative changes and (presumably) die leaving empty lacunae (Bloom and Fawcett, 1975).

The vascular system of the embryo develops simultaneously to reach and invade the perichondrium. This vascular invasion induces the cells of the inner layer to differentiate into osteogenic cells, probably by increasing the local oxygen tension (Hall, 1978). A thin layer of bone, the primary bone collar, is formed around the cartilage shaft (Figure 5B). Unmineralized hyaline cartilage resists vascular invasion (Einstein et al, 1973). When the bone collar and contained cartilage are calcified at two months, they are invaded by a bud of capillaries and cells from the osteogenic periosteum. The calcified cartilage fragments. The mechanism of this is not clear. It has been suggested that this is due initially to enzymes released from either the degenerating or decreased chondrocytes, and then further digestion of the fragments by chondroclasts. The thin-walled vessels of the periosteal bud branch and form capillary loops that extend into the cavities formed in the cartilage (Figure 5D). Osteoblasts then deposit (Figure 5E) bone over the remnants of the calcified cartilage in primary centers of ossification. The source of these osteoblasts, and the chondroclasts proposed above, is controversial. Most authors believe that they develop from osteoprogenitor cells that accompany the vessels of the periosteal bud. Others propose that the hypertrophied chondrocytes are not destroyed during osteogenesis, but rather are released and modulated into osteoprogenitor cells (Crelin, 1967; Wilsman and Van Sickle, 1970). The ossification center expands towards the ends of the bone as cartilage distal to it continues to pro-

liferate, mature, calcify and be replaced by trabecular of bone. These trabeculae are continuous with the periosteal collar which also expands along the length of the bone, stopping at the margin of the zone of Ranvier at the level of the future physis (Ogden, 1978). The bone also continues to grow in width by periosteal appositional growth. The periphery of the bone undergoes remodelling and strengthens, providing support, while the central cancellous bone is resorbed leaving a central marrow cavity.

The marrow first formed in this cavity is non-hematopoetic, becoming hematopoietic three months after birth. The blood vessels of the primary marrow differentiate into medullary arteries and sinusoids drained by venous sinuses and nutrient veins (Brookes, 1972). The nutrient artery pierces the cortex midshaft as did the periosteal bud vessels from which it was derived. As the endosteal surface of the widening shaft is resorbed, and many medullary blood vessels become confluent with the cortical vessels.

At nine to twelve weeks (Brookes, 1972; Trueta, 1968) of fetal life, perichondral vessels are incorporated into canals in the growing epiphyseal cartilage at the ends of the long bone. There is disagreement as to how this takes place since it is known that uncalcified cartilages normally resists penetration by blood vessels. Some (Waterman, 1961) propose that the cartilage cells degenerate and lyse to prepare a pathway for actively ingrowing vessels. Wang et al. (1975) observe that the perichondral vessels form into vascular loops about which the perichondrium and then cartilage cells proliferate, eventually burying the loops in cartilage as the epiphysis grows outwards. Each "in-growing" arteriole develops a leash of about six capillaries which expand into a glomerulus at its tip and drain into one venule. The capillary endothe-

lium is the fenestrated type, very thin with 60nm pores covered by diaphragms (Stockwell, 1979). The cartilage is nourished by nutrients that diffuse from the blood vessels which are separated by a distance of 1.2 to 1.5 mm (Wilsman and Van Sickle, 1970). Thus, as the epiphyseal cartilage grows, the blood vessels branch and sub-branch, each branch forming its own glomerulus. By birth, there are 27 glomeruli in the human femoral head. Some vessel branches extend through the region of the future growth plate to anastomose with the metaphyseal circulation. These "transphyseal vessels are more frequent at the periphery than at the center" (Ogden, 1978).

The cartilage canals serve not only as sources of nutrition, but are also a source of chondro-and perhaps osteoprogenitor cells. The walls of the canals are lined with connective tissue that is continuous with the perichondrium and contains mesenchymal cells (Wilsman and Van Sickle, 1970). The mesenchymal cells gradually differentiate into chondral cells as they radiate outwards from the canal. In the first months of fetal life the epiphyseal cartilage grows mainly by perichondral apposition, but after three to four months the cartilage canals contribute most of the new chondrocytes (Wang, 1975).

The above is an overview of the prenatal development of bone (Figure 5F). At birth, the long bone consists of two cartilaginous epiphyses and a ring of woven cortical bone surrounding the non-hemopoietic marrow of the diaphysis and the primary (trabeculae with cartilaginous cores) and secondary (bony cores) spongiosa of the two metaphyses. The vasculature of the epiphyses is enclosed in cartilage canals, and is connected with the circulation of the metaphysis via transphyseal blood vessels. The vascular pattern of the metaphysis and diaphysis is similar to that of

the child, described below.

Postnatal

In the human, all of the epiphyseal or secondary ossification centers appear after birth except that of the distal femur. In the dog, all appear postnatally; the first centers to appear radiographically are those of the heads of the humerus and femur, during the first or second week (Hare, 1961). In two day old pups (corresponding to 4-6 months old humans), Wilsman and Van Sickle (1970) observe three or four foci of calcified cartilage adjacent to glomerular endings in canals. Surrounding this is a zone of hypertrophied cartilage cells in radiating columns 2-5 cells long. Outside of this is a layer of germinal cells. The foci of calcification subsequently enlarge and coalesce into one focus. At six days of age the glomerular endings dilate and resemble the dilations of the capillary loops of the metaphyseal side of the growth plate. Osteoid appears at the center of the focus the following day (Figure 5G). The situation appears to be similar in the human (Ogden and Southwick, 1976; Wang, 1975). The secondary center of ossification expands outward and the blood vessels of previous canals anastomose and continue to extend into the degenerating zone of hypertrophied cartilage. When the region of the growth plate is reached, first in the center and then in the periphery, the process of expanding ossification ceases (Figure 5H). It also ceases at the joint surface, leaving the articular cartilage. The basic microvasculature of the epiphysis at this time (2-3 years in the human femoral head) is essentially the same as in the adult except for the vascular expansions over the growth plate. Both were described earlier.

The articular cartilage has two separate layers of dividing chondrocytes during growth (Trueta, 1968). One is that associated with the

expanding secondary ossification center. The other is located three to four cells below the articular surface and remains after the ossification center stops growing. The mitotic figures disappear, however, though the cells continue to secrete matrix to compensate for that lost by wear and tear (Ham, 1974). These cells overlie more hypertrophied cartilage cells which overlie a thick, but discontinuous, layer of calcified cartilage. During growth many subchondral vessels extend up into the uncalcified layer of cartilage. These long tortuous vascular loops decrease in number with age, but a few still persist in adulthood (Trueta, 1968) (Figure 6C). The number of canals in the articular cartilage also decreases with age; these totally disappear by 18 months in the rabbit (Stockwell, 1979).

The cartilage of the growth plate is the most well studied area of endochondral ossification. Above it lies the saccular expansions and varicosities of the epiphyseal end arteries whose epithelium is closed (Brookes, 1972). These overlie and nourish a zone of closely packed and small resting cartilage cells, and a zone of proliferating, flattened, cartilage cells. The latter cells are stacked in vertical columns and secrete the greater part of their matrix between columns. Brookes (1972) suggests that the alignment into columns is somehow due to the influence of vertical metaphyseal vascular loops. In the adjacent zone of maturation, the cells secrete more matrix, gradually accumulate glycogen and hypertrophy, and give off membrane vessicles which induce the matrix to calcify. In the zone of calcified cartilage, the chondrocytes either degenerate and/or differentiate into osteoprogenitor cells and osteoblasts, leaving empty lacunae. The intracellular substance starts to break down and the thin horizontal partitions within columns of lacunae, as well as the thinner vertical partitions between columns, disintegrate. The remaining thicker

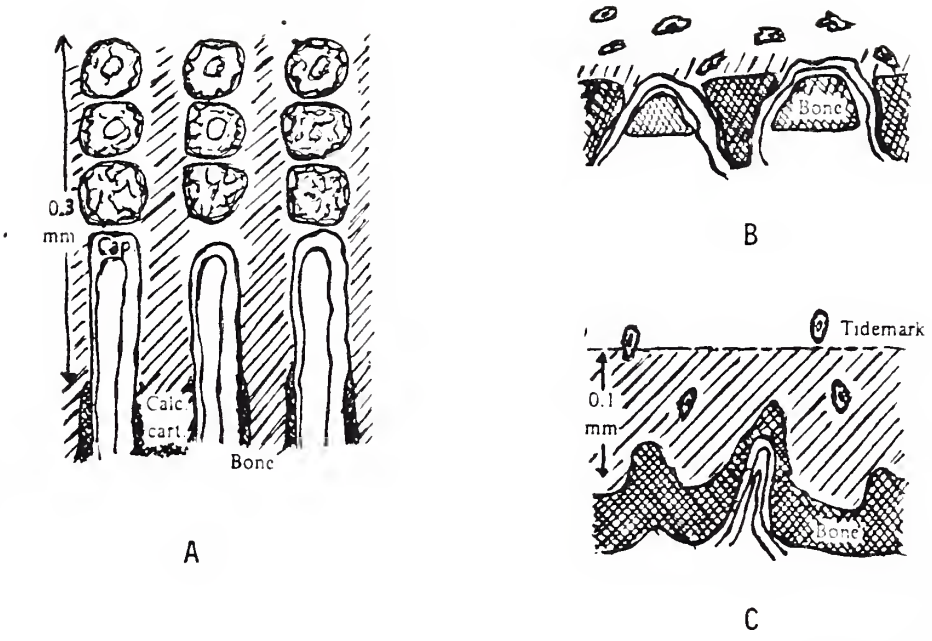

Figure 6

Three Types of Osseochondral Junction

(A) A thick lamina of calcified cartilage penetrated by numerous vascular spaces or capillaries (Cap.) apposed to columns of uncalcified cartilage, as at the metaphyseal side of the growth plate. (B) A thin lamina of calcified cartilage penetrated by numerous blood vessels, as at the epiphyseal side of the growth palte. (C) A thick lamina of calcified cartilage where vascular penetration is sparse or absent as at the deep surface of articular cartilage

(Stockwell, 1979)

vertical partitions of calcified cartilage are in the shape of hollow cylinders. Vascular loops invade each cylinder, perhaps carrying the chondroclasts that aid the disintegration. The loops are vertical and composed of continuous epithelium (Ogden, 1978; Brookes, 1972). The diameter is narrow in ascent and dilates at its tip so that it is wider in the descending limb. The dilation is less and the caliber more regular than on the epiphyseal side of the physis. Some vessels reach through the lower half of the calcified zone to abut on columns of yet uncalcified but degenerating cartilage that extends through the upper half of the calcified zone (Figure 6A) (Stockwell, 1979). Osteoid is secreted onto the cartilaginous walls of the vascularized cylinders. The osteoid is calcified to form primary spongiosa. This is eventually resorbed by osteoclasts and is either left as marrow space or remodelled into secondary spongiosa.

The number of transphyseal vessels appears to vary with age. Most investigators seem to feel that there are a significant number of connections between the circulations of the epiphysis and metaphysis in the infant and in the adult after epiphyseodesis, but not in the child with a fully ossified epiphysis and well developed growth plate (Irving, 1964; Bassett et al, 1969). Brookes (1972) says that transphyseal vessels exist as long as the secondary ossification centers are expanding and also at the approach of epiphyseodesis. Ogden (1974) says that the number of vessels crossing the growth plate region in the femoral head begins to decrease as the secondary ossification center develops at one year of age; there are none by 15-18 months. Trueta (1968) found no blood vessels crossing a growth plate in over 2,000 specimens. He implicates the physis as a circulatory barrier which prevents the

spread of childhood hematogenous osteomyelitis from the metaphysis to the epiphysis. This barrier isolates the circulation of the femoral capital epiphysis, rendering it more vulnerable to vascular insult and ensuing osteochondritis disease or necrosis. Nevertheless, there are some reports of the existence of blood vessels in well developed growth plates. Wang et al, (1975) portray the proximal tibia of a seven-year-old containing a good many of these vessels. Transphyseal vessels are also noted at twelve years in the tibial tuberosity (Ogden et al, 1975). Despite these reports, the general consensus is that in the older child, the circulations of the major epiphyses are isolated from the rest of the bone by well developed growth plates. The only vascular connections between the shaft and the epiphysis are extra-osseous via the periosteal vessels around the zone of Ranvier.

The tibial tuberosity is an example of an apophysis, a secondary ossification center that is subjected to tensile rather than compressive forces. In Trueta's opinion (1968), while pressure encourages osteogenesis, tension induces mesenchymal stem cells to undergo fibrous changes. The immature tibial tuberosity is divisible into three histological sections. Among these three segments the most tension is exerted on the distal fibrous section (Ogden, et al, 1975). Tensile forces are less in the middle fibrocartilage section and are minimal in the proximal section which undergoes normal endochondral ossification. The fibrous areas undergo membranous ossification.

The bone continues to grow longitudinally as long as the growth cartilage undergoes interstitial growth with some peripheral perichondrial apposition. The rate of growth is the product of the chondrocyte proliferation rate and the length of the hypertrophied

cells. Growth at opposite ends of a fetal bone is equal (Brookes, 1972). After birth, however, the physes adjacent to the knee joint grow faster than the physes at the other ends of the tibia and femur. The growing end of the femur contributes 70% of the total bone growth, the non-growing proximal end contributing 30% (Stockwell, 1979). The rate is affected by a variety of factors discussed in Section VIII, though it probably is regulated and limited by periosteal tension. The periosteum is attached to the physeal cartilage at the zone of Ranvier. If the growth of one growth plate is limited, the tension transmitted through the periosteum to the opposite physis is limited, permitting that physis to grow more and compensate for the other. Although the growth rate may vary, the thickness of the physis varies little; the rate of growth at the E-side of the plate is equalized by the rate of resorption and ossification at the M-side. At high rates of growth, the vasculature is noted to be increased on both the E-side (Stockwell, 1979) and the M-side (Trueta, 1968) of the physis. At the time of epiphyseodesis, however, the rate of growth at the E-side falls behind the rate of activity at the M-side. An increasing percentage of the remaining cartilage becomes calcified and is replaced by bony trabeculae, eventually uniting the cancellous bone masses and the vasculature of the epiphysis and metaphysis (Figure 5I,J).

Concurrent with continued bone growth, the shaft continues to form and remodel. The spongy bone of the metaphysis is being converted into compact bone of the shaft. The primary spongiosa consists of cylinders of calcified cartilage covered or lined by lamellae of bone and housing blood vessels and osteogenic cells. In histological sections the walls of these cylinders appear as trabeculae with cartilage cores. As the osteoblasts secrete successive layers of bone, the canal in the center

of the cylinder narrows. Thus, an osteon of the Haversian system of compact bone is formed. The flared metaphysis is wider than the diaphyseal shaft into which it is incorporated. Hence, bone is resorbed from the periosteal surface of the metaphysis.

In the diaphyseal cortex new Haversian systems are created around periosteal capillaries while bone is resorbed on the endosteal surface. Hence, the shaft increases in width while the cortex thickness changes relatively little. The bone surface of a young, rapidly widening shaft is not smooth, but covered by ridges and grooves in which blood vessels lie (Ham, 1974) (Figure 7). Osteoblasts from the osteogenic periosteum selectively lay bone onto the ridges until they fuse, leaving a canal where each groove had been. The canal contains a capillary and is lined by the former periosteum of the groove, now designated endosteum. Endosteal osteoblasts secrete concentric layers of bone to narrow the canal and form a Haversian system. When the rate of growth in width of the shaft slows, the cortical surface becomes smoother. The periosteum lays down uniform layers of bone encircling the entire shaft, forming circumferential lamellae. In certain areas, the bone of circumferential lamellae has troughs eroded by osteoblasts; periosteal osteoblasts subsequently create a Haversian system about each vessel in a trough. The bone between these Haversian systems is now designated interstitial lamellae. Volkmann's canals contain blood vessels that are connected to and perpendicular to the vessels of the Haversian canals. When Haversian bone systems are being laid down about the more or less longitudinal blood vessels, spaces are left where a transverse periosteal vessel descends into the developing canal. These spaces are the canals of Volkmann. The Haversian systems are also constantly being renewed. When an osteocyte in a lacuna of an osteon dies, the dead bone is eventually

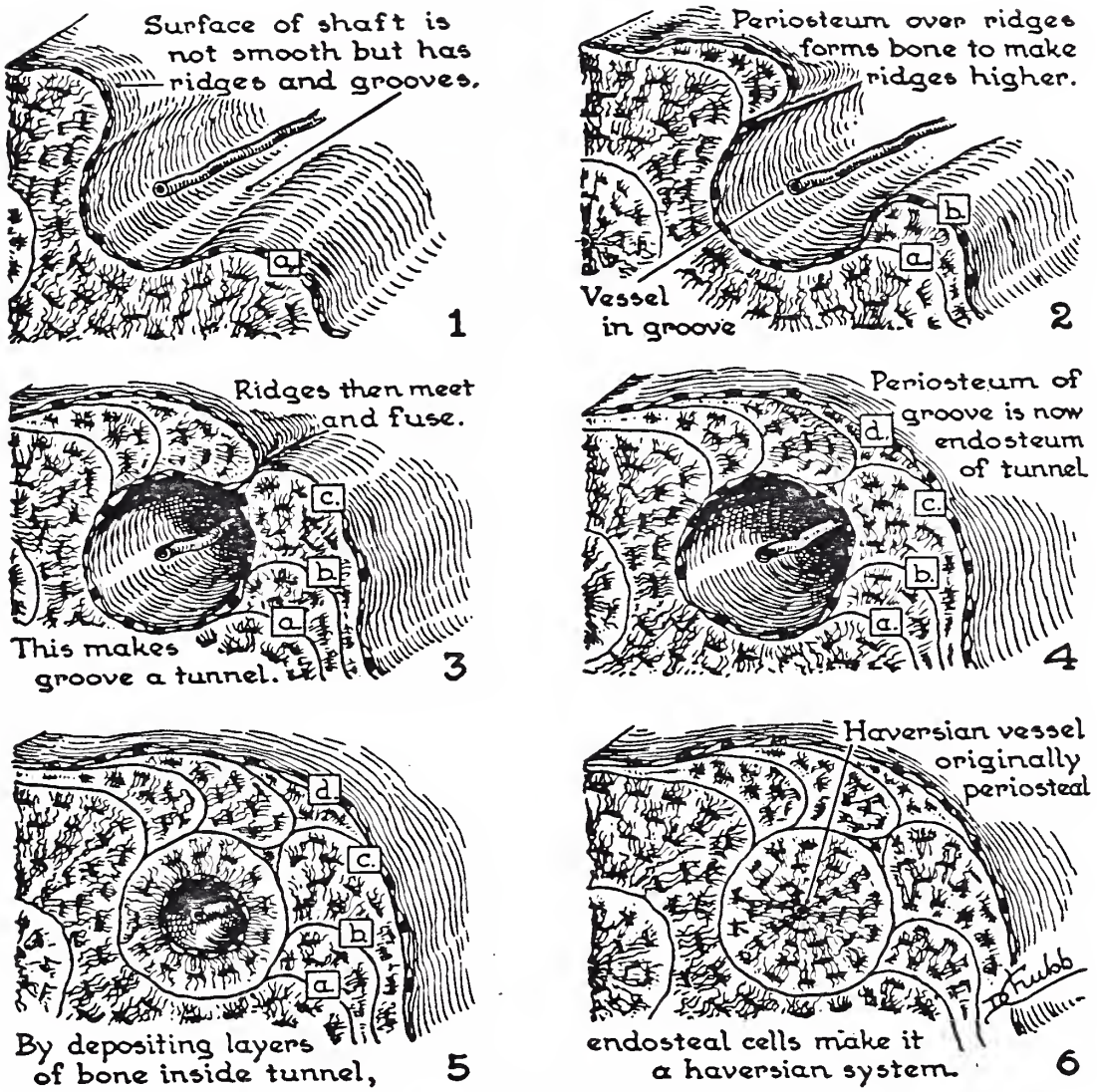

FIG. 17 Three-dimensional diagrams showing how the longitudinally disposed grooves on the exterior of a growing shaft become roofed over to form tunnels and how these become filled in to form haversian systems which thereupon are added to the exterior of the shaft. These diagrams also show how the blood supply of a shaft of a long bone comes to be derived, when it is fully grown, to a great extent from the periosteum by means of vessels having been buried in its substance.

(Ham, 1974)

resorbed by osteoclasts. In time, the expanding resorption cavity encompasses a blood vessel and osteoprogenitor cells. Some of these differentiate into osteoblasts which create a new Haversian system, its outer cement line being the edge of the previous resorption cavity. When the growing bone has finally attained its adult width, osteoblasts from both the endosteal and periosteal surfaces lay down a few final circumferential lamallae. Nevertheless, internal remodelling continues throughout adulthood. Cortical bone is normally replaced at a rate of 5-10% per year (Ham, 1974).

As a result of periosteal apposition and endosteal resorption, all the cortical vessels are derived from periosteal vessels (Ham, 1974). It should be noted that although the vessels of the Haversian canals are generally referred to as being longitudinal, most run somewhat obliquely (Brookes, 1972) (Figure 8). The canals are truly vertical only in endochondral bone in which the vessesl were previously M-side vascular loops. In bone formed by periosteal apposition, the vessels tend to radiate out from the center of the bone. The vessels in bone laid down by the endosteum tend to converge on an imaginary point outside the bone. The cause of the obliquity is unknown. Brookes proposes that as the bone elongates, periosteum is stretched between the two growth plates where it is anchored to the bone. Because of the stretching, the periosteal vessels are obliquely oriented; oblique canals are formed about oblique vessels. The situation in the endosteal bone would be "analogous".

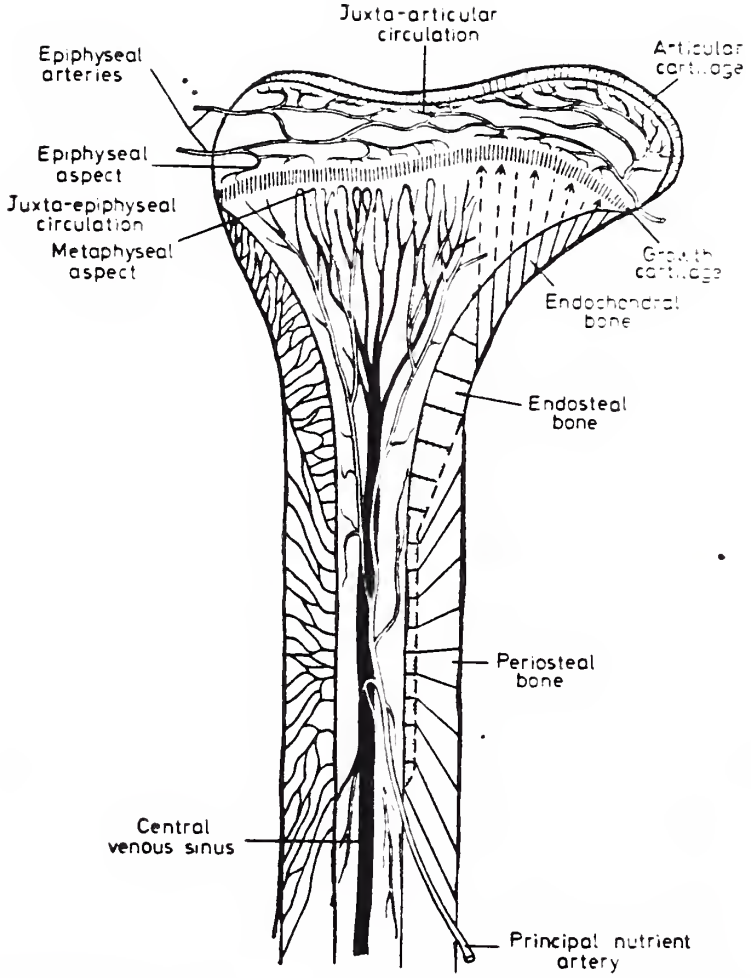

Figure 8. The three vascular patterns in bone cortex, corresponding to the three types of bone present

(Brookes, 1972)

C. Functional Vascular Anatomy

Anatomical studies reveal anastomoses in the adult between the vascular systems of the nutrient metaphyseal and epiphyseal arteries. Interconnections also exist between the medullary, cortical and periosteal vascular networks. Many investigations have been conducted to delineate the relative contribution of each artery and to define the region(s) of bone each artery normally supplies. The individual contribution to bone blood flow by an artery has generally been studied by either occluding the given artery or by occluding all flow except that through the artery under study.

Most investigators who have tried to obstruct flow by ligating the nutrient artery or by stripping the periosteum from the cortex have found few, if any, histologic changes. Drinker et al, (1922) measured bone flow and did not detect any alteration by ligation or stripping. He attributed this to the profuse interconnections that exist within bone's vascular lattice. More recent workers have been able to measure decreased flow as a result of these procedures. Whiteside et al. (1978) found the flow through the epiphyseal area was depleted in mature rabbits, and absent in immature rabbits after periosteal stripping. No area was affected by medullary reaming. Shim et al. (1968) found adult bone flow to be reduced in all areas after ligation of the nutrient artery. With the diaphyseal flow reduced more (70%) than epiphyseal and metaphyseal (35%) flow is reduced; the total bone flow was reduced by 50%. From this study and the work of Trueta (1968), the nutrient artery has been estimated to contribute 50-70% of the total bone flow.

Johnson (1927) and Trueta and Cavidias (1955, 1965) performed studies in which the flow through only a single source was preserved while flow

from two other sources was obliterated. To obliterate flow, the nutrient artery was ligated, and the metaphysis sealed off with wax, or the periosteum was stripped and the outer shaft sealed with wax or polythene. The results were interpreted in the following manner. The nutrient artery is felt to supply the entire marrow and the inner two-thirds of the cortex. The periosteal flow maintains and is necessary for the survival of the peripheral third of the cortex. The combined epiphysometaphyseal arteries can maintain the entire medulla and inner cortex in the adult. When the epiphyseal flow to the shaft is blocked by a growth plate, however, the isolated metaphyseal arteries are able to maintain only the metaphyseal ends of the shaft; the midsection dies.

Brookes (1972) and Rhinelander disagree with the above interpretation of cortical blood supply. In Brookes's opinion, all cortical flow is from the vessels of the medulla; the periosteum only supplies centripetal flow to the cortex in certain instances, such as when the nutrient artery medullary blood supply is greatly diminished during experiments or in senescense. Rhinelander (1974) points out that the cortical capillaries represent a closed system between the vessels of the marrow and the periosteum. Flow through the cortex can be blocked by either blocking inflow or outflow with tightly fitting medullary rods or tight metal plates, for example. Rhinelander (1976) believes that the periosteal capillaries are outflow vessels.

It is evident that there is a controversy over which vessels supply the peripheral cortex. Older opinion has held that the inner cortex is supplied by the nutrient artery and the outer cortex supplied by the periosteal capillaries. The fact that most cortical capillaries are derived from the periosteum has been taken to support this view. Never-

theless, as Brookes (1972) points out, the dynamics of flow are determined by pressure differences and resistances, rather than vessel etiology. The periosteal role in supplying the cortex is repeatedly supported by microangiographic studies which demonstrate that the cortex is perfused centripetelly from the periosteal side. Rhinelander refutes these studies claiming that the perfusion pressures were excessive and not physiologic. In 1959, Brånemark performed vital microscopy in rabbit bone and observed capillaries from the nutrient medullary arteries entering the Haversian canals to supply the cortex. However, Rhinelander (1974) points out that normal flow had been interrupted "because all the external cortex had been ground away [so that] the only flow possible was back to the medulla."

There is a greater abundance of evidence supporting the theory of centrifugal flow through the cortex. Brookes (1961) proposed this theory after noting the centrifugal spread of hypaque which was added to the arterial injections of salicylates administered to patients with refractory bone pain. The dye spread out into the muscles. A similar phenomenon is observed following the injection of intravital dye in humans at operation; first the marrow is stained, then the inner cortex, then the outer cortex (Lamas et al, 1946). Brookes also reported that the nutrient veins are smaller than the nutrient artery and reasoned there must be an additional route to drain the venous side of the nutrient system; this could be through the cortex to the periosteal and interfascicular vessels. Since most of the canals in the diaphyseal cortex have one functioning vessel, blood can only flow in one direction through a canal. Although intravascular pressures are unavailable, the tissue pressure of the bone medulla is higher than that of the periosteum (Azuma et al, 1964). Intraosseous pressure averages about 50 mm Hg in the diaphyseal marrow of the dog (Stein et al, 1957; Herzig and Root, 1957), the cat (Bloomthal et al, 1952) and the

rabbit (Kalser et al, 1959). Brookes (1972) estimates that the intravascular pressure of the sinusoids starts at about 75 mm Hg, dropping to about 55 mm Hg in the collecting sinusoids. The high pressure might be attributed to the lack of precapillary sphincters. Periosteal tissue pressure is probably close to that of the rest of the body: 0 mm Hg. Thus, there is probably a pressure gradient across the cortex from the marrow sinusoids to the periosteal capillaries. Blood would flow centripetally if the pressure in the periosteal vessels were greater than about 55 mm Hg, but this is unlikely as the periosteal vessels are generally "capillaries or small venules, but not arteries" (Nelson et al, 1960). The intravascular pressure of most extra-osseous capillaries ranges from about 35 mm Hg on the arterial side to about 15 mm Hg at the venous end (Guyton, 1976).

As stated earlier, Rhinelander (1976) does find periosteal arterioles penetrating the cortex at fascial attachments; his perfusion studies reveal that in these select areas the periosteal circulation does supply the outer third of the cortex. Rhinelander, like Brookes, states that the periosteal vessels can also supply the outer cortex if the medullary supply is obliterated or pathologically insufficient. Brookes feels that this is due to decreased intraosseous pressure, while Rhinelander states that it is due to the ingrowth of new arterial vessels (as occurs in the repair of fractures). Thus, in the view of Rhinelander, the periosteal vessels supply the flow to the outer cortex in certain areas normally, or to the whole cortical thickness in pathological situations; otherwise, blood from the medulla supplies the whole thickness of the cortex.

The cortex is not the only region of bone where there is controversy regarding the source of nutrition. Disagreement also exists over the

major blood supply to the metaphysis, the articular cartilage and the growth plate. The metaphyseal blood supply changes with development. In early fetal life, the metaphysis receives blood only from the nutrient artery. In later fetal life metaphyseal arteries derived from the periosteum begin to take over the supply of the peripheral metaphysis (Root, 1963). By adulthood, the metaphysis of the proximal femur is totally supplied by the metaphyseal arteries. Yet, studies of other adult metaphyses show that most of the flow stems from the nutrient artery. Brookes (1972) resolves the controversy stating that in the growing ends of adult bone, the nutrient artery supplies the central three-fifths of the metaphysis and the metaphyseal arteries supply the peripheral zone. The metaphyses at the non-growing ends receive all of their blood from the metaphyseal arteries.

In early fetal life the epiphyseal cartilage is not vascularized. The area of the growth plate can be nourished by diffusion from the vessels of the perichondrium and the metaphysis (Brookes, 1972). Later cartilage canals develop and send branches to the resting cells of the future growth plate as well as transphyseal vessels, which extend across into the metaphysis. No experiments have yet documented the relative contribution to physeal nutrition by the various vessels at this early age. It is likely that the cartilage surrounding the transphyseal vessels is nourished by them, wherever and whenever these vessels exist.

The mature growth plate is adjacent to and could be nourished by three vascular systems: (1) the perichondral vessels of the zone of Ranvier, and, (2) epiphyseal side (E-side), and, (3) metaphyseal side (M-side) vascular loops. It is generally agreed that the periphery of the physis receives diffused nutrients from the perichondral circulation. Hence, if the epiphyseal and metaphyseal circulations are disrupted, the

central growth plate dies while the periphery continues to survive, supported by the perichondral circulation (Trueta, 1968). Conversely, disruption of the periosteal circulation results in peripheral ischemia and eccentric growth (Ogden, 1978). It is also generally agreed that the vessels on the E-side of the growth plate maintain the zone of resting cells and the zone of proliferation. This is demonstrated by studies on slipped epiphyses, in which the line of fracture is usually through the growth plate's zone of hypertrophy. If the epiphyseal arteries and veins remain intact, the germinal and proliferative zones of cartilage continue to grow and thrive (Dale and Harris, 1958). In intact bones the rate of chondrocyte proliferation varies directly with the amount of E-side vascularity.

It is not known whether the E-side vascular loops supply the whole thickness of the growth plate or whether the mature chondrocytes are maintained by substances which diffuse from the M-side loops. Ham (1974) denies that the M-side could supply nutrition, since the calcified intracellular matrix is essentially impermeable. While the calcified zone may be thick, it is not continuous, and M-side vessels do abut on uncalcified cartilage. Radioactive phosphate and adenine have been found to cross the growth plate from the metaphysis to the epiphysis (Prives et al, 1959; Stockwell, 1979). Ham's argument is thus invalid. In 1960, Trueta and Amato blocked off E-side vessels by hollowing out a narrow space with a spatula immediately adjacent to the growth plate and filling the space with polythene. As a result, the central physis died and was subsequently invaded by M-side vessels and bony trabeculae. When the M-side vessels were obliterated in the same fashion, the growth cartilage did not die, but continued to thicken. The cells were normal in that they underwent hypertrophy, accumulated glycogen and became vacuolized. The cartilage was abnormal in that that the

matrix neither contained alkaline phosphatase nor calcified, and the cells did not die. The absence of alkaline phosphatase suggests that the M-side blood flow may be needed to maintain normal metabolism in the lower zones of the growth plate as well as providing the calcium and phosphate necessary for cartilage mineralization. A minority of investigators suggest that the M-side vasculature may even supply the upper zones of the physis. Holdsworth (1966) destroyed the epiphyseal arteries extravascularily, yet the growth plate did not die. Brookes notes the greater rate of the flow in the metaphysis compared to the epiphysis, and proposes that therefore it is likely that the M-side vessels would contribute a greater amount of nutrition to the physis. This is not necessarily so. Brookes refers to the flows of the entire metaphysis and epiphysis rather than the more relevant areas immediately adjacent to the growth plate; the flows to these particular regions previously have never been measured. Moreover, the high metaphyseal flow may be secondary to the high metabolic demands of the osteoid secreting osteoblasts, and have little to do with the cartilage of the growth plate. In summary, past experiments seem to reveal that the growth cartilage can survive with only the E-side or only the M-side vessels alone, but in intact bone both are probably needed to maintain a normal growth plate.

The nutritional needs of the articular cartilage are few, as it has a slow anaerobic metabolism (Ham, 1974). Prior to epiphyseal ossification, the articular cartilage receives nutrition from the synovial fluid, the perichondral vessels, and the epiphyseal cartilage canals when present. Eventually the epiphyseal cartilage is replaced by vascularized cancellous bone, and the remaining canals in the articular cartilage gradually disappear. The role played by the epiphyseal subchondral blood vessels in the nutrition of the articular cartilage is disputed. The old, established

view is that everything diffuses from the synovial fluid, which is essentially a dialysate of plasma from the synovial blood vessels. This view is supported by clinical evidence. A loose body of detached articular cartilage in a joint may live and grow with only synovial fluid for nourishment. In osteochondritis dissecans, a large piece of spongiosa and attached articular cartilage may dehiss from the epiphysis to survive and sometimes grow while suspended in the synovial fluid. There is also clinical evidence supporting the nutritive role of subchondral circulation. In avascular necrosis, the articular cartilage survives in general, but the deeper layers adjacent to the subchondral bone degenerate (Stockwell, 1969). Various experiments show that substances injected into a previously intact epiphyseal spongiosa will diffuse out into the articular cartilage and, with exercise, into the joint space (Trueta, 1968). These substances include silver nitrate, large starch particles of 1μm diameter, and radioactive phosphate and gold chloride. Although these substances diffuse across the joint cartilage in both directions, the rate of passage from the epiphysis is greater than from the synovial cavity. The rate of passage into the knee joint is greater from the distal femur than the proximal tibia (Brookes, 1972). One might want to attribute this to the higher flow rate of the distal femur delivering the solute to the articular cartilage more quickly, but there have been no previous studies comparing the flow rates of the epiphysis on opposite sides of the knee joint. In conclusion, it seems not only possible, but likely, that the articular cartilage is nourished by the subchondral vessels beneath it as well as by the synovial fluid above.

D. Quantitative Measurement of Bone Blood Flow

Investigators have attempted to quantitatively measure osseous flow for nearly sixty years. The widely differing results tabulated in Table 1 point to the difficulty of measuring blood flow through this organ. The complex vascular organization of bone frustrates many experimental designs.

The direct measurement of flow involves monitoring arterial inflow or venous outflow. Traditionally, this has been accomplished through the use of flow meters or by collecting the outflow from a vein. However, the mean phasic flow meters or electromagnetic flow meters are usually used on single, large arteries, while the arteries of bone are multiple and small; even the largest nutrient artery is too small for the application of flow meters (Brookes, 1974). Moreover, "the uncertainty as to which part is supplied by which artery as well as the probability that the part supplied may vary from time to time does not even permit one to estimate the perfusion of a particular region. A further complication arises from the possibility that the surgical manipulation required to isolate the arteries or veins of the calcified tissue has in itself a profound influence on the magnitude of flow" (Kane, 1968). The only direct measurements that have been made are those of venous outflow. Drinker et al, pioneered the field in 1922, by perfusing the nutrient artery of an isolated tibia and collecting all the effluent blood in a beaker. The rest of the arterial input was ignored, and the results were highly variable, 3.5 - 41 ml/100 grams/min. In 1962 Cumming ligated every branch of the femoral artery and vein except the nutrient ar-

KEY FOR TABLE 1

Animals

rbt = rabbit
GP = Guinea Pig

Age

I = Immature
M = Mature
A = Aged
V = Various ages
W = Week
m = month

Bone

F = Femur
T = Tibia
R = Radius
H = Humerus
Tf = Tibio-fibula
S = Entire Skeleton
V = Various bones

Bone Region

mc = medial condyle
lc = lateral condyle
d = distal (with respect to trunk)
p = proximal (with respect to trunk)
M = Metaphysis
E = Epiphysis
D = Diaphysis
Fh = Femoral head
Fn = Femoral neck

1 = not corrected for extraction ratio
* = animal awake (otherwise anesthetized)
2 = corrected from ml/min/100ml tissue to cc/min/100g tissue (assume densities of cortex= 1.94, bone = 1.7)
*3 = awake & anesthetized
ER = Extraction Ratio

TABLE 1

OSSEOUS BLOOD FLOW: SUMMARY OF THE LITERATURE

YEAR	AUTHOR(S)	METHOD	ANIMAL	AGE	BONE	BONE REGION	BONE TISSUE FLOW cc/min/100g CORTEX	MARROW	SPONGIOSA	MIXED	% CARDIAC OUTPUT TO SKELETON
1922	Drinker et al	isolated bone perfusion	dog	I	T						
1945	Edholm et al	plesmography	man	M							
1955	Fredrickson et al	$^{45}Ca^{1}$	rat							10-30	
1957	Copp	$^{45}Ca^{1}$	dog								
1959	Branemark	observation of RBC velocity (Brookes volumetric data)	rbt		F		2.6	13			
1960	Copp et al	$^{45}Ca^{1}$	dog							4.9	3.5-9
1961	Barnes et al	^{85}Sr	man	M						1.25	
1961	Hollings et al	plesmography[2]	man	M						.5	
		plesmography[2]	dog	M						3.3	
		plesmography[2]	dog	I						4.5	
1962	Cumming	venous collection	rbt	V	F			51			7.6
1963	Shim	$^{85}Sr^{1}$	rbt		HTF					16.4	
1963	Weinman et al	$^{45}Ca^{1}$	dog	M						5.6	5-7
		$^{85}Sr^{1}$	dog	I						7.7	8-10
1964	Ray	$^{45}Ca^{1}$	dog	M						4.9	
		$^{45}Ca^{1}$	dog	I						6.5	
1964	Copp & Shim	$^{85}Sr^{1}$	dog							9-12	
1964	Kane & Grim	^{42}K,^{86}Rb,^{46}Na-mics	dog	M						12	

TABLE 1

OSSEOUS BLOOD FLOW: SUMMARY OF THE LITERATURE

YEAR	AUTHOR(S)	METHOD	ANIMAL	AGE	BONE	BONE REGION	BONE TISSUE FLOW cc/min/100g CORTEX	MARROW	SPONGIOSA	MIXED	% CARDIAC OUTPUT TO SKELETON
1965	Osmond	^{59}Fe-RBC wash-out	GP		F			1.6			
1965	Copp & Shim	^{85}Sr[1]	dog				10				12.5
1965	Van Dyke et al	^{18}F[1]	rat							8.5	4.3
1966	Pasternak et al	^{85}Sr[1]	dog	M	T					3.25	
		^{85}Sr[1]	dog	I	T					9.34	
		^{85}Sr	dog	M	T					12	
		^{85}Sr	dog	I	T					21	
1966	Semb	^{85}Sr[1]	dog		R	M			5-14		
		^{85}Sr	dog		R	M			25-30		
1966	Stein & White	^{51}Cr-RBC wash-out	rbt	M	T					16	
1967	Shim et al	^{45}Ca[1]	dog	M	F					9.3	
		^{45}Ca[1]	dog	M	T					10.5	
		^{45}Ca (ER=75%)	dog	M	F					12.4	
		^{45}Ca (ER=75%)	dog	M	T					14	
		^{45}Ca (ER=75%)	rbt	M	T					10.3	
		^{45}Ca[1]	rbt	M	T					13	7.1
		^{45}Ca[1]	rbt	M	F		7.5			9.7	
		^{45}Ca[1]	rbt	M	F	FH			18.7		
		^{45}Ca[1]	rbt	M	F	Gt			10.4		

TABLE 1

OSSEOUS BLOOD FLOW: SUMMARY OF THE LITERATURE

YEAR	AUTHOR(S)	METHOD	ANIMAL	AGE	BONE	BONE REGION	BONE TISSUE FLOW cc/min/100g				% CARDIAC OUTPUT TO SKELETON
							CORTEX	MARROW	SPONGIOSA	MIXED	
		$^{45}Ca^{1}$	rbt	M	F	dE			12.		
1967	Ray et al	$^{45}Ca^{1}$, ^{85}Sr	dog	M	F					8.2	5.5
1967	Brookes	^{51}Cr-RBC wash-out (if hct = 43%)	rat	I	F		17	29			
		^{51}Cr-RBC wash-out (if hct = 43%)	rat	I	F	pM			22		
		^{51}Cr-RBC wash-out (if hct = 43%)	rat	I	F	dM			30		
		^{51}Cr-RBC wash-out (if hct = 43%)	rat	I	F	dE			21		
1968	Brookes	^{51}Cr-RBC wash-out (if hct = 43%)					14	25			
1968	Shim et al	$^{85}Sr^{1}$	rbt	M	TF		8.5			9.6	
		$^{85}Sr^{1}$	rbt	M	TF	E&M			10.8		
1968	Kane	^{86}Rb	dog							12	
1968	Kane	^{42}K	man	M	T		1				
1969	Hruza & Wachtlova	$^{45}Ca^{1}$	rat	2m	T					19.5	
		$^{45}Ca^{1}$	rat	4m	T					6.9	

TABLE 1

OSSEOUS BLOOD FLOW: SUMMARY OF THE LITERATURE

YEAR	AUTHOR(S)	METHOD	ANIMAL	AGE	BONE	BONE REGION	BONE TISSUE FLOW cc/min/100g				% CARDIAC OUTPUT TO SKELETON
							CORTEX	MARROW	SPONGIOSA	MIXED	
		^{45}Ca[1]	rat	11m	T					2	
1969	Kane & Grim	^{42}K, Na mics*[3]	dog	I	T					18.5	
		^{42}K, Na mics*[3]	dog	I	F		12.3	17.7	19.7 (E)	17.7	
1969	Mizuno & Matumoto	phlebography	man	M	F	Fh			1.8-8.8		3-12
		phlebography		I	F	Fh			1.2-11.8		3-16
1970	Brookes	^{59}Fe-resin mics (30-70μ)	rat	I	S					19	27
1970	Shim & Kelly	^{85}Sr[1]	man	M	T					3.8	
1970	Lunde & Michelson	mics (15μ)	rbt	M	F		1	25			
1970	Shim et al	^{85}Sr[1]	man	M	T					2.5	4.7
1970	Kato et al	Pressure flow curve of nutrient artery	dog	M	T					4-6	
1970	Cofield	^{85}Sr	dog	M	T					6.9	
1970	McElfresh et al	^{125}I-AP washout[2]	dog	M	T		.9				
1971	Kelly et al	^{125}I-AP washout[2]	dog	M	T		.75				
		^{85}Sr[1]	dog	M	T					3.83	
1971	Van Dyke et al	^{18}F partition[1] bone:kidney	man	M	S						3.3

TABLE 1

OSSEOUS BLOOD FLOW: SUMMARY OF THE LITERATURE

YEAR	AUTHOR(S)	METHOD	ANIMAL	AGE	BONE	BONE REGION	BONE TISSUE FLOW cc/min/100g CORTEX	MARROW	SPONGIOSA	MIXED	% CARDIAC OUTPUT TO SKELETON
1972	Brookes	^{51}Cr-RBC wash-out (hct not constant)	rat	I	F	D	18	21			28
		^{51}Cr-RBC wash-out (hct not constant)	rat	I	F	pM			26		
		^{51}Cr-RBC wash-out (hct not constant)	rat	I	F	dM			30		
		^{51}Cr-RBC wash-out (hct not constant)	rat	I	F	dE			29		
1972	Ray	^{125}I-AP washout[2]	dog	M	T		1.5				
1974	McElfresh & Kelly	^{125}I-AP washout[2]	dog	M	T		.8				
1974	Veal	^{18}F partition[1] bone:kidney	man	M	S					7	11
1975	Tothill & McCormick	^{59}Fe resin mics, (35-75μ)	rat								3
		^{99}Tc-albumin mics	rat								3
1976	Wooton et al	^{18}F partition	man	M	S					4.1	
1977	McPherson & Tothill	mics (15μ)	rat	10W	Tf					14.7	
		mics (15μ)	rat	11m	Tf					8.1	
		mics (15μ)	rat	A	Tf					4.8	
		mics (15μ)	rat	V	S					14	3

TABLE 1

OSSEOUS BLOOD FLOW: SUMMARY OF THE LITERATURE

YEAR	AUTHOR(S)	METHOD	ANIMAL	AGE	BONE	BONE REGION	BONE TISSUE FLOW cc/min/100g				% CARDIAC OUTPUT TO SKELETON
							CORTEX	MARROW	SPONGIOSA	MIXED	
1977a	Whiteside et al	H_2 washout[2]	rbt	V	V	D	3.6				
		H_2 washout[2]	rbt	V	V	M			10.0		
		H_2 washout[2]	rbt	V	V	E			7.6		
1977b	Whiteside et al	H_2 washout[2]	rbt	M	T	D	2				
		H_2 washout[2]	rbt	M	T	M			6		
		H_2 washout[2]	rbt	M	T	E			6		
		H_2 washout[2]	rbt	I	T	D	4				
		H_2 washout[2]	rbt	I	T	M			8		
		H_2 washout[2]	rbt	I	T	E			10		
		H_2 washout[2]	dog	M	T		3.3				
1979	Schoutens et al	mics (low #s)	rat	4m	F					9.6	
		mics (low #s)	rat	4m	T				12(E)	8	
		^{45}Ca[1]	rat	4m	F					4.5	
		^{45}Ca[1]	rat	4m	T				6(E)	4.3	
1979	Morris & Kelly	mics (15μ)*	dog	M	T		3	3.3		6.6	12
		mics (15μ)*	dog	I	T		7	2.3			
1979	Niv & Hungerford	mics (9μ)*	dog	M	F	D	2.2				
		mics (9μ)*	dog	M	F	Fh			13		
		mics (9μ)*	dog	M	F	Fn			16		
		mics (9μ)*	dog	M	F	Gt			9		
		mics (9μ)*	dog	M	F	pM			14		
		mics (9μ)*	dog	M	F	mc			3.8		
		mics (9μ)*	dog	M	F	lc			2.5		
1980	Niv et al	H_2 washout[2]	dog	M	F	Fh			13		

tery and vena comitans so that all of the limb flow was channeled through the femur. By collecting the blood from the femoral vein he presumed he was measuring blood flow through the marrow. His results of 51 ml/mm/100g is higher than that obtained by any other investigators. Bränemark (1959) attempted to quantitate flow by directly observing red blood cell velocities during vital microscopy of the rabbit diaphysis. In the marrow he observed velocities of 1.5 mm/second in the arteries, .5 mm/second in the capillaries, .2 mm/second in the sinusoids and .1-.3 mm/second in the venules, giving an arteriolar-sinusoidal velocity ratio of 10:1. Velocities were higher in the cortical vessels ranging from .2 to .8 mm/second. Brookes extrapolated volume flow from rates from these velocities and his own volumetric data to obtain values of 13 and 2.6 ml/min/100g in the marrow and cortex, respectively.

In the 1950's and early 1960's, for the most part, a number of investigators attempted to correlate flow with the measurements of 1) intraosseous pressure (Kane, 1970), 2) the partial pressure of oxygen in bone blood, and 3) intraosseous temperature (Brookes, 1972). The first method erroneously assumes that flow is directly proportional to intraosseous pressure (Kane, 1968). Intramedullary manometry yields highly variable recordings which vary independently of flow, as discussed in Section E. The second method assumes that changes in the partial pressure of oxygen reflect changes in bone flow, thus incorrectly assuming that oxygen utilization remains constant. The third method assumes that clearance of heat or cold is proportional to flow and is uninfluenced by metabolism. Although this method might be applicable in some organs, such as bone, there is no suitable probe for bone. The commonly used probes are rapidly poisoned and lie in a

pool of extravasated blood (Brookes, 1972). These three methods all involve invasive manipulation which injures the tissue and disrupts normal flow patterns in the immediate area (Michelson, 1967).

Attempts have been made to measure human bone flow via plasmography and venography but these methods are qualitative at best. In 1945 Edholm et al designed a plesmograph which recorded a humeral nutrient artery flow of 1 cc. blood/100 ml. bone/minute or about .5 ml/min/100g. All other arterial flow to the distal limb was occluded by the application of a tourniquet just distal to the nutrient canal. The venous drainage accumulated in the arms by means of cuff at diastolic pressure placed just proximal to the nutrient foramen. Inaccuracies resulted because venous blood may have pooled in the potential spaces of the marrow sinusoids or preferentially escaped through the proximal bone, and because 30-50% of inflow that normally would have come from the non-principle nutrient arteries was occluded. Plesmographic studies have shown massive qualitative increases in flow through bone affected by Paget's disease (Edholm et al, 1945) and pulmonary hypertrophic osteoarthropathy (Holling et al, 1961).

In 1966, Matumoto and Mizuno introduced phlebography to evaluate flow through the femoral head. The technique involves injecting contrast directly into the cancellous bone, followed by densiometric analysis of the radiographs using a nomogram to calculate flow. The authors admit that phlebography "is not a direct measure and there are many inherent potential errors that may lead to misinterpretation" (Mizuno and Matumoto, 1969). A similar procedure had been employed by Laing and Ferguson (1959) who injected I^{131}-labelled albumin directly into the femoral head and monitored clearance of the isotope by surface counting. Not only was this a poor way to measure

flow, but every one of the patients available for follow-up developed avascular necrosis (Ray, 1972).

Attempts also have been made to correlate human bone flow with the rate of osseous uptake of radioactive isotopes from the systemic circulation, namely ^{32}phosphate, ^{18}fluorine, ^{85}strontium, and ^{42}postassium, the latter two used to determine flow just before amputation (Kane, 1968; Shim et al, 1970). Tucker (1950) used radioactive phosphorus to estimate viability of the femoral head after fracture. Other authors propose that there is increased flow through human bones affected with osteogenic sarcoma, Paget's disease, fracture, myelofibrosis and anemia (Shim et al, 1970; Van Dyke et al, 1971; Van Dyke, 1968; Wooten et al, 1976). However, the uptake of these isotopes is not only determined by flow as is discussed below.

The majority of experiments designed to determine osseous flow in laboratory animals have employed the Fick principle in which the rate of uptake of a radioactive isotope by bone divided by the arteriovenous isotope concentration difference is equal to flow through bone:

$$Q = \frac{\text{Bone}}{\int_0^t A\,dt - \int_0^t V\,dt}$$

Since all arterial blood would have the same concentration, it can be sampled from any artery. It is impossible to get an accurate assessment of concentration of radioactivity in venous blood as it would be impossible to cannulate all of the veins of a bone. Most workers have assumed that the venous concentration is zero and that 100% of isotope is extracted or cleared from the blood in one circulatory transit. Thus, bone flow equals the amount of isotope in the bone per area under the arterial dilution curve. This would artificially lower the calculated flow values.

In some cases the extraction ratio, the arteriovenous concentration difference divided by the arterial concentration of the isotope ($\frac{A-V}{A}$), has been determined by assuming that blood obtained from a hole drilled in the marrow is equivalent to venous blood (Semb, 1966). This assumption is most probably erroneous due to resistance discrepancies. In addition, this invasive procedure upsets the normal physiologic conditions. Others have obtained venous samples from the femoral vein; however, this is a mixture of blood from the soft tissues as well as from bone.

It has not been sufficiently substantiated that the exchange of the tracer ions occurs solely in bone (Brookes, 1972). Moreover, the extraction ratio changes with time, being different at one minute, five minutes, and ten minutes after injection (Schoutens et al, 1979). Extraction ratios also vary with the age of the animals, within different regions of a bone, and in different species (Kelly, 1968; Van Dyke, 1965). By measuring flow with microspheres, Schoutens et al (1979) showed that the extraction ratios of ^{45}calcium and ^{99m}technetium diphosphate decrease markedly as flow increases; the extration ratio of 60-70% at flows under 6 ml/mm/100g was reduced to 20-25% at flows above 12 ml/min/100g.

Incorrect or undetermined extraction ratios are not the only problem with using the Fick principle to measure bone flow. The final figures are given for the net weight of the bone; this includes the vessels of the marrow, which add further inaccuracy. Ray (1972) points out that radioactive blood may pool in the "dead space" of the marrow sinusoids, thus increasing the calculated total bone flow. Brookes (1974) states that the marrow vessels clear little, if any, tracer into bone, thus causing the perfusion rate to be underestimated.

The isotopes that have been used can be grouped as bone-seeking or nonbone-seeking radioisotopes. The bone-seeking isotopes include ^{45}calcium, ^{85}strontium, ^{32}phosphate, ^{18}florine and the various ^{99}technetium tagged phosphate compounds. In addition to the problems listed in the previous paragraph, the uptake of these isotopes by bone is not flow limited. Uptake also depends on the amount of isotope in the blood, the rate of diffusion through the interstitial fluid to the bone, the rate of exchange with bone mineral, and the rate of incorporation into bone crystals by bone metabolism (Kane, 1968; Brookes, 1972). Despite all the inaccuracies, measurement of clearance of bone-seeking isotopes probably yields more accurate results than the methods previously described, especially if corrected for the extraction ratio. But as one can see in Table 2, the majority of the results in the literature assume 100% extraction. This was true for all the early studies using ^{45}Ca and ^{85}Sr uptake. Later, in 1966, results were corrected for extraction. Nevertheless, subsequent work from these same authors and others reverted to calculating clearance without correcting for the incomplete extraction, possibly because of the near impossibility of getting an accurate extraction ratio.

Most of the studies that found fault with the bone-seeking isotope experiments dealt with calcium, strontium and phosphate. ^{18}Fluorine was introduced more recently and was proclaimed at the outset to have a 100% extraction ratio, as had been the case with other isotopes. Since then Wooten (1975) confirmed that the extraction of ^{18}F was complete by comparing it to ^{51}Cr labelled microparticles which are totally "extracted at the first capillary bed". On the other hand, Veal (1975) stated that there is no evidence that ^{18}F does not have significant reflux from bone to blood. Stadal-

TABLE 2

SUMMARY OF AVERAGE VALUES FOR TOTAL BONE FLOW (ML/MIN/100G)

	SPECIES					
	DOG			RAT		
METHOD	MATURE	IMMATURE	RABBIT	MATURE	IMMATURE	MAN
perfusion	3-40					
pressure	5					
plesmography	3.3	4.5				2
venography						2-12
^{45}Ca assume 100%	5	7	10	3	19	
^{85}Sr extration	4	9	16			2
^{45}Ca	8		14		20	
^{85}Sr corrected for extration	10	21	11			
^{18}F				8		
^{42}K, ^{86}Rb	12	19				
Cr-red cells			16			
arteriolar blockade	10	15	14	5		

nik et al (1975) found the ^{18}F "flow" is proportional to the rate bone deposition measured with tetracycline. Because of the two hour half-life of ^{18}F, it has been used to measure flow in human bone. Gross qualitative differences can be appreciated with a positron camera. Quantitative determinations involve the injection of a known amount of another isotope, ^{81}Cr-EDTA, which distributes in the extracellular fluid space in a manner similar to that of ^{18}F, thus allowing the amount of ^{18}F in the bone to be calculated.

The nonbone-seeking isotopes accumulate in bone and in other tissues of the body. Most were first used to measure flow through non-skeletal organs. Isotopes used in bone include ^{42}potassium (^{42}K), ^{86}rubidium (^{86}Rb), and ^{125}iodoantipurine (^{125}I-AP). The studies utilizing ^{42}K and ^{86}Rb employ the concept of fractional distribution. If an intravenously injected isotope is 100% extracted from the blood by all tissues of the body, then the fraction of the total amount of injected isotope that is in any one organ equals the fracture of cardiac output perfusing that organ. Thus,

$$\frac{\text{organ blood flow}}{\text{cardiac output}} = \frac{\text{amount isotope in organ}}{\text{amount isotope injected}}$$

Cardiac output is determined on arterial dilution curve after injection of the isotope. In 1952, Walker and Wilde reported that 90% of the injected ^{42}K passes out of the circulation in one minute. Sapirstein (1958) found that the distribution of ^{86}Rb was much the same as ^{42}K and that their concentration in an organ barely changed during the first minute despite much recirculation of the isotopes in and out of cells. He therefore concluded that 100% extraction ratios could be assumed for ^{42}K and ^{86}Rb. Delaney

and Grim (1964) pointed out that since the extraction ratios differed in different regions of the body and all were less than 100%, the principle of fractional distribution was invalid for these isotopes. Nevertheless, Kane and Grim (1964, 1969) proposed that their results of 12 and 18 cc/min/100g for mature and immature canine bone (respectively) were validated by their finding that the distribution and venous outflow of ^{42}K and ^{86}Rb closely agreed with that of ^{24}Na-labelled glass microspheres of 16μ and 25μ diameter.

Flow has been determined by yet another technique using ^{125}I-AP washout, in which flow is said to be responsible for washing the isotope out of the bone (Kelly et al, 1971; Kelly, 1973; McElfresh and Kelly, 1974). The procedure entails advancing a cannula down the femoral artery until the tip is just opposite the opening of the tibial nutrient artery. ^{125}I-AP is perfused into the nutrient artery until a steady state concentration in the bone is reached. The amount of radioactivity in the bone is monitored in this experiment with an external scintillation detector placed over the bone. Once equilibrium between bone tissue and blood has been reached, ^{125}I-AP perfusion ceases and the rate of radioactive washout is recorded. Flow can be determined from the washout curve. The rate of washout is also affected by the rate of diffusion from the bone to the bloodstream and by the partition coefficient. The authors assume that diffusional resistances are negligable and that washout is purely flow limited. The partition coefficient, λ, equals the ratio of the solubility of the indicator in the tissue to that of the indicator in the blood. Similar to clearance studies using the extraction ratio, obtaining an accurate partition coefficient is "subject to many sources of error" (Whitesides et al, 1977a). The partition coefficient has an advantage over the extraction ratio in that solubility parameters are independent of hemodynamics. Thus, the partition coefficient

remains constant as flow rate changes. But, like the extraction ratio, it will vary in different species, bones, and bone regions.

The marrow region of the bone may present additional problems in the washout technique. If the larger sinusoid spaces can be regarded as "dead spaces" (Ray, 1972), washout from the marrow may be limited by diffusion rather than flow. A source of error inherent in the ^{125}I-AP experiments is the method of monitoring radioactivity. An external detector will receive emissions non-selectively from all adjacent tissues, skin, muscle, and bone. Furthermore, counts from different bone regions cannot be distinctly measured unless the bone is removed from the leg and cut so the regions that can be physically separated from one another. Intact, the cortex is inseparable from the marrow it encases. The epiphyseal counts will be contaminated by counts deflected from the metaphysis. Perfusing the bone via the nutrient artery may only establish equilibrium in the diaphyseal marrow and not in the epiphysis, for example. This would almost certainly be true in the immature animal. The total ^{125}I-AP washout procedure does have the advantage of being simple and relatively non-invasive.

Bone blood flow has also been measured by the washout of hydrogen gas, H_2 (Whitesides et al, 1977a, b). The principles and problems of the washout are the same as above; however, the experimental procedure is quite different. H_2 is administered nasally until equilibrium between the blood and organs is attained throughout the body. Radioactivity is monitored with an electrode inserted in the tissue, thus allowing discrete areas of flow to be measured. However, the lesion created by the probe locally alters the normal architecture of the tissue and creates a pool of blood which has its own diffusion characteristics possibly leading to the misrepresentation of

blood flows. This could happen in any tissue, but especially in bone where a hole must be drilled for insertion of the electrode. The normal flow through the cortex, described by Rhinelander (1974, 1976) as being a closed system, could be easily upset even by a much less invasive procedure. Multiple areas must be sampled and averaged to attain an accurate flow for a larger region of bone or the whole bone. Furthermore, it has been observed that the administration can lead to tachycardia and arhythmias in dogs, deranging flow patterns throughout the body (Schnitzer, 1979).

Several workers have determined bone blood flow by the rate of accretion of radiolabelled red blood cells tagged with ^{51}Chromium (White et al, 1964, 1966; Brookes, 1967, 1968, 1972) or ^{59}Iron (Osmond and Everett, 1965). After the labelled erthrocytes are injected into the circulation, flow to the bone is halted at approximately one second intervals in different animals. This is accomplished by either applying a tourniquet or chopping off the limb with a guillotine, then immediately freezing the leg at -50°C. The rate of change of bone radioactivity over time is proportional to red blood cell velocity. In order to calculate whole blood flow, the hematocrit must be determined and corrections must be made for red blood cell volume, determined in a separate set of experiments. Not surprisingly, Brookes claims that the hematocrit varies in different regions of a bone. He directly measured the hematocrit of the marrow using blood from the nutrient vein and calculates it for other regions of the bone. In these calculations he makes multiple assumptions and has a deficiency of data for his "known" variables so that at best his results are a first order approximation. Nevertheless, the results for the rabbit femur may be verified in the future and are as follows:

bone area:	arterial blood	Diaphysis		Metaphysis		distal epiphysis
		marrow	cortex	proximal	distal	
hematocrit:	33	60	42	39	50	31

The greatest deficiency of this technique of determining osseous flow lies in the assumption that circulation is instantaneously halted at the various intervals. It is also a laborious procedure requiring the sacrifice of many animals in order for the results to be statistically significant. A different set of animals must be used for each time interval and yet another set to determine red blood cell volume. However, calculation of flow using radiolabelled red blood cells may well be more precise than some of the other methods which are hampered by the errors inherent in extraction ratios, partition coefficients, or invasive procedures.

The final major method used to measure blood flow in bones is that of arteriolar blockade by radionuclide labelled particles. This technique has been widely used to measure flow in other organs, especially the heart. The microspheres are injected into the arterial circulation, usually the left atrium, and travel to the small peripheral arterioles or capillaries where they are trapped and embolized. The fraction of total injected microspheres and thus the fraction of radioactivity in an organ is equal to the fraction of total flow or cardiac output. This is the principle of fractional distribution described earlier. It holds true for all organs so that

$$\frac{\text{cardiac out put}}{\text{total microsphere injected}} = \frac{\text{flow to organ A}}{\text{\# microspheres in A}} = \frac{\text{flow to organ B}}{\text{\# microspheres in B}}$$

The most commonly used method of quantitation flow in any unknown organ A is the reference sample technique in which organ B is a surrogate organ with

a known flow. The surrogate organ is usually a syringe connected by a catheter to any systemic artery and placed in a Harvard withdrawal pump which can be set at a constant withdrawal rate, or "known flow", during the injection of the microspheres. Withdrawal is continued long enough for extraction or entrapment of all of the microspheres, about two minutes. After this, the organ A being measured is removed and its radioactivity measured, as is the radioactivity of the blood collected in the syringe, organ B. With this data, the flow to organ A is calculated. Microspheres are thus one of, if not the most, simple and potentially most accurate ways to measure flow. They give results that vary only 6% and 3% from those obtained with electromagnetic flow meters or venous effluent collection, respectively, in organs in which these two techniques are applicable (Heymann et al, 1977).

However, many errors can result if the basic principles of microspheres use are not understood, or one does not adhere to the proper technique. Mistakes may result from vascular skimming and streamlining secondary to poor mixing, and from insufficient numbers or improperly chosen size of microspheres. The microspheres must be well mixed and evenly distributed in the blood so that streamlining does not occur and the concentrations reaching all arterial branching sites are solely flow dependent. The best mixing occurs if the injection site is the left atrium, but injections in the left ventricle also get good measurements. Buckberg et al (1971) found a 20% difference between the concentrations of microspheres in the carotid and femoral arteries after injection into the left ventricle in dogs, versus no difference after left atrial injection. In sheep there was no difference for either injection site. Occasionally, if samples are being taken distal

to the kidneys, injection into the root of the aorta (preferably an upstream injection) may suffice. The evenness of mixing can be checked by comparing the radioactivity of the left to the right kidney, or by making a second injection of microspheres using a different radionuclide label. Accuracy depends on a sufficient number of microspheres in the organ and the reference sample. As the number of microspheres increases, so does the accuracy. If there are 385 in a given sample, the results are distributed within 10% of the mean at a 95% confidence level. 1538 microspheres per sample have a 95% probability of being within 5% of the mean. With only 100 microspheres, this error is 40% (Buckberg et al, 1971). On the other hand, there is a possibility of injecting too many microspheres and blocking enough capillaries in a short time span to cause cardiac ischemia and altered cardiac function. In the dog, up to 21.6 x 10^6 microspheres can be injected without apparent adverse affects (Heyman et al, 1977).

It is important that microspheres of the proper size are chosen. They must be large enough so that all are trapped in the first circulation, but small enough to be indicative of capillary flow (microcirculation), not large arteriole flow. The optimal microspheres are the smaller ones that approximate red blood cells in size ($\simeq 8\mu m$) and distribution. Microspheres are currently manufactured as insoluable, inert plastic spheres, available in a variety of specified sizes with a specific gravity close to that of whole blood. Since the 8μ-10μ microspheres fail to be trapped in many organs, the next size of 15μm is often the best size. These will pass through most arteriovenous anastamoses, most of which are larger than 25μm in diameter, with the result that 5-10% of the 15μ microspheres injected into a dog's systemic arterial circulation will be trapped in the lungs (Heymann et al, 1977). Significant numbers of normally closed arteriovenous

connections may be open by certain experimental conditions such as increased environmental temperature and anesthetic agents (Heymann et al, 1977; Sasaki and Wagner, 1971).

The proper microsphere size cannot be chosen without prior knowledge of the vasculature of the organ whose flow is being measured. If there are many arteriovenous anastamoses, microspheres are not a good method by which to study flow in that organ. Obviously, microspheres cannot be used to measure flow for the second of two capillary networks in series, as, for example, in the portal system. Fifteen μm microspheres are totally entrapped in bone with minimal shunting in the rat, dog, and man (Morris and Kelly, 1979; MacPherson and Tothill, 1977; Rhodes et al, 1972). MacPherson and Tothill (1972) also found no change in flow in the anesthetized rat, leading to the conclusion that ether anesthesia does not open up any shunts in bone.

It appears that 15μm microspheres are the ideal size for a bone, for 50% of the microspheres of 9μm diameter escape entrapment in unanesthetized dogs, resulting in flows half as high as those obtained with 15μm spheres (Niv and Hungerford, 1979). Furthermore, larger microspheres tend to over or underestimate flow depending on the anatomical circulatory pathways (Heymann et al, 1977).

Niv and Hungerford unfortunately did not study the cortex separately from the marrow. The bone cortex may contain a portal system of capillaries that is not accessible to microspheres. Many investigators believe that part of the flow to the diaphyseal cortex occurs through the majority of cortical capillaries which are in a series with another set of capillaries, either in the marrow or the osteogenic periosteum. According to past histo-

TABLE 3

REPORTS OF VESSEL DIAMETER

SOURCES	SPECIES	VESSEL	DIAMETER (μM)
Weiss & Greep, 1977	man	non-bone terminal arterioles	100 → 10
Weiss & Greep, 1977	man	non-bone precapillary sphincters	may decrease to 5μ
Bloom & Fawcett, 1975	man	non-bone capillary	8
Bloom & Fawcett, 1975	man	non-bone small venule	15-20
Brooks, 1972	rabbit	bone marrow arterioles	smallest may reach 5μ
Trueta, 1968	?	bone marrow sinusoids	15-50
Bloom & Fawcett, 1975	man	Haversian canals	22-100, average 50
Trueta, 1968	man	bone cortex capillaries	(hyperperfused) nearly fill canals
Brooks, 1972	rabbit	bone cortex capillaries	15-30 (wider near endosteum)
Branemark, 1959	rabbit	bone cortex capillaries	$\leq$ 15

logical studies (Table 3), it appears that 15 μm spheres would be entrapped in the marrow arterioles which precede the marrow sinusoids, or in the extraosseous arterioles of the fibrous periosteum. However, there are arterioles which go directly to the cortex. Most of these stem from marrow arteries and a few are the periosteal arterioles which enter at fascial attachments. Microspheres could be entrapped in these arterioles either before or after they penetrate the cortex, respectively underestimating arteriolar flow to the cortex. The reliability of using microspheres should be tested by comparing the cortical flows attained by microspheres, and another method, perhaps radiolabelled red blood cells dilution, in the same animal model under the same experimental conditions. This was done in a crude experiment with questionable statistical significance by Lavender et al (1979) who compared the gamma counter profiles of bones injected with 15μm microspheres and Krypton^{81m}, a short-lived gas with flow dependent distribution. Since the profiles of the two tracers were nearly identical, the authors concluded that bone does not have a portal type of circulation and that microspheres are a valid method of assessing flow in bone.

There are a few past microsphere experiments in which flow to the diaphyseal cortex is measured separately from the marrow flow. The results of all are questionable and conflicting. Lunde and Michelson (1970) used 15μm microspheres in anesthetized adult rabbits and obtained cortical flow of about 1 ml/min/100g versus marrow flows averaging 25 ml/min/100g. This is the lowest cortical flow recorded by any method in the rabbit (Table 1). Conversely, in conscious dogs, Morris and Kelly (1979) obtained a cortex: marrow flow of 2.9:3.3 in adults and 7.0:2.4 ml/min/100g in immature animals.

This is the only recorded case where cortical flow exceeds marrow flows, but both are low with respect to most of the literature. One might postulate that the vessels of the vasculature supplying the cortex of the smaller mammel, the rabbit, are too small to permit entry of any microspheres, while entry is attained in the larger dog. But the rat is smaller than the rabbit and Schoutens (1979) still found a significant percentage of total bone microspheres in the rat cortex, fifteen to twenty percent as opposed to ten percent in the marrow. Tissue weights were not given. Schoutens' results are extremely unreliable as there were only 150 microspheres in a whole bone. The technique of Lunde and Michelson is also unreliable. Mixing most probably was poor since the injection was made just above the aorta's iliac bifurcation. The numbers of microspheres per sample were probably quite low as the results have standard deviations of 50-70% of the means. The technique of Morris and Kelly is omitted in their abstract. But, their results of 6.6 and 6.9 ml/min/100g for total bone flow in mature and immature dogs are quite low as compared to these measured by the better techniques listed in the lower half of Table 2. They are also lower than the results of Kane (1968) and Kane and Grim (1969) who, using 16-25μ glass microspheres in dogs, got flows of 12 and 18 ml/min/100g. The small amount of microsphere perfusion may well be due to technical error. In sum, other than the data of Lavender et al (1979), it appears that past experiments reveal little concerning the validity of using microspheres to measure cortical flow except that microspheres are entrapped in the cortical circulation of dogs and rats. Any quantitative blood flow value of these experiments has little statistical relevancy so that regional and even developmental circulatory differentiation cannot be accurately surmised.

It has been recognized that microsphere use is probably the most accurate means of quantifying overall osseous flow and can be used to evaluate other methods. In fact, Brookes (1974) states that arteriolar blockade may provide a means of establishing the extraction ratio of isotopes. In 1969, Kane and Grim used glass microspheres containing ^{24}sodium to show that the extraction ratios of ^{42}K and ^{86}Rb were nearly 100%. Tothill and McCormick also used microspheres in the rat, and thereby determined that the ten minute extraction ratios of ^{18}F, ^{85}Sr, and ^{99}Tc-labelled diphosphate were respectively 100%, 60%, and 35%. They used ^{99}Tc-labelled albumin microspheres and ^{59}Fe-labelled resin particles of highly variable size, 20-100μm, and injected them into the aorta. These results are somewhat inaccurate since the microspheres were larger than the ideal size of 15μm. Using a better experimental protocol involving left ventricle injection of 15μm microspheres, Tothill later obtained nearly the same results (MacPherson and Tothill, 1977). Wooten (1975) also used microspheres to determine the extraction ratio for ^{18}F to be 100%. A few workers have used microspheres to compare qualitative changes in flows to changes in ^{99}Tc-diphosphonate uptake (see Section X).

Brookes (1970) injected ^{59}Iron coated resin particles of 30-70μm diameter into rats. His estimated finding that 28% of cardiac output is distributed to the rat skeleton agreed with his results using ^{51}chromium labelled erythrocytes, and he concluded that the two methods validated each other. However, Brookes used large particles that were probably unevenly mixed since they were injected into the base of the carotid artery.

Hence, a fair number of investigators have used microspheres to validate or evaluate other methods of quantitating bone flow. A few investi-

gators have taken advantage of these agents which can be consistently 100% extracted by all bone tissues in all age groups and have attempted to measure bone blood flow in various regions of a bone, or compare mature to immature bone. As of December, 1979, however, there were no reports in the literature of quantitative osseous flow in which the investigators clearly showed that they used microspheres properly, with even mixing, sufficient number and the appropriate diameter.

E. Physiologic Control of Osseous Flow

The preceding data in section D was ideally intended to deal with osseous blood flow unaffected by experimental alterations. Many other experiments have been designed to alter flows and measure qualitative or quantitative changes from the control situation. Evidence accumulated from such studies indicates that the blood circulation within bone is normally regulated by and responsive to neural, hormonal, metabolic and mechanical influences.

Most studies concerned with the hemodynamics of bone marrow have recorded flows and pressures that vary widely and independently of each other. Bone as a tissue is unique because it is volume limited. Unlike extraosseous tissue, which may expand, increases in interstitial fluid volume within a bone result in a rise in marrow interstitial pressure. Thus, flow is affected by three pressures: arterial (Pa), venous (Pv) and marrow (Pmar). Marrow pressure may be raised by increasing intravascular pressure via increased systemic arterial pressure or nutrient vein ligation. Likewise, marrow pressure falls after ligation of the nutrient artery (McPherson, 1967; Hawk and Shim, 1970). Nutrient arterial pressure normally exceeds marrow hydrostatic pressure by 10-30 cm saline.

Bone blood flow is limited by two sets of resistances, arterial (Ra) and venous (Rv). Thus, flow = $Q = \frac{Pa - Pmar}{Ra}$ and $Q = \frac{Pmar - Pv}{Rv}$, $Q = \frac{Pa - Pv}{Rtotal}$. Since the resistances are in series, $Q = \frac{Pa - Pv}{Rv}$ (Michelson, 1967). Arterial resistance is provided primarily by the arterioles. Though there are no precapillary sphincters in bone, the muscles of the arterioles respond to nervous, hormonal and metabolic biochemical influences by contracting to increase resistance or by relaxing

to decrease resistance. At physiological perfusion pressures, resistance in the arteries far exceeds that in the veins and is thus responsible for most of the total resistance. However, at high perfusion pressures, venous resistance rises sharply, eventually becoming the more significant resistance in the marrow (Michelson, 1967). The thin-walled veins are more affected by the limited volume in bone. If arterial hydrostatic pressure increases, interstitial fluid volume increases along with marrow pressure so that the veins are compressed and venous resistance increases. At any given time in bone there is not just one venous resistance; since the marrow pressure changes, the resistance of a vein changes as it traverses the various regions of the bone. For example, in the tibia the pressure of the diaphyseal marrow exceeds that of the proximal metaphysis, which exceeds that of the distal metaphysis (Michelson, 1967). Metaphyseal pressure is higher than epiphyseal pressure (Stein et al, 1957). Lower pressures occur in areas where the net arterial resistance is increased.

The hemodynamics of bone are further complicated by the effect of multiple arterial anastomoses, which may create collateral circulation. If the perfusion pressure through one artery is increased relative the another aretery, flow from the first will take over the supply of capillary beds normally supplied by the second artery. Thus, flow through the first artery increases not only from increased pressure, but also from the decreased total resistance of parallel flow (where $\frac{1}{R_{total}} = \frac{1}{R1} + \frac{1}{R2}$). Each artery further affects flow through other arteries by influencing marrow pressure.

Many nerves accompany the afferent blood vessels into bone. Some of these are pain fibers, which are stimulated by vascular dilation (Helal, 1965). This accounts for much of the "bone pain" in diseases characterized

by vascular engorgement including osteoarthritis, Brodies abscess, Paget's disease, metastatic tumors, osteogenic sarcoma and multiple myeloma (Brookes, 1972; Trueta, 1968). In such diseases, increasing intravascular pressure by a valsalva maneuver may increase the bone pain (Root, 1967).

The afferent nerves travel the same path as the efferent sympathetic fibers. Sympathetic filaments form plexuses about all marrow arterial vessels up to the capillary level (Brookes, 1974) and are responsible for vasoconstriction of the marrow arterioles. Experimental evidence supporting sympathetic control has been compiled in Tables 4 and 5. Sympathetic stimulation decreases osseous flow and secondarily decreases marrow pressure (Herzig and Root, 1959). Flow increases if the sympathetic influence is blocked. This can be accomplished by administration of an alpha-adrenergic blocker, such as dibenzyline, or by sympathectomy at the level of the lumbar sympathetic ganglia or the sciatic nerve, which carries most of the sympathetic fibers to the distal leg. Thus, with exercise bone flow decreases along with skin flow (Kane and Grim, 1969) consequent to increased sympathetic stimulation. These flows decrease by the same mechanism during hemorrhagic shock. Brookes (1972) has proposed that the vascular dilation and increased flow observed following fracture of the contralateral bone is a vascular reflex mediated by the lumbar sympathetic ganglia.

Bone vessels also constrict in response to hormonal vasopressors, such as vasopressin and the sympathominetics, epinephrine and noradrenalin. These hormones caused decreased flow into bone and resulting decreased intraosseous pressure, despite increased systemic arterial pressure (Hawk and Shim, 1970; Shim, 1968; Bloomenthal et al, 1952). Conversely, vagal stimulation and administration of acetocholine cause vasodilation, reduced flow and reduced pressure, both intraosseously and systemically.

TABLE 4

FACTORS ASSOCIATED WITH INCREASED OSSEOUS FLOW

FACTOR	SOURCE	METHOD	IF QUANTITATIVE: % INCREASE OVER CONTROL
Animal Experiments:			
sympathectomy (sciatic nerve-temporary effect)	Shim, 1968		5-45
sympathectomy (lumbar ganglia)	Trotman and Kelly, 1963	^{42}K, ^{86}Rb-dog	27
sympathectomy (lumbar ganglia)	Rockoff et al, 1969	^{86}Rb-sheep	
sympathectomy (lumbar ganglia)	Yu et al, 1972	venous outflow-dog,rabbit	
sympathetic blocker:dibenzaline	Yu et al, 1972	venous outflow-dog, rabbit	20
increased temperature	Schoutens et al, 1979	microspheres, ^{45}Ca	
increased metabolic rate	Lauren and Kelly, 1967	^{85}Sr-dog	
increased metabolic rate	Pasternak et al, 1966	^{85}Sr	
rebreathing air (with $\downarrow O_2$ & $\uparrow CO_2$)	Cumming, 1962	venous outflow-rabbit	
IV lactic acid	Woodhouse	nutrient artery, flow meter	
IV HCL	Post and Shoemaker	venous outflow	
Clamp Nutrient Artery $\rightarrow$			
temporary ischemia $\rightarrow$ reactive hyperemia	Shim, 1968		
increased remodelling	Stadelnik, 1975	^{18}F(tetracycline)	
increased osteoblast concentration	Whiteside et al, 1977b	H_2 (tetracycline)	
increased remodelling secondary to thyroxine ($\uparrow$ formation, $\uparrow$ resorption)	Sim and Kelly, 1970	^{85}Sr (tetracycline)	
increased remodelling secondary to PTH ($\uparrow$ resorption)	Sim and Kelly, 1970	^{85}Sr	
increased remodelling secondary to PTH 30 minutes after PTH	Boelkins et al, 1977b	microspheres	
bone growth	Sudan, 1968	thermocouple (+tetracycline)	
bone growth	Pasternak, et al, 1966	^{85}Sr-dog	

TABLE 4 (CONT.)

FACTORS ASSOCIATED WITH INCREASED OSSEOUS FLOW

FACTOR	SOURCE	METHOD	IF QUANTITATIVE: % INCREASE OVER CONTROL
barbituate injection (acute effect)	Niv et al, 1980	H_2-dog	200
chronic immobilization (>10 days)	Semb, 1969	^{85}Sr-dog,rabbit	
Human Diseases:			
osteoporosis, Sudeck's Atrophy	Miller and DeTakats, 1942	plesmography	60-80
pulmonary hypertroppic osteoarthropathy	Holling et al, 1961	plesmography	1200%
Paget's Disease	Edholm et al, 1945	plesmography	2000
Paget's Disease	Van Dyke, 1965, 1967	^{18}F	
Paget's Disease	Rhodes et al, 1972	albumin microspheres	
Paget's Disease	Wooton, 1976	^{18}F	63-195
fracture	Johnson, 1927	primary arterial ligation rate healing	
fracture	Lauren and Kelly, 1969	^{85}Sr	2 wks.-600%;3wks-350%
fracture	Paridis and Kelly, 1979	^{125}I-AP	
fracture	Lavender et al, 1979	microspheres	100% in fx. area
infection	Morris and Kelly, 1979	microspheres	25
Ewings tumor; osteogenic sarcoma	Shim, 1968	man	
acute leukemia	Petrakis et al, 1953	^{131}I	
multiple myeloma	Petrakis et al, 1953	^{131}I	
myelofibrosis	Van Dyke et al, 1971	^{18}F-man	136
anemia (→with↑hematopoiesis)	Van Dyke et al, 1971	^{18}F-man	
osteoarthritis	Lange et al, 1979	H_2 washout-dog	209

TABLE 5

FACTORS ASSOCIATED WITH DECREASED OSSEOUS FLOW

FACTOR	SOURCE	METHOD	% DECREASE FROM CONTROL
Animal Experiments:			
ligate nutrient artery	Shim et al, 1968	^{85}Sr	46
ligate nutrient artery	Siegel et al, 1976	microspheres	56
epiphyseal arterial occlusion from forced frog position	Schoenecker, et al, 1978	H_2	
ligate nutrient vein (temporary effect)	Singh & Brooks, 1971	arteriolar blockade	
vagal stimulation, acetocholine	Shim & Patterson, 1967	^{85}Sr	
sympathetic nerve stimulation	Drinker et al, 1922	venous outflow	
sympathetic nerve stimulation	Yu et al, 1972	venous outflow	
vasopressors: noradrenalin & adrenalin	Cumming, 1962	venous outflow	75
vasopressors: noradrenalin & adrenalin	Yu et al, 1972	venous outflow	50
vasopressors: adrenalin	Stein & White, 1966	^{51}Cr-red blood cells	89
vasopressors: pitressin	Shim, 1968	^{85}Sr	
hemorrhage→↓systemic blood volume→↑sympathetic action	Yu et al, 1972	venous outflow	
exercise	Kane & Grim, 1969	^{42}K	
exercise	Reeve et al, 1977	?	0
isometric muscle contraction	Sudan, 1968	thermocouple	
PTH-only during 1st three minutes after injection	Boelkins et al, 1976	microspheres	18
decreased remodelling - secondary to PTH or thyroxin depletion	Sim & Kelly, 1970	^{85}Sr	
acute immobilization ($\leq$ 1 wk.)	Semb, 1966, 1968, 1969	^{85}Sr	
cooling limb in ice	Genant et al, 1974	microspheres	60
excessive intra-articular pressure	Shim, 1968		

TABLE 5 (CONT.)

FACTORS ASSOCIATED WITH DECREASED OSSEOUS FLOW

FACTOR	SOURCE	METHOD	% DECREASE FROM CONTROL
excessive intra-articular pressure 150 mmHg	Borgsmiller, 1980	H_2 washout	100
following atmospheric decompression	Hills & Straley, 1972	thermal dilution	
Human Diseases:			
sickle cell crisis (marrow flow)	Hammel et al, 1973	^{99}Tc sulphur colloid	
osteopetrosis (experimental model)	Trueta, 1968	suppress flow to metaphysis	
Diseases Associated With Aseptic Necrosis of Femoral Head:			
Legg-Perthes disease (model)	Lemoine, 1957	suppress flow to epiphysis	
Legg-Perthes disease (model)	Schoenecker et al, 1978	H_2 washout	
Legg-Perthes disease	Tucker, 1949		
Legg-Perthes disease	Trueta, 1968		
fracture of femoral neck	Tucker, 1950	$^{32}PO_4$	
fracture of femoral neck	Minzuno & Matumoto, 1969	phlebography	
fracture of subcapital femur	Shim, 1968		83 (72-90)
fracture of subtrochanteric femur	Shim, 1968		52 (23-70)
caisson disease	Minzuno & Matumoto, 1969	phlebography	
epiphyseolysis	Minzuno & Matumoto, 1969	phlebography	
dislocation	Minzuno & Matumoto, 1969	phlebography	
idiopathic osteonecrosis	Minzuno & Matumoto, 1969	phlebography	
pyogenic/toxic arthritis (experimental model)	Borgsmiller et al, 1980	H_2 washout	

Flow through bone tissue appears to be autoregulated much as the rest of the body, save the lungs. Vascular dilation and consequent increased flow occurs in response to the by-products of increased metabolism: low pH, excess carbon dioxide and/or insufficient oxygen. Hence, intravascular administration of lactic acid or a small amount of hydrochloric acid causes increased osseous flow.

Pasternak et al (1966) and Lauren and Kelly (1969) found increased bone flow associated with immaturity and fracture without a change in arterovenous oxygen or carbon dioxide difference. These authors concluded that the increased flow was the consequence of the increased metabolism required for bone growth or repair. Flow is augmented to areas of bone containing heightened numbers of osteoblasts and presumably heightened metabolic rate (Whitesides et al, 1977b). It follows that flow is proportional to bone deposition (Stadelnik, 1975). Flow also responds to the metabolic demands of osteoclasts that carry on resorption. This has been demonstrated by the enhancement of flow and oxygen consumption that follows administration of parathyroid hormone, which is known to stimulate osteoclast formation and action.

Bone blood flow is increased when an animal rebreathes air high in carbon dioxide and low in oxygen. Shim and Patterson (1967) reported that if air is rebreathed in the face of blood loss, bone flow was maintained while the skin vessels constricted. They postulated that this is a homeostatic mechanism which allows the marrow to mobilize erythrocytes to meet the increasing oxygen demands. By transiently clamping the femoral artery, Shim was able to produce reactive hyperemia in which flow rose two to three fold. This phenomenon was not abolished by nerve stimulation, vasopressor hormones, or cutting all the nerves to bone. On the other hand, Michelson (1967) was unable to produce reactive hyperemia in his rabbit bone

perfusion studies. This may have been an artifact of perfusion, since such a process has been known to change the properties of blood in regard to its influence on vascular smooth muscle (Michelson, 1967). Reactive hyperemia is clinically manifested by the increased bone bleeding seen when a tourniquet is released after bone surgery (Shim, 1968). Chronic ischemia stimulates vasodilation and hypervascularity as well. Brookes (1972) finds increased bone vascularity in senile arterialsclerosis with peripheral gangrene characterized by invasion of the cortex by periosteal arterioles, enlargement of the cortical canals, and increased vascularization of the spongiosa. According to Trueta (1968), diseases manifested by sclerosis initially become ischemic due to occlusion of the vascular spaces by new bone or bony collapse, and subsequent neovascularization and hypervascularity. Neo-and hypervascularity also occur at the site of fracture repair in response to the chronic increased metabolic demands of the osteoblasts. This is especially evident at the peripheral surface when medullary blood flow has been blocked (Rhinelander, 1976).

Mechanical forces may also influence the circulation of blood through bone. It is generally thought that the distribution of fluid through the cartilaginous growth plate and articular cartilage is favored by the pump-like affect of intermittent compression (Trueta, 1968). The intermittent contraction of the muscles of the limb aides venous return. At the sites of fleshly muscle attachment to bone, the cortical capillaries are directly continuous with the interfascicular venules; elsewhere the cortical capillaries probably empty into periosteal vessels, which are continuous with intramuscular vessels. During muscular contraction venous blood can only be squeezed towards the heart due to the one-way venous valves. Since valves are lacking in intraosseous vessels, there is a transient decrease

in flow and increase in pressure in the bone while the muscle is actively contracting (Suden, 1968). When the muscle relaxes the veins are empty and ready to be refilled with blood that flows out of the higher pressure system of bone. Muscle action can be inhibited by casting the limb in plaster, nerve sectioning, muscle or tendon excision, or neuromuscular disease, such as poliomyelitis. This results in the equivalent of venous obstruction or decreased flow for one week, but after 10 days flow increases above control values (Semb, 1969). The bone becomes hypervascularized with a widening of the marrow cavity and cortical canals, and hyperemia of the periosteum (Brookes, 1972; Trueta, 1968). The mechanism that brings this about is unknown. The hypervascularization might be a reaction to ischemia, but one would expect this to return flow to control levels rather than above them. Furthermore, the blood in the marrow of these bones has high oxygen, high pH and low carbon dioxide content compared to normal bone (Semb, 1969). This suggests that arterial blood has been shunted away from the metabolically inactive muscle and through the bone. It could be that the increased pressure head resulting from higher resistance in the inactive muscle caused normally non-patent osseous vessles to open up secondarily. Alternatively, due to the ischemia, the vascularity may have increased enough to normalize flow. The flow then rose excessively as the blood was shunted from the high resistance systems in inactive muscle to the abnormally low resistance system of primarily hypervascularized bone. This problem might be resolved by measuring the changes in flow through muscle and bone as well as the changes in the pressures in the nutrient and muscular arteries during chronic immobilization.

F. The Association Between Bone Blood Flow and Bone Growth

In the undisturbed state the bone growth rate and flow rate vary directly with one another. Thus, flow is increased at the same time or in the same bone region characterized by augmented growth. During the growth spurt, increased vascularity on both the E-side (epiphyseal) and the M-side (metaphyseal) of the growth plate has been noted (Stockwell, 1979; Trueta, 1968). In the tibia, the ratio of growth in the growing and non-growing metaphysis is the same as the ratio of blood flow, 3:2 (Brookes, 1972). Greater numbers of osteoblasts and increased metabolism and oxygen concumption characterize the areas of greater growth and flow.

As shown in Section IIE , flow normally is determined by metabolic needs. However, in the abnormal conditions of the laboratory or in pathological states, growth may be flow-limited. As reported in Section II C, total ablation of flow to the E-side of the growth plate causes the cartilage to cease division and usually die. Following ligation of the nutrient artery, metaphyseal flow decreases 35% (Shim et al, 1968), but growth only falls 3% (Brookes, 1972) or not at all (Kelly, 1968). Root (1963) claims this is because the fall in flow is only transitory since collateral circulation quickly develops. Another explanation is that epiphyseal flow is minimally affected by nutrient artery ligation in immature animals. Excessive unremitting pressure exerted at the ends of bone retards growth by compressing the M-side vasculature then the E-side vasculature, eventually causing premature epiphyseodesis (Trueta and Trias, 1961). This may be the

mechanism by which growth is inhibited when rigid staples are inserted across the growth plate. Many people think that normally growth is regulated or inhibited by periosteal tension (Stockwell, 1979). Thus, if one physis is prevented from growing by stapling, the consequent decrease in periosteal tension may be the mechanism which allows the compensatory growth that occurs at the opposite end of the bone. It is possible that periosteal tension limits growth by limiting flow, probably E-side flow. Growth is stimulated by periosteal stripping which may also reduce the blood supply to the M-side of the physis (Tachdjian, 1972). The mechanism may solely be the removal of the inhibitory effect of tension. It is alternatively or additionally possible that if flow is decreased through the medullary arteries, the excess blood is shunted through the epiphyseal arteries to supply the E-side of the growth plate. Increased flow could only increase growth if growth were normally a flow limited phenomenon.

There are investigators who believe that growth is flow limited and that any condition which increases flow to the physis causes overgrowth. This is not easy to prove. It is extremely difficult to experimentally produce and sustain high flow rates for an extended period of time without altering many other factors as well. Dickerson (1966) was able to accelerate growth by implanting the total femoral artery into the shaft of the femur. He assumed that this highly invasive procedure increased bone flow, but failed to even measure the flow qualitatively. Sudan (1968) increased flow by sympathectomy and documented faster growth by a greater uptake of tetracycline. However, sympathectomy increases flow only temporarily (Shim, 1968) and other investigators have found that his process does not cause bone to lengthen (Kelly, 1968). Other experiments have produced overgrowth by altering the

circulation without increasing total bone flow. Ligation of the nutrient vein caused flow to fall temporarily then return to normal values (Singh and Brookes, 1971). Brookes (1972) suggests that this procedure shunts excess blood to the region of the growth plate, increasing flow in that region without affecting total fow. He has no experimental evidence to back this up. Arteriovenous fistulas also stimulate longitudinal bone growth. The overgrowth is greater in the femur than in the tibia with an iliac fistula, and greater in the tibia with a femora fistula (Tachdjian, 1972). In the first three weeks after creation of a femoral AV fistula, an increase in growth and bone turnover and venous emptying via phlebography is noted (Vanderhoft and Kelly, 1964), but flow measured with ^{45}Ca and ^{85}Sr has decreased to both bones. Flow in the femur subsequently rises above normal then returns to normal values by 9 weeks. Tibial flow remains below normal. Weineman et al (1964) conclude that no relationship between flow and growth can be found in this situation. Nevertheless, Kelly and James (1968) report that the pressure of the epiphyseal marrow increased, raising the possibility that the overgrowth could be secondary to increased perfusion of the E-side of the growth plate.

Clinically, pathologic conditions that are accompanied by increased total bone flow such as fracture, chronic infection and tumor (Table 4) have been associated with overgrowth. Ferguson (1933) proposed that this is because these conditions interrupt normal flow through the nutrient arterial system in the medulla and divert it to the epiphyseo-metaphyseal arteries on either side of the growth plate. Trueta (1968) proposes that synovitis can stimulate bone length by stimulating the E-side vascularity.

In summary, it appears that in the face of abnormally decreased flow, growth can be flow limited. It is possible that increasing flow to the

physeal area above normal values causes increased growth but at this point in time there is no concrete evidence that this it true. Experiments are needed in which changes in bone length are compared to quantitative changes of blood flow to specific regions of the bone. Even so, any experimental procedure that chronically increases flow is going to affect other parameters as well.

G. Blood Supply and Age

All related experiments consistently prove that flow to mature bone is lower than that to immature bone (see Tables 1 and 2). Immature bone has greater bone turnover, a greater number of osteoblasts and a greater oxygen consumption. Its periosteum is more highly vascularized and reactive. Injured bone heals faster and more completely in the immature animals (Rhinelander, 1979). However, little evidence is available concerning the changes of flow through mature bone with advancing age. MacPherson and Tothill (1977) find that osseous flow in adult rats of 11 months is half of that in immature 10 week old rats, and that flow rates are halved again in senescense. Brookes (1975) reports that flow steadily drops from 20 ml/min/100g in 8 week old rats to only 2 ml/min/100g in senescent animals. Hruza and Wachtlova (1969) also find that flow continues to decrease from 2½ to 4 to 11 months and this is associated with a concomitant decrease in cortical capillary density. On the other hand, when Trueta (1968) perfused bones taken from humans ranging 20 to 100 years old, he found no change in the blood vessels. He acknowledges that there are numerous workers who disagree and report that the arterial supply of bone decreases with advancing age. These workers also get their information from anatomical and histological studies. Obviously, more studies are needed correlating quantitative changes in bone blood flow with advancing age.

H. Osseous Blood Flow and Pathology

As can be seen in Tables 4 and 5, many diseases are associated with increase or decrease in flow compared to that in normal bone. Some investigators have postulated that nearly all disease in bone can be attributed to primary changes in flow. It is probably more often true that the disease the primary event, then blood being autoregulated, responds secondarily to the changes in metabolism wrought by the disease process. However, there are a limited number of diseases which blood flow plays an important role in the etiology; these include diseases which are spread hematogenously and diseases associated with ischemia and necrosis due to lack of blood supply.

I. HEMATOGENOUSLY SPREAD BONE DISEASE

a. ACUTE HEMATOGENOUS OSTEOMYELITIS

Diseases that are borne to bone by the bloodstream include acute hematogenous osteomyelitis, both bacterial and tuberculous, and cancer metastases. The organisms responsible for causing osteomyelitis in order of decreasing frequency, are staphlococcus aureus, streptococcus, pneumococcus, gonococcus, and hemophilus influenza (Robbins and Angel, 1976). Since 50 to 70% of osseous blood is delivered through the nutrient artery, the majority of the bacteria enter the bone by this route. But they are also delivered by the numerous smaller bone arteries. The pattern of disease localization is determined by vascular pattern and hemodynamics and by the immune response of the host. Trueta (1959) divided acute hematogenous osteomyelitis

into three clinical entities; childhood, infant, and adult osteomyelitis. These entities are separable by their clinical features and patterns of bone microvasculature.

Childhood osteomyelitis is the most common and is seen in children between the ages of one and sixteen years. During this time the epiphysis and metaphysis are separated by a well-developed physis which is not traversed by many vessels as discussed in Section I. It is generally believed that the bacteria travel from the nutrient artery through the vascular loops on the M-side of the growth plate and into the sinusoids of the metaphysis and diaphysis (Figure 9). Because the sinusoids are wider and more numerous than the arterioles, the blood flows more slowly through the sinusoids (Brookes, 1972). The relative blood stasis provides a favorable environment for bacterial colonization and growth. This, in turn, causes venous thrombosis and more stasis, documented by the initial decrease in ^{99m}Tc-sulphur colloid uptake after IV injection of bacteria (Feigin et al, 1976). Because of the decreased flow, the influx of inflammatory cells is limited. The thrombus spreads retrograde to occlude the capillary loops causing transudation, increased marrow pressure to 180 cm H_2O (Kelly, 1968) and marrow necrosis. The high marrow pressure is probably due to a) increased hydrostatic pressure secondary to venous occlusion and b) increased inflow due to decreased resistance because of reactive hyperemia, accumulation of waste products and/or release of histamine, a vasodilator. The infection spreads laterally to perforate the thin cortex on the M-side of the physis and lift the periosteum, disrupting the vessels between the two. A subperiosteal pus collection forms, followed by the deposition of involucrum of the reactive periosteum. Morris and Kelly (1979) found that flow to an infected tibia was 1.25 times that in the healthy contralateral bone.

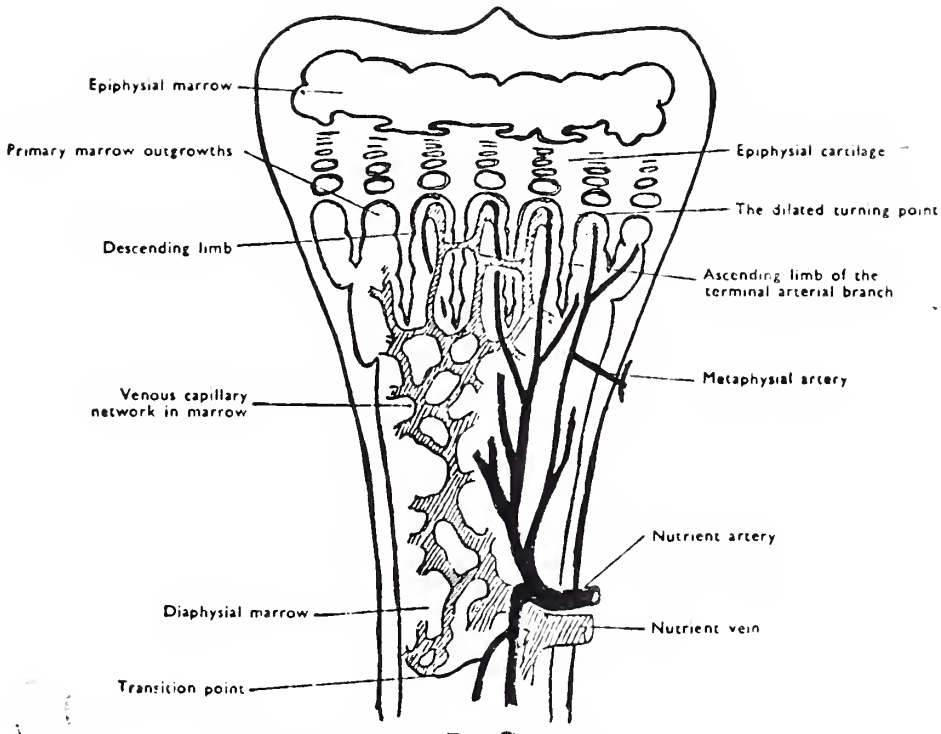

FIG. 9
Diagram of the course of the blood vessels in the marrow of a young rabbit. (After Hobo 1921)

Nutrient Vascular System With M-Side Vascular Loops

Trueta (1968) postulated that the increased flow is due to increased vascularity on the M-side of the physis since 30% of individuals get increased growth in the infected bone. However, the overgrowth could also be due to increased blood being shunted through the epiphyseal arteries to the E-side of the plate.

Childhood osteomyelitis nearly always centers in the metaphysis, though it may spread into the joint space if the metaphysis is intracapsular (Brookes, 1972). Infection may localize in the metaphysis because of 1) increased delivery, 2) favorable local conditions for bacterial colonization, and 3) decreased clearance. Delivery of bacteria is proportional to blood flow. Unfortunately, since most quantitative studies of blood flow are unreliable, the studies comparing the various regional flows are also unreliable. Nevertheless, flow to the diaphyseal marrow is reported to be lower than that in the metaphysis, 21:30 cc/min/100 gm (Brookes, 1972) and lower than in the epiphysis, 17.7:19.7 cc/min/100 gm (Kane and Grim, 1969). A number of workers have found slightly lower blood flow in an epiphysis compared to its adjacent metaphysis with the following epiphyseal:metaphyseal flow ratios: 29:30 (Brookes, 1972), 7.6:10.0 (Wooten et al, 1976), 8:10 (Whiteside et al, 1978), and 13:16 (Niv and Hungerford, 1979). Although better studies are needed, the past studies indicate that the metaphysis is the region of bone that receives the highest flow. One would expect the metaphysis with the highest flow to be the most frequently infected. The disease localizes in the following metaphyses in decreasing order of frequency: proximal tibia > distal femur > distal tibiofibula > proximal femur > ilium > proximal humerus > distal radius > distal humerus (Hart, 1937). The only osseous blood flow study that compares the separate metaphyses is that of Brookes (1972) who found the proximal femoral metaphysis to receive 27 cc/min/100g

while the distal femoral metaphysis received 30 cc/min/100g. This makes sense in light of the general finding that infection is more frequent in the distal than the proximal femur, but more data is obviously needed.

Local slowing of blood flow velocity in the metaphyseal sinusoids is thought to favor bacterial colonization. Yet, the epiphyseal sinusoids are wider and more irregular in caliber than those in the metaphysis (Brookes, 1972; Stockwell, 1979). This would lead one to expect that the epiphysis is a more favorable place for colonization.

Studies with india ink uptake indicate that there is decreased phagocyte activity in the medullary cavity of bone (Robertson, 1927), especially in the metaphyseal region. Hobo (1921) created an animal model of the disease and reported that in the first three hours after IV inoculation the bacteria were distributed in both the metaphysis and diaphysis; by six hours there were substantially fewer organisms in the diaphysis as a result of active phagocytosis in that region. The relatively less competant immunological defense system of the metaphysis would favor local infection; however, only Hobo has documented phagocytic activity. Modern studies are needed.

To summarize, in childhood osteomyelitis, the highest number of bacteria are carried to the metaphysis. Here, rhealogic conditions are favorable for colonization. The infection may persevere because of the limited immunological activity in the metaphysis.

The infection also starts in the metaphysis in infant or neonatal osteomyelitis. There are no studies to date which quantify osseous blood flow in any bones before the physis is fully formed. Hence, it is impossible to compare metaphyseal to epiphyseal flow in the infant. Nor are there any re-

ports on regional or absolute bone phagocytic activity in this age group. The only studies available are anatomical. The metaphyseal vasculature is similar to that in the child. The secondary ossification center, however, is still forming. Since the transverse sinusoidal system is less well developed, it is likely that the infant has relatively less favorable conditions for primary bacterial colonization in the epiphysis than the child does. But, the primary infection in the metaphysis can spread to the epiphysis through the transphyseal blood vessels that are present at this age. Occlusion of the vessels which provide nutrition to the physis may result in permanent damage to the growth plate in that area. This age group has a very thin cortex which allows easy spread of the infection into the joint space, beneath the easily elevated periosteum, and into the soft tissue (Ogden and Lister, 1975). The marrow pressure probably does not increase as much as it does in childhood osteomyelitis and hence, there is less massive necrosis (Potter, 1954).

Acute hematogenous osteomyelitis is much rarer in adults than in the younger age groups. Adults lack a physis and have wide venous connections and small arterial or capillary anastamoses between the epiphysis and metaphysis. The sinusoids are essentially the same as in the child. The decreased incidence of infection may be a result of the decreased delivery due to lower blood flow, coupled with the vascular anastomoses which would allow influx of inflammatory cells and oxygen, provide an outlet for waste products, and prevent as much pressure build up. In the adult, epiphyseal infections are relatively more common, because the infection spreads from the metaphysis. The sole study comparing epiphyseal to metaphyseal blood flow in the adult reports that they both receive 6 cc/min/100g (Whiteside, et al, 1978). If, indeed, epiphyseal flow is as high as metaphyseal flow,

there may be primary epiphyseal infections in this age group, providing that the immune system is not significantly more competant in the epiphysis. The infection can spread from the epiphysis into the joint space. Subperiosteal abscess and involucrum formation are rare since the periosteum is firmly adherent to the thickened cortex.

In our study, we hope to shed light on the role that hemotogenous delivery of bacteria plays in the localization of infection in infant, childhood and adult osteomyelitis in the tibia and femur.

b. CANCER METASTASES

The skeleton is one of the most common sites of distant metastases from carcinoma and sarcoma. Seventy percent of patients who die of cancer are found to have bone metastases at autopsy (O'Mara, 1974). These lesions make up two-thirds of all bone malignancies (Robbins and Angell, 1976). They most frequently originate from the prostate, breast, lung, thyroid, kidney and bladder. Tumors are conveyed through lymphatic, venous or arterial channels. Carcinomas tend to be spread more by lymphatics, sarcomas more by blood (Bertino, 1977). Most tumor cells travel to bone through the blood; for most skeletal metastases are not accompanied by tumor deposits in regional lymph glands (Willis, 1960). However, spread through the blood is often initiated by way of lymphatic channels. The tumor cells are carried first to regional lymph nodes which then become the source of further metastases or to the thoracic duct and through it to the jugular vein, the right heart and finally, the lungs. When spread is initiated by way of the bloodstream, it is more often via venous invasion, clumps of tumor cells adhere to the vascular endothelium of a venule where they multipy, induce fibrin formation and invade through the endothelium (Bertino, 1977). The low blood velocity in the medullary sinusoids of bone provides a favorable environment for primary bone cancer cells to

multiply and produce metastatic tumors (Trueta, 1968). Most tumor emboli are 50 μm to 100 μm in diameter and are arrested in the first arteriole they encounter. Hence, if they enter and are carried in the portal vein they are trapped in the liver, from the systemic veins they go to the lungs, and abortive emboli from the lungs enter the pulmonary veins and left heart from whence they can go to any peripheral organ or tissue. In the latter case, seeding of a particular organ is determined by the rate of blood flow to that organ and by how favorable the tissue environment is for tumor cell invasion, survival and growth.

In general, the distribution of blood borne metastases among the various organs in the body roughly corresponds to the proportion of cardiac output flowing through these organs, as indicated in Table 6.

The metastatic data is taken from a study by Willis (1960) of the organs of five hundred cancer patients at necropsy. The cardiac output data was collected from various sources by Brookes (1972), and the skeletal flow value is his own. The lungs, skin and muscle have a lower incidence of metastasis than would be expected if flow were the sole determining factor, while a higher incidence is found in the liver and spleen. Willis (1960) found that nearly all lungs devoid of visible metastases still contained minute degenerating tumor emboli, indicating that growth had been arrested and that the lung is often an unfavorable environment for tumor growth. Degenerating emboli were rarely found in the liver; Willis concluded that nearly all emboli grow into metastases in this tissue, and that growth might be favored by the poor oxygenation and high carbohydrate content or some growth promoting substance secreted by the liver. He postulated that tumor growth in skeletal muscle is inhibited by lactic acid. Muscle also has a low incidence of infection. With such inconstant findings for

TABLE 6

	% ALL BLOOD BORNE METASTASES IN ORGAN	% CARDIAC OUTPUT TO ORGAN
Liver (Portal v. and Hepatic a.)	36	25
Lungs	29	100
Skeleton	14	26
Adrenals	9	--
Kidneys	8	20
Brain	6	14
Heart	5	5
Thyroid	4	--
Ovary	3	--
Pancreas	3	--
Detramater	3	--
Spleen	3	1
Intestine	2	--
Skin	1	7
Muscle	0.5	8

skeletal flow, it is nearly impossible to correlate incidence of metastases with blood flow. If the skeleton receives as much flow as Brookes claims, it is neither an excessively favorable or unfavorable area for tumor growth. However, all other investigators report that the skeleton receives a lower percentage of cardiac output, with values ranging from 3% to 18%. The average of all experiments, including Brookes', is 10%. If this figure is used, it appears that bone is a fertile environment for tumor growth. Moreover, most skeletal metastases are found in the bone with red marrow, which "in adult man is exclusively limited to the bones of the body trunk and head as well as the proximal portions of the limbs" (Root, 1963). Metastases are found in the following bones in decreasing order of frequency: vertebrae > proximal femur > pelvis > ribs > sternum > proximal humerus (Krane, 1977). It is interesting to note that growth is favored in the three areas of actual or potential hematopoiesis in the human body: the liver, spleen and red marrow. A future pertinent study would involve comparing the regional frequency of skeletal metastases to regional marrow activity measured with a ^{52}Fe scan, and to regional osseous blood flow measured with microspheres.

From the above information it appears that the hematogenous seeding of neoplastic metastases is determined by blood flow but that certain tissues, such as the liver, bone marrow and spleen, favor tumor growth while other areas, notably skeletal muscle and, to a lesser extent, lung, limit tumor growth. This is a gross generalization, for certain tumors show a definite preference for one site of metastasis over another.

In addition, there is a second mechanism of hematogenous spread. Thoracic, abdominal and pelvic tumor cells may also undergo retrograde spread through the vertebral vein system which communicates with the caval

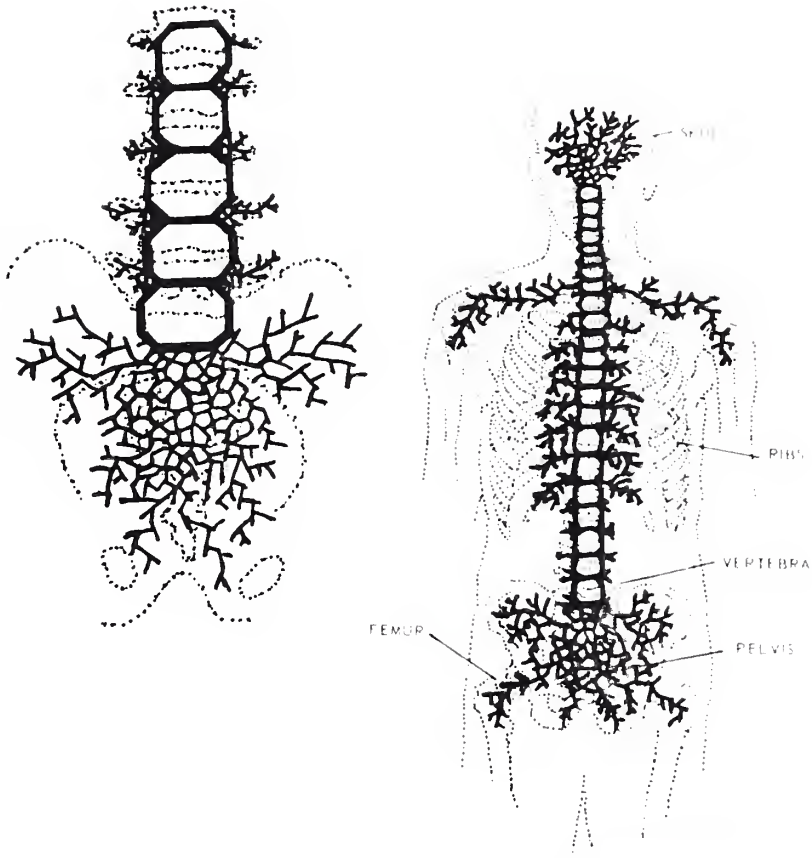

Figure 10

Vertebral Vein System
(Regato, 1977)

system (Figure 10). There are no valves in the vertebral venous plexus (Brookes, 1972) and the direction of flow is not constant. Retrograde "spread is favored by increased abdominal pressure such as takes place in chronic coughers" (Regato, 1977). Similarly, tumor cells may spread to bones via interfascicular venules at the sites of direct muscle attachment. The relative importance of retrograde venous spread versus arterial embolization in the creation of skeletal metastases is an area of controversy. The proponents of venous spread point the frequency of pelvic and vertebral metastases in cancer of the prostate and the shoulder girdle and pelvis metastases in cancer of the breast (Bateson, 1940; Regato, 1977). The results of Belliveau et al (1975) compiled in Table 7 substantiate this claim for prostatic cancer. However, the distribution of metastases from breast cancer is highly similar to that from all cancers combined; there is no increased incidence in local bone. The proponents of retrograde flow also point to the rarity of metastases in bone below the knee and beyond the elbow, and claim that arterial transport of tumor emboli would result in a greater number of metastases in the distal extremities (Regato, 1977). An alternative explanation has already been raised; tumor growth is enhanced in the red marrow. Some light might have been shed on this dilemma if Willis had meticulously dissected the long bones looking for degenerating tumor emboli as he did in the lung and liver. Degenerating emboli in the tibia would indicate that there was arterial spread, but the environment was unfavorable for tumor growth. An alternate experiment would involve three stages. First, the frequency of metastases in all the various regions of long bones (or just the femur) should be determined. This distribution could secondly be compared to regional osseous arterial

TABLE 7

PRIMARY SITE OF CANCER	% PATIENTS WITH BONE METASTASES	% OF TOTAL BONE METASTASES							
		SKULL	CERVICAL	SPINE: THORACIC	LUMBAR	RIBS	PELVIS	LOWER EXTREMITY	UPPER EXTREMITY
All	59	15	2	12	22	22	17	7	3
Breast	56	18	4	10	23	23	15	4	1
Lung	65	18	3	14	8	33	14	6	3
Prostate	81	8	-	19	25	19	25	4	0

flow, measured with microspheres. Thirdly, the regional distribution of retrograde flow could be grossly and qualitatively determined by injecting a tracer into the prostatic venous plexus. At this point in time, it can only be said that since the skeletal metastases from tumors in general, or from the lungs or breast, all have a similar distribution, they are probably seeded predominantly by arterial embolization. Retrograde venous spread to bone may be an important route for skeletal metastases from prostatic cancer, as opposed to cancer in general, since prostatic metastases are more frequent in the lower spine and pelvis, and relatively less frequent in the skull, humerus and cervical spine.

Although both acute hematogenous osteomyelitis and tumor metastases are spread by bone flow, their distribution is vastly different with the proximal tibia being the most frequent site of infection in the former disease, yet rarely involved in the latter.

2. BONE DISEASE FROM DECREASED OSSEOUS BLOOD FLOW: ASEPTIC NECROSIS

One group of bone diseases caused by a variation in blood flow have a very similar distribution. Aseptic necrosis of bone results from an interruption of its blood supply which may be due to a physical injury or to non-traumatic occlusions of its blood vessels. The femoral head is the most common site of aseptic necrosis (Tachdjain, 1972). Its blood supply

particularly susceptible to damage from a number of causes, both in childhood and adulthood. Because of this, a discussion of the developmental vascular anatomy will be presented. The proximal femur is supplied by two anastamotic rings of blood vessels: 1) the more important extracapsular ring formed by the medial circumflex artery (MCA) and the lateral circumflex artery (LCA), and 2) an intra-articular ring, which is often incomplete,

especially in males, composed of small synovial arteries (Chung, 1976). At birth the proximal femoral epiphysis is a single mass of cartilage with a single planar extra-articular growth plate penetrated by transphyseal blood vessels. The LCA supplies blood to the greater trochanter and the portion of the growth plate below it, and the anterior part of the future femoral head. The MCA supplies the posterior femoral head analogue and the entire femoral head growth plate (Ogden, 1974). The central area of the physis grows more quickly than the rest so that the femoral neck forms. The femoral neck metaphysis is nourished by the LCA (anterior cervical branches), which ceases to directly supply the anterior femoral head. They are still transphyseal vessels which can supply blood to the epiphysis until fifteen months. By two to three years of age, the femoral head is supplied by two branches of the MCA. The posterior inferior branch, also known as the inferior reticular, medial ascending cervical and medial metaphyseal arteries, runs along the lower border of the femoral neck to deliver blood to the posterior femoral head. The posterior-superior branch, also known as the superior retinacular, lateral ascending cervical or lateral epiphyseal artery, carries the major blood supply to the femoral head. It normally supplies 70% of the epiphysis in puppies (Bassett et al, 1969) and can supply 100%, if necessary, (Chung, 1976). Its course along the upper border of the femoral neck and through the intertrochanteric notch renders it susceptible to tamponade. This, in turn renders the femoral head, particularly the anterior portion, susceptible to ischemia. Whereas early in life this area was supplied by multiple small vessels each a few millimeters apart, after three years the LCA branches only supply the metaphysis, and the physis segregates the epiphy-

seal and metaphyseal circulations, leaving the entire anterior area to be supplied by one artery, the posterior-superior branch of the MCA. However, if the subsynovial intra-articular anastomotic ring of blood vessels is complete, it may be able to compensate for a deficiency of blood flow through the MCA.

Many authors claim that the susceptibility of the anterior femoral head epiphysis to ischemic damage decreases at about eight years of age due to the ingrowth of muscular arteries which run through the ligamentum teres. These vessels are large and enter the femoral head to anastamose with the branches of the MCA in 33% of individuals. The other 67% have smaller vessels which only distribute to a small local area of the femoral head (Werthheimer and Lopes, 1971); these smaller vessels have a limited ability to supply collateral circulation acutely if the MCA vessels are damaged. Ischemic changes can be produced experimentally in adult animals if both the extracapsular and the ligamentum arteries are cut (Lemoine, 1957). Trueta (1968) claimed that black infants were less susceptible to aseptic necrosis due to their relatively high flow through the round ligament. However, Chung (1976) found no difference between the ligamentum teres of black and white babies.

The susceptibility of the femoral head to ischemia is further decreased after epiphyseodesis, at about age sixteen in males, when the vasculature of the metaphysis and the epiphysis can freely communicate at this time when there are three possible sources of blood supply: the MCA, the metaphyseal vessels fed by the metaphyseal and nutrient arteries, and the ligamentum teres vessels, all of which must have inadequate flow for avascular necrosis of the femoral head to occur.

The changes wrought by vascular insult are similar at any age. The initial decrease in flow has been grossly and qualitatively documented by

a number of methods including phlebography, $^{32}PO_4$- uptake, ^{99m}Tc-EHDP uptake, tetracycline labelling and H_2 washout (see Table 5). This is followed by aseptic necrosis of the involved area of bone. If there is residual blood flow or revascularization, the necrotic area is invaded by dilated vessels, and new bone is laid down over the dead bone which is gradually resorbed (Trueta, 1968; Tachdjian, 1972). Meanwhile, the old bone may collapse and fragment. These processes result in a patchy sclerosis (Brookes, 1972). The reparative stage is marked by an increase in flow and metabolism shown by an increase in uptake of ^{99m}Tc-EHDP and tetracycline compared to control limbs (D'Ambrosia et al, 1976). If blood flow is not re-established and there is total necrosis of the epiphysis, there obviously will be no uptake of any tracer and no x-ray changes unless weight bearing results in collapse, fragmentation and/or pathologic fracture, and then secondary ossification (Trucker, 1949).

The osetochondroses, also called juvenile osteochondritis or epiphyseal anemia, are the result of temporary interruptance of flow in the epiphysis or apophysis. The best studied is osteochondritis of the head of the femur, Legg-Calve-Perthes disease. The exact etiology is not known, but much can be construed from the following findings: (1) it most commonly occurs between three and eight years of age, (2) in males more often than females, and (3) it is often preceded by synovitis. As discussed above, the femoral head is highly susceptible to vascular insult between the ages of three and eight when the physis is fully developed, yet there is no collateral circulation from the ligamentum teres vessels (Trueta, 1968). Males may be a greater risk because they more commonly have an incomplete intra-articular vascular ring

(Chung, 1976). Alternatively, Trueta (1968) proposed that boys play more roughly than girls and that the vascular insult might result from repetitive minor trauma. It is known that the posterior-superior branch of the MCA can be compressed by the acetabular lip when the hip is in a position of forced abduction, internal rotation and extension. Immobilization in this position has been shown to decrease perfusion by angiography (Nicholson, 1964) and hydrogen washout (Schoenecker et al, 1978) and can produce an experimental aseptic necrosis (Salter et al, 1969). The increased incidence of Legg-Perthes disease in children with CDH was probably secondary to fixation of the hips in this position. Because of this and the finding that immobilization of the hip in at least 90% of flexion and minimal abduction will minimize the subsequent occurrence of avascular necrosis. If there is any validity to Trueta's theory that transient repetitive internal rotation, abduction and extension leads to Legg-Perthes disease, then the relative incidence of the disease should be increasing in girls considering the current surge of participation in women's athletics, particularly in gymnastics.

Aseptic synovitis may play an important role in the etiology of Legg-Perthes disease. Whereas the intra-articular pressure of the hip joint is normally 49 mmHg, it may exceed 150 mmHg in 59% of children with synovitis (Tachdjian and Grana, 1968). Avascular necrosis can be produced by experimentally maintaining the intra-articular pressure at 200 mmHg for over 10 hours (Tachdjian and Grana, 1968). Hydrogen washout studies show that epiphyseal blood flow decreases at an intra-articular pressure of 50 mmHg and ceases at 150 mmHg (Borgsmiller et al, 1980). Hence, it

is likely that aseptic necrosis may often be a consequence of the joint effusion of aseptic synovitis, but not always; for only 12% of the children with synovitis subsequently get Legg-Perthes disease.

The next period in development when the femoral head epiphysis has increased susceptibility to avascular necrosis is during the period of rapid growth at twelve to sixteen years of age in human males and eleven to thirteen years in females (Trueta, 1968), or in dogs of four to eight months of age (Whittick, 1974). At this time the M-side of the physis is hypervascularized with concomitant enlargement of the cylindrical housing the vascular loops. The growth plate is consequently weaker than usual, increasing the risk of epiphyseolysis. If mechanical forces cause a rapid traumatic slip, the extracapsular vessels may be ruptured and avascular necrosis of the epiphysis may ensue (Ham, 1974). Epiphyseolysis can occur in the distal femoral epiphysis, and is frequent there in dogs; but the distal femoral epiphyseal vessels are intracapsular and generally are left intact. Thus, blood flow is not interrupted and avascular necrosis is rare in this location.

Rupture of the femoral head extracapsular vessels following traumatic dislocation of the hip can occur at any age. Obstruction of or damage to the vessels supplying the epiphysis, and thus the incidence of avascular necrosis, is increased by posterior dislocations and when there is a delay before reduction.

The most frequent cause of aseptic necrosis in the adult is fracture of the femoral neck. Necrosis follows one-half to one-third of these fractures. Again, it is the posterior-superior branch of the MCA which is most vulnerable. The vessels are medial to and not damaged by extracapsular fractures. However, intracapsular fractures usually interrupt arterial

blood flow, especially the adduction fractures with rotation, angulation and proximal displacement of the limb. Decreased blood flow may result from hematoma or torquing, kinking or rupture of the artery (Bell and Subramanian, 1979).

Non-traumatic avascular necrosis of the femoral head occurs in sickle cell anemia, caisson disease, Gaucher's disease due to vascular occlusion by gaucher cells, idiopathic osteonecrosis, and also is associated with chronic renal failure, chronic steroid treatment and alcoholism. Bone infarcts caused by the "log-jam" of sickled red blood cells can occur anywhere but are most often in the femoral head (Tachdjian, 1972). Caisson disease may also cause avascular necrosis in both the femoral epiphysis and diaphysis. The bone lesions are usually symmetrical and may be found in more than 50% of the professional divers or caisson workers. Most theories attribute the ischemia to vascular occlusion by various agents formed during decompression such as gas bubbles, thrombi, and fat emboli. However, as there is no statistically significant correlation between the incidence of the bone lesions and other symptoms of decompression, it is possible that the mechanism may be partly due to changes in vascular hemodynamics (Hills and Straley, 1972). After decompression, marrow pressure increases (Harrelson and Hills, 1970), and flow, measured by thermodilution, decreases (Hills and Straley, 1972). The reverse occurs with compression. The decrease in bone blood flow after decompression was minimal, nevertheless, and not by itself sufficient to cause aseptic necrosis.

In all the above diseases, knowledge of decreased or absent blood flow to the femoral head is of value in making clinical decisions concerning therapy. The changes in flow precede any x-ray changes. Various methods

to clinically assess femoral head blood flow and viability have been used in the past. These include aspiration of the bone to see if it will yield blood, phlebography, and bone scans depicting the uptake of the various bone seeking radioisotopes discussed in Section X.

Two other diseases that may be associated with decreased osseous blood flow are hemophilia and osteopetrosis. The articular cartilage damage from the hemarthrosis in hemophilia can be reproduced experimentally only if there is excessive pressure in the joint space (Rival, 1961). This pressure tamponades flow through the epiphyseal blood vessels and the capillaries of the synovial membrane, thus cutting off both sources of nourishment for the articular cartilage. Although certain authors (Trueta, 1968) propose that the failure of bone resorption and restricted bone formation in osteopetrosis, or osteosclerosis fragilis, may be a result of primarily poor vascularity, it seems more likely that the primary defect lies in the modelling cells and flow is decreased secondarily to decreased metabolism.

3. BONE DISEASES WITH INCREASED OSSEOUS BLOOD FLOW

Increased blood flow has been measured in bones with fractures, infection, healing rickets, osteoarthritis and various tumors. Immediately after fracture occurs there is decreased flow on either site of the fracture line with a very slight increase of flow above baseline values at the opposite ends of the bone (Lockwood and Latta, 1980). Total bone blood flow is increased by the end of one day. In ten days to two weeks total bone flow is six times normal (Lauren and Kelly, 1969) and flow at the site of fracture is one hundred times normal (Lavender et al, 1979) with neo-and hypervascularity. From three until ten weeks post fracture total bone flow is about 3½ times normal, and if healing is not delayed, flow values return to normal

by about twelve weeks (Lauren and Kelly, 1969). Although the increased bone flow is predominantly due to the increased metabolic demands of the osteoblasts at the fracture site, neurogenic factors may also play a role, for flow through the intact contralateral leg also rises above baseline values (Brookes, 1972). If blood flow is limited, healing is delayed. There have been numerous past experiments comparing the relative delay in fracture repair when the various arteries are cut. Bone that is poorly vascularized heals slowly and is at increased risk for non-union. Thus, aged rat bones are more slowly repaired than young rat bones (Brookes, 1972). "The tibia is an ideal example of the rate of bone healing in relation to vascular supply for there exists one of the richest vascular areas of bone tissue--the upper metaphysis, and... one of the poorest---the distal part of the shaft...The upper region... produces the early union and [the distal shaft is] more likely to be affected by delay or lack of union." (Trueta, 1974).

In osteoarthritis of the hip, flow to the femoral head is doubled, probably mainly due to augmented flow through the metaphyseal anastamoses (Lange et al, 1979). The stimulus for this is unknown but a likely explanation is that increased or uneven wear causes microscopic stress or fatigue fractures in the subchondral bone and the hemodynamic response to the increased metabolic demands or repair is the same as in microscopic fractures.

Most tumors in bone, whether primary or secondary, are associated with increased blood flow. A few neoplasms to which augmented flow has been measured are listed in Table 4; in addition, 98% of tumors show increased local blood flow (Bell and Subramanian, 1979). The other 2% of tumors, aggressive malignant neoplasms which have replaced bone, almost certainly have increased flow but the scan is negative because no bone remains

for the bone-seeking tracer to seek. The increased blood flow can be attributed to several causes. The most obvious and probably the most important cause is the autoregulatory response of the circulation to supply enough nutrition to meet the demands of tissue metabolism. Growing tumor cell masses have very high nutritional needs. They also may stimulate a local reparative response in the bone tissue, thus increasing the metabolism of the non-malignant bone cells. Certain tumors associated with bone destruction and lymphoid cell accumulation, notably myelomas and lymphomas, are thought to elaborate a serum factor quite like OAF (Luben et al, 1979). OAF, osteoclast activating factor, is a lymphokine which stimulates osteoclast resorption. Since OAF acts much like PTH, increasing cAMP in the same cells, it probably increases osseous blood flow as PTH does. A final mechanism by which tumors can augment blood flow is by the elaboration of tissue angiogenesis factor, TAF, a macromolecule which results in the local proliferation of blood vessels (Bertino, 1977).

In the diseases mentioned in the above paragraph, the increased flow is probably predominantly secondary to increased metabolism. There are a few diseases in which it has been claimed that the increased flow is primary to the pathologic bone changes, namely Paget's disease, hypertrophic pulmonary osteoarthroplathy and osteoporosis. Paget's disease or osteitis deformans has markedly increased osseous flow that has been estimated to be as high as twenty times normal (Holling et al, 1961). This high flow has the same effect as multiple arteriovenous fistulae would have, and has been known to cause high output cardiac failure. Yet, there are no AV shunts in pagetoid bone (Rhodes et al, 1972), but rather hypervascularity in the form of many new arterioles and sinusoid capillaries (Putshar, 1972). The stim-

ulus for neovascularization is not known. It may be largely secondary to the abnormal excess rate of bone metabolism. Pagetoid bone contains abundant osteoblasts and osteoclasts (Robbins and Angell, 1976) and bone turnover may be twenty times normal (Krane, 1977c). But, the hypervascularity is increased beyond the metabolic needs, for the venous oxygen content is elevated (Rhodes et al, 1972). Thus, it remains possible that the vascular abnormality is, at least in part, a primary change in the disease process.

There is also increased vascularity and blood flow with high oxygen content along with high pH and low CO_2 content in experimental models of immobilization osteoporosis. The possibility of muscle disease causing venous obstruction with a secondary response of bone hypervascularization and shunting of blood away from muscle through these osseous vessels was discussed at the end of Section VI. Nevertheless, there is also an increase in bone resorption and formation in chronic immobilization (Kramer, 1977b). Whether this contributes to the hypervascularity or is a consequence of the high flow and increased oxygen saturation is not known. Increased blood flow has been measured through osteoporotic bones with Sudeck's atrophy or post-traumatic dystrophy of the extremities (Miller and deTackets, 1942). In this disease the initial decrease in bone flow is probably secondary to the sympathetic vasoconstrictive reaction to injury coupled with the muscle disuse that results because movement of the limb is painful. If the pain and muscle disuse continues, the pathogenesis of increased flow may be like that in chronic immobilization osteoporosis. Alternatively, the injury somehow causes increased resorption and the blood flow increases accordingly (Miller and deTackets, 1942).

The final disease with increased vascularity and blood flow in bone with an unknown etiology is pulmonary hypertrophic osteoarthropathy (PHOA). This condition is manifested by a symmetric periostitis and subperiosteal deposition of friable vascular bone. The bulk of the increase in blood flow, measured by plesmography, is thought to be directed to this newly formed bone (Holling et al, 1961). PHOA is associated with a variety of diseases including certain cancers and pulmonary, cardiovascular, liver and some gastrointestinal diseases (Robbins and Angell, 1976). The disease process reverses with successful treatment of the underlying disease. PHOA has been produced experimentally in dogs by anastomosing the pulmonary artery to the left atrium (Mendolwitch and Leslie, 1942). Therefore, it has been proposed that the bone changes are secondary to the increased peripheral flow in excess of the nutritional needs of the tissues. "However, the increased vascularity is probably an essentail feature of the syndrome and not the primary cause" (Ginsbur, 1965). Because PHOA has been reversed in humans after vagotomy and limb flow fell in a dog after bilateral cervical vagotomy in the absence of cardiac output change, Holling et al (1961) proposed that the afferent fibers of the reflex underlying osteoarthropathy were carried by the vagus. Vagal stimulation causes a fall in osseous blood flow and marrow pressure acutely (Shim and Patterson, 1967). It is conceivable that chronic vagal stimulation might elicit the same response of neo- and hypervascularity that chronic ishcemia elicits, but that still does not account for the periosteal inflammation. Though the pathogenesis of PHOA remains an enigma, it is most likely that the periostitis is the primary change, and there is increased flow in response to the increased bone formation by a reactive periosteum. This di-

sease is probably like disease in general (except when TAF-like factors come into play); blood flow responds to tissue needs, needs which are abnormal in abnormal or disease tissue.

I. Bone Seeking Radionuclides and Bone Scanning

Nearly every disease of bone is characterized by an increase or decrease in blood flow to the diseased areas. Although the various bone-seeking radionuclides do not give accurate quantitative measurements of osseous blood flow, they certainly show qualitative changes in flow. Thus, diseased areas of bone can be identified as the areas with a pattern of tracer uptake that varies from the norm. Uptake is increased by primary or metastatic tumors, inflammatory diseases, arthritis, fractures, metabolic diseases, Paget's disease, reactive vascularity, and transient migratory or traumatic osteoporosis, all of which are associated with increased blood flow. Decreased uptake may be found in regions that have undergone radiation with acute osteonecrosis, bone cysts, aggressive bone-eroding non-osseous tumors, and plasma cell cytomas (Bell and Subramanian, 1979). Hence, bone scans following IV injection of bone-seeking radionuclides can be used to discover or localize bone neoplasms, to diagnose the cause of an atraumatic fracture or unexplained bone or joint pain, or to find soft tissue calcification in a patient with renal failure.

The increased or decreased uptake is seen early in the disease process, usually before roentgenographic changes manifest. X-ray changes depend on differences in bone density which are not visualized until 30-50% of the mineral matrix has been resorbed. Experimental osteomyelitis can be detected within 24 hours of innoculation by bone scans while it takes 7-10 days before discernable roentgenographic changes occur (Trevas et al,

1976). Stress fractures may not show up on x-ray films for up to six weeks, but they light up on bone scans immediately (Bell and Subramanian, 1979). Bone scans are an aide in predicting avascular necrosis as the scan immediately reflects decreased arterial flow to the femoral head, days before the degenerative changes begin to appear on x-ray. Bone lesions must be at least 1-1.5 cm. in diameter to be seen on x-ray. Metastases can be seen in bone scans 36-146 days before alteration in x-rays are noted (O'Mara, 1974). Moreover, roentgenograms can only detect osteolytic or osteoblastic tumors, while bone scans reveal tumors which involve no changes in bone density. They also identify neoplasms in the sternum and ribs, where they are often missed on x-ray. In one series, 72% of the metastatic lesions picked up by bone scans were missed on x-ray films (Hopkins et al, 1974). Bone scans can also be used to follow the efficacy of therapy on the tumors; roentgenogram changes reflecting density changes occur much too slowly for this. Nevertheless, since the bone "scan is highly sensitive but non-specific, abnormal areas should never be interpreted without corresponding roentgenograms to exclude benign causes of demonstrated lesions" (Hopkins et al, 1974).

The first bone-seeking radionuclides, ^{45}Ca and ^{32}P, became available forty-five years ago, but it was not until 1942 that an external radiation detector adequate to measure in vivo tracer distribution was developed. At this time, Treadwell moved a scintimetric probe over the skeletons of patients injected with ^{85}Sr and found increased radioactivity over breast and prostatic carcinoma metastases. "With the introduction of the rectilinear scanner in 1951, the commercial availability of the scintillation camera in 1963, and the subsequent development of a number of safer bone-seeking radiopharmaceuticals, tracer diagnosis of bone disorders has now come into

its own as one of the more widely used applications of nuclear medicine" (Bell, 1972).

A rather large number of nuclides are taken up by bone; these are listed in Table 8. Yet, most of these do not have the properties that would make them ideal for clinical use. An ideal bone-imaging agent has the following characteristics: 1) it is available on an immediate basis and easily prepared, 2) is easily sterilized, 3) is of low cost, 4) has no pharmacological effect, 5) causes no or minimal adverse reactions, 6) has rapid clearance from and low retention in soft tissue and blood, 7) has high bone uptake with high bone extraction efficiency (#6 and #7 giving a high target/background ratio), 8) can be imaged effectively with a conventional gamma counter (which requires relatively low gamma energies for high resolution studies) and 9) gives a low radiation dose, allowing scans to be performed in benign disease and in children (i.e., it should have a short half-life).

The properties of some of the bone-seeking radionuclides are listed in Table 9. The first six compounds have the greatest clinical use. ^{85}Strontium, one of the first tracers used, has a number of problems. It is slowly cleared from the blood and excreted in the colon, obscuring the pelvis. It requires a three to seven day wait between injection and scanning to clear the colon, unless a laxative is used. Its long half-life is associated with a high radiation dose, and therefore only small amounts of it are administered (.15 mCi); consequently, the patients must be scanned for long periods of time. Finally, ^{85}Sr has a gamma energy that is too high for high resolution studies with conventional gamma counters (O'Mara, 1974). ^{87m}Strontium has a lower gamma energy and a low radiation dose, but its half-life is too short considering its slow clearance from

TABLE 8*

BONE-SEEKING NUCLIDES

Alkaline Earth Metals	Be, Mg, Ca, Sr, Ba, Ra
Aluminum Metals	Ga, In
Transition Metals	Sc, Y, La
Lanthanides	Lu, Er, Sm, Dy
Actinides	Uranyl Ion
Group IVB Metals	Sn, Pb
Group IVA Metals	Zr, Hf
Group VB Metals	Bi
Group VIA Transition Metals	W
Halogens	F
Compounds	Alizarin, Tetracycline Tc-labelled phosphorous Compounds

*Adapted from McAfee, J.G. and Subramanian, G., 1966.

TABLE 9*

PROPERTIES OF BONE-SEEKING RADIONUCLIDES

RADIONUCLIDE	HALF-LIFE	GAMMA-ENERGY (KeV)	B ENERGY EBmeV	RECOMMENDED ADULT DOSE (mCi)	RADIATION DOSE (RADS) SKELETON	MARROW
^{85}Sr	65 days	514	.015	.15	3.89	1.35
^{87m}Sr	2.7 hr.	388	.082	10.	.71	.21
^{157}Dy	8.1 hr.	326	.014	10.	1.27	.55
^{18}F	1.85 hr.	511	.250	5.	.75	.20
^{99m}Tc-PyroP	6.02 hr.	140	.015	20.	1.08	.76
^{99m}Tc-MDP	6.02 hr.	140	.015	20.	.76	.49
^{135}Ba	28.7 hr.	268	.200	3.	4.08	.87
^{131}Ba	11.7 hr.	(124-496)	.043	.3	4.28	1.35
^{113m}In	1.7 hr.	390		5.	.	.
^{171}Er	7.5 hr.	296,308	.380	4.	3.0	.76
^{153}Sm	47 hr.	103	.290	1.	3.3	.85

*Adapted from Genant, 1974; O'Mara, 1974; Bell and Subramanian, 1979.

the blood. Scans must be performed one hour after injection, when there is still high blood and soft tissue background activity (Hopkins, 1974). ^{87m}Sr is also expensive. Expense makes another potentially useful agent, ^{157}Dysprosium, unavailable for clinical use (Bell, 1972). ^{18}Fluorine has many qualities that make it a good imaging agent. It has rapid clearance from blood, and the short half-life confers very little radiation. However, its short half-life limits its availability. It is only available at or near facilities that can produce ^{18}F with a nuclear reactor or a cyclotron. In addition, it emits high energy photons that are poorly detected by conventional scintillation cameras.

^{99m}Technetium-labelled polyphosphate was introduced in 1971 (Subramanian et al, 1971). Since then a number of ^{99m}Tc-labelled phosphorous compounds have been introduced. These can be classified into the following four groups according to the atoms between their phosphate groups: 1) pyrophosphates (P-O-P), 2) diphosphonates (P-C-P), 3) iminodiphosphates (P-N-P), and 4) analogues of the chelating agents EDTA and DPTA (P-C-N-P) (Bell and Subramanian, 1979). Those with the widest clinical use are pyrophosphate (PYro P), polyphosphate (Poly P), ethane-1, hydroxy-1, diphosphonate (EHDP) or edidronate; and methylene diphosphonate (MDP) or medronate (Russel and Cash, 1979).

The ^{99m}Tc-labelled phosphorus compounds are available at relatively low cost from commercial sources as freeze-dried kits containing stannous ion added as either chloride or fluoride. They are easily reconstructed when technetium pertetnetate (Na $^{99}TcO_4$) in isotonic saline is mixed with the freeze-dried ligand. This yields a tracer that satisfies all the requirements of an ideal bone imaging agent. The gamma energy (140 KeV) is low, the half-life (6.02 hr.) is relatively short, and the urine and blood

clearances are rapid. This allows for a high target/background ratio and high resolution studies with a low radiation dose. Scans are performed about three hours after injection. Of the various ^{99m}Tc-phosphates, blood clearance is as follows: MDP > EHDP > PYro P > Poly P. ^{99m}Tc-MDP is the most ideal compound presently available with the highest target: non-target ratio and the lowest radiation dose (Bell and Subramanian, 1979).

The skeletal distribution of the various bone-seeking radionuclides is mainly determined by blood flow. As discussed in Section V, however, with the possible exception of ^{18}F, the extraction ratios are not 100%, indicating that distribution is not flow limited. The extraction ratio of ^{99m}Tc-diphosphonates is low, 35% on single passage (Tothill and McCormick, 1975), though the overall skeletal uptake is eventually 50-60% of the injected dose (Treves et al, 1976). Uptake is affected by many parameters besides flow including the capillary permeability and amount of vascular surface area or the combined PS product, the amount of interstitial fluid and the rate of diffusion through it, the amount of absorptive bone surface available, the volume of rapidly exchangeable bone mineral, the rate of diffusion or tracer through bone, and the metabolic rate of bone turnover. Washout experiments reveal that nuclides pass through four compartments at four different rates, passing through 1) blood and across the capillary endothelium to 2) the interstitial fluid, then 3) across a bone cell-functional membrane of periosteum, endosteum, or osteocyte and perhaps peri-bone fluid to 4) be incorporated in the bone mineral (Kelly and Bassingthwaighte, 1977; Khan et al, 1979).

The transcapillary exchange is thought to be one of passive diffusion where the ions pass through either 10nm clefts between endothelial cells or

through pores of channels composed of chains of vesicles (Kelly and Bassingthwaighte, 1977). The rate of diffusion decreases as molecular size increases, and hence is relatively slow for the ^{99m}Tc-labelled diphosphonates, but is reportedly unaffected by charge (Davies et al, 1976). The transcapillary exchange occurs in the first 30 seconds after IV injection and is known as the early or vascular phase of uptake. At this time the tracer distribution is determined by blood flow and is high in areas of greater flow such as the metaphysis just under the growth plate in adolescents (Khan et al, 1979).

The late phase scans reflect uptake of the tracer into the bone matrix in a non-exchangeable form. The various bone-seeking radionuclides are taken up by different mechanisms. ^{18}F undergoes anionic substitution for hydroxyl and perhaps bicarbonate groups in the inorganic bone matrix. ^{141}Ce is deposited in osteoid (Genant et al, 1974). Strontium is a calcium analogue which undergoes cationic substitution in the hydroxyapatite crystals. Kinetic studies are interpreted as showing a rapid initial endothelial adsorption (vascular phase), a slower exchange with the surface (exchangeable bone) ions, and then the slowest phase of diffusion in the bone to become part of the non-exchangeable bone mineral (Bell, 1972). The ^{99m}Tc-labelled phosphorous compounds combine with solubilized Ca++ and bind hydroxyapatite crystals, displacing orthophosphate. The binding probably occurs via a chemical reaction because the rate increases with temperature (Jung et al, 1972).

King et al (1977) have developed a mathematical model describing the uptake of ^{18}F and ^{47}Ca from blood into the bone (Figure 10).

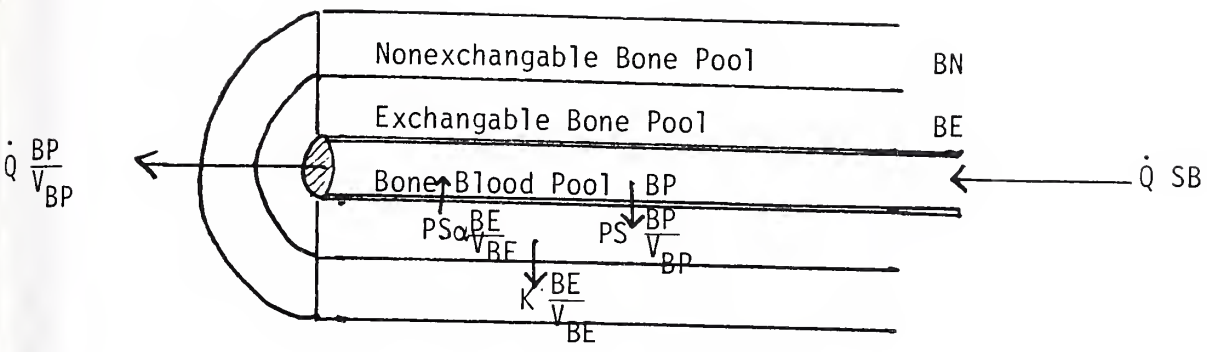

FIGURE 11

Using the symbols:

SB, BP, BE, BN = the concentration of radionuclides in Systemic Blood, local Bone blood, Exchangable Bone, and non-exchangable bone.

V = Volume

Q = Volume blood flow

PS = the capillary permiability x capillary surface area at the blood/bone interface

α = the partition coefficient between blood and exchangable bone

K = the rate constant for long term bone exchange and accretion

The equations governing the model are:

$$dBP/dt = \dot{Q}\left(SB - \frac{BP}{V_{BP}}\right) - \left(PS\frac{BP}{V_{BP}} - \alpha\frac{BE}{V_{BE}}\right.$$

$$dBE/dt = PS\left(\frac{BP}{V_{BP}} - \alpha\frac{BE}{V_{BE}}\right) - k\frac{BE}{V_{BE}}$$

$$dBN/dt = k\frac{BE}{V_{BE}}$$

Since ^{99m}Tc-diphosphonate has a slower blood clearnace than ^{18}F or ^{47}Ca, the effect of V_{BE} on uptake would be enhanced at the expense of the effect of Q.

The above model is simplified. The rate of calcium and phosphorous exchange is not one of simple kinetics for the local environment is affected by alkaline and acid phosphatases released by osteoblasts and osteoclasts, respectively. These cells in turn are regulated by many circulating substances, a few of which are Osteoclast Activating Factor (OAF), thyroxine, parathyroid hormone, and ultimately serum calcium and phosphate concentrations. Pyrophosphate may have a regulatory role in bone. It inhibits hydroxyapatite formation and breakdown both in vivo and in vitro (Jung et al, 1972). The diphosphonates also have these inhibitory functions but their action in vivo is greater as they are resistant to hydrolysis by the pyrophosphatases. The effects of the different phosphorous compounds vary, implicating that there is more than one class of phosphate binding sites on the hydroxyapatite crystals. In binding site affinity, ability to displace orthophosphate and inhibition of crystalization of calcium phosphate, the effects of EHDP > PYro P > MDP. Yet, PYro P > EHDP > MDP in total binding capacity and the degree of inhibition of hydroxyapatite disolution (Jung et al, 1972). The authors suggest that the second set of effects is because the larger diphosphonate molecules occupy more space or because there are a greater number of sites that will bind pyrophosphate.

Autoradiographic studies show that nuclides that bind hydroxyapatite have the highest uptake in areas of active mineralization, the metaphysis, the endosteal and periosteal surfaces of the cortex, and at the cement lines of the osteons (Khan et al, 1979; Tilden et al, 1973). There is higher up-

take in the trabecular bone of the epiphysis and metaphysis than in the cortex; not only are these areas of rapid growth, but trabecular bone has a surface to volume ratio three to four times that of compact bone (Genant et al, 1974). Nevertheless, these tracers still distribute diffusely throughout the whole bone, wherever hydroxyapatite is present. Lavender et al (1979) made a gross comparison of regional tibial blood flow to ^{99m}Tc-MDP uptake. They found that flow was maximal at the proximal tibia with relatively little in the shaft and distally. The ^{99m}Tc-MDP followed the same trend, but had a much more uniform distribution throughout the bone.

Although all of the above information indicates that the distribution of ^{99m}Tc-labelled phosphorous compounds is not due solely to osseous blood flow, the relative importance of flow is unknown. A number of investigators have attempted to ascertain this by comparing flow and ^{99m}Tc-phosphate uptake in abnormal bones. Genant et al (1974) decreased flow to the right lower extremity of the rat by immersing it in ice and found that while flow measured with albumin microspheres decreased 60% from that in the control limb, ^{99m}Tc-EDPH and ^{99m}Tc-Pyro P uptakes only dropped by 30% (^{18}F and ^{85}Sr uptakes showed greater flow dependence, dropping by 55% and 50%, respectively). Siegel et al (1976) decreased flow to the rat lower limb by ligating the femoral artery. They, too, found that the number of microspheres, or flow, decreased more over the control leg than did the ^{99m}Tc-EHDP after 3 hours, with the decreases respectively being 56% and 33%. Thus, though uptake does decrease with decreased blood flow, it appears that the extraction of the ^{99m}Tc-phosphate compounds is significantly increased at low flow rates.

Siegel et al (1976) increased flow rates by fracturing rat bones and found that flow to the fractured limb increased to a greater extent than

^{99m}Tc-EHDP uptake. This finding is at variance with later studies, all of which find increased extraction of ^{99m}Tc-labelled phosphates at the site of fracture. However, Siegel's group did not find increased uptake in a fractured leg if the femoral artery was ligated; in this case, tracer uptake increased despite decreased blood flow. Garnett et al (1975) compared ^{99m}Tc-Pyro P uptake in abnormal/normal human bone to ^{18}F uptake, which was supposed to represent flow. The ratios of percent increase in ^{99m}Tc-Pyro P over the percent increase in ^{18}F were as follows: 1.31 in an old fracture, 1.41 in a united osteotomy, and 1.32 in a metastatic tumor. Hughes et al (1978) found an increased uptake of ^{99m}Tc-MDP at osteotomy sites and attributed it to a) increased flow and capillary surface area secondary to recruitment and dilation of the capillary beds, and b) increased number of mineral binding sites on the new bone. They concluded that there was no change in capillary permeability since the extraction of ^{85}Sr did notchange. Lavender et al (1979) also performed osteotomies to obtain increases in flow, measured by 15 μm microspheres and ^{81m}Kr gas. Flow increased by 100% at the osteotomy site compared to an 800% increase in ^{99m}Tc-MDP uptake. The increased uptake at fracture sites is consistent with the autoradiographic studies in normal bone in that both studies show high uptake in areas of new bone formation. Similarily there is marked increased uptake in rachetic rat bone after treatment (Genant et al, 1974) and in reparative bone that forms in response to experimental tumors (Galasko, 1975). This may be partly due to the fact that the hydroxyapatite crystal in new bone are smaller and thus have a greater surface area and number of binding sites (Termine and Posner, 1967). Galasko (1975) proposes that tracer uptake is determined by the proportion of osteoid and woven new bone.

In summary, ^{99m}Tc-MDP has been found to be an ideal and clinically valuable agent for bone scanning. The main determinant of uptake appears to be flow, but uptake remains more constant than flow in conditions of abnormally decreased flow. Uptake seems to be increased more than flow in areas of new bone formation which have increased osteoid and increased surface area due to both the trabeculae and spicule formation and the smaller hydroxyapatite crystals. The increased extraction in areas of pathology serves to make ^{99m}Tc-MDP a better, more sensitive scanning agent than if it were purely a flow limited. The determinants of the local distribution of ^{99m}Tc-MDP are still only conjectured. The above experiments, with the exception of Siegel et al, have questionable statistical significance with N = 2 or 3. Several groups of investigators assume that the uptake of ^{18}F or ^{85}Sr is directly correlated to blood flow and that their extraction ratios do not vary with varying flow rates even though the extraction of the ^{99m}Tc-phosphate compound does. They examine changes in total bone flow and uptake in pathological situations. In the "normal" bone of Lavender et al (1979), all of the branches of the tibial artery, except the nutrient attery, are ligated. The correlation of blood flow to tracer uptake in the different tissues of normal, healthy bone under physiological conditions is not presently known. The only current information on regional uptake are autoradiographic studies which show where there is qualitatively increased uptake. These studies are neither quantitative nor do they correlate ^{99m}Tc-phosphate uptake with regional osseous blood flow. This study compares blood flow to ^{99m}Tc-MDP uptake in the various skeletal tissue types in many regions of bone under physiologic conditions.

III. MATERIALS AND METHODS

A canine model was chosen because "among common laboratory animals, the dog appears to have an osseous structure and circulation closest to those of man" (Cumming, 1962). Osseous flow was quantitated in the tibae and femora of dogs in three different developmental stages: neonatal, immature, and mature. The distribution of a bone scanning agent, technetium-99m labelled methylene diphosphonate (Tc-99m MDP), was compared to blood flow in all immature and in many of the mature animals.

The neonatal group was composed of five day old German Shephard litter mates weighing 400-500 grams each. In this group the secondary centers of ossification were not radiographically evident. These physiologically labile animals were injected with microspheres while anesthetized.

In the immature group, well defined secondary ossification centers and growth plates were desired. In the canine tibia and femur, the various secondary ossification centers appear between five days and eleven weeks (Hare, 1961), and fuse with the primary ossification centers between eight and twelve months of age (Hare, 1960; Chapman, 1965). Hence, four month adolescent pups were used. These five mongrels were of both sexes and weighed between twenty-eight and thirty-eight pounds. Three came from one litter, two from a second one. All dogs appeared healthy at the time of injection. One animal, however, (from the litter of three) had recently recovered from a severe bout of tracheal bronchitis and had been recently treated with antibiotic medication. The results of injection in this animal were excluded from the composite results.

In the mature dogs over two years old, all the secondary centers of ossification had fused, as verified by radiographs of the lower extremity long bones. These five dogs were of mixed breed from both sexes. Four were large (60-77 lbs.) and one of medium size (30 lbs.).

A. Surgery

After an IV injection of surital (adolescent and adult dogs), the older dogs were intubated and respirated with 50:50 O_2:NO_2 while being maintained under anesthesia with halothane. Infant pups were anesthetized with an intraperitoneal injection of sodium pentabarbitol and were ventilated via a midline tracheostomy. A muscle relaxant (1-2 ml. Flaxidyl) was administered and an IV drip of Ringer's lactate was started via a left jugular vein catheter. The left carotid artery was cannulated.

A left thoracotomy via the fourth or fifth intercostal space exposed the heart. After a small pericardial incision, the left atrial appendage was isolated and catheterized with a fine polyethylene multipore catheter. The immature and mature animals were awakened. Catheters were flushed with heparinized saline and covered with dressings.

Prior to microsphere injection, blood samples were analyzed to verify normal hematocrits and blood gases. The neonatal pups were injected in the anesthetized state while the immature and mature dogs were injected only when alert and ambulatory. Cardiac pressure tracings demonstrated normal patterns.

B. Injection

1. Tc-99m MDP

Regional technetium-99m methylene diphosphonate was quantitated in all the immature and three of the mature dogs. Fifteen mCi of a commercial preparation of Tc-99m MDP (Osteolyte) was injected into the left jugular catheter. Bone scans were performed three hours later, when blood levels of the tracer were 3-5% of the injected dose. After the dog had been scanned it was prepared for microsphere injection.

The tibiae and femora were scanned a second time after they had been removed from the dog. The second set of scans revealed no apparent change of distribution of Tc-99m within the lower extremity bones. Sev-

eral animals had preliminary Tc-99m MDP bone scans performed one week prior to surgery. The preoperative and postoperative scans were indistinguishable.

2. Microspheres

Radioactive microspheres injected via the left atrial catheter were employed to quantitate blood flow in all animals. The spheres were suspended in 10% dextran with .05% Tween 80 surfactant to prevent aggregation. Minimal aggregation was observed under light microscopy. One milliliter of suspension contained 4.3×10^6 microspheres with a specific activity of 100 μCi. The activity of the microsphere in the energy windows used was sufficient to minimize gamma counting errors to less than 15% when as few as 100 microspheres were present per sample. Radionuclides used included Chromium-51, Strontium-85, Niobium-95, and Scandium-46. Because these radionuclides and Technetium-99m possess distinct energy peaks, it was possible to carry out multiple injections on a single animal and reliably quantitate the distribution of each injection.

A calibrated Harvard withdrawal pump collected the reference flow from the carotid artery catheter at a calibrated rate dependent on the animal size. Five seconds after withdrawal had commenced, microspheres were injected gradually into the left atrial catheter over a 30 to 60 second period to average heterogeneity in the cardiac output or osseous circulation. The neonatal animals received 1 ml. injection while the immature animals received 3 to 4 ml. The withdrawal was continued for at least 90 seconds after completion of injection.

Three animals had a second 2 ml. injection of microspheres with a different radionuclide label in the same manner as the first injection. Close agreement of flow values were obtained in the doubly injected animals.

Animals were sacrificed with an overdose of sodium pentobarbital injected into the left atrium, followed by an air embolus.

C. Processing of Bones

The tibiae and femora were removed from the dogs and thoroughly cleaned of all muscle, tendon and ligaments. The periosteum was placed into preweighed glass scintillation vials and its weight determined. The intact uncut bones were weighed. Bones were sectioned into as many anatomically and physiologically relevant sections as possible while maintaining a sufficient number of microspheres in each sample to provide statistically significant figures. The small bones of the neonatal animals were sectioned into 13 segments as depicted in Figure 14. As shown in Figure 12, the immature tibiae and femora were cut in 32 and 41 sections, respectively. Each mature animal femur was divided into 32 segments, while each tibia had 25 sections (see Figure 13). Sectioning was accomplished using a band saw, a fine bladed zigsaw, a fine toothed electric hand held circular saw, curettes and scalpel. Each segment was immediately sealed in a preweighed glass scintillation vial and was reweighed. Uncut segments were maintained in saline moistened sponges to prevent drying. A 10% loss in total bone weight which occurred in the cutting process was primarily due to sawdust loss rather than drying.

1. Neonatal Bones

The bones were cut as depicted in Figure 12. The cartilages of the greater trochanter (GtC) or tibial tuberosity (TubC) were cut away from the proximal epiphyseal cartilage of the femur or tibia, respectively. (The lesser trochanter was indistinguishable). The bone was then cut in half lengthwise and the marrow scraped out (DMar). The epiphyseal cartilage

was peeled off from either end of the bone and divided into an inner core (iEC) and an outer shell (oEC) of about 1.5 mm thickness. The masses of each oEC and iEC were approximately equal. The first 1.5 mm of metaphyseal spongiosa adjacent to the epiphyses (pMS) was cut away at either end of the bone. The cortex surrounding this area was too thin to be detected. The remaining 4 mm of metaphyseal (dMS) spongiosa was scraped out with a curette. The surrounding metaphyseal cortex was saved as the MCx. The remaining piece of bone was diaphyseal cortex (DCx).

2. Immature Bones (Figure 13)

First, the epiphyseal cartilage was peeled off and any spongiosa that remained attached to the inner surface was scraped away and put into a vial labelled "Unwanted Waste (UW)". If an avulsing force was applied to the remaining epiphyseal spongiosa while the shaft was held stable, the growth plate generally fractured through the zone of hypertrophy. The physis could then be peeled away from the epiphyseal spongiosa. Any red spongiosa which occasionally remained on the clear, white cartilaginous growth plate, was discarded into UW. The epiphyseal secondary ossification centers were then divided into an outer shell and inner sphere. The outer shell was about 1.5 mm wide, except in the larger distal femur where it was 3 mm wide. These widths were chosen so that the inner and outer sections were approximately equivalent in weight. The secondary ossification center of the lesser trochanter was left in one piece because it was so small. The distal femoral epiphyseal areas were further divided into medial and lateral halves.

The metaphyseal areas were enclosed by a very fine cortex extending

from the growth plate to the diaphyseal marrow where the cortex began to thicken. As shown in Figure 12, each metaphyseal spongiosa was divided into four regions. The distal metaphyseal portion (dMS) was furthest from the physis and extended from the midpoint of the metaphysis to the diaphysis. The distal metaphyseal cortex (dMCx) had the same boundaries. The remaining metaphysis was again divided in half with the piece adjacent to the dMS being the middle distal metaphyseal spongiosa (mdMS). The final quarter of metaphysis included the larger middle proximal metaphyseal spongiosa (mpMS) and the proximal metaphyseal spongiosa (pMS), a segment 1.5 mm in width located just under the growth plate. The proximal metaphyseal cortex (mPCx) was the extremely thin cortex surrounding the pMS, mpMS, and mdMS.

Because of anatomical differences, the metaphysis of the proximal femur was cut differently than just described. The pMS was still 1.5 mm wide with the mpMS adjacent to it, but these two areas were found in both the femoral neck (Fn-mPS and Fn-mpMS) and the metaphysis of the greater trochanter (Gt-pMS, Gt-mpMS). The cortices of these two areas were saved as the Fn-MCx and Gt-MCx. The remaining metaphysis was divided through the area where the lesser trochanter had been to create an introchantic (It-MS and It-MCx) and distal metaphysis (dMS, dMCx). The cortex and spongiosa were separated with a hand saw, minimizing any visible red cancellous bone on the inner surface of the white cortex. If at any time it was very difficult to ascertain whether a bone fragment was cancellous or compact, it was discarded into the UW vial.

The diaphyseal marrow (DMar) of the immature long bone was fatty and yellowed in the mid-bone region (mDMar), turning to a deep red, bloody marrow towards the ends of the bone. It was divided at the junctions of fatty

and bloody marrow to create a proximal, middle, and distal marrow (pDMar, mDMar, distal DMar) according to the anatomically defined proximal and distal ends of the whole bone. The surrounding cortex was cut at the same junctions, creating the pDCx, mDCx, and dDCx. The marrow was reamed out thoroughly with curettes, again leaving a white inner cortical surface. This process may have deleted up to 50% of the endosteum; however, there was no other conceivable way to divide the irregular marrow-cortex junction cleanly. In preliminary experiments, the cortical segment was divided into inner and outer hollow cylinders, but since the flows in the two areas were not significantly different and the task was extremely tedious, this practice was stopped.

3. Mature Bones (Figure 14)

Since many distinct anatomical areas fuse with age, the mature bones were cut into fewer sections than the immature bones. The mature femora were each divided into 32 areas and the tibiae, into 25 areas. The differences between mature and immature bone areas were as follows. Rather than epiphyseal cartilage, the adult had articular cartilage (AC) over all secondary ossification centers except the greater and lesser trochanters and the tibial tuberosity, and thin shells of cortex (ECx) over all but the tibial tuberosity, where the cortex (Tub-Cx) was much thicker. Each epiphyseal spongiosa was left as one piece rather than being divided into outer shells and central cores. As in the immature femora, the mature femoral epiphyseal spongiosa for three dogs was divided into medial and lateral halves (me-ES and l-ES).

Of course, there were no physes in the mature bones. The epiphyseal-metaphyseal junction was not separated by a distinct growth plate and was

difficult to delineate. Therefore, it was impossible to accurately cut the first 1.5 mm of the metaphysis. The whole quarter of each metaphysis adjacent to the epiphysis, the immature pMS and mpMS was cut as one piece in the adult, the pMS. The mature mMS and dMS were equivalent to the immature mdMs and dMS, respectively. The distal metaphyseal cortex (dMCx) was that surrounding the pMS and mMS. In the mature proximal femur, the metaphyseal spongiosa of the femoral neck (Fn-MS) and the greater trochanter (Gt-MS) were each left as one piece. Otherwise this area was cut the same as in the immature femur. The distal femoral metaphysis was cut differently, as its spongiosa was visibly separable into a red central cylinder and an outer cylinder of white cancellous bone. Thus, a distal central MS (dcMS) was cut, surrounded by the distal outer MS (doMS), which in turn was surrounded by the dMCx. The middle and proximal central MS (mcMS, pcMS) were both enclosed by the proximal outer MS (poMS) which was in turn enclosed in the pMCx.

The mature diaphyses were composed of a central fatty marrow (DMar) sandwiched between two regions of spongiosa (pDS, dDS) which corresponded to the immature pDMar and dDMar. The DSs were distinguished from the dMSs by the more friable spongiosa and thicker surrounding cortex of the diaphysis. The pDCx, mDCx, and dDCx were the cortices enclosing the pDs, DMar, and dDS, respectively.

D. Computation of Results

Tissue flow rates were calculated by the reference-flow microsphere technique where the adjusted radioactive count rate (cpm) in each sample was related to the flow by the following equation:

$$F_T = F_R \left(\frac{C_T}{C_R} \right)$$

where

C_T = radioactive count rate in the tissue sample, cpm

C_R = radioactive count rate in the reference flow blood, cpm

F_T = flow rate to the tissue sample, cc/min

F_R = withdrawal flow rate, cc/min.

This flow was normalized by the tissue weight so that all flows were expressed in cc/min/100g. The cpm were adjusted for the cross-over ratio between energy windows of different isotopes whenever more than one isotope was used. The number of microspheres was calculated using a standard sample with a pre-determined number of microspheres. The mean, standard deviation, coefficient of variation, and standard error were calculated for all flow rates. In order to examine regional and developmental differences in osseous circulation, the samples were compared to each other using the two-tailed Student's T-test. Equivalent regions between the three age groups also were compared. Histograms illustrating the mean flow value with its standard deviation were drawn to depict the results.

E. Bone Region Recombination For Developmental Circulation Comparison

In order to compare the bones of the three age groups, the weights and flows of certain adjoining regions in a bone were combined so that each age comparison would have equivalent bone regions with respect to number, relative size, and distribution.

For the immature and mature comparisons, the immature outer and inner ossification centers were combined as epiphyseal spongiosa (ES).

In the distal femoral epiphysis, the me-o20, l-o20, me-c20, and l-c20 were combined as one ES. The immature pMS and mpMS were combined as the pMS, the equivalent of the original mature pMS. In the distal femur, the immature pMS, mpMS and mdMS all became the pMS. The mature pcMS, mcMS, and poMS were added together as the new pMS; the mature doMS and dcMS were combined as the dMS. Because the adult has articular cartilage and cortex over its epiphyses while the immature canine only has cartilage, the various mature ACs ECxs were combined to make EC/Cxs. The immature EC was considered the same as the EC/Cx. In the distal femur, the me-EC and l-EC became D.EC/Cx. The mature diaphyseal spongiosa was considered equivalent to the immature red marrow; hence, the pDS and pDMar were renamed the pDS/Mar, and so on for the middle and distal regions. The resulting divisions of the immature vs. mature comparison are depicted in Figures 15 and 16.

Furthermore, to compare the three developmental ages, the various tibial and femoral regions were recombined as illustrated in Table 11. The resulting areas used for the 3-age comparisons are illustrated in Figures 17 and 18.

Finally, in order to evaluate tissue collection according to the histological type rather than the anatomic location, the various regions were recombined into five primary osseous tissue types:

1) Cartilage (Cart.) included any cartilaginous region, i.e., oEC, iEC, AC, EC.
2) Cortex included all cortices, regions ending in "Cx".
3) Spongiosa (Spong.) included epiphyseal spongiosa or secondary ossification centers, all metaphyseal spongiosa and mature pDS and dDs.

4) Marrow (Mar.) included only soft diaphyseal marrow.

5) Growth Plate (GP) was present only in the immature bones since the neonatal "growth plate" was part of the oEC and was not distinct.

As with the original regions, the flow values for the immature vs. mature comparisons were evaluated via computer to obtain the mean, standard deviation, coefficient or variation, and standard error for each region in an age group. Two-tailed Student's T-tests were done comparing first all the region to its equivalent mature region. The same computer work was done for the nine-region developmental comparisons including multiple T-tests. In addition to comparing the regions within each bone, and comparing immature vs. mature, immature vs. neonatal, and neonatal vs. mature tibiae and femur, the tibia and femur within each age group were compared via two-tailed T-tests.

The flows to the histologically-defined osseous tissues for each age group were similarly evaluated and compared.

3-Age Comparison	Infant	Adolescent	Adult
P.Epi	P-oEC + iEC	P + EC + o20 + c20	P-AC + ECx + ES
Tub	Tube	Tib C + Tub 20 + Tub fib	TubS + Tub Cx
P.MCx	MCx	pMCx + dMCx	pMCx + dMCx
P.MS	pMS + dMS	pMS + mpMS + mdMS + dMS	pMS + MMS + dMS
DCx	DCx	pDCx + mDCx + dDCx	pDCx + mDCx + dDCx
DMar	DMar	pDMar + mDMar + dDMar	pDS + DMar + DDs
D.MS	PMS + dMS	pMS + mpMS + mdMS + dMS	pMS + mMS + DMS
D.MCx	MCx	pMCx + dMCx	pMCx + dMCx
D.Epi	D-oEC + iEC	D-EC + o20 +c20	D-AC + ECx + Es

TABLE 10

FEMUR

P.Epi	E-oEC + iEC	FhEC + Fho20 + Fhc20	AC + FhES + FhECx
Gt	GtC	GtEC + Gto20 + Gtc20	GtES + GtECx
P.MCx	MCx	FhMCx + GtMCx + ItMCx + dMcx	FhMCx + GtMCx + ItMCx + dMCx
P.MS	pMS + dMS	FhpMS + Fh-mpMS + Gt-mpMS+ ItMS + dMS	GhMS + GtMS + ItMS + dMS
DCx	DCx	pDCx + mDCx + dDCx	pDCx + mDCx + dDCx
DMar	DMar	pDMar + mDMar + dDMar	pDS + DMar + dDS
D.MS	pMS + dMS	pMS +mpMS + mdMS + dMS	pcMS + mcMS +dcMS + poMS +doMS
D.Mcx	MCx	pMCx + dMCx	pMCx + dMCx
D.Epi	D-oEC +iEC	me-EC + l-EC + me-o20 + me-c20 + l-c20	AC + ECx + ES

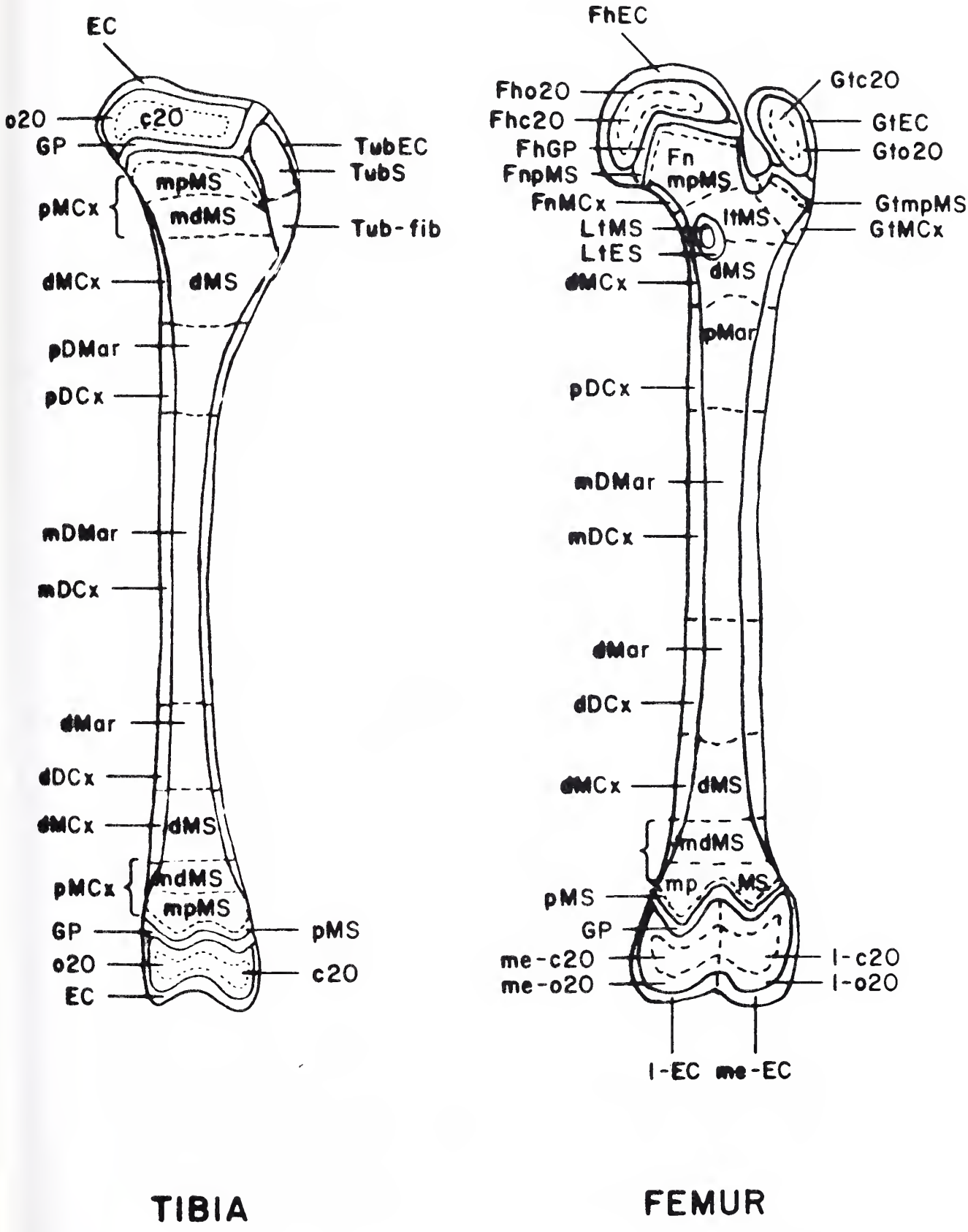

FIGURE 12
IMMATURE PUP BONE REGIONS

FIGURE 13
MATURE DOG BONE REGIONS

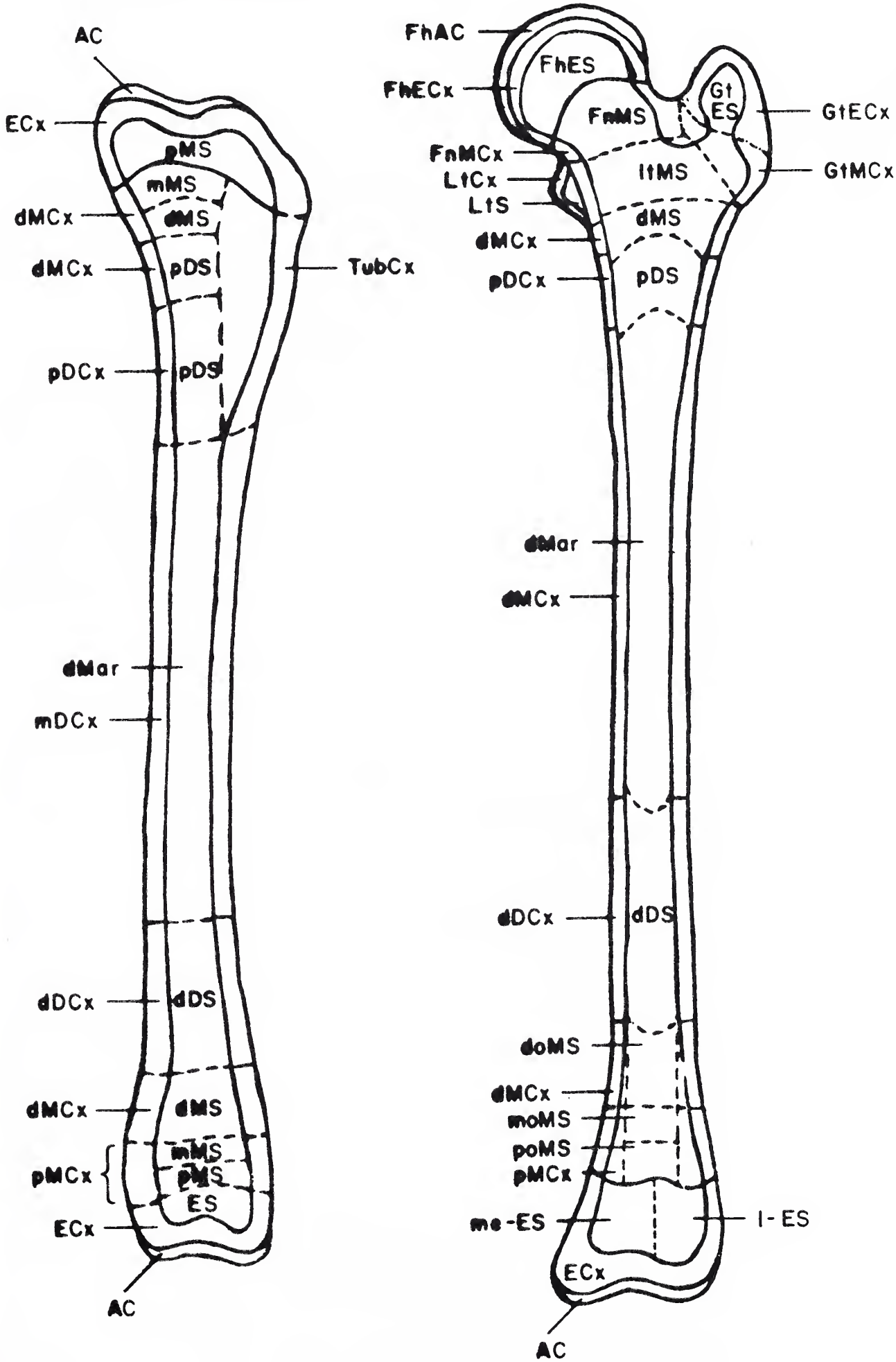

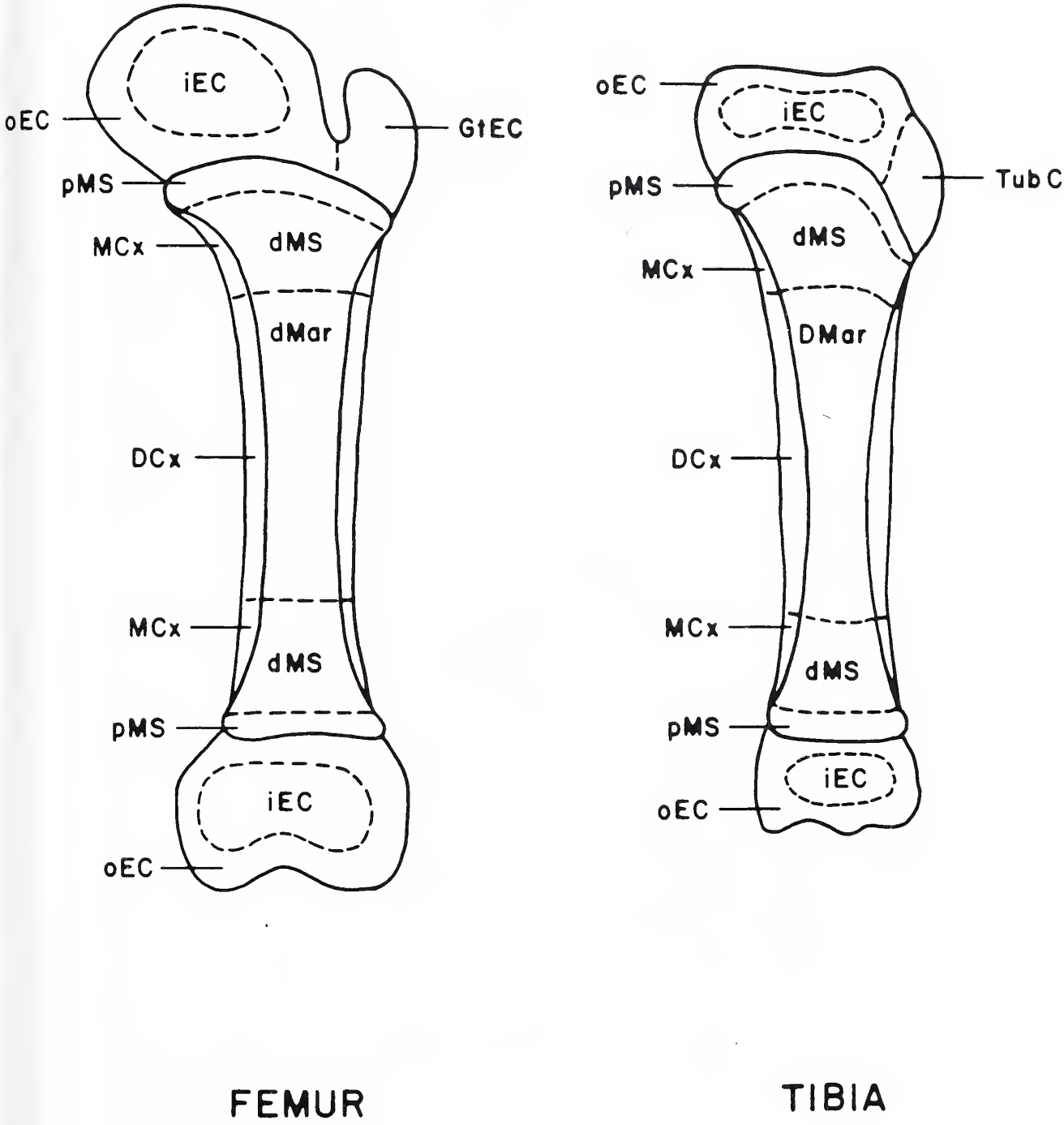

FIGURE 14
NEONATAL PUP BONE REGIONS

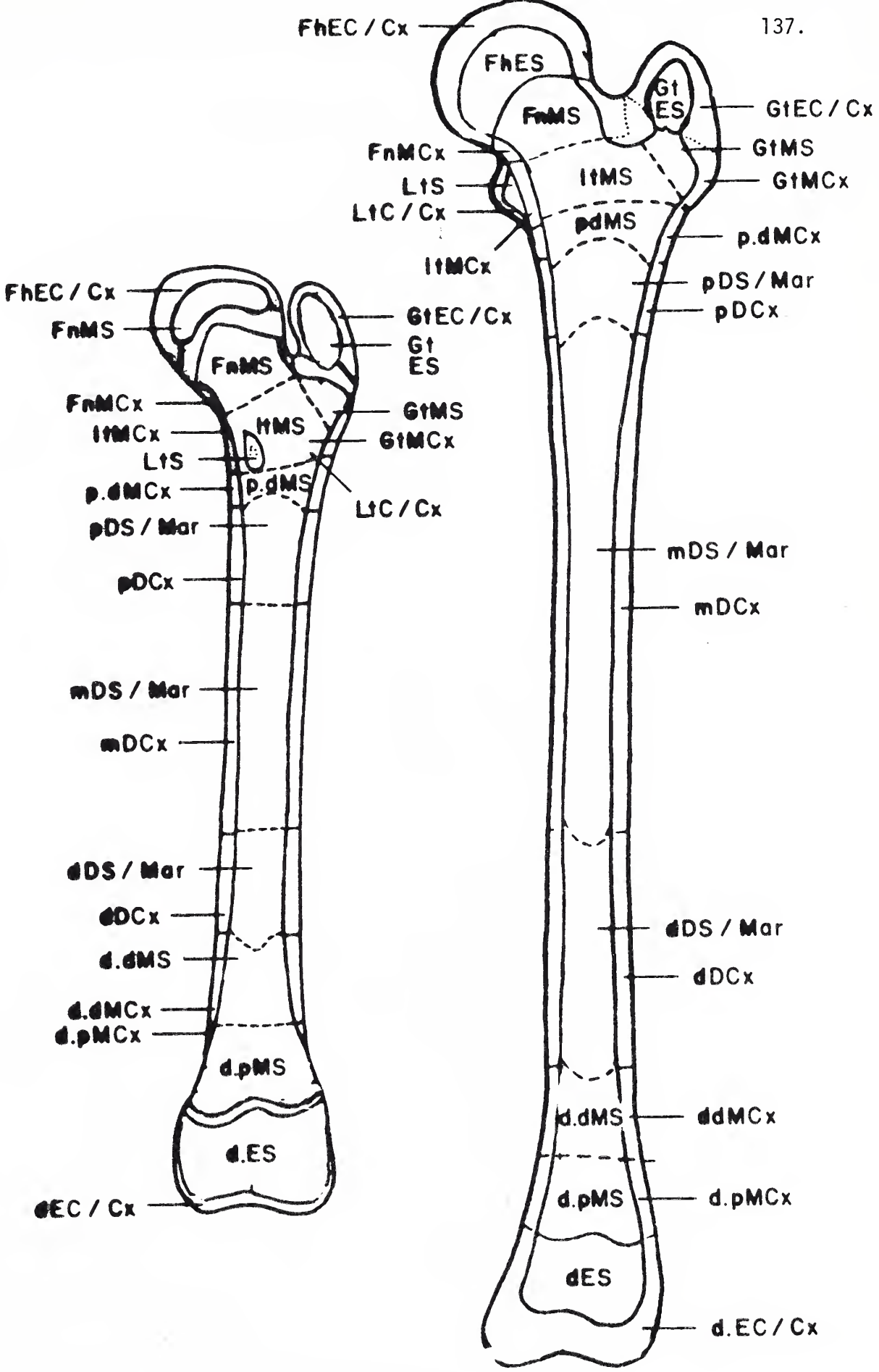

FIGURE 15
BONE REGIONS FOR COMPARISON OF IMMATURE VS. MATURE FEMUR

IMMATURE MATURE

FIGURE 16
BONE REGIONS FOR COMPARISON OF IMMATURE VS. MATURE TIBIA

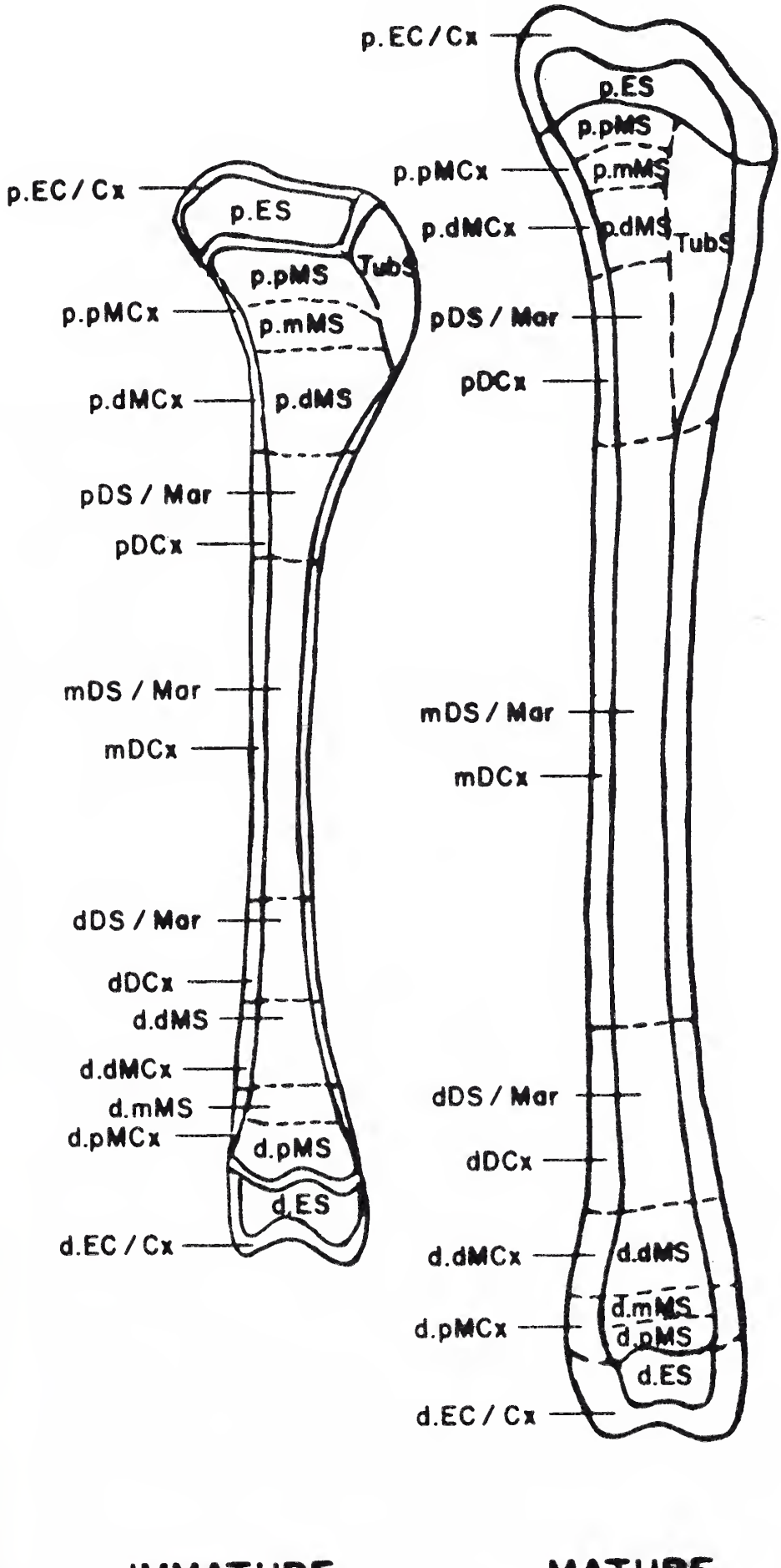

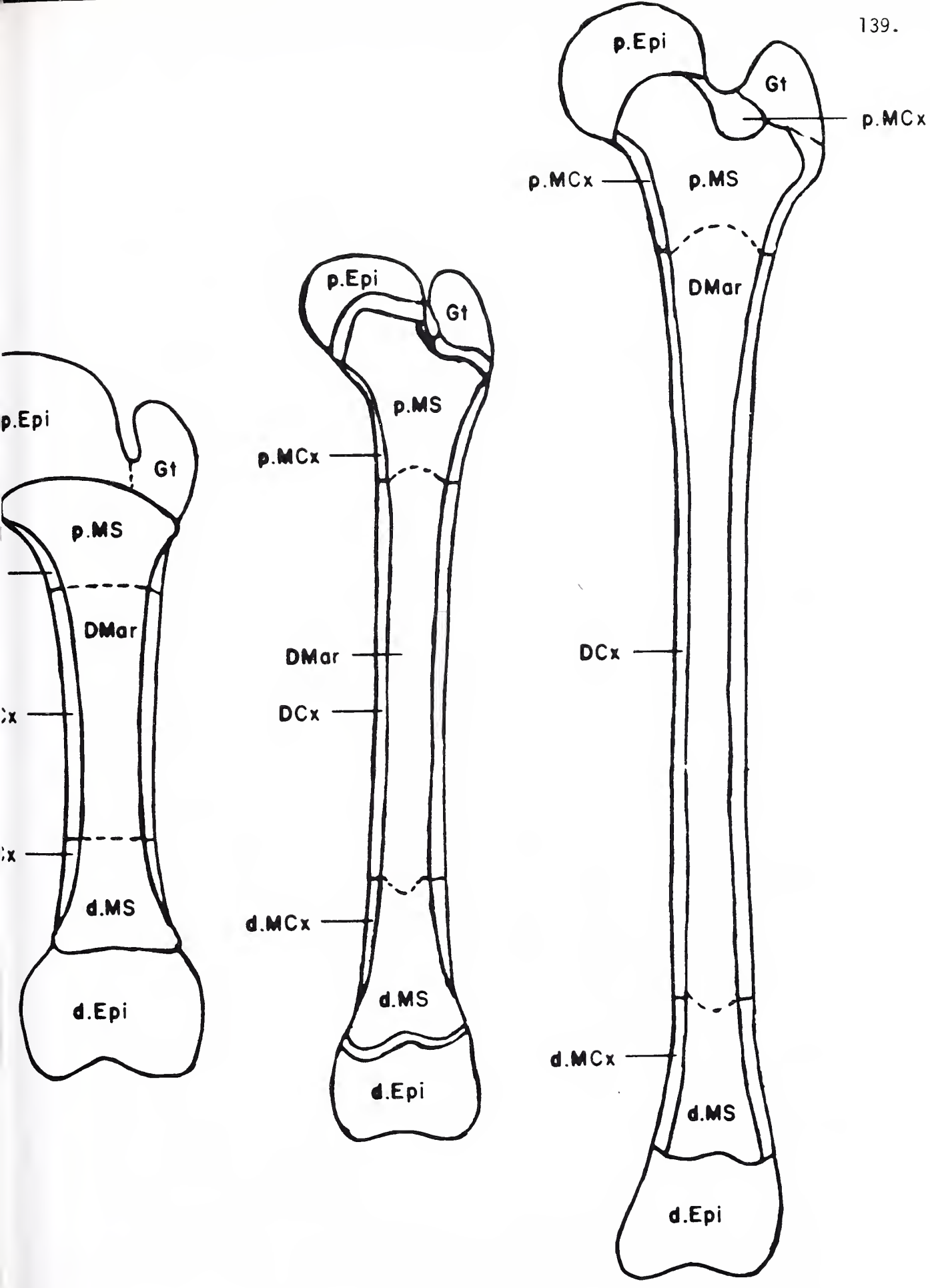

FIGURE 17
RECOMBINED FEMORAL BONE REGIONS FOR THREE-AGE COMPARISON

NEONATE IMMATURE MATURE

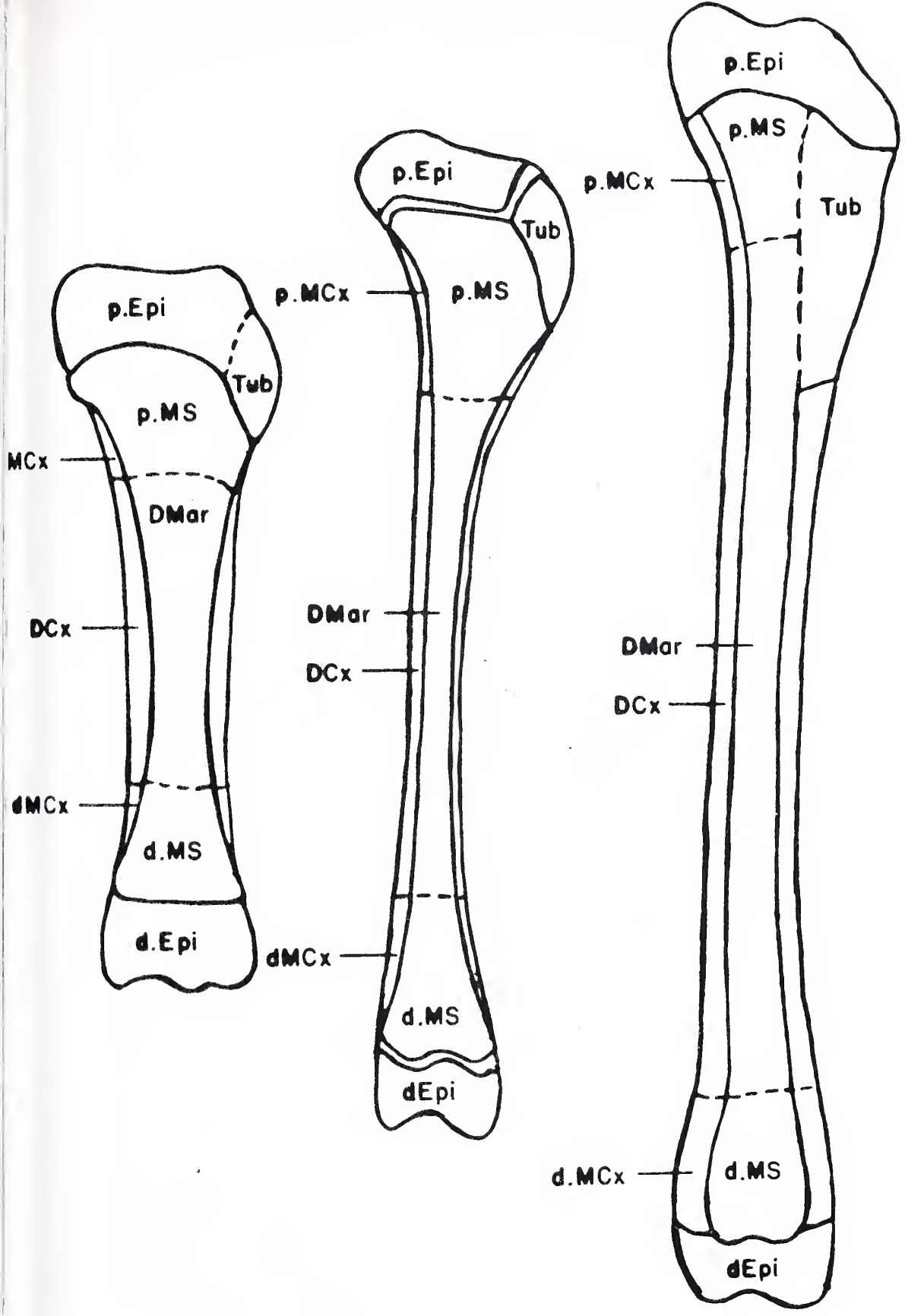

FIGURE 18
RECOMBINED TIBIAL BONE REGIONS FOR THREE-AGE COMPARISON

IV. RESULTS

The results are plotted as bar graphs (Graph 1-60). Each bar represents the mean value (± standard deviation) for that region. The graphs are all at the end of this section, followed by the computer outputs of means, standard deviations (S.D.), coefficients or variation (CV) and standard (STD) errors of the mean.

The T-test results are included in part on the bar graphs. Here no mark between two bars means they are definitely different ($p \leq .01$), "*" means probably different ($p \leq .05$), "◇" means not statistically different, "=" means probably the same, ($p \geq .90$), and "≡" mean definitely the same ($p \geq .99$). If two adjacent bars or several bars, for example, are not different, this is represented as follows:

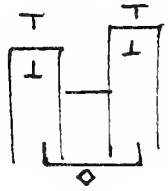

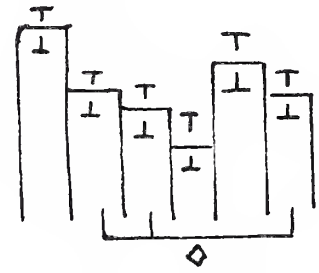

In the written body of the paper a third though similar set of figures is used to show that the mean values are significantly different or the same. These are >, >*, ≥, =, ≡. "A ≥ B" means that although the mean of A is greater than the mean of B, the distribution of values in A are not statistically different than the distribution of values in B. The sets of symbols are as follows:

	Bar Graphs	Written Text
definitely different, $p \leq .01$		>
probably different, $p \leq .05$	*	>*
not different, not equal	◇	$\underline{>}$
probably the same, $p \geq .90$	=	=
definitely the same, $p \geq .99$	≡	≡

The number of microspheres in each bone region are represented on the graphs by circles above the upper standard deviation where

0 means <100 microspheres

● means 100-400 microspheres

no marks means >400 microspheres.

The results are also tabulated in Tables 11 through 38. In these tables, Age = 1, 2, or 3 corresponds to neonatal, immature, or mature bones, respectively. Bone = 1 refers to the femur while Bone = 2 refers to the tibia.

A. Quantitative Osseous Circulation

1. Technique

To check the validity of our technique, T-tests comparing the equivalent bone regions in the right vs. the left limbs are performed. In nearly every instance, the right and left regions are not significantly different. This verifies the evenness of microsphere mixing and the consistency of the cutting of the various bone regions. Theoretically, there must be a mean of 400 microspheres per sample to limit the error to 15% at a 95% confidence level. With only 100 microspheres, the random error is 40%. Our results compared favorably with the theoretical expectations. In a given bone, the adolescent femur, the average coefficient of variation ± S.D. for blood flow bone regions containing more than 400 microspheres was 19 ± 5. Regions with 100-400 microspheres had a mean coefficient of variation of 28 ± 10, and regions with less than 100 microspheres had a mean coefficient of variation of 41 ± 11. In all bones except the adult femur, more than half of the regions had over 400 microspheres apiece. There were only a few regions with less than a mean of 100 microspheres. These regions included the following: in the adolescent bones, all the epiphyseal cartilage of the lesser trochanter regions and the tibial tuberosity; in the infant tibia, the metaphyseal cortices and the distal dMS; and in the adult bones, the articular cartilages, the periosteum, the lesser trochanter cortex and the distal tibial metaphyseal cortex. In the regions just listed, the microsphere technique can show only qualitative differences in osseous blood flow. In all the other regions, it is an accurate method for quanti-

tating osseous circulation.

The simplest way to examine the results is first look at the largest areas (the total bones) then the largest divisions (the gross tissue types) and progressing to even smaller regions.

2. Total Bone Flow

	cc/min/100 grams			cc/min/total bone		
	infant	adolescent	adult	infant	adolescent	adult
femur	34.4	23.7	16.6	40 ± 16	1785 ± 558	1711 ± 858
tibia	36.9	15.4	5.2	26 ± 11	851 ± 137	380 ± 195
tibia and femur	35.4	20.2	11.8			

Because there was variation in total bone mass among the dogs of the same age group, it is more relevant and accurate to compare flow in relative terms, cc/min/100g rather than absolute flow, cc/min/bone. Flow in cc/min/100g to both bones in the lower extremity drops with increasing maturity, $p \leq .01$. This drop is more prominent in the tibia than in the femur which respectively have 86% and 52% as much flow/gram in adulthood as they had in infancy. The tibia has slightly higher flow than the femur in infancy, then receives 65% as much blood/gram as the femur does in adolescence, and only 31% as much by adulthood. In terms of absolute total bone flow, the tibia receives less flow at all three ages since the tibia weighs less than the femur. The tibias get 65% as much absolute flow as the femur in infancy, half as much in adolescence, and one-fifth as much flow in adulthood.

3. Gross Tissue Flow

The flows to major tissue types in the three ages are plotted in Graphs 1-3. Within each group of three bars, the first bar represents neonatal, the middle bar immature, and the third bar mature animal tissue. In Graph 3, 'osseous' tissue refers to the composite means of both tibia and femur tissue data.

In five of the six bone groups studied, the spongiosa tissue has the highest flow. The exception is the immature animal femur in which spongiosa blood flow is second to, but not statistically different from, marrow blood flow. In the neonatal bone, flow to the spongiosa, which includes only metaphyseal spongiosa, far exceeds that to other tissue types. Although the relative rank order of flow to tissues in the neonatal femur (cortex $\geq$ cartilage $\geq$ marrow) is different than that in the neonatal tibia (cartilage $\geq$ marrow $\geq$ cortex), flows to these three tissues are not significantly different.

As the scales of the graphs are identical, it can be appreciated that each tissue in the neonatal femur receives about the same amount of blood flow as the corresponding tissue does in the neonatal tibia. The rank order of flow among the tissues in the immature animal is more similar than in the neonatal animals. Flow to the immature tibial tissues was ranked in the following order: spongiosa $\geq$ marrow $\geq$ growth plate > cortex > cartilage. Since the small cartilage sample contained less than 100 microspheres, its position in this sequence of regional blood flows is not well substantiated. The femur is similar except that the marrow receives more flow than the spongiosa. The order of flow is similar in both bones of the mature animals: spongiosa > marrow > cortex > cartilage. In the adult tibia, flows to the spongiosa and marrow are not significantly dif-

ferent. Flow to each femoral tissue exceeds that to the same tibial tissue in maturity and in immaturity in all significant cases.

When the flow values of the three ages in each tissue are compared, neonatal > immature > mature in all tibial tissues and in the femoral cortex and perhaps spongiosa. In the latter tissues, we find: neonatal > immature $\geq$ mature. The femoral marrow is different with the immature > mature > neonatal bone blood flow.

4. Developmental Regional Osseous Flow: Neonatal vs. Immature vs. Mature

In Graphs 4-7, the tibia and femur are each divided into nine regions. Again, the three bar clusters depict neonatal, immature, and mature flows, respectively. In all regions, the neonatal group has either the highest flow or is not significantly different from the adolescent (in the proximal and distal femoral epiphysis and the greater trochanter). The mature bone has the lowest flow in all regions except the femoral marrow, where the neonate is lowest, and the proximal femoral metaphysis, where flow in the adult is less than the neonate but greater than in the immature proximal femoral metaphysis.

Graphs 4 and 5 also demonstrate that the areas with the highest blood flow in the mature tibia and femur and in the immature femur are the metaphyseal spongiosa and the diaphyseal marrow. In the immature femur and the mature tibia femur, the diaphyseal cortex receives the least blood flow. The immature tibia differs in that its proximal epiphysis has a relatively low flow so that the order is proximal MS > proximal Epi $\geq$ DMar $\geq$ distal MS >.....> DCx > distal Epi. The immature tibial proximal Epi, however, is not significantly different from the DMar or the dMS.

The neonatal bone segments may be grouped into two regions according

to flow: 1) the metaphyseal spongiosa, none of which are significantly different, with high blood flows of 75 to 90 cc/min/100g, and 2) the rest of the bone with low blood flows ranging 15 to 30 cc/min/100g. The blood flow to the tibial tuberosity decreases with age. The tibial tuberosity receives about the same amount of blood flow as the distal tibial epiphysis of the same bone in the neonate and the adult.

In all bone regions except the greater trochanter, flow is higher during infancy than in the older age groups. The greater trochanteric epiphysis is unique in that it receives less flow during infancy than in adolescence. This latter age group receives about the same amount of blood flow as the capital and distal femoral epiphyses. At maturity the trochanteric flow value is intermediate between the mature distal femoral and femoral head epiphyses.

In every bone but one the order of regional cortical flow from highest to lowest is proximal MCx, distal MCx, DCx. The exception is the neonatal tibia in which DCx $\geq$ proximal MCx $\geq$ distal MCx, though there is no statistical difference in the flows to the three cortices. The differences in cortical flow are not significant in the immature tibia in which distal MCx $\geq$ DCx and the mature tibia in which proximal MCx $\geq$ distal MCx. In other areas the differences in flow are significant. The flow to each region of femoral cortex in a given age group is greater than to the corresponding region of the tibia, except for the neonatal tibial DCx (where tibia DCx > femoral DCx). Tibial cortical flow is very low in mature animals, especially in the midshaft area where the DCx receives only 2.1 cc/min/100g.

5. Neonatal Bones (Graphs 8-11)

Both the neonatal tibial and femoral bones were initially cut into thirteen regions. In general, the proximal metaphyseal spongiosas (pMSs) received the highest flow. All the other regions received less than one-fifth the flow of the pMS value. There is no significant differences between any of the pMS regions or between any of the dMS regions. The dMSs generally receive the lowest flow among all the bone regions. In all four major epiphyses, the oEC definitely receives less blood flow than the iEC.

6. Immature Bones (Graphs 12-19)

The epiphyses of the immature animals are divided into three regions. In every epiphysis, flow to the outer epiphyseal spongiosa or secondary ossification center (o20) > central spongiosa (c20) > cartilage (EC). Since the small cartilage sample contained less than 100 microspheres, its position in this sequence of regional blood flows is not well established. The distal femoral epiphysis is separated into medial and lateral condyles. In each of the three regions, 1) cartilage, 2) outer ossification center, and 3) inner ossification center, the medial condyle receives higher flows of gram tissue than the lateral condyle, $p \leq 0.1$, $p \leq .01$ and $p \leq .05$, respectively.

IMMATURE SECONDARY OSSIFICATION CENTER FLOW
(cc/min/100g)

	Fh	Gt	Distal Femur Me/Lat	Proximal Tibia	Tub.	Distal Tibia
o20	36.6	27.0	28.8/25.3	25.7		6.2
c20	18.4	19.8	25.1/18.6	18.8		3.5
Total 20	27.4	24.2	24.5	20.3	13.6	4.6

Among the various secondary ossification centers, flow rates are higher proximally and diminish in the distal portion of the limb. Flow is highest in the femoral head followed by the greater trochanter and distal femur, then the proximal tibia, and finally, the distal tibia. The distal tibia epiphysis receives substantially lower flow than any other epiphysis in the tibia or femur. The more proximal outer secondary ossification centers have flows of 25 to 36 ml/min/100g, far exceeding the 6 ml/min/100g of the distal tibia. The same is true for the distribution of flow to the inner secondary ossification center; the distal tibia c20 receives 4 ml/min/100g while the other four c20s receive 19 to 25 ml/min/100g.

The metaphyseal spongiosa in the adolescent animals is divided into four regions, with a slight modification in the proximal femur. As in the neonate, substantially higher flow is documented in the pMS, the segment of each metaphysis within 1.5 mm of the growth cartilage. Graphs 12 and 13 illustrate the vastly higher flow to these regions when contrasted to the rest of the bone. The metaphyseal area receiving the second highest flow is the region adjacent to the diaphysis, the dMS. This is followed by the mdMS, or the ItMS in the proximal femur. The mpMS, which is adjacent to the pMS, receives the least flow of the four regions. The flow value differences are all significant except in the proximal femur where dMS $\geq$ ItMS. The flow values for the various pMS regions are as follows: proximal tibia > distal femur $\geq$ greater trochanter $\geq$ femoral head > distal tibia.

FLOWS NEAR PHYSIS (cc/min/100g)

	Femur			Tibia		
	Gt	Fh	Distal	Proximal	Distal	Tub.
ø20	27	36	29/25	26	6	(14)
GP	26	21	17	20	11	15
pMS	113	108	118	179	55	
dMS		36	35	31	23	

The growth plate lies between the outer secondary ossification centers and the pMSs. In all but one location, the growth plate receives significantly less blood flow than the two adjacent regions. The exception is the Gt where the GtGP and Gto20 flows are not statistically different. Among the growth plates, the relative rank order of blood flow rate is: proximal femur $\geq$ proximal tibia > distal femur > distal tibia, differing from the order in the pMSs and the o20's.

With both the immature tibial and femoral diaphyseal marrows, the middle or fatty marrow has lower documented flow than that of the adjacent marrow on either side. The red marrow closer to the knee joint receives more flow than the red marrow farther from the knee in both bones. Each of the four red marrow regions is not differentiable from the region of metaphysis (dMS) adjacent to it. In fact, the dMS and pDMar of the proximal tibia have the equivalent flow rates ($p \geq .95$). Each area of marrow in the femur receives more flow than the analogous region in the tibia.

The cortices and cartilage are garphed in Graphs 14, 15, 18, and 19. As discussed previously, the cartilage seemingly receives the least flow; however, regional differentiation is not statistically relevant. Three of the adolescent metaphyseal cortices are divided into proximal and distal regions (pMCx and dMCx), and the fourth, the proximal femoral metaphysis cortex, is broken into four areas. However, the regions within each of the four metaphyseal cortices are not separable by blood flow differences. In the proximal femur, the flow to the ItMCx and dMCx are indistinguishable ($p \geq .99$). The diaphyseal cortices are divided into three regions with each region receiving comparable flows. In both the immature tibia and femur, the highest flow occurs in the pDCx, followed

generally by the dDCx and then the mDCx.

7. Immature vs. Mature (Graphs 20-27); Mature (Graphs 28-35)

To allow comparison of the immature animal data to the mature animal data certain bone regions are combined. The o20 and c20 are combined as the epiphyseal spongiosa (ES), and the mpMS and pMS are combined into the pMS. In the distal femur, the "pMS" of comparison also includes the mdMS. It includes to pc-, mc-, and po-MS of the mature animal.

The immature tibia receives more blood flow than the mature tibia in virtually every region. In the femur, the comparative results are mixed. More flow occurs in all the proximal femur metaphyseal spongiosa regions of the mature animals. The difference is statistically significant in all but the greater trochanter (GtMS).

When each immature animal metaphyseal spongiosa is divided as described in the preceding paragraph, there is less difference in flow between the regions although the dMS always receives the greatest flow within a given metaphysis. In the proximal femur, the flows to the FnMS, ItMS, and dMS are not statistically separable, but all are greater than the flow to the GtMS. The same is true in the mature animal. In the distal femur, the pMS and dMS have equal flows in the mature animal and are not statistically separable in the immature. In the immature proximal tibia, the dMS receives the same amount of flow as the pMS; these two get more flow than the mMS. In the mature animal no significant difference is discernable between the flows to the three regions of the proximal tibial metaphysis. In the distal tibia, dMS > mMS $\geq$ pMS in the immature animal. In the mature animal there is no distinguishable difference between the three regions.

The diaphyseal medulla follows the same trends in the mature as in the immature animals. The middle or fatty section receives the least flow of the three areas in a given bone. In the mature, diaphyseal marrow, the proximal and distal segments contain cancellous bone, while in the immature diaphysis these segments are only soft, non-osseous red marrow. The only area where the relative bone flows differ is the femur where dDMar >* pDMar in the immature animal while the pDS and dDS are indistinguishable in the mature animal. Although each immature marrow region receives greater amounts of blood flow than the corresponding region in the mature animal, the difference is only significant in the proximal and distal tibial diaphysis.

To compare the epiphyseal region in the analysis of the two age groups, the spongiosa, cortex, and cartilage were combined. In both ages, the rank order of flow rates among the epiphyseal spongiosa alone is: femoral head > distal femur $\geq$ proximal tibia > distal tibia.

EC/Cx flow in the mature animal exceeds that in the immature, (except in the GtC/Cx) probably because the immature EC/Cx is entirely cartilage while the adult EC/Cx is primarily cortical bone with a small fracture composed of articular cartilage. In the mature animals, the cartilage and cortex are separated (Graphs 30, 31, 34, 35). The epiphyseal cortex segments alone have higher flow rates which in all but one case are not significantly different from the spongiosa they enclose. The exception is the tibial tuberosity in which there is a thick cortex which has approximately half as much flow as the spongiosa. The other cortices are very thin. It is thus possible that the similarity in flow between the cortex and spongiosa is in part a reflection of the difficulty of differentiating cortex from spongiosa in the mature bone at the time of cutting.

The adult articular cartilage fails to receive significant blood flow. It is not possible to exactly quantitate regional flow for each articular cartilage area since these regions only trapped an average of 10 microspheres. Thus, there is very low flow, if any, in these regions of low weight.

There is no significant difference in blood flow to the subdivisions within any of the four metaphyseal cortices in the immature animal or within the mature animal proximal tibia or distal femur. However, within the mature femoral and distal metaphyseal cortices, the dMCx receives the least flow, $p \leq .05$. As in the immature bones, there is little difference between any of the three regions of diaphyseal cortex in the mature tibia. In the mature femur, however, the pDCx has higher blood flow than in the mDCx and dDCx.

The periosteum of the immature animal receives two to three times as much blood flow as the periosteum of the mature animal in both the femur and the tibia. The immature animal's femoral periosteum receives higher flow than the tibial periosteum and the femoral diaphyseal cortex. Tibial periosteal flows are indistinguishable. The adult tibial and femoral periosteal blood flows are not distinguishable from one another or from diaphyseal cortical flows. With the paucity of microspheres in the adult periostea, these comparative results may be subject to significant error.

Analysis of the graphs of the adult bone medulla (Graphs 28 and 29) demonstrate that the femur gets far more flow than the tibia. This is true in both medullary and cortical tissues (Graphs 31 and 32). The graphs of the mature animal medullary flows illustrate that most of the blood flows to the proximal femoral metaphysis. This is followed by the

femoral diaphysis and distal metaphysis, then the femoral head epiphysis, then the rest of the femur and all of the tibia. The tibia has a low, narrow range of blood flow; the region with the most flow, the proximal dMS, only receives 13.8 cc/min/100g.

The distal femoral metaphysis was cut uniquely in the mature dog in that it was divided into a central core and an outer cylinder. The central core receives significantly higher flows, ranging 30 to 38 cc/min/100g, than the outer part which received 11 and 13 cc/min/100g.

B. ^{99m}Technetium-Methylene Diphosphonate Uptake

Tc-MDP was injected intravenously into adolescent and adult dogs. The results given are three hours post injection. Because there was no monitoring of ^{99m}Tc-MDP levels in the blood with time, measurement of the amount of tracer in the bone can only be relative. Thus, the comparisons here are %uptake of total ^{99m}Tc-MDP per bone/%total weight of bone (%^{99m}Tc-MDP/%TW), %total bone blood flow/%TW (%TBF/%TW) and %total ^{99m}Tc-MDP uptake/%total blood flow per bone (^{99m}Tc-MDP/blood flow). This is the disadvantage in that it does not allow one to compare the amount of ^{99m}Tc-MDP in the femur to that in the tibia, or to compare adult versus adolescent uptake. However, it is an excellent way to evaluate the flow dependency of ^{99m}Tc-MDP uptake in one bone.

1. Gross Tissues (Graphs 37-45)

As with the blood flow data, probably the easiest way to examine such a multitude of data is to first look at a smaller number of sections, the gross tissues. In all but one of the four bones, adolescent femur, adolescent tibia, adult femur and adult tibia, the order of %^{99m}Tc-MDP/%TW is growth plate (if present) > spongiosa > cortex > soft marrow > cartilage, $p \geq .01$. The only variation is in the adolescent tibia where marrow $\geq$ cartilage, but there is no significant difference. When examined by %TBF/%TW, the tissues of the four bones are also all in the same order with the exception of the adolescent tibial marrow. The order in the other three bones is marrow > spongiosa > growth plate (in the adolescent) > cortex > cartilage, with $p \leq .01$ except in the adult tibia where the difference between marrow and spongiosa is not statistically significantly different. The adolescent tibial marrow receives a relatively low percentage

flow and is less, though not significantly less, than the spongiosa and nearly the same, though more, %TBF/%TW than the GP ($p \geq .90$). In both $\%^{99m}$Tc-MDP/%TW and %TBF/%TW, the relative order of three tissues: spongiosa > cortex > cartilage is the same. Thus, in the ratio of $\%^{99m}$Tc-MDP/%blood flow for these tissues is somewhere around one, with the exception of the adult dog femoral cartilage. As mentioned in the flow results, the adult dog cartilages only included articular cartilage a minute amount of tissue that only received about 10 microspheres apiece. Therefore, the flow values and the Tc-MDP/blood flow ratio for adult cartilage should be disregarded. In both adolescent bones and the adult tibia, the ratio of ^{99m}Tc-MDP uptake to blood flow is near one. The decreasing order in the adolescent is cortex, cartilage, spongiosa, though the cortex $\geq$ cartilage in the adolescent tibia.

The ratios of $\%^{99m}$Tc-MDP uptake/%bloodflow for the marrow and growth plate are not near unity. The adolescent growth plate absorbs by far the most ^{99m}Tc-MDP per weight but is only intermediate among the other tissues in the percent blood flow it receives. In all four bones, the soft diaphyseal marrow receives either the greatest or not significantly less than the greatest %TBF/%TW, and gets the lowest or next to the lowest $\%^{99m}$Tc-MDP/%TW, resulting in a very low ^{99m}Tc-MDP/blood flow ratio. Thus, the overall order of $\%^{99m}$Tc-MDP uptake/%blood flow is growth plate > cortex $\geq$ cartilage > spongiosa > marrow, if one disregards the adult cartilage which is greater than cortex.

2. %Total ^{99m}Technetium-Methylene Diphosphonate Uptake/%Total Weight

Each pair of graphs for the means for the four bones, Graphs 46-52, is drawn to the same scale. Graphs 46A and 48A have been enlarged as 46B and 48B in order to visualize more clearly the differences within the cor-

tices. Each pair shows in general medullary flow is higher than cortical flow as would be expected from the tissue data: GP > spongiosa > cortex > marrow > cartilage. Looking first at the adolescents, it is apparent that the pMS has by far the highest uptake per gram, followed by the growth plate. There is little difference among the femoral head, greater trochanter or distal femmur pMSs or among these GPs. The uptake in the proximal pMS and GP is greater, but not significantly greater than the equivalent regions in the distal femur. In the femur, the next highest ^{99m}Tc-MDP uptake occurs in the o20s femoral head and greater trochanter LtGP, then the metaphyseal cortex. In each MCx there is less tracer uptake midshaft than at the ends of the bone. The %^{99m}Tc-MDP/%TW is about one in the proximal c20s the distal epiphyses (in which o20 > c20 and me > 1), and all the rest of the metaphyseal spongiosa. The femur and tibia are again similar in that next is the proximal part of the proximal metaphyseal cortex, FnMCx and GtMCx in the femur and P.pMCx in the tibia. Then there are a group of areas where %^{99m}Tc-MDP/%TW is about one, the rest of the metaphyseal cortices and spongiosa, in which the concentration decreases as one goes towards midshaft, the Fhc20 and Gtc20, and all the other epiphyses, in which o20 > c20, and m > 1 in the distal femur. Next is the diaphyseal cortex, in which again, the most midsection gets the least tracer, and the proximal and distal diaphyseal marrow, followed by the various epiphyseal cortices, then the periosteum. The middle diaphyseal marrow gets the least uptake of all.

In the adult femur, the highest uptake of ^{99m}Tc-MDP is in the femoral head and neck, followed by the femoral head and neck cortices, and the rest of the proximal femoral spongiosa, including the metaphysis, the GtES

and pDS. Next is the central distal spongiosa: metaphyseal, (in which central > outer) dDS and epiphyseal. The adult tibia follows somewhat similar lines, except that there is no femoral head and neck with highest uptake. Thus, most ^{99m}Tc-MDP goes to the proximal tibial metaphysis, then the proximal epiphysis, tuberosity and pDS, followed by the distal metaphyseal, epiphyseal, and diaphyseal spongiosa. In the distal metaphyses of both bones, the uptake decreases as one goes towards midshaft. Cortical uptake is next in order, with the exception of the aforementioned femoral head and neck cortex; in both bones the cortices at either end of the bones have %^{99m}Tc-MDP to %TW ratios of about one; the ratio decreases as one goes midshaft to reach .6 in the tibia and .3 in the femur. The uptake of ^{99m}Tc-MDP is quite constant throughout the tibial cortex. Finally, the lowest %^{99m}Tc-MDP/%TW goes to the periosteum, the articular cartilage, and as in the adolescent, to the mDMar.

3. %Total Blood Flow/%Total Weight (Graphs 16-19, 33-36)

Although %TBF/%TW has nearly the same distribution as blood flow in cc/min/100 grams, which was discussed under the Flow Results, it would be helpful to review the percent flow distribution in order to compare it to the percent ^{99m}Tc-MDP distribution.

In the adolescent bones, by far the most blood goes to the pMS. The next highest areas are the proximal and distal diaphyseal marrows (unlike the %^{99m}Tc-MDP) and the metaphyseal spongiosas on either side of the marrow, ItMS and dMSs. In the tibia the proximal dMS gets more flow than the distal dMS. In the next set of regions where %TBF/%TW is about equal to one, the femur and tibia diverge somewhat. In the adolescent femur, the highest flow regions of the group are the o2Os, proximal more than distal epiphysis, the mDMar and distal mdMS, and the c2Os and growth plates. The tibia has

the proximal epiphysis, o20 > c20, and growth plate, followed by the tibial tuberosity regions, the rest of the metaphyseal spongiosa and the distal growth plate. Then both bones are alike with the metaphyseal cortices leading the cortices, proximal > distal, then periosteum, then diaphyseal cortex, and finally the epiphyseal cartilages. The tibial distal epiphyseal spongiosa, o20 > c20, gets about the same small %TBF/%TW as the cartilage.

In the adult bones, like in the adolescent, the medullary %TBF/%TW ratio is mostly greater than one and in the cortex is mostly less than one. The highest flows in both bones go to the proximal metaphyseal and diaphyseal spongiosas. In the latter group, the %TBF/%TW ratio is close to one. Next are the cortices led by the femoral head and neck and proximal tibial epiphyseal cortex. In both bones, the cortical flows are highest at the extreme ends, i.e., the epiphyseal cortices, then decrease as one goes towards the middle so that the mDCx has the lowest of cortical flows. However, the variation in %TBF/%TW is to a smaller degree and more symmetrical in the tibia than in the femur, where flows are higher proximally. Percent blood flows to the cortical regions in both bones are relatively lower than %99mTc-MPD uptake in the same regions. Yet, the cortices of both bones have little variation in %TBF/%TW as opposed to %99mTc-MDP/%TW. The cartilage gets the lowest or is not significantly different from the lowest flows.

4. %99mTc-MDP Uptake/%Blood Flow (Graphs 54-61)

When %99mTc-MDP is divided by %blood flow per region, this tends to cancel out the role blood flow plays in distributing ^{99m}technetium-methylene diphosphonate to the tissues: the resulting number shows the rela-

tive affinity of Tc-MDP for the bone regardless of flow (if one ignores the affect of flow on extraction ratios). The weight or density of the bone is not a consideration in this figure.

The ^{99m}Tc-MDP graphs are paired so that the medulla and cortex of each bone are drawn to the same scale. Graphs 54-57 show that the growth plates stand out and exceed all other regions in the adolescent bones in ^{99m}Tc-MDP uptake per blood flow. The physes are among the medullary regions receiving the lowest amount of blood flow yet have high ^{99m}Tc-MDP uptake, being second only to the pMS. The tibial tuberosity and lesser trochanter growth plates have lower ^{99m}Tc-MDP/blood flow ratios than the other growth plates, but these figures are less accurate and have large standard errors, especially the lesser trochanter. The region for which tracer affinity is next highest is the metaphyseal cortex. In each of the four MCxs, the ^{99m}Tc-MDP/blood flow ratio is greater in the area proximal to the physis and decreases as one goes towards midshaft to the diaphyseal cortex. However, before the dCx are the mpMSs, followed by the secondary ossification centers and the pMSs. In each case the pMS ^{99m}Tc-MDP affinity is close to that of the epiphysis on the opposite side of the physis from it, and the c20 > o20 ($p \leq .01$ or .05)in each epiphysis. The relative %^{99m}Tc-MDP uptake and %TBF are about the same, giving a ratio near one, in the diaphyseal cortex and the various epiphyseal cartilages. This is excepting the distal tibial EC, which had a Tc uptake/flow ratio near that of the growth plates; the %TBF/%TW in this region was the lowest of any region in any bone in any age group. There was less ^{99m}Tc-MDP uptake relative to blood flow in the distal metaphyseal spongiosa, i.e. the ItMS and dMS in the proximal femur and the mdMS and dMS in the other three metaphyses.

Within each metaphysis, the dMS gets more blood flow and less ^{99m}Tc-MDP/blood flow than the adjacent mdMS or ItMS. The three diaphyseal marrow regions and the periosteum had the lowest affinity for ^{99m}Tc-MDP in both bones.

The ^{99m}Tc-MDP/blood flow results in the adult bones are portrayed in Graphs 58-61. Although the articular cartilages' values are highest among the femoral regions and not different from the region with the highest value in the tibia, the articular cartilage ^{99m}Tc-MDP/blood flow values are not significantly different from the values of any region in either bone. The same is true for the adult tibial periosteum. Of the remaining bone regions, those for which the tracer has the highest affinity are the epiphyseal spongiosa, none of which is significantly different from another. As is mostly the case with the blood flow data, there is no significant difference between each epiphyseal spongiosa and its surrounding epiphyseal cortex. Following the epiphyseal spongiosa, the next highest area of %^{99m}Tc-MDP/%blood flow includes all of the cortex regions. ^{99m}Tc-MDP affinity is quite constant throughout the cortex in both bones, especially in the tibia. There appears to be greater affinity for the epiphyseal cortices, but the differences are not significant because of the large standard deviations. The proximal femoral metaphyseal cortex has slightly lower relative tracer uptake than the rest of the femoral cortex; and in the tibial cortex there is minimally lower relative uptake in the distal metaphyseal and diaphyseal cortex. However, statistical analysis shows there is almost no significant difference between ^{99m}Tc-MDP affinity for any of the cortical regions. Following the cortex in ^{99m}Tc-MDP/blood flow is the metaphyseal spongiosa. Within each metaphysis, the tracer affinity decreases as one goes towards the middle of the bone, so that it is lower in diaphyseal spongiosa and least in the non-boney mDMar. Affinity for the femoral periosteum

is very low. In the distal femoral metaphyseal spongiosa, the $\%^{99m}$Tc-MDP uptake/%blood flow is higher in the outer cylinder than in the central core. This is expected since the central part receives more blood flow while there is little difference between outer and central $\%^{99m}$Tc-MDP uptake/%TW. In summary, the general decreasing order of ^{99m}Tc-MDP uptake/blood flow in the adolescent is GP > MCx (proximal > distal) > mpMS > pMS, ES (c20 >* o20), DCx, EC > mdMS $\geq$ dMS > periosteum, DMar. In the adult it is ES > Cortex > MS (pMS $\geq$ mMS $\geq$ dMS) > DS > periosteum, DMar. The main difference is that there is higher affinity of the ^{99m}Tc-MDP for the adolescent proximal metaphysis, metaphyseal cortex and growth plate. After this, from the epiphyseal spongiosa on down, the ^{99m}Tc-MDP/blood ratios for adolescent and adult bone regions are quite similar, both in amount and distribution.

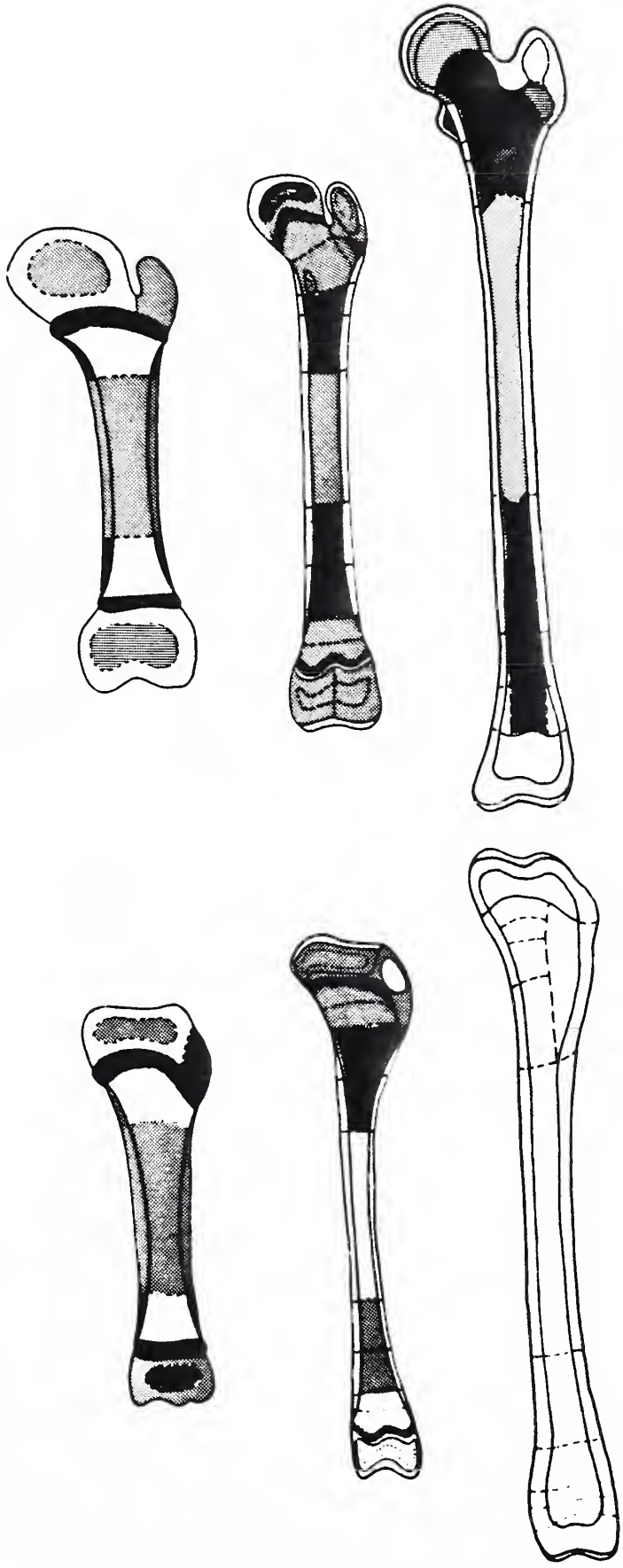

FIGURE 19
DOT DENSIOGRAM: OSSEOUS BLOOD FLOW IN THREE AGE GROUPS

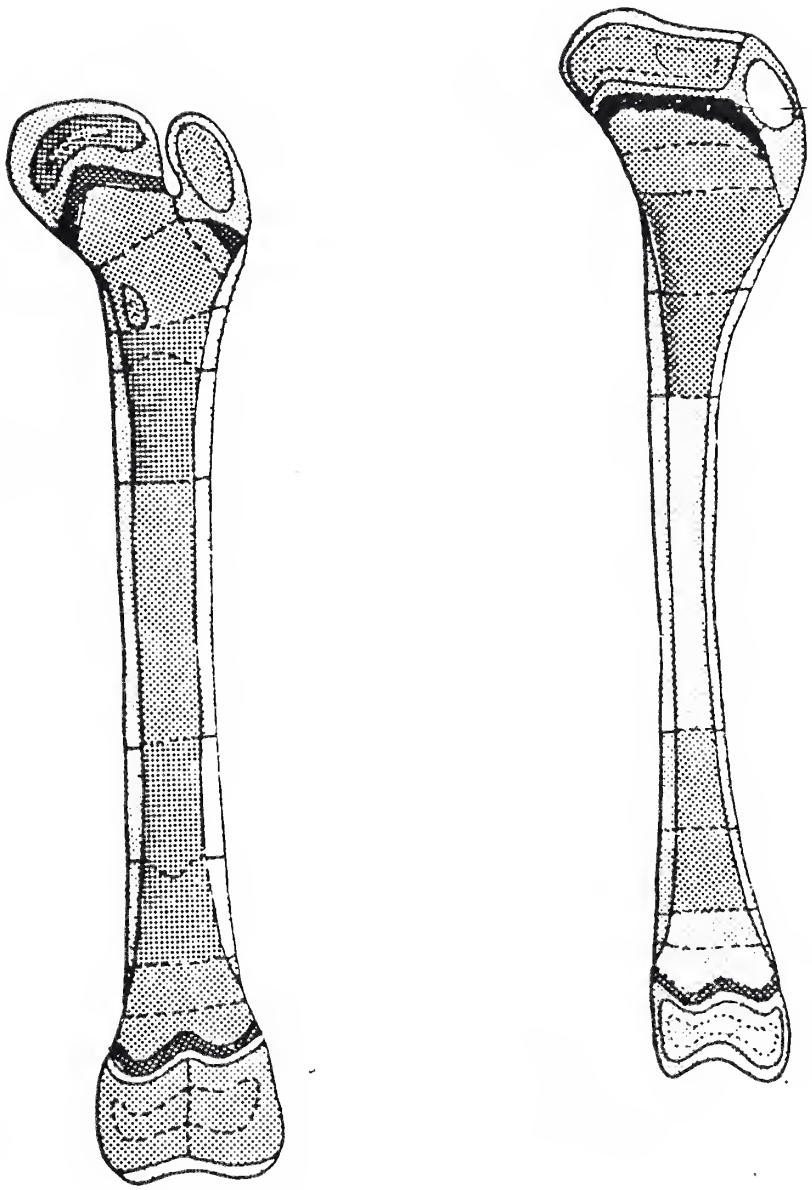

FIGURE 20

Dot Densiogram: Immature Bone Blood Flow

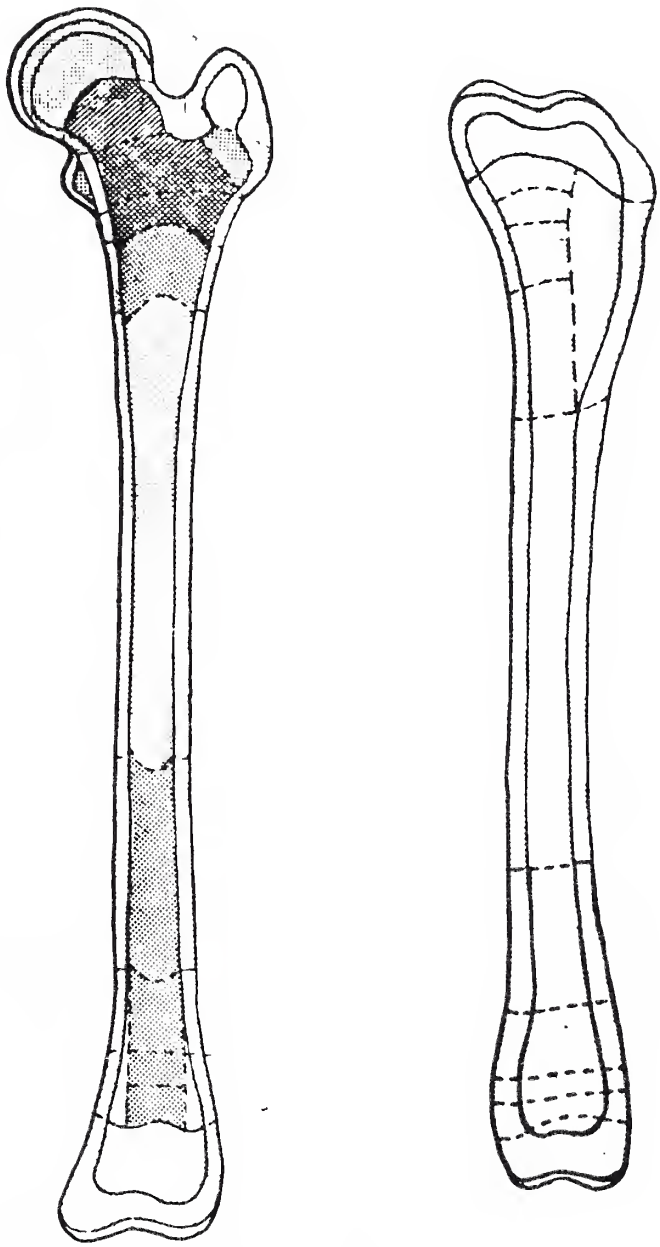

FIGURE 21

Dot Densiogram: Mature Bone Blood Flow

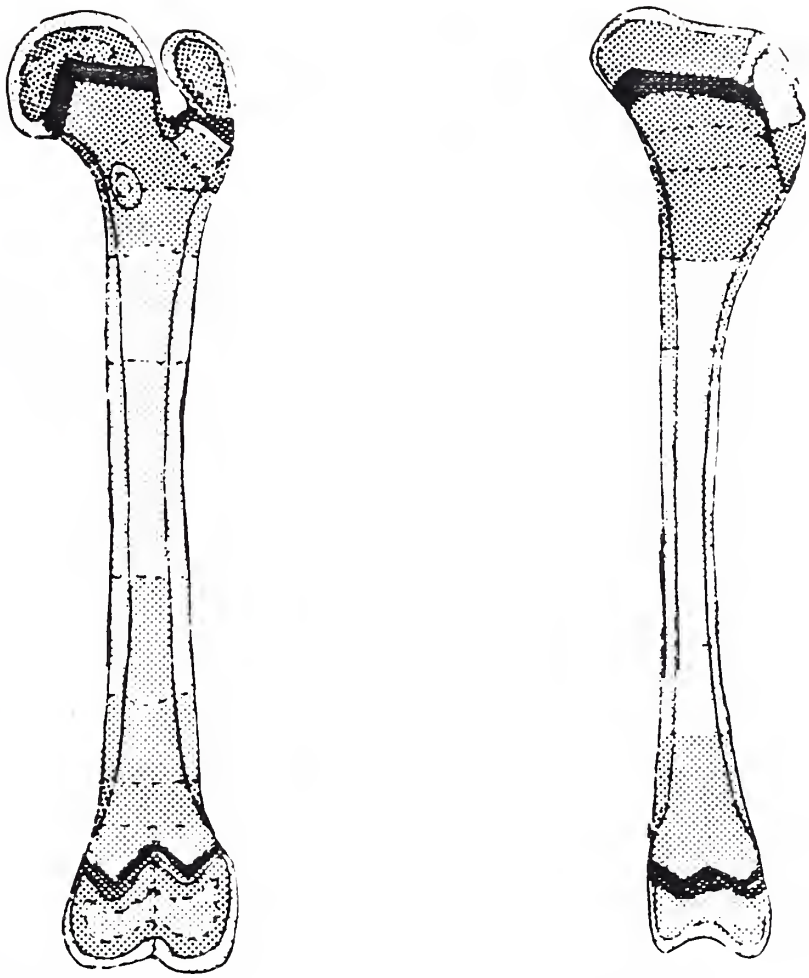

FIGURE 22

Dot Densiogram: Immature Bone: %Tc-99m MDP/%Total Weight

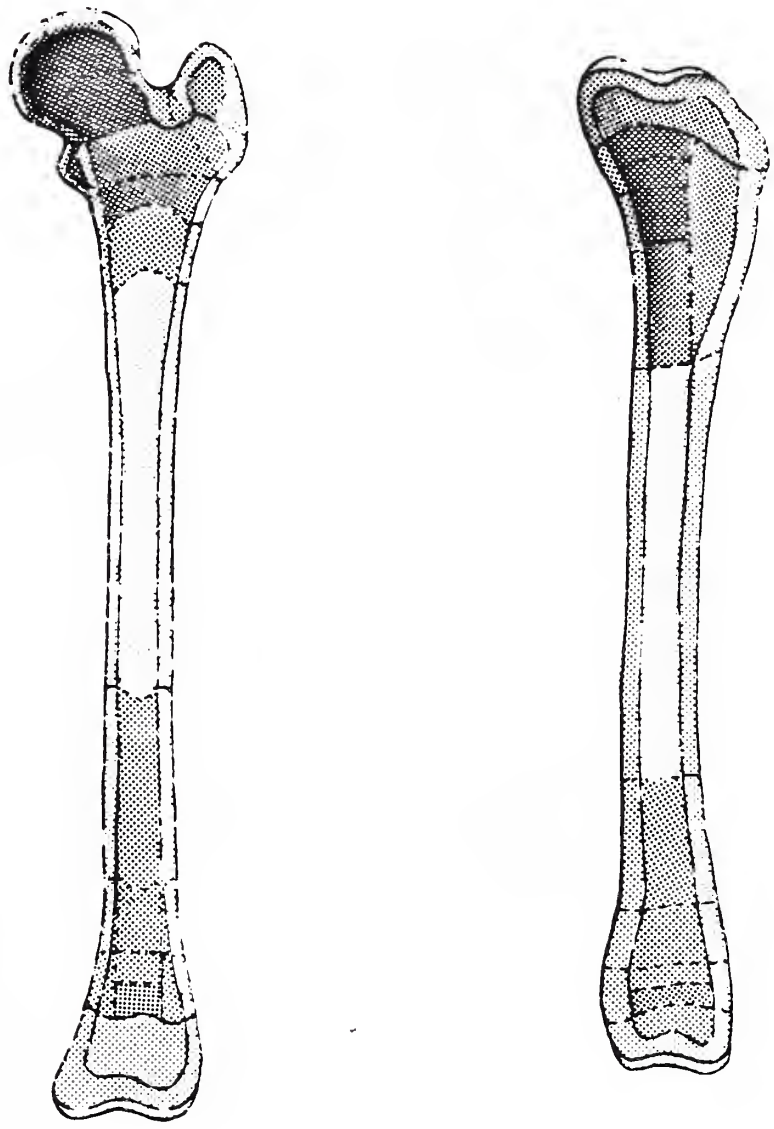

FIGURE 23

Dot Densiogram: Mature Bone: %Tc-99m MDP/%Total Weight

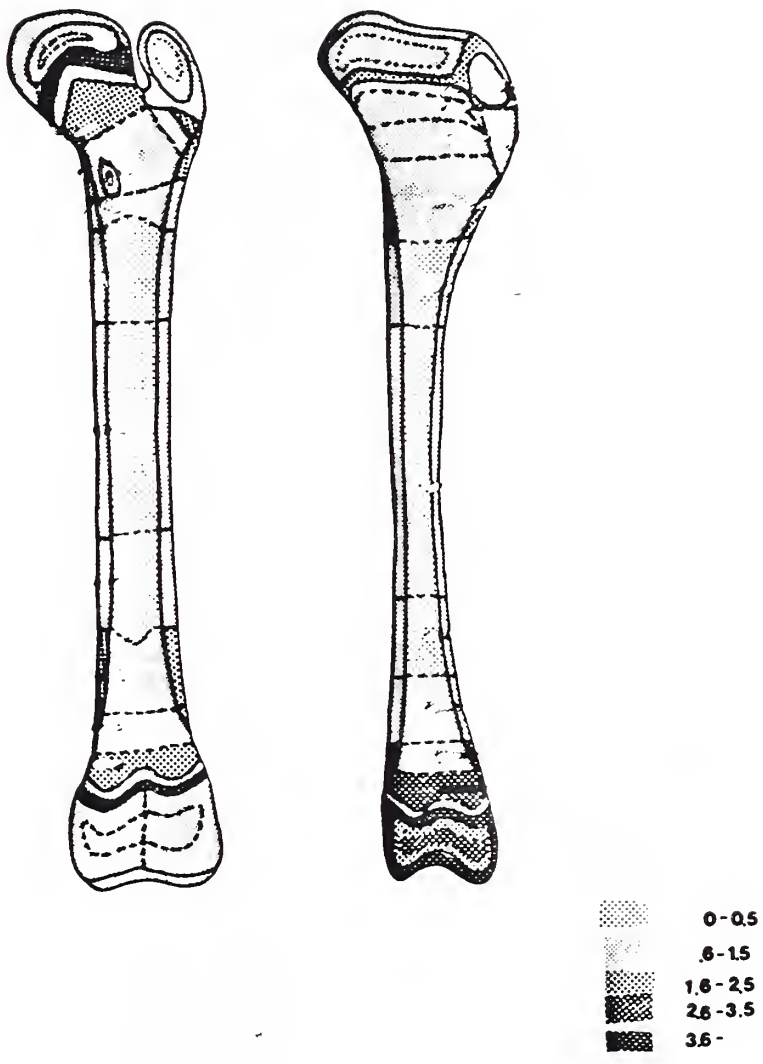

FIGURE 24

Dot Densiogram: Immature Bone: Tc-99m MDP/Blood Flow

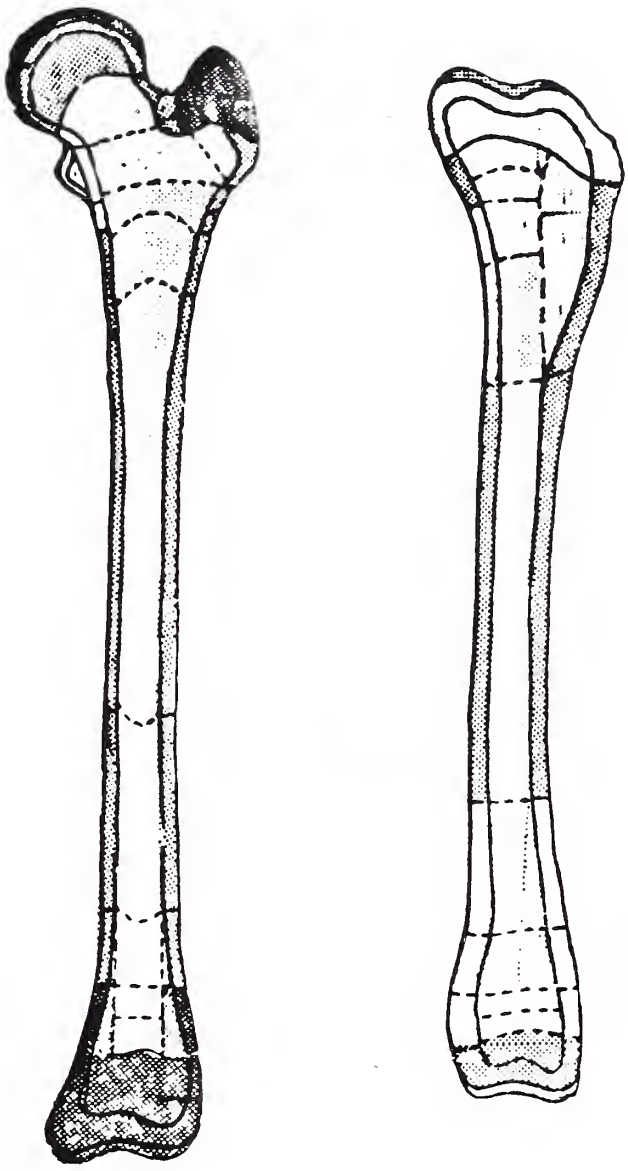

FIGURE 25

Dot Densiogram: Mature Bones: Tc-99m MDP/Blood Flow

GRAPH 1

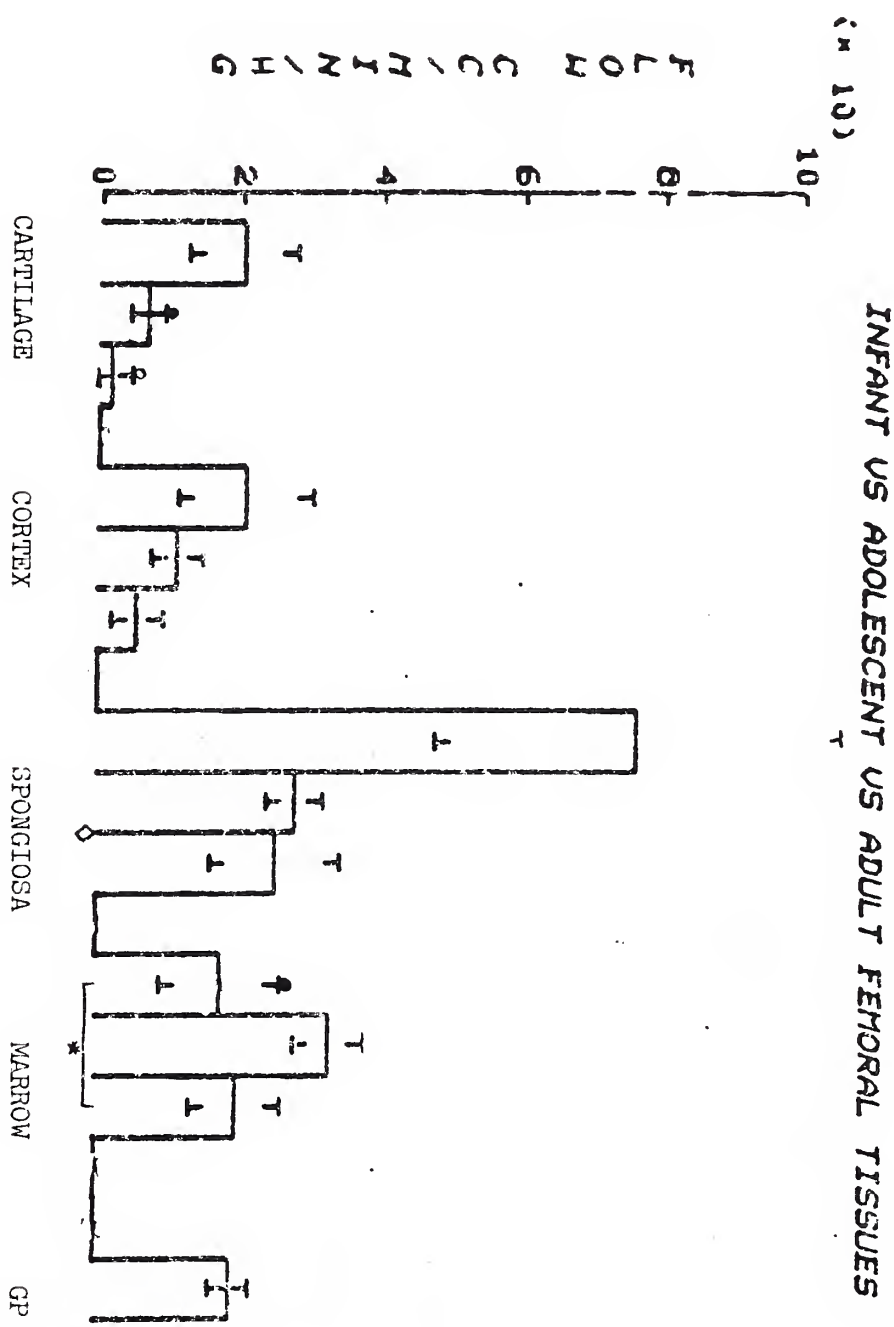
INFANT VS ADOLESCENT VS ADULT FEMORAL TISSUES
(x 10)
FLOW CCC/MIN/HG
0
2
4
6
8
10
CARTILAGE
CORTEX
SPONGIOSA
MARROW
GP

GRAPH 2

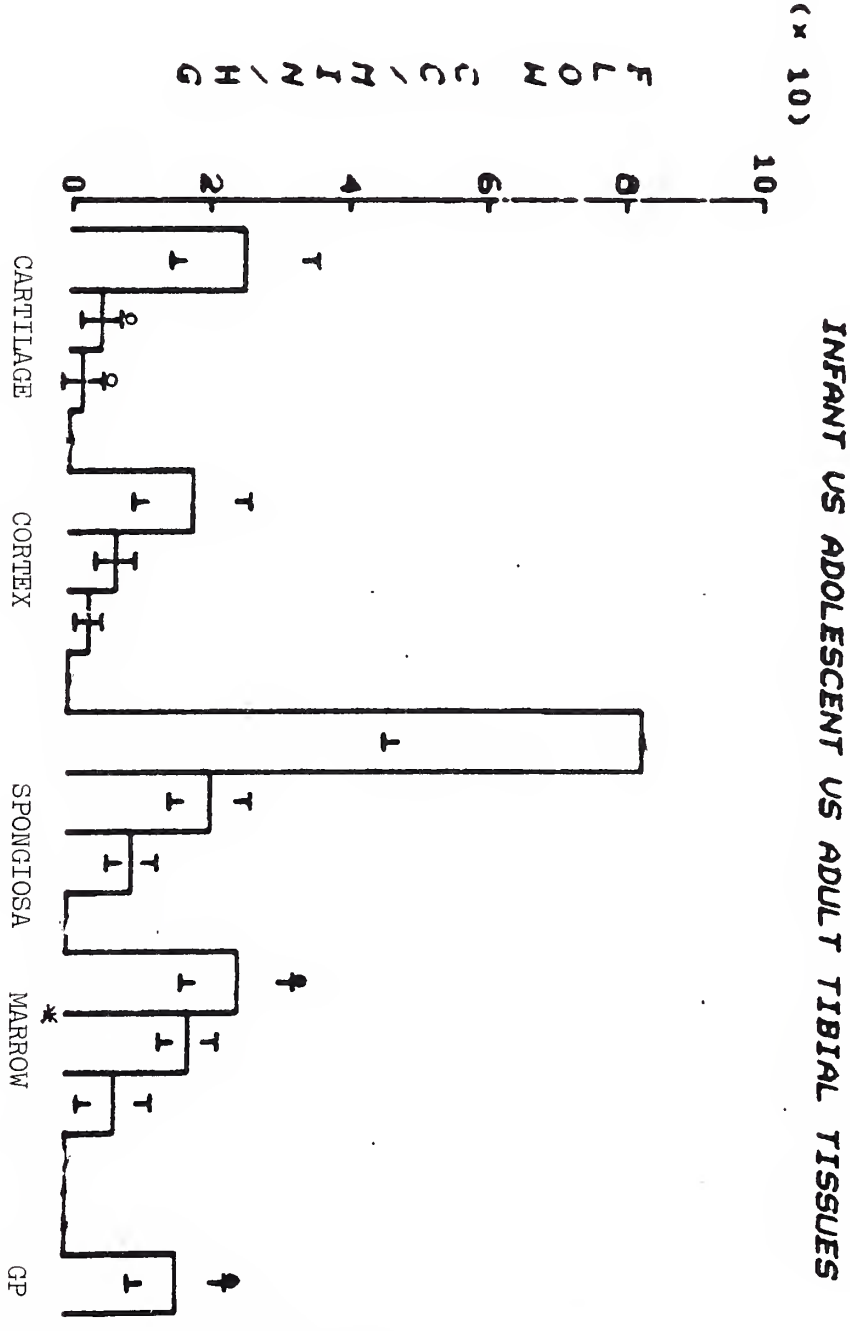
INFANT VS ADOLESCENT VS ADULT TIBIAL TISSUES
FOLLOW SCINTIN/HG
(× 10)
10
8
6
4
2
0
CARTILAGE
CORTEX
SPONGIOSA
MARROW
GP

GRAPH 3

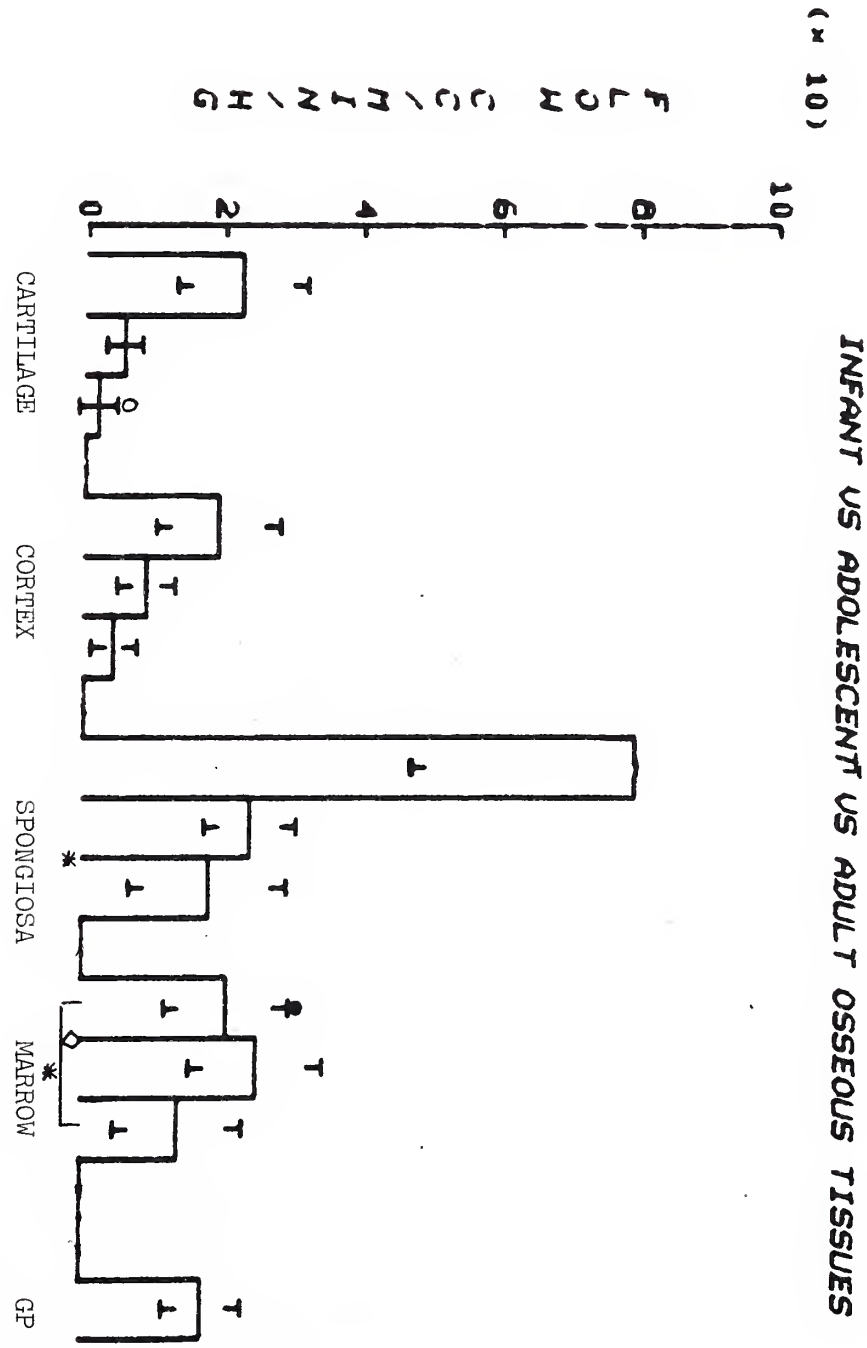
INFANT VS ADOLESCENT VS ADULT OSSEOUS TISSUES
(× 10)
0
2
4
6
8
10
CARTILAGE
CORTEX
SPONGIOSA
MARROW
GP

GRAPH 4

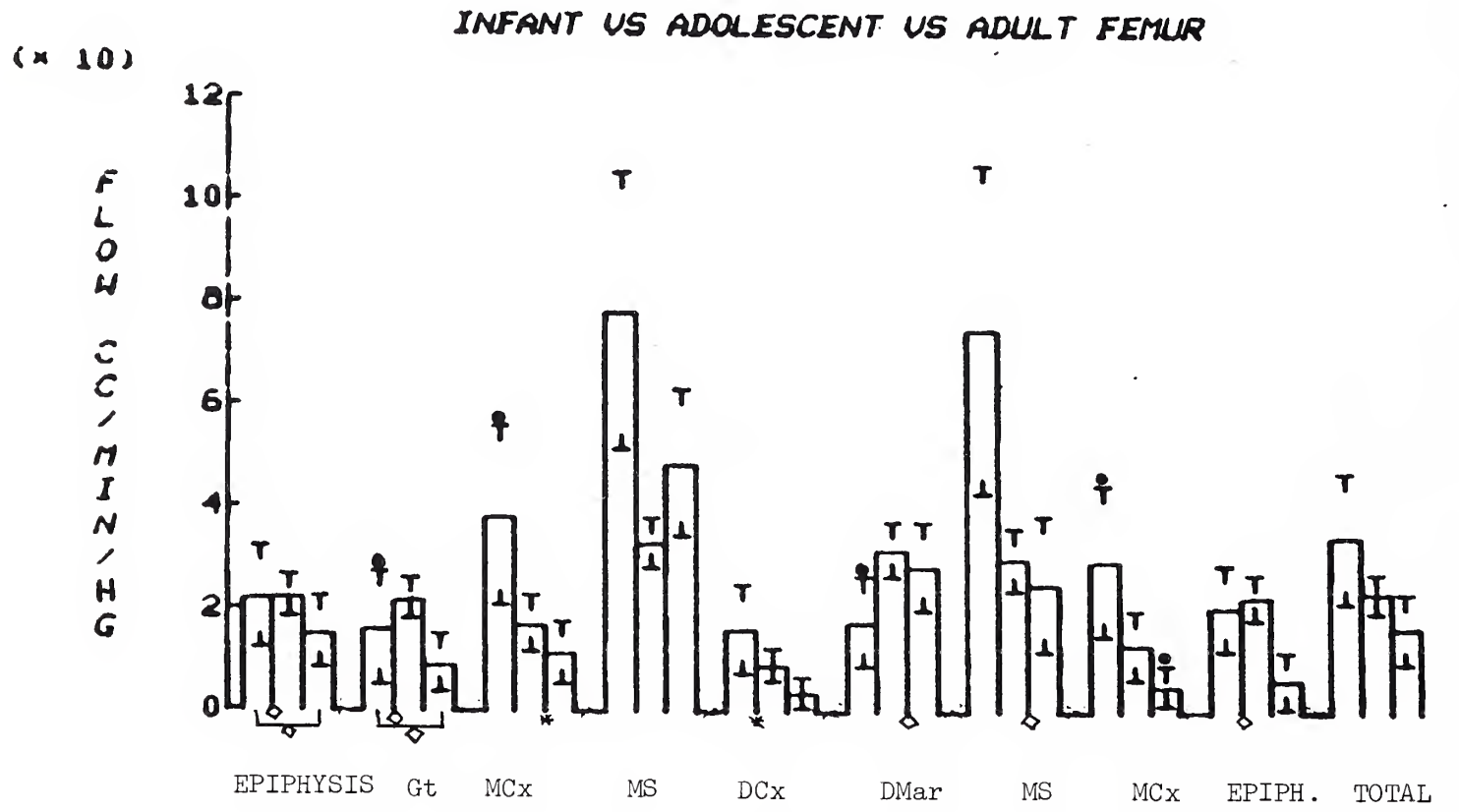
INFANT VS ADOLESCENT VS ADULT FEMUR
(× 10)
FLOW CC/MIN/HG
12
10
8
6
4
2
0
EPIPHYSIS
Gt
MCx
MS
DCx
DMar
MS
MCx
EPIPH.
TOTAL
PROXIMAL
DISTAL

GRAPH 5

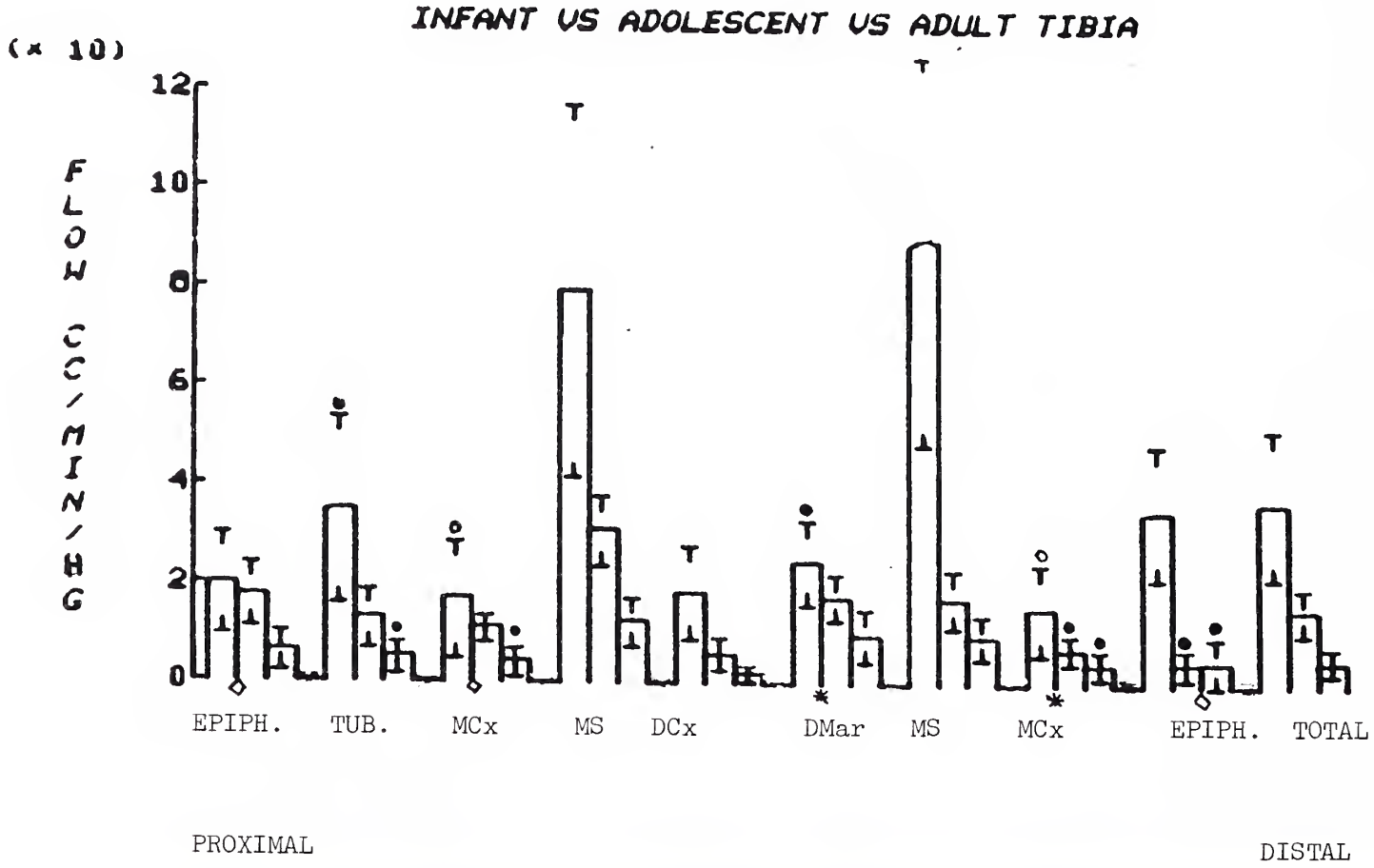
INFANT VS ADOLESCENT VS ADULT TIBIA
(× 10)
FLOW CC/MIN/HG
12
10
8
6
4
2
0
EPIPH.
TUB.
MCx
MS
DCx
DMar
MS
MCx
EPIPH.
TOTAL
PROXIMAL
DISTAL

GRAPH 6

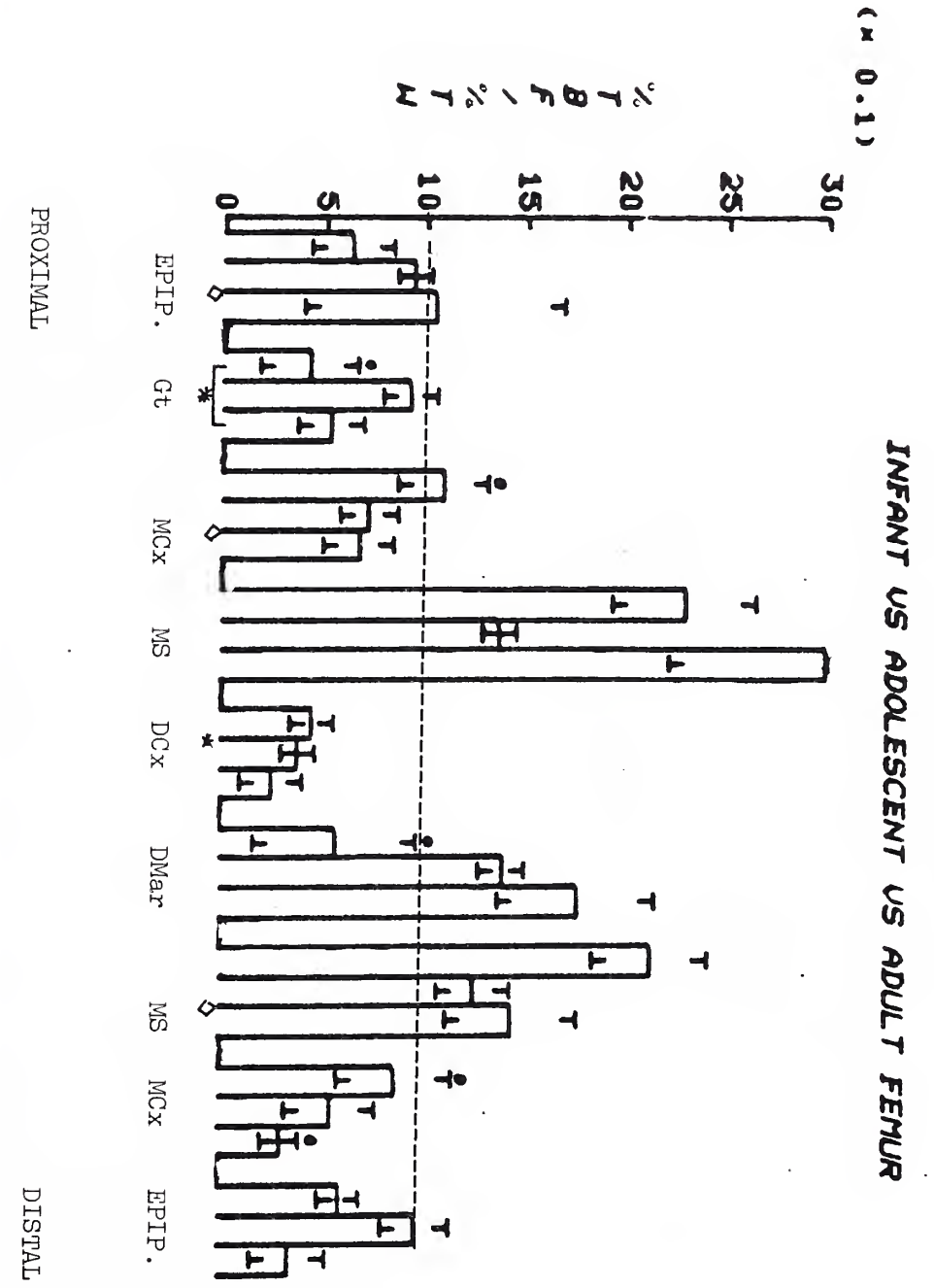
INFANT VS ADOLESCENT VS ADULT FEMUR
(× 0.1)
% TBF / % TM
0
5
10
15
20
25
30
EPIP.
Gt
MCx
MS
DCx
DMar
MS
MCx
EPIP.
PROXIMAL
DISTAL

GRAPH 7

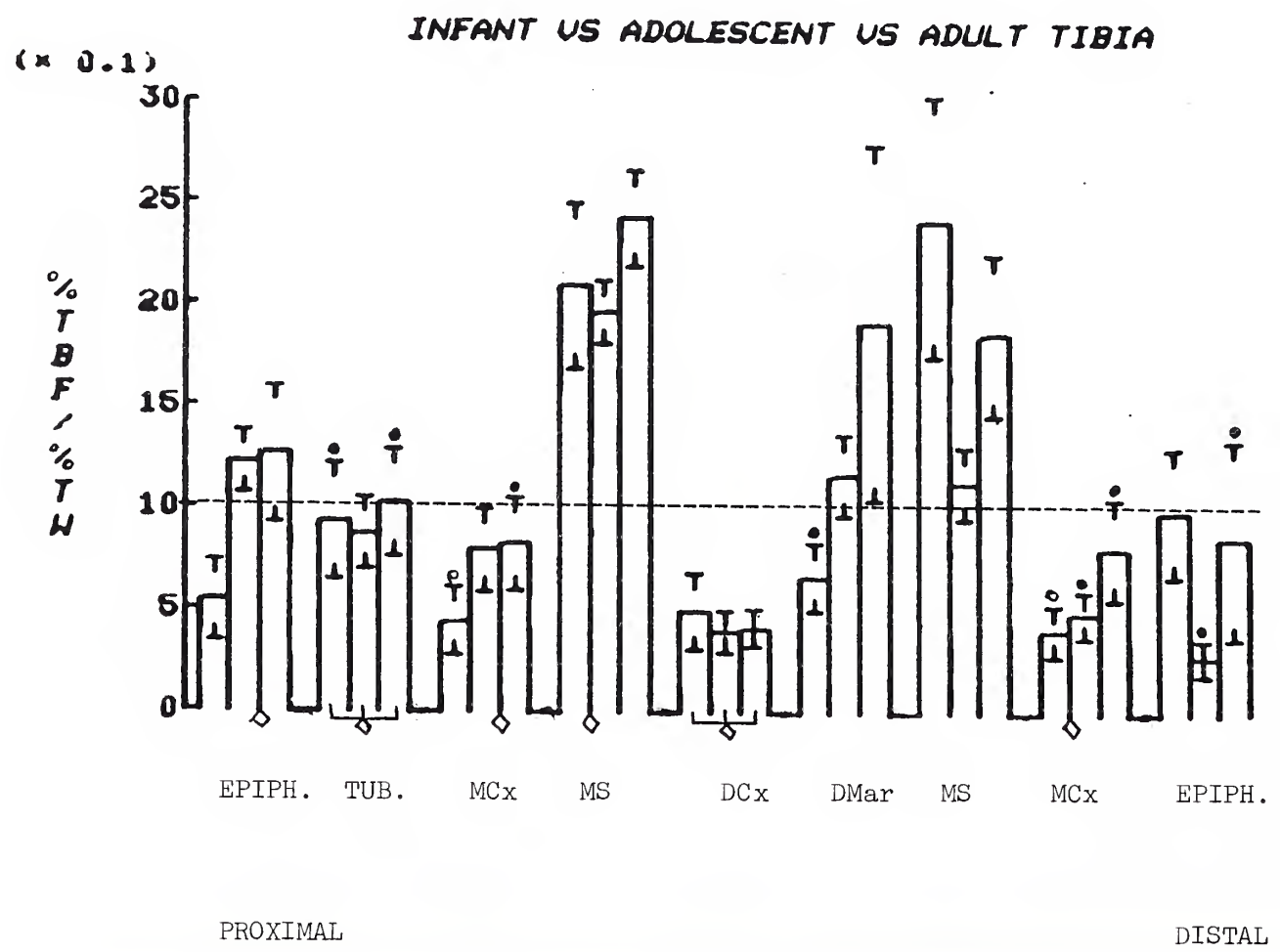
INFANT VS ADOLESCENT VS ADULT TIBIA
(× 0.1)
30
25
20
15
10
5
0
% TBF / % TH
EPIPH.
TUB.
MCx
MS
DCx
DMar
MS
MCx
EPIPH.
PROXIMAL
DISTAL

GRAPH 8

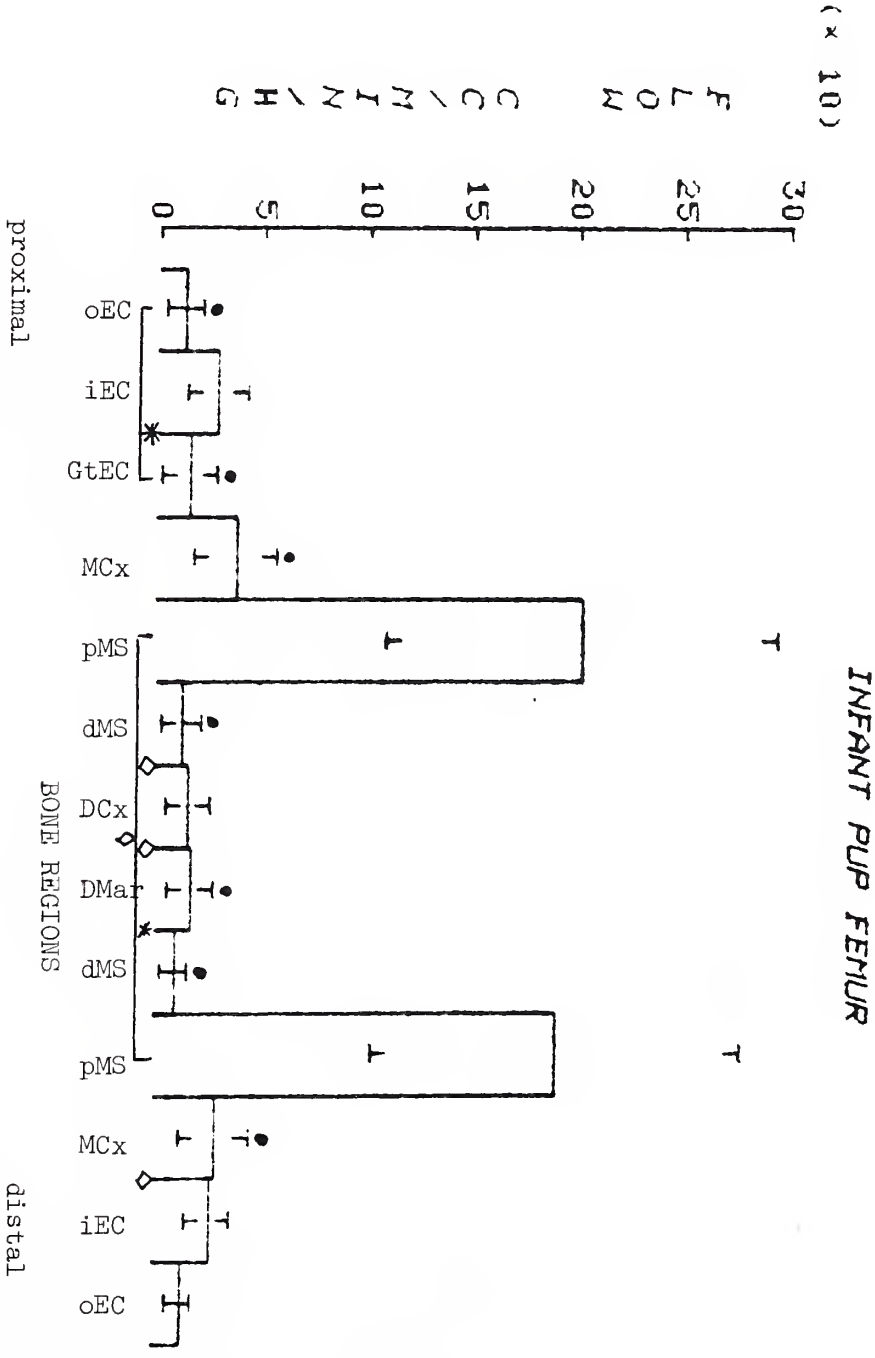
INFANT PUP FEMUR
COCHRAN FILM
(× 10)
0
5
10
15
20
25
30
proximal
distal
BONE REGIONS
oEC
iEC
GtEC
MCx
pMS
dMS
DCx
DMar
dMS
pMS
MCx
iEC
oEC

GRAPH 9

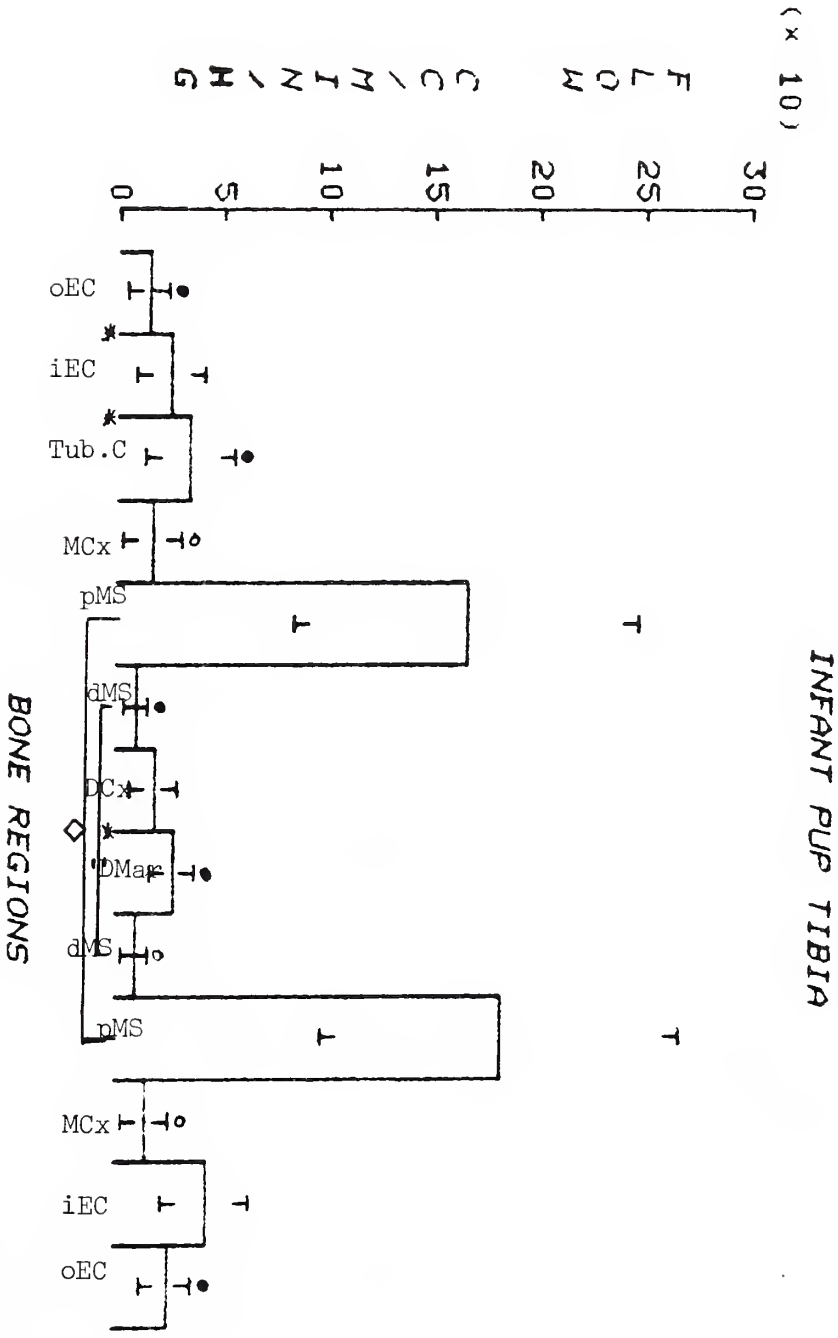
INFANT PUP TIBIA
FLOW
CC/MIN/HG
(× 10)
0
5
10
15
20
25
30
BONE REGIONS
PROXIMAL
DISTAL
oEC
iEC
Tub.C
MCx
pMS
dMS
DCx
DMax
dMS
pMS
MCx
iEC
oEC

GRAPH 10

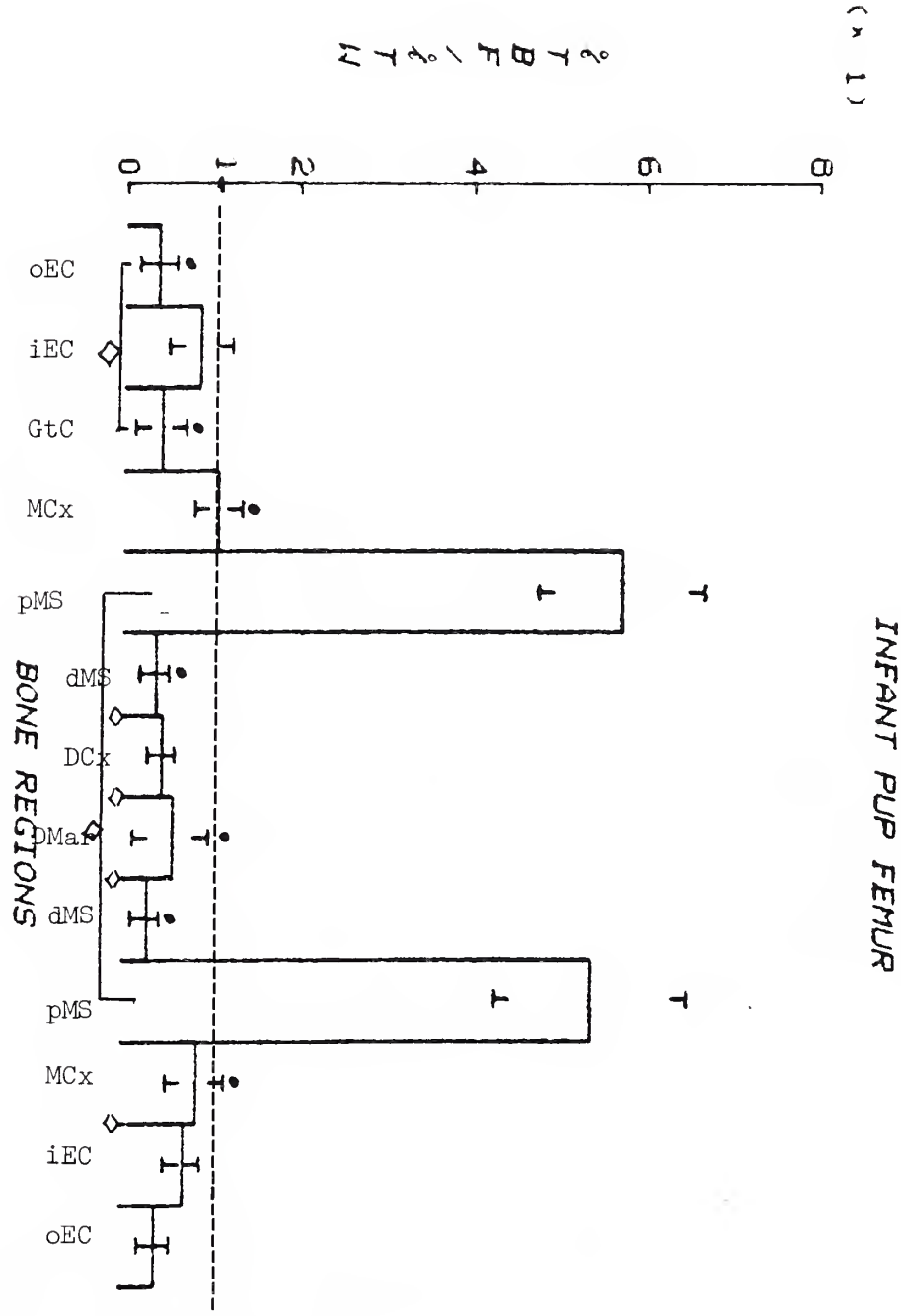
INFANT PUP FEMUR
BONE REGIONS
PROXIMAL
DISTAL
oEC
iEC
GtC
MCx
pMS
dMS
DCx
DMar
dMS
pMS
MCx
iEC
oEC
0
1
2
4
6
8

GRAPH 11

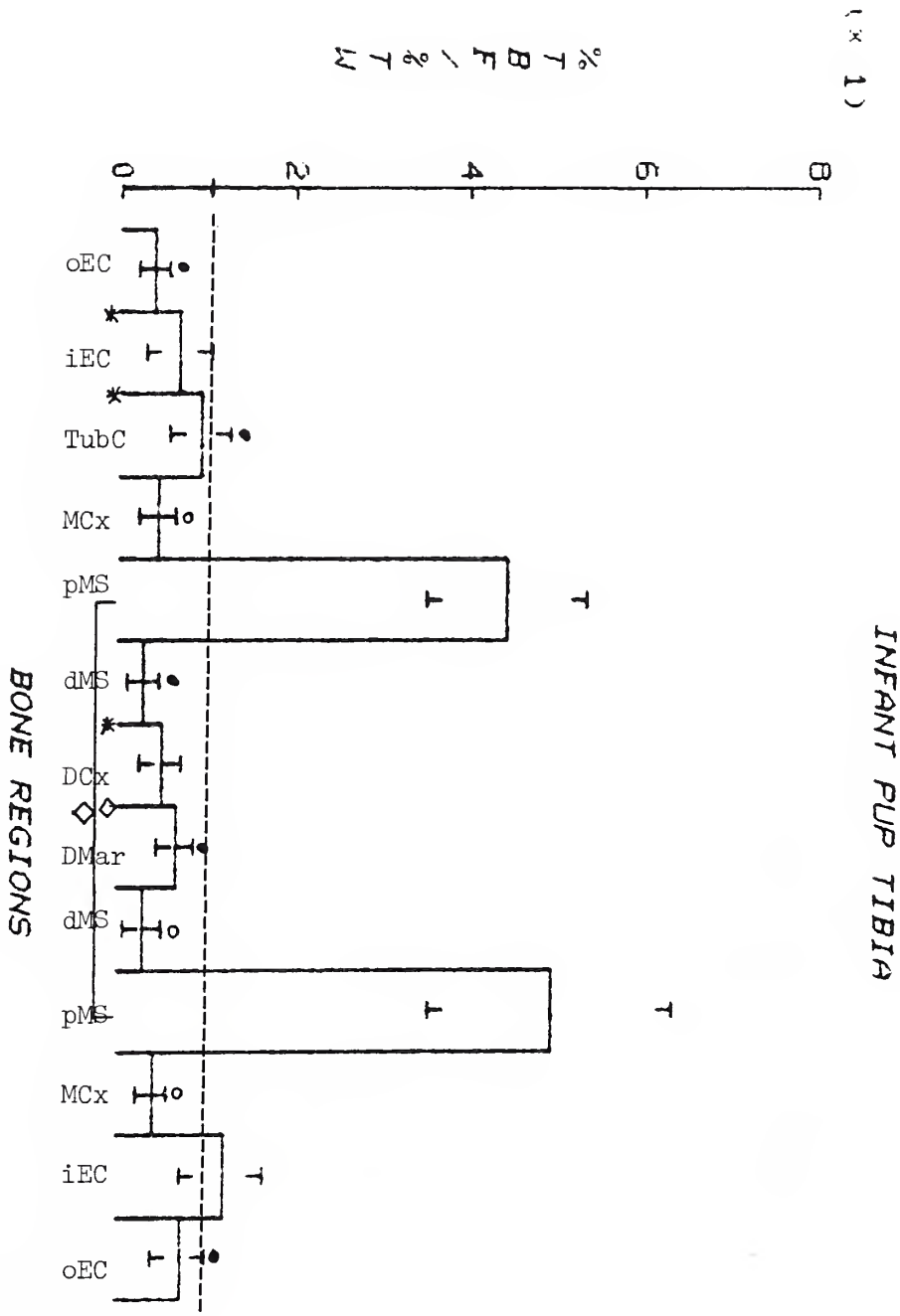
INFANT PUP TIBIA
% TBF/TTM (x 1)
0
2
4
6
8
BONE REGIONS
oEC
iEC
TubC
MCx
pMS
dMS
DCx
DMar
dMS
pMS
MCx
iEC
oEC
PROXIMAL
DISTAL

GRAPH 12

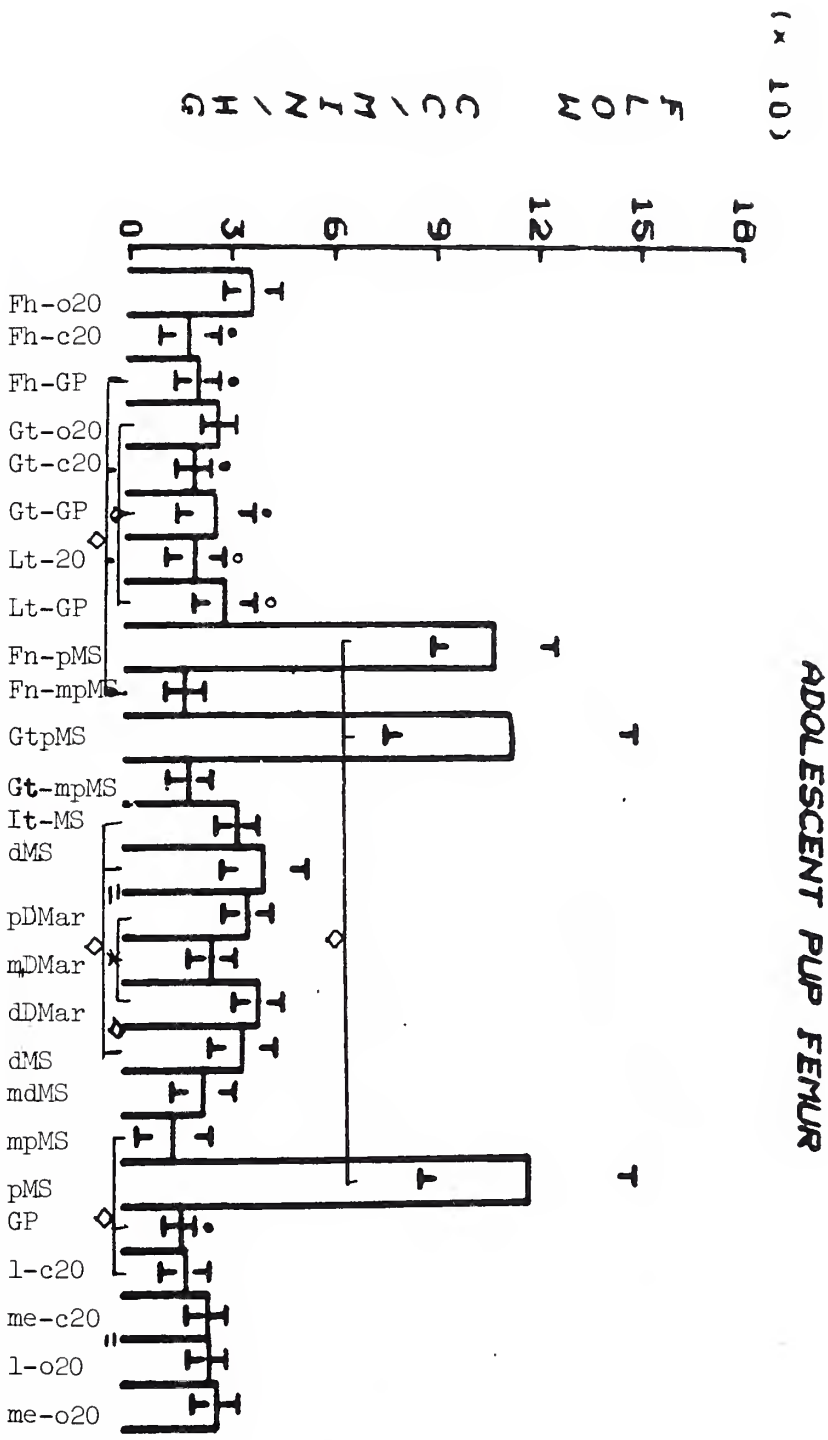
ADOLESCENT PUP FEMUR
FLOW
(× 10)
0
3
6
9
12
15
18
PROXIMAL
DISTAL
BONE REGIONS
Fh-o20
Fh-c20
Fh-GP
Gt-o20
Gt-c20
Gt-GP
Lt-20
Lt-GP
Fn-pMS
Fn-mpMS
GtpMS
Gt-mpMS
It-MS
dMS
pDMar
mDMar
dDMar
dMS
mdMS
mpMS
pMS
GP
l-c20
me-c20
l-o20
me-o20

GRAPH 13

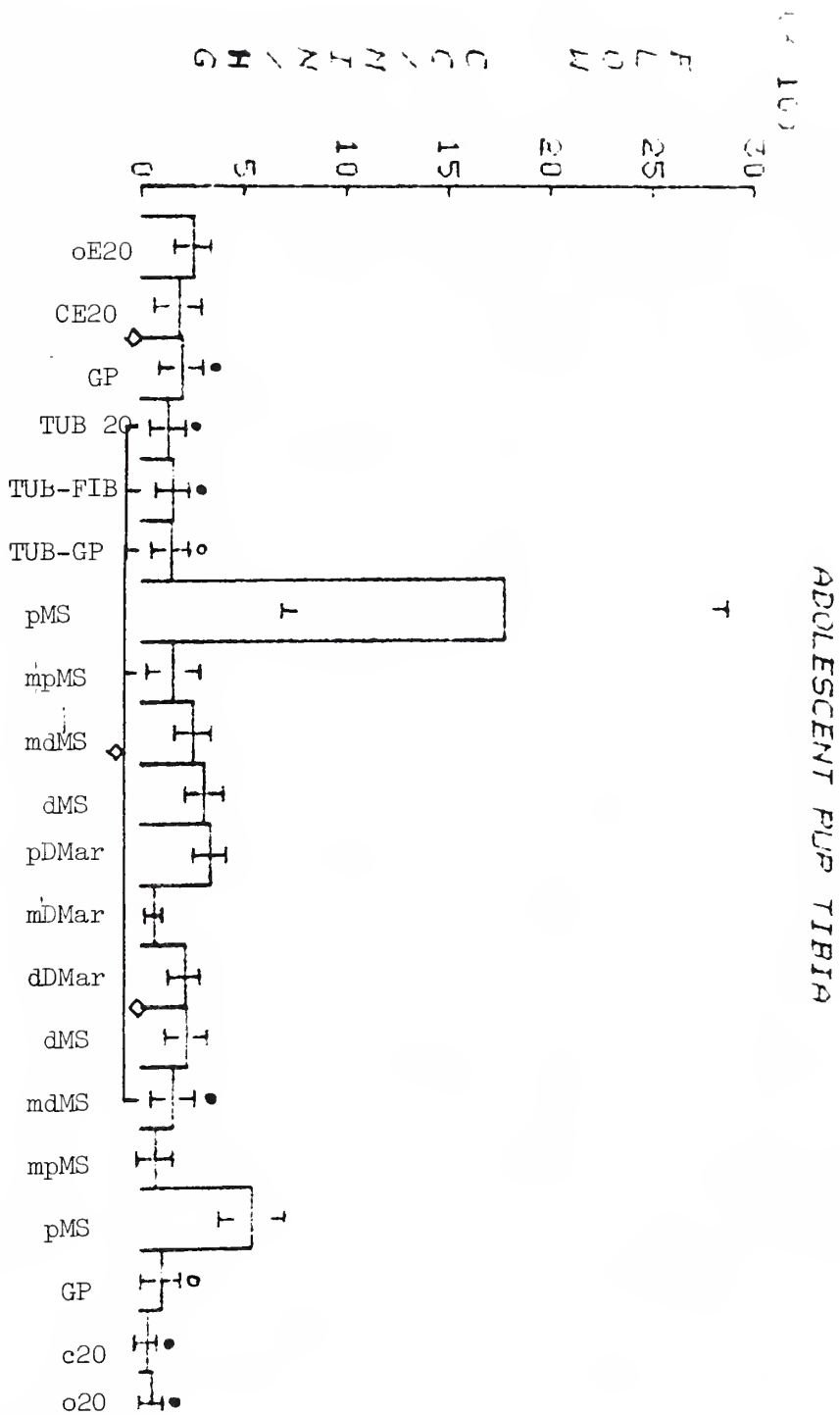
ADOLESCENT PUP TIBIA
GRAIN COUNT
0
5
10
15
20
25
oE20
CE20
GP
TUB 20
TUb-FIB
TUB-GP
pMS
mpMS
mdMS
dMS
pDMar
mDMar
dDMar
dMS
mdMS
mpMS
pMS
GP
c20
o20
BONE REGIONS
PROXIMAL
DISTAL

GRAPH 14

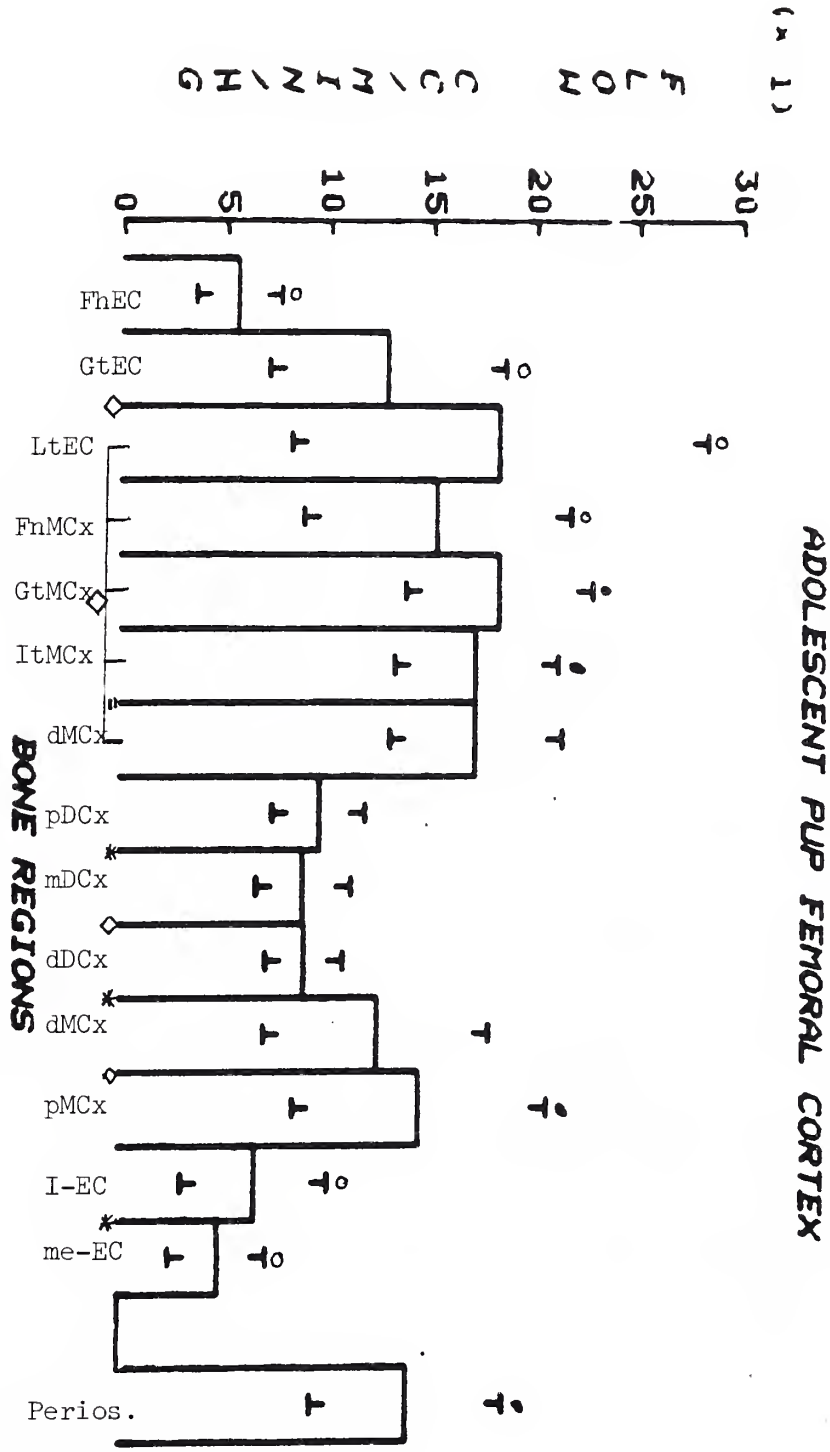
ADOLESCENT PUP FEMORAL CORTEX
BONE REGIONS
PROXIMAL
DISTAL
FhEC
GtEC
LtEC
FnMCx
GtMCx
ItMCx
dMCx
pDCx
mDCx
dDCx
dMCx
pMCx
I-EC
me-EC
Perios.
0
5
10
15
20
25
30

GRAPH 15

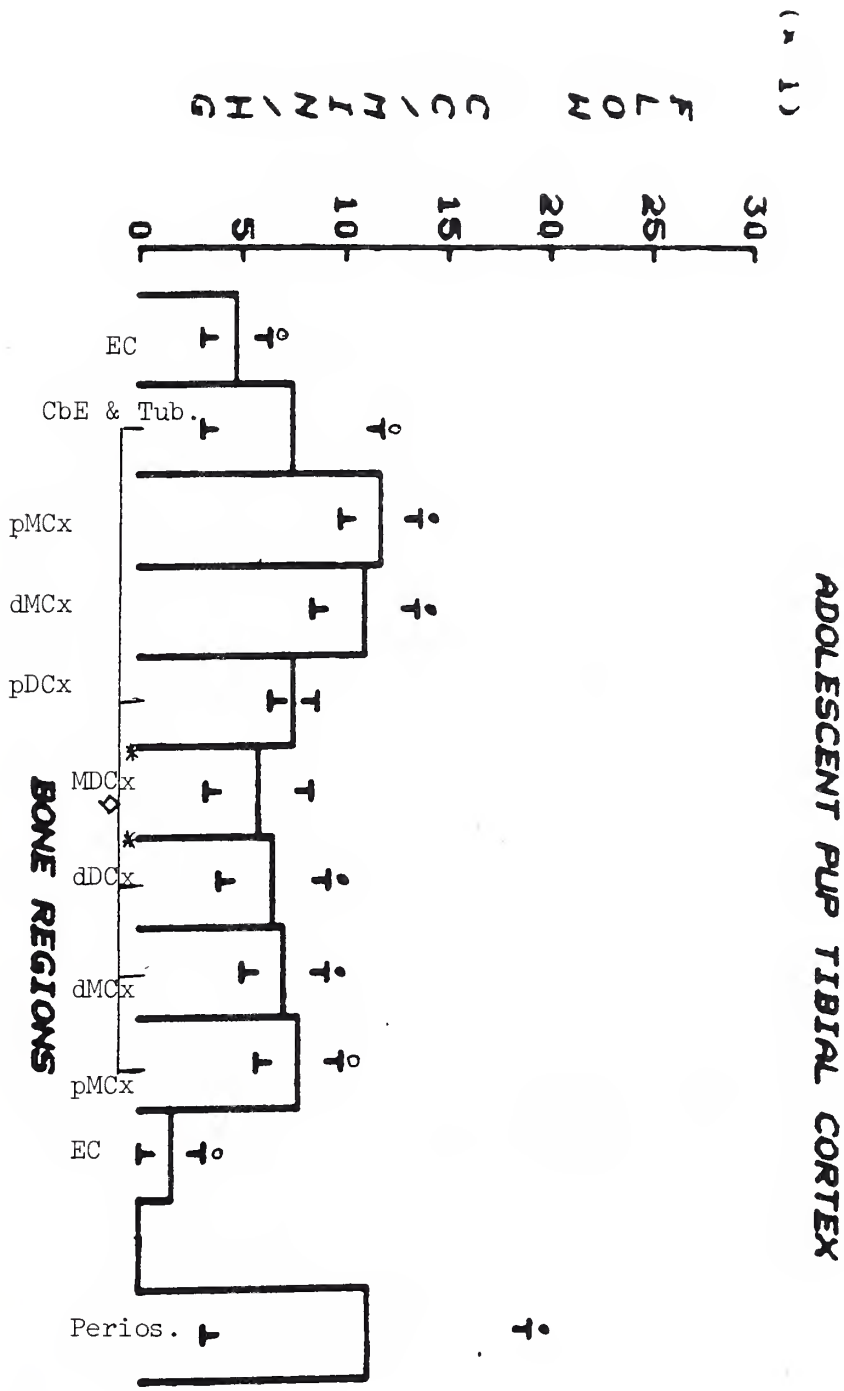
ADOLESCENT PUP TIBIAL CORTEX
BONE REGIONS
PROXIMAL
DISTAL
EC
CbE & Tub.
pMCx
dMCx
pDCx
MDCx
dDCx
dMCx
pMCx
EC
Perios.
0
5
10
15
20
25
30

GRAPH 16

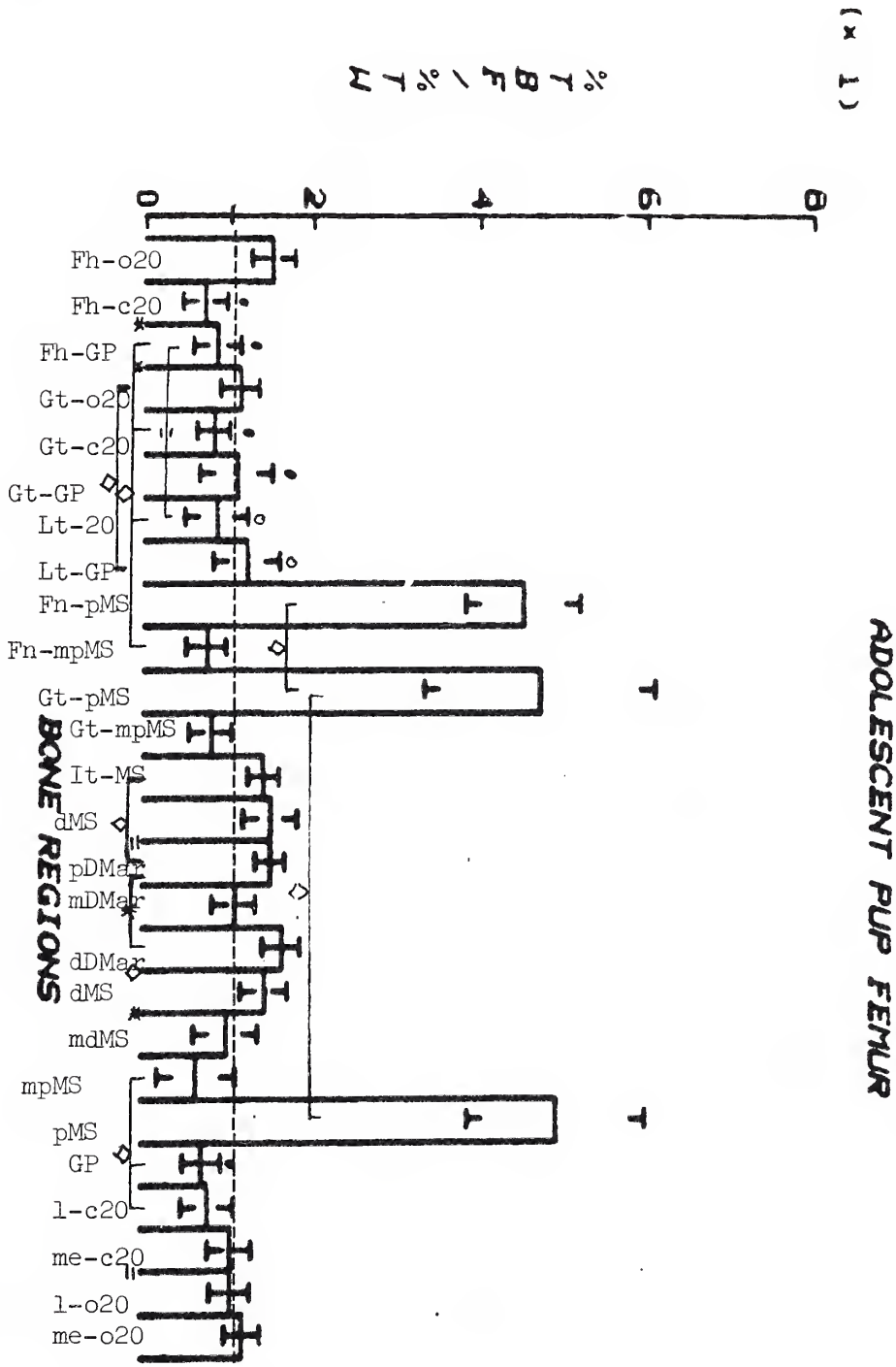
ADOLESCENT PUP FEMUR
MEAN % BFT (x 1)
0
2
4
6
8
PROXIMAL
DISTAL
BONE REGIONS
Fh-o20
Fh-c20
Fh-GP
Gt-o20
Gt-c20
Gt-GP
Lt-20
Lt-GP
Fn-pMS
Fn-mpMS
Gt-pMS
Gt-mpMS
It-MS
dMS
pDMar
mDMar
dDMar
dMS
mdMS
mpMS
pMS
GP
l-c20
me-c20
l-o20
me-o20

GRAPH 17

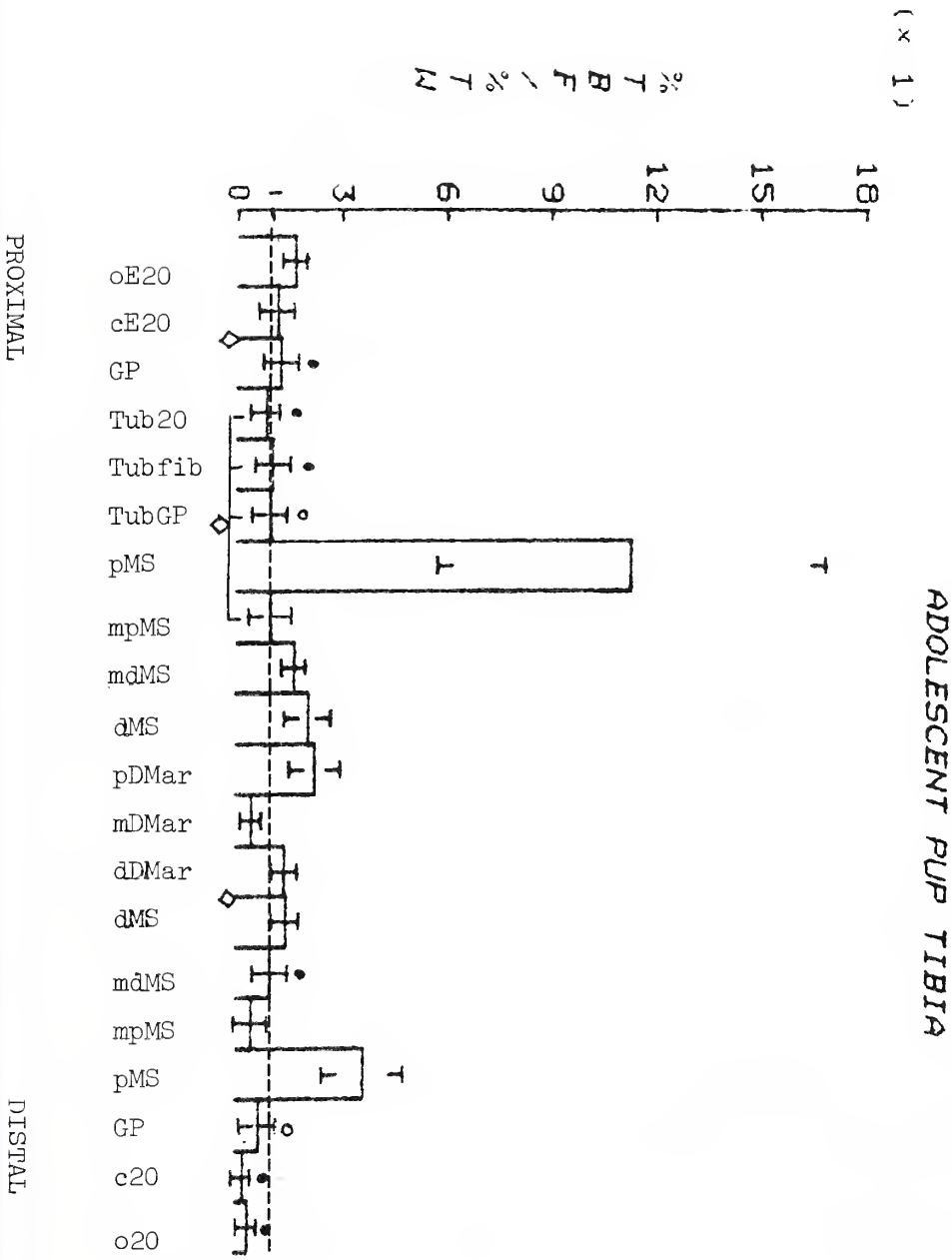
ADOLESCENT PUP TIBIA
% TOTAL BFV (× 1)
0
3
6
9
12
15
18
PROXIMAL
DISTAL
oE20
cE20
GP
Tub20
Tubfib
TubGP
pMS
mpMS
mdMS
dMS
pDMar
mDMar
dDMar
dMS
mdMS
mpMS
pMS
GP
c20
o20

GRAPH 18

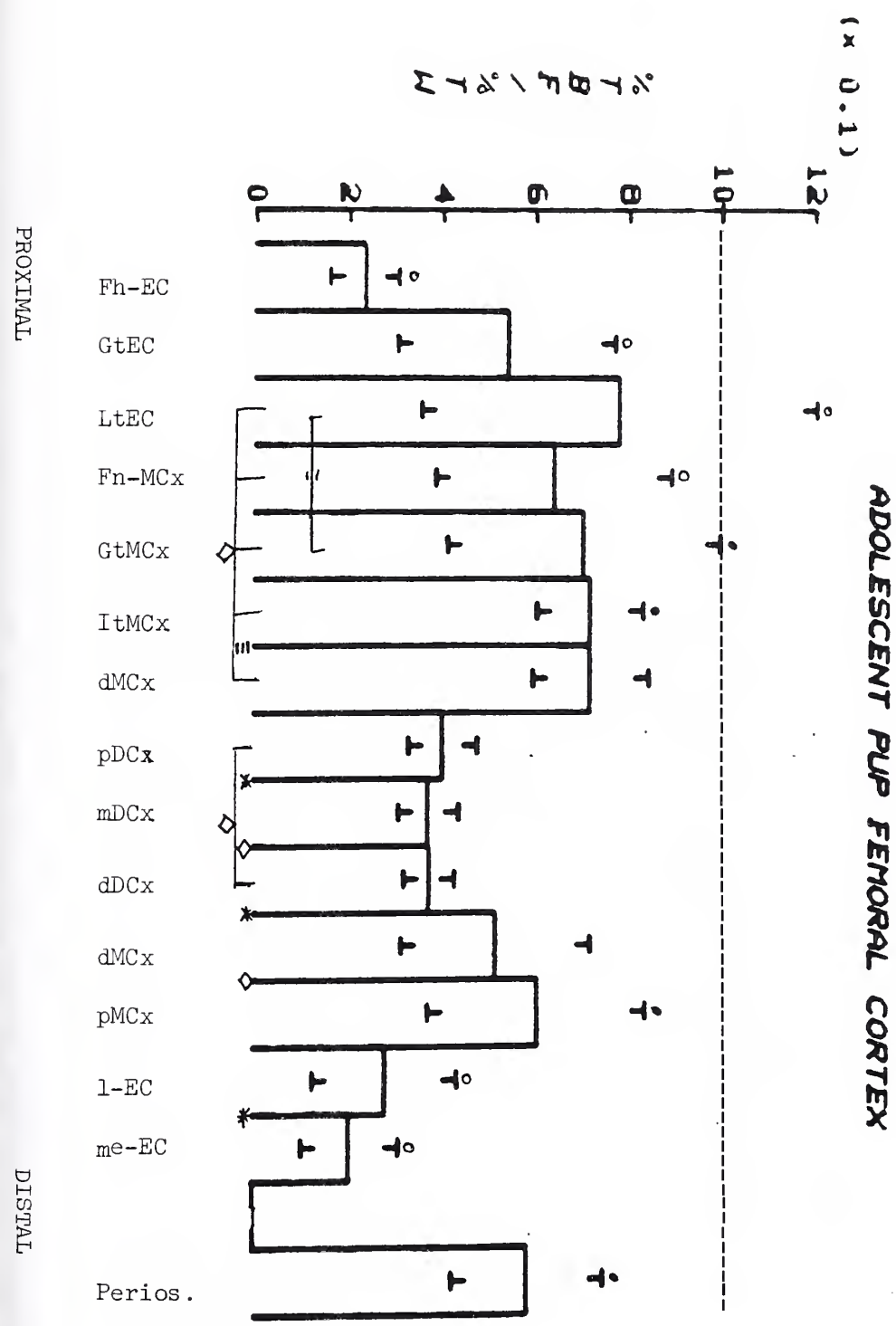
ADOLESCENT PUP FEMORAL CORTEX
% T / B F T
(x 0.1)
0
2
4
6
8
10
12
PROXIMAL
DISTAL
Fh-EC
GtEC
LtEC
Fn-MCx
GtMCx
ItMCx
dMCx
pDCx
mDCx
dDCx
dMCx
pMCx
l-EC
me-EC
Perios.

GRAPH 19

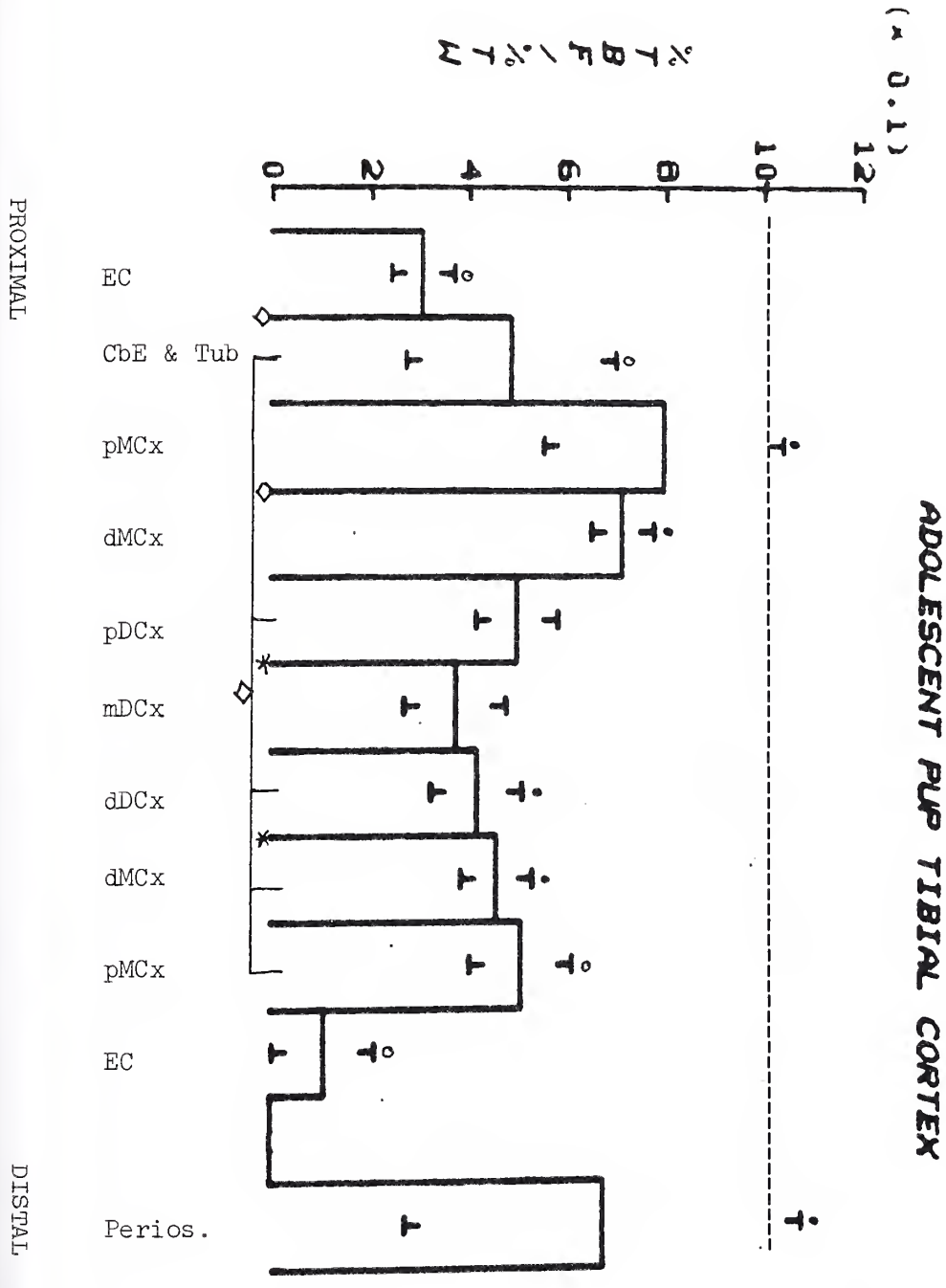
ADOLESCENT PUP TIBIAL CORTEX
% TBFV
(× 0.1)
0
2
4
6
8
10
12
PROXIMAL
DISTAL
EC
CbE & Tub
pMCx
dMCx
pDCx
mDCx
dDCx
dMCx
pMCx
EC
Perios.

GRAPH 20

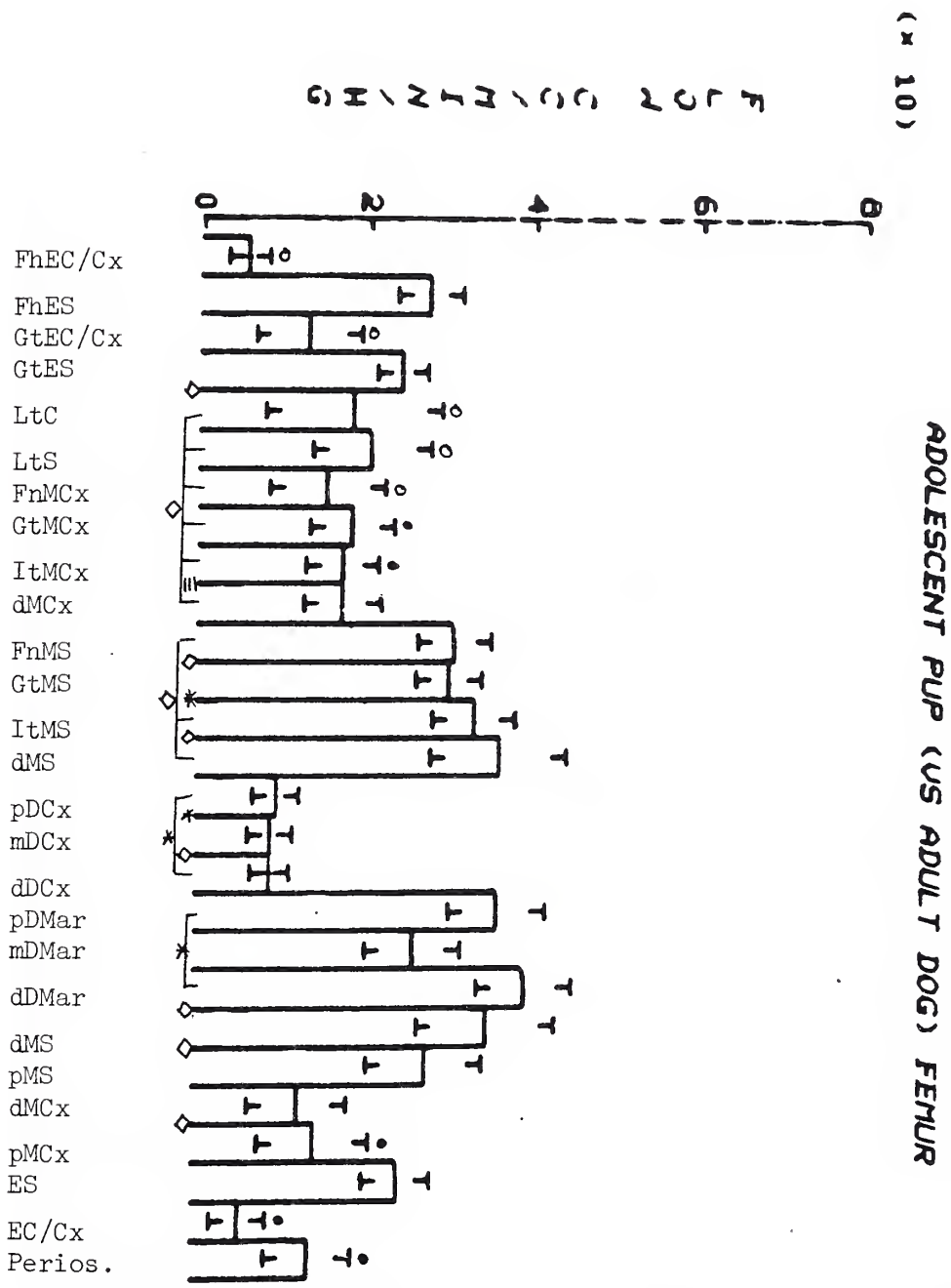
PROXIMAL
DISTAL
FhEC/Cx
FhES
GtEC/Cx
GtES
LtC
LtS
FnMCx
GtMCx
ItMCx
dMCx
FnMS
GtMS
ItMS
dMS
pDCx
mDCx
dDCx
pDMar
mDMar
dDMar
dMS
pMS
dMCx
pMCx
ES
EC/Cx
Perios.
0
2
4
6
8
(× 10)
ADOLESCENT PUP (VS ADULT DOG) FEMUR

GRAPH 21

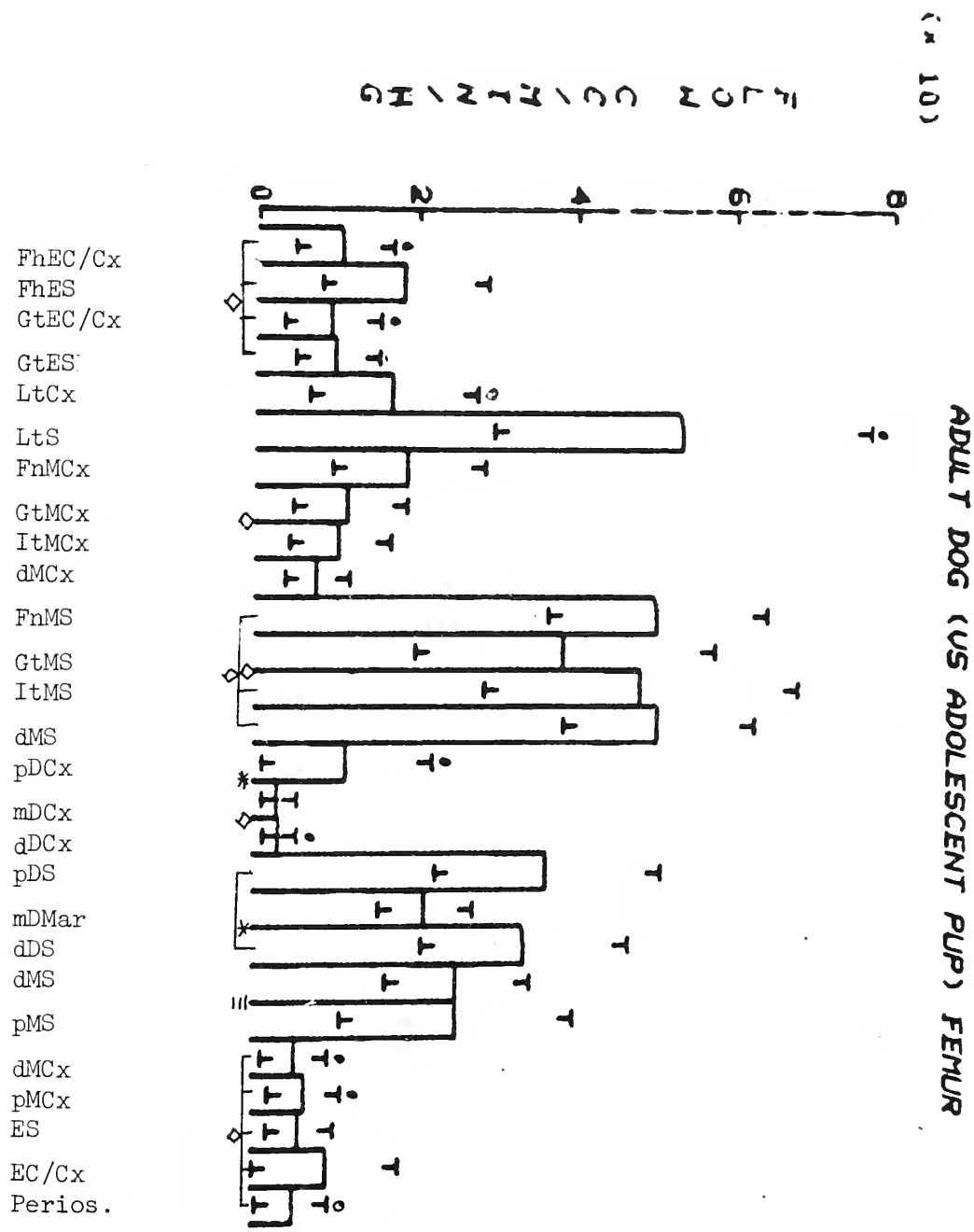
ADULT DOG (VS ADOLESCENT PUP) FEMUR
FLOW CONTRAST (x 10)
0
2
4
6
8
FhEC/Cx
FhES
GtEC/Cx
GtES
LtCx
LtS
FnMCx
GtMCx
ItMCx
dMCx
FnMS
GtMS
ItMS
dMS
pDCx
mDCx
dDCx
pDS
mDMar
dDS
dMS
pMS
dMCx
pMCx
ES
EC/Cx
Perios.
PROXIMAL
DISTAL

GRAPH 22

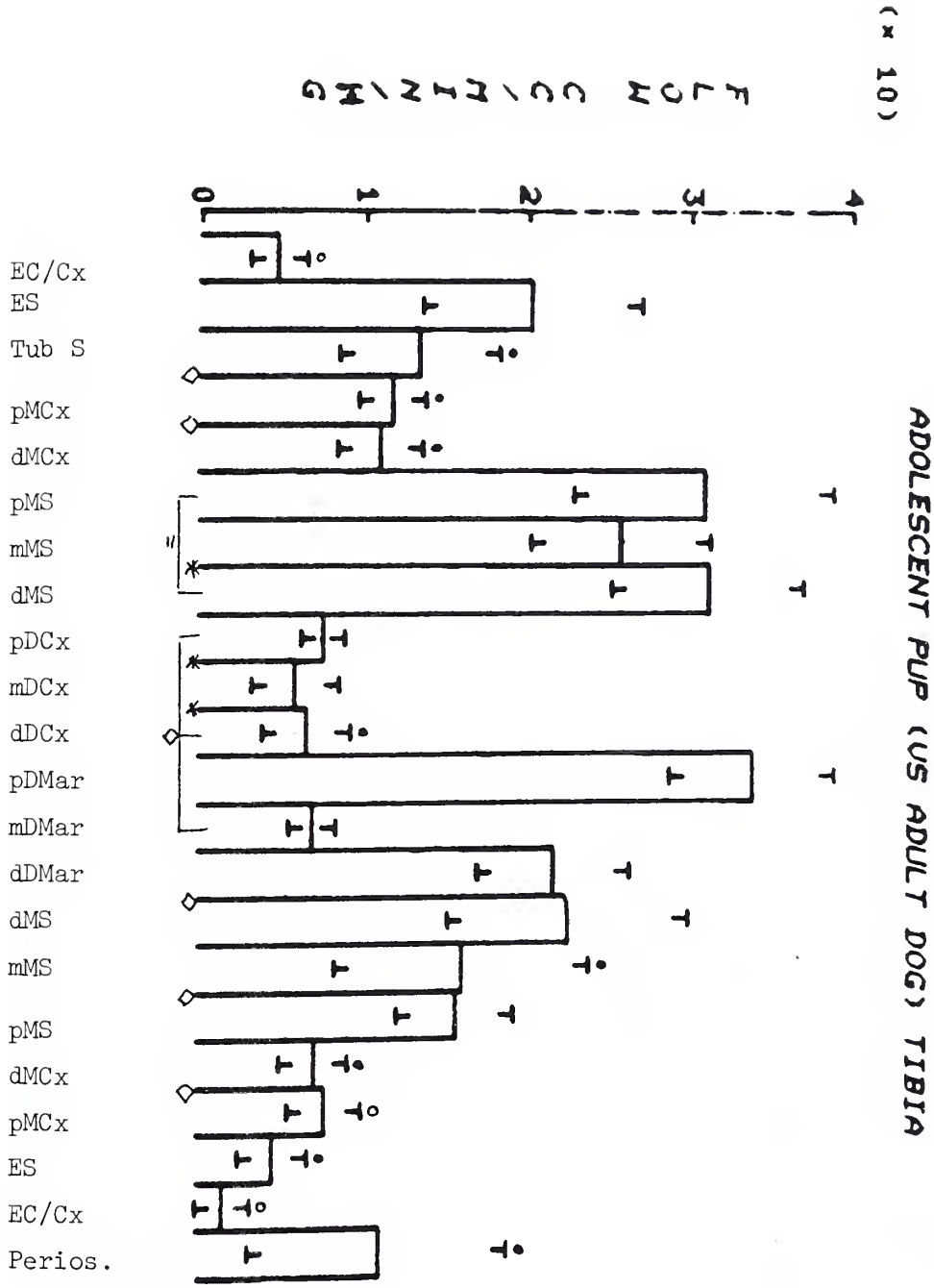
ADOLESCENT PUP (VS ADULT DOG) TIBIA
(× 10)
0
1
2
3
4
EC/Cx
ES
Tub S
pMCx
dMCx
pMS
mMS
dMS
pDCx
mDCx
dDCx
pDMar
mDMar
dDMar
dMS
mMS
pMS
dMCx
pMCx
ES
EC/Cx
Perios.
PROXIMAL
DISTAL

GRAPH 23

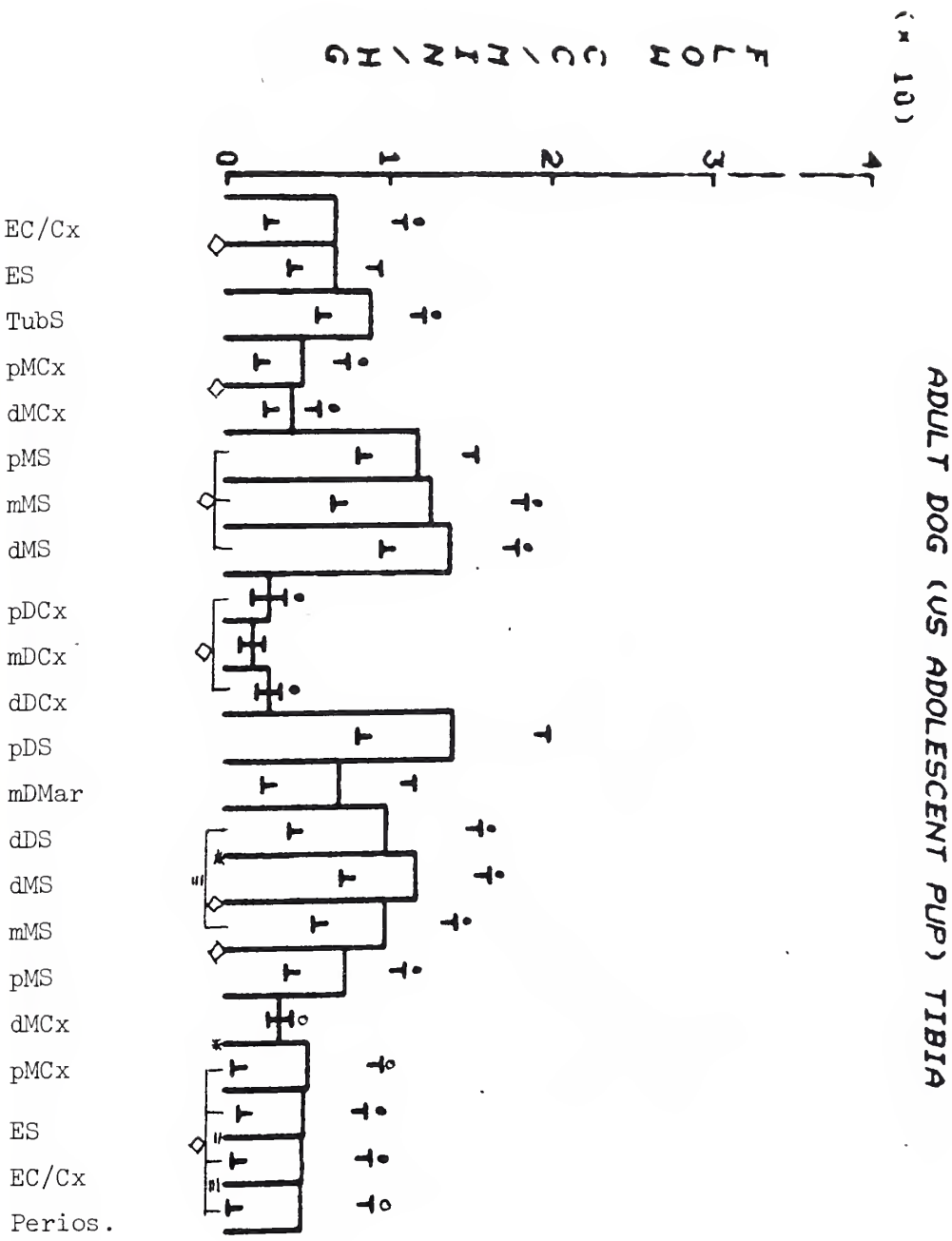
ADULT DOG (VS ADOLESCENT PUP) TIBIA
FOM SCHENKS
(x 10)
0
1
2
3
4
PROXIMAL
DISTAL
EC/Cx
ES
TubS
pMCx
dMCx
pMS
mMS
dMS
pDCx
mDCx
dDCx
pDS
mDMar
dDS
dMS
mMS
pMS
dMCx
pMCx
ES
EC/Cx
Perios.

GRAPH 24A

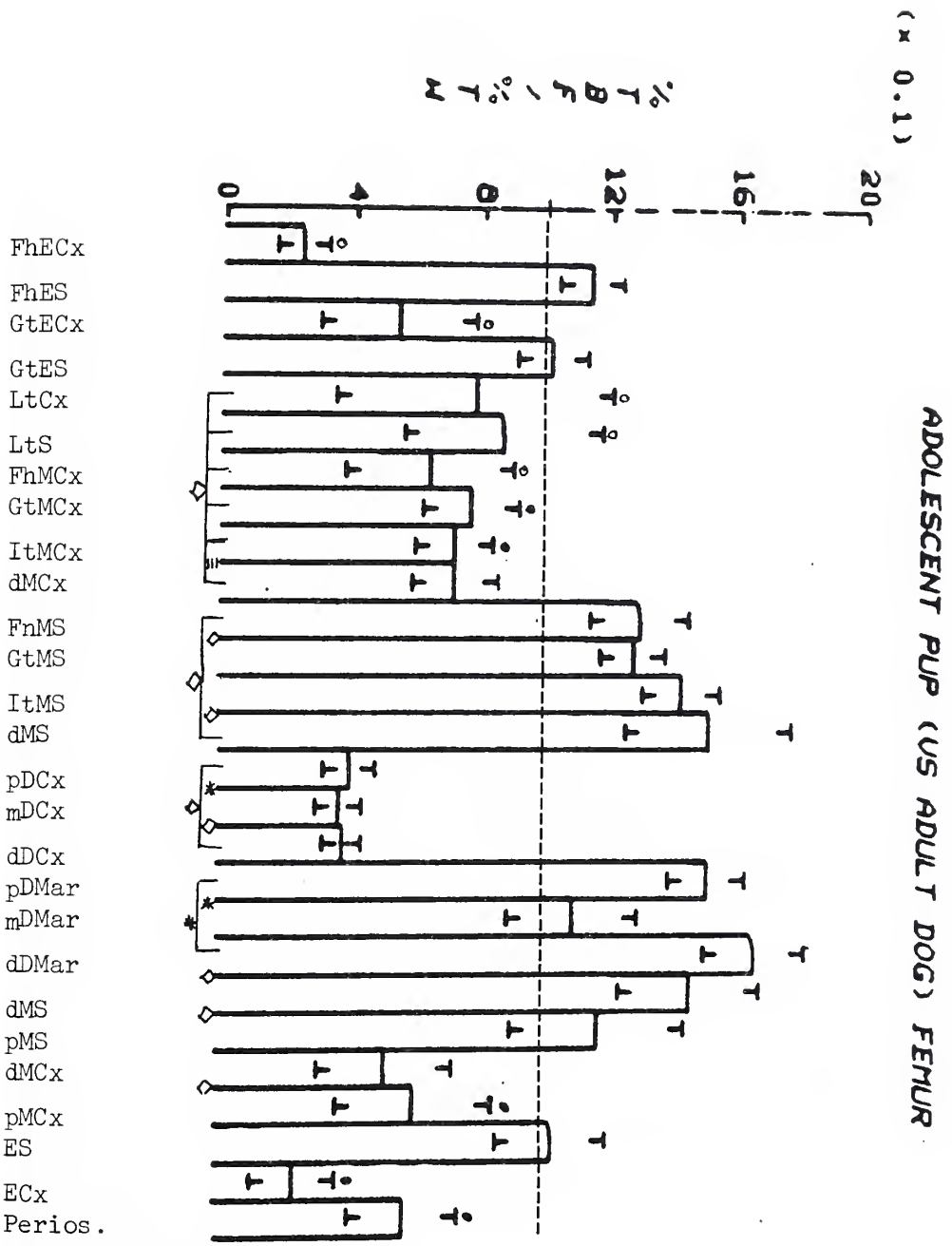
ADOLESCENT PUP (VS ADULT DOG) FEMUR
(× 0.1)
0
4
8
12
16
20
FhECx
FhES
GtECx
GtES
LtCx
LtS
FhMCx
GtMCx
ItMCx
dMCx
FnMS
GtMS
ItMS
dMS
pDCx
mDCx
dDCx
pDMar
mDMar
dDMar
dMS
pMS
dMCx
pMCx
ES
ECx
Perios.
PROXIMAL
DISTAL

GRAPH 24B

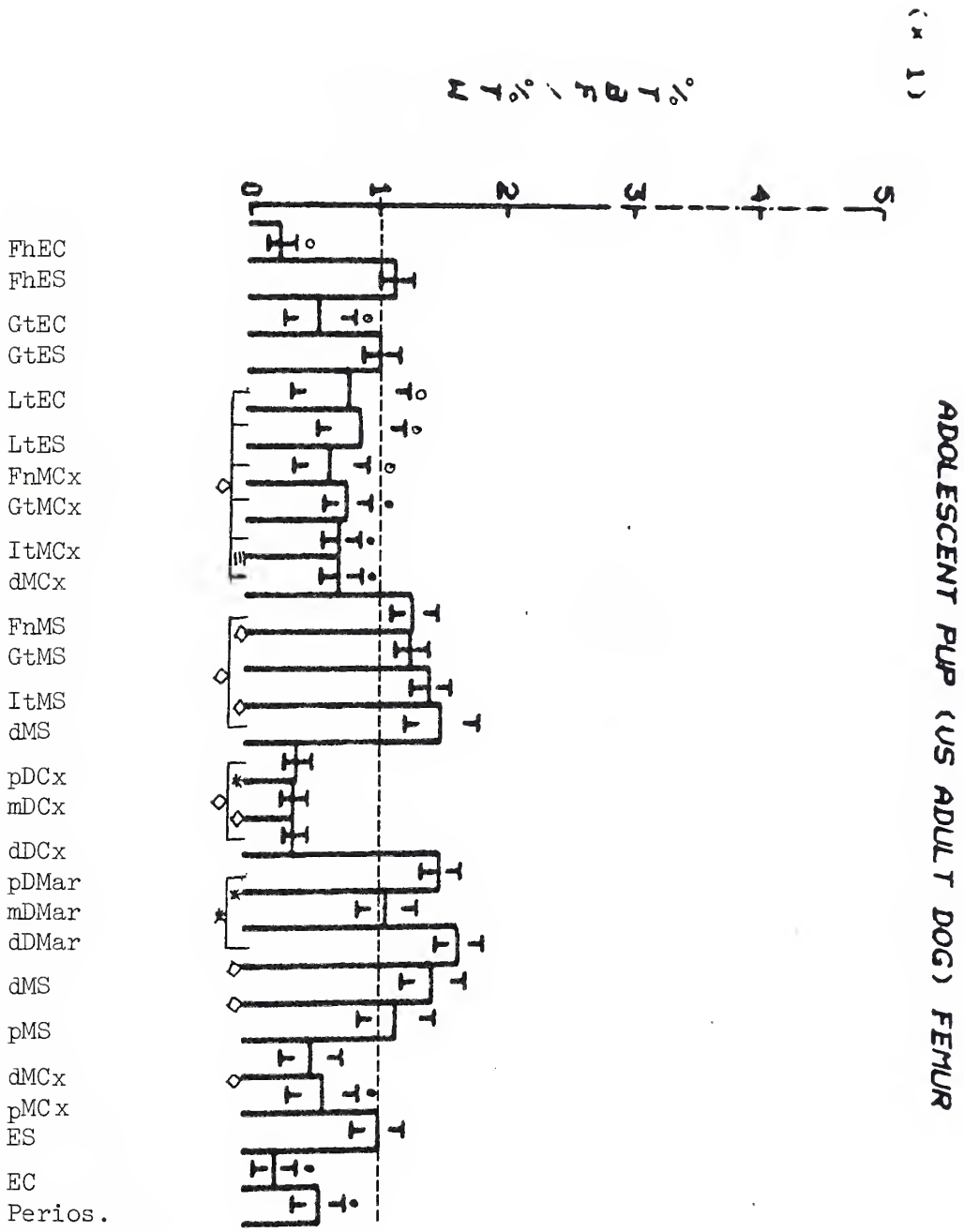
ADOLESCENT PUP (VS ADULT DOG) FEMUR
0
1
2
3
4
5
FhEC
FhES
GtEC
GtES
LtEC
LtES
FnMCx
GtMCx
ItMCx
dMCx
FnMS
GtMS
ItMS
dMS
pDCx
mDCx
dDCx
pDMar
mDMar
dDMar
dMS
pMS
dMCx
pMCx
ES
EC
Perios.
PROXIMAL
DISTAL

GRAPH 25

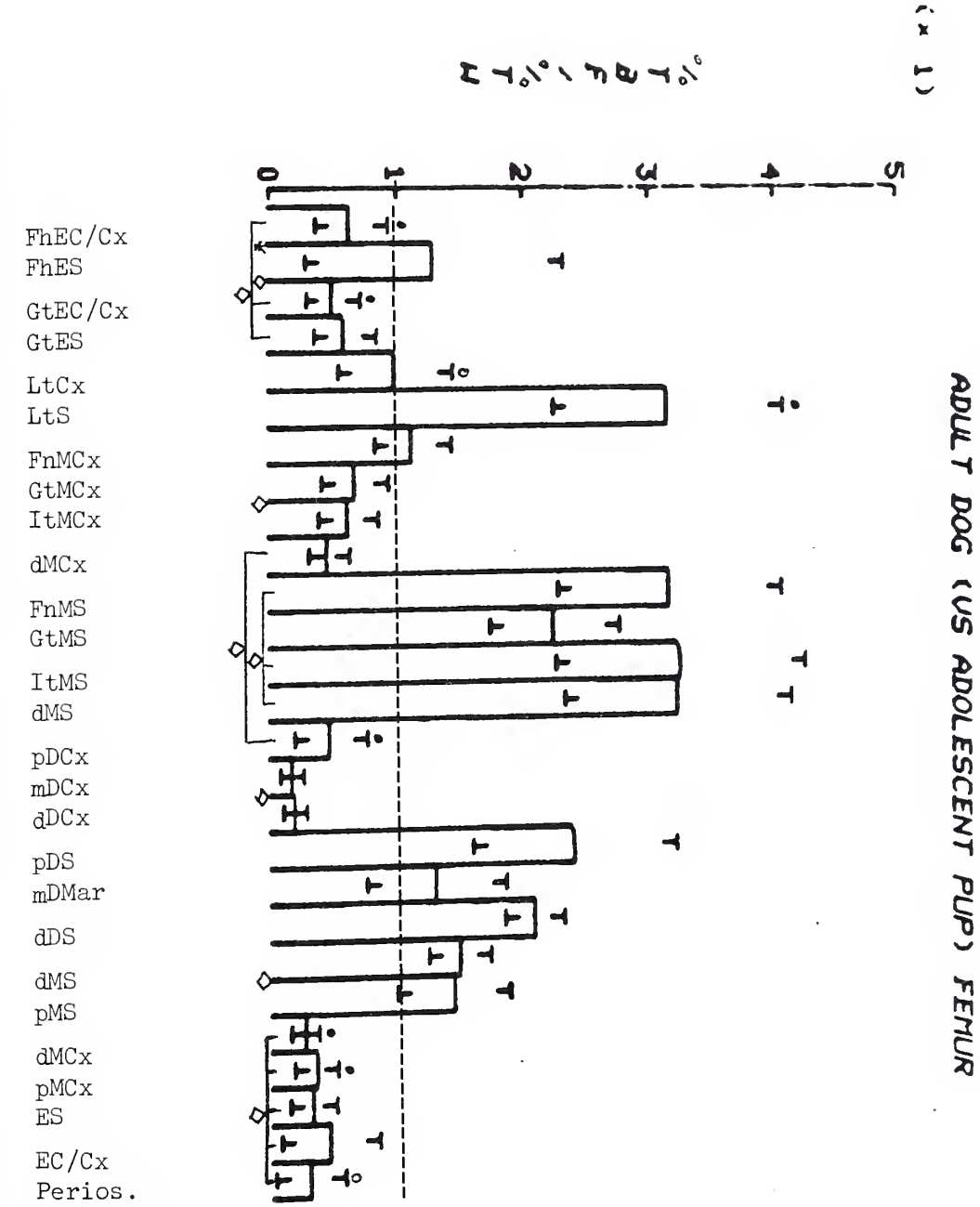
ADULT DOG (VS ADOLESCENT PUP) FEMUR
0
1
2
3
4
5
FhEC/Cx
FhES
GtEC/Cx
GtES
LtCx
LtS
FnMCx
GtMCx
ItMCx
dMCx
FnMS
GtMS
ItMS
dMS
pDCx
mDCx
dDCx
pDS
mDMar
dDS
dMS
pMS
dMCx
pMCx
ES
EC/Cx
Perios.
PROXIMAL
DISTAL

GRAPH 26

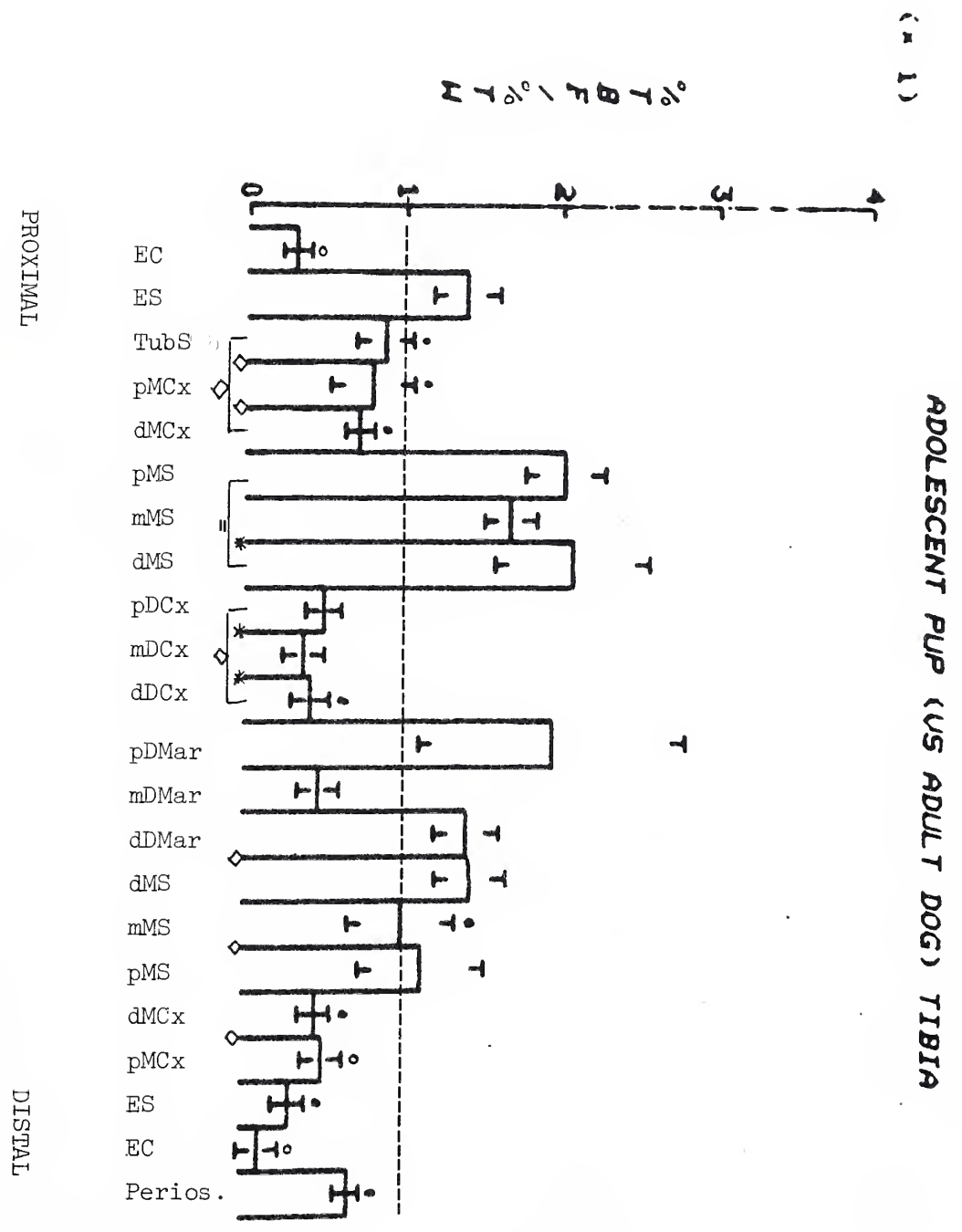
ADOLESCENT PUP (VS ADULT DOG) TIBIA
PROXIMAL
DISTAL
EC
ES
TubS
pMCx
dMCx
pMS
mMS
dMS
pDCx
mDCx
dDCx
pDMar
mDMar
dDMar
dMS
mMS
pMS
dMCx
pMCx
ES
EC
Perios.

GRAPH 27

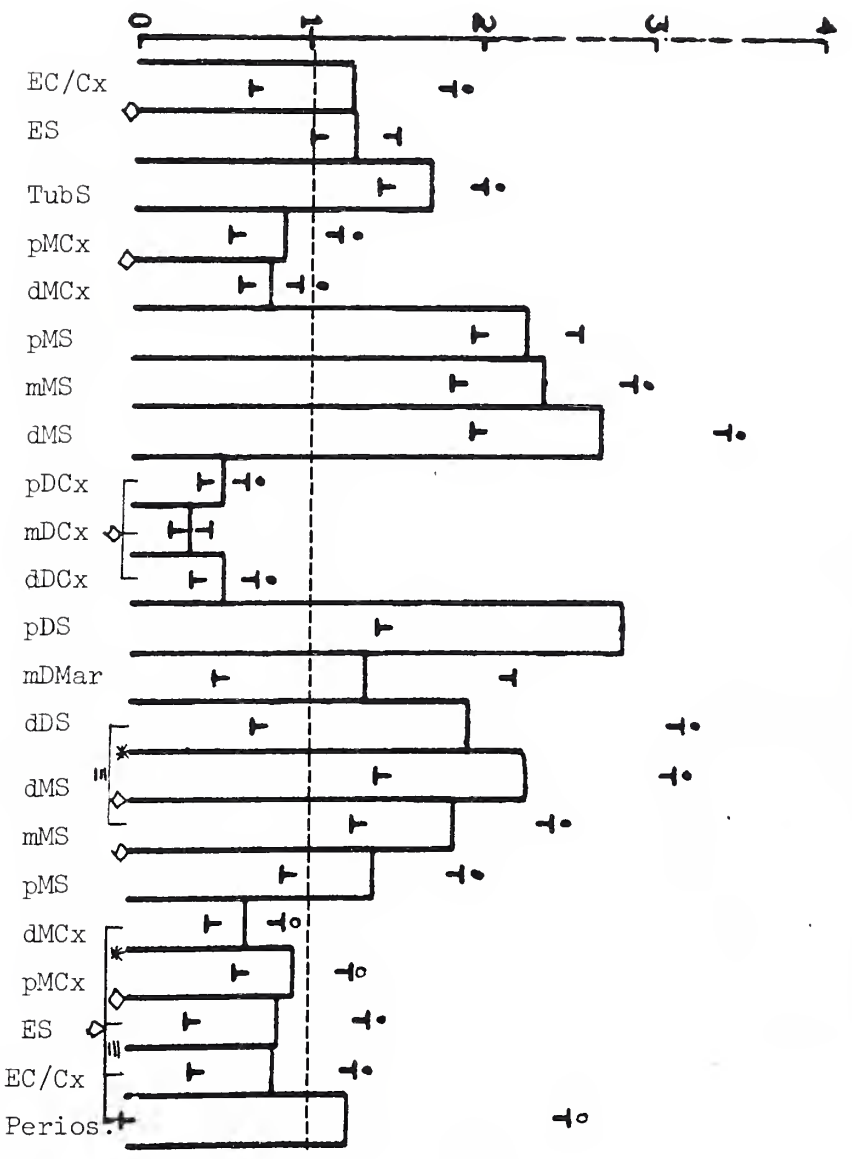
ADULT DOG (VS ADOLESCENT PUP) TIBIA
(x 1)
0
1
2
3
4
EC/Cx
ES
TubS
pMCx
dMCx
pMS
mMS
dMS
pDCx
mDCx
dDCx
pDS
mDMar
dDS
dMS
mMS
pMS
dMCx
pMCx
ES
EC/Cx
Perios
PROXIMAL
DISTAL

GRAPH 28

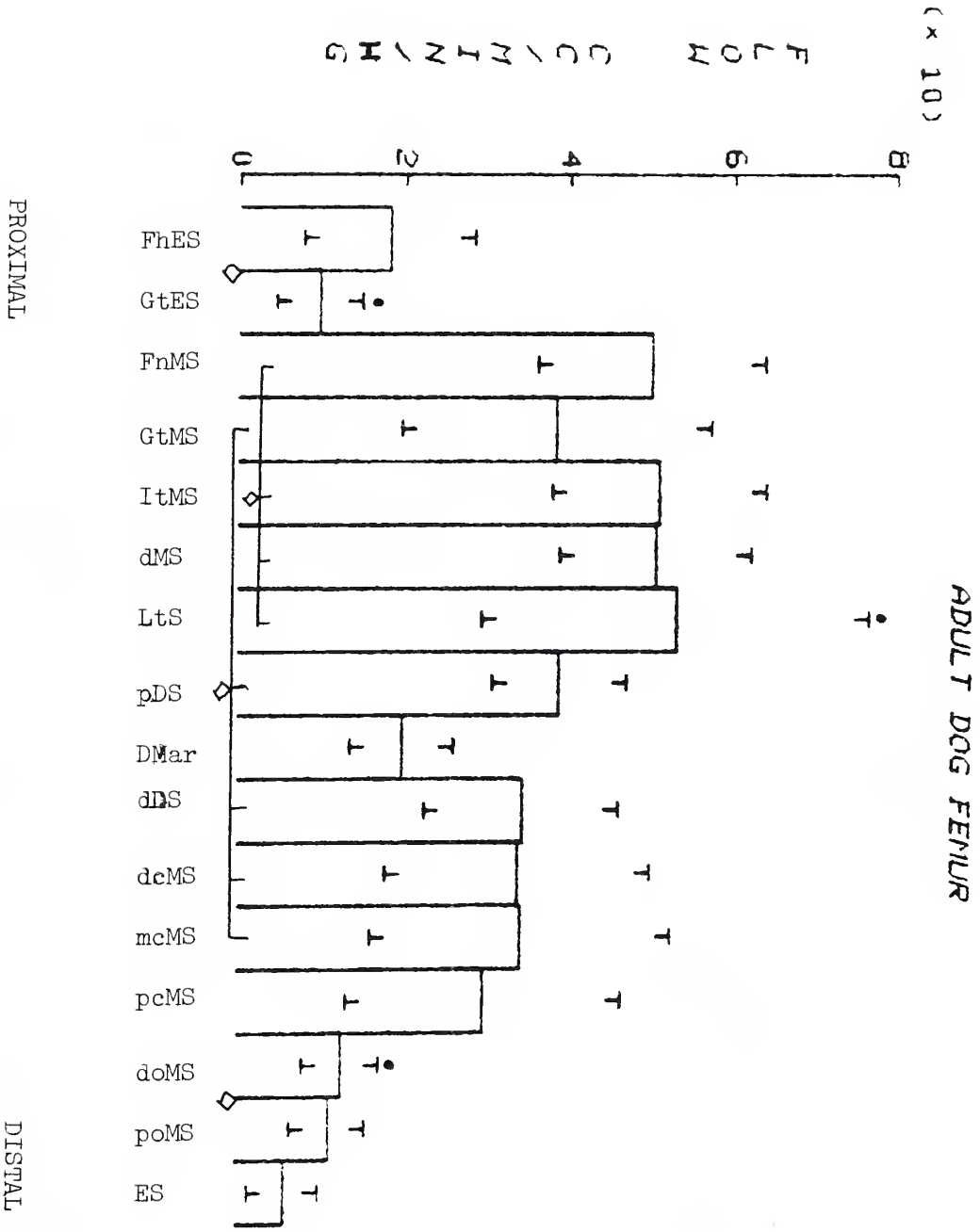
ADULT DOG FEMUR
PROXIMAL
DISTAL
FhES
GtES
FnMS
GtMS
ItMS
dMS
LtS
pDS
DMar
dDS
dcMS
mcMS
pcMS
doMS
poMS
ES
0
2
4
6
8
(× 10)
NO. OF CEMENTUM

GRAPH 29A

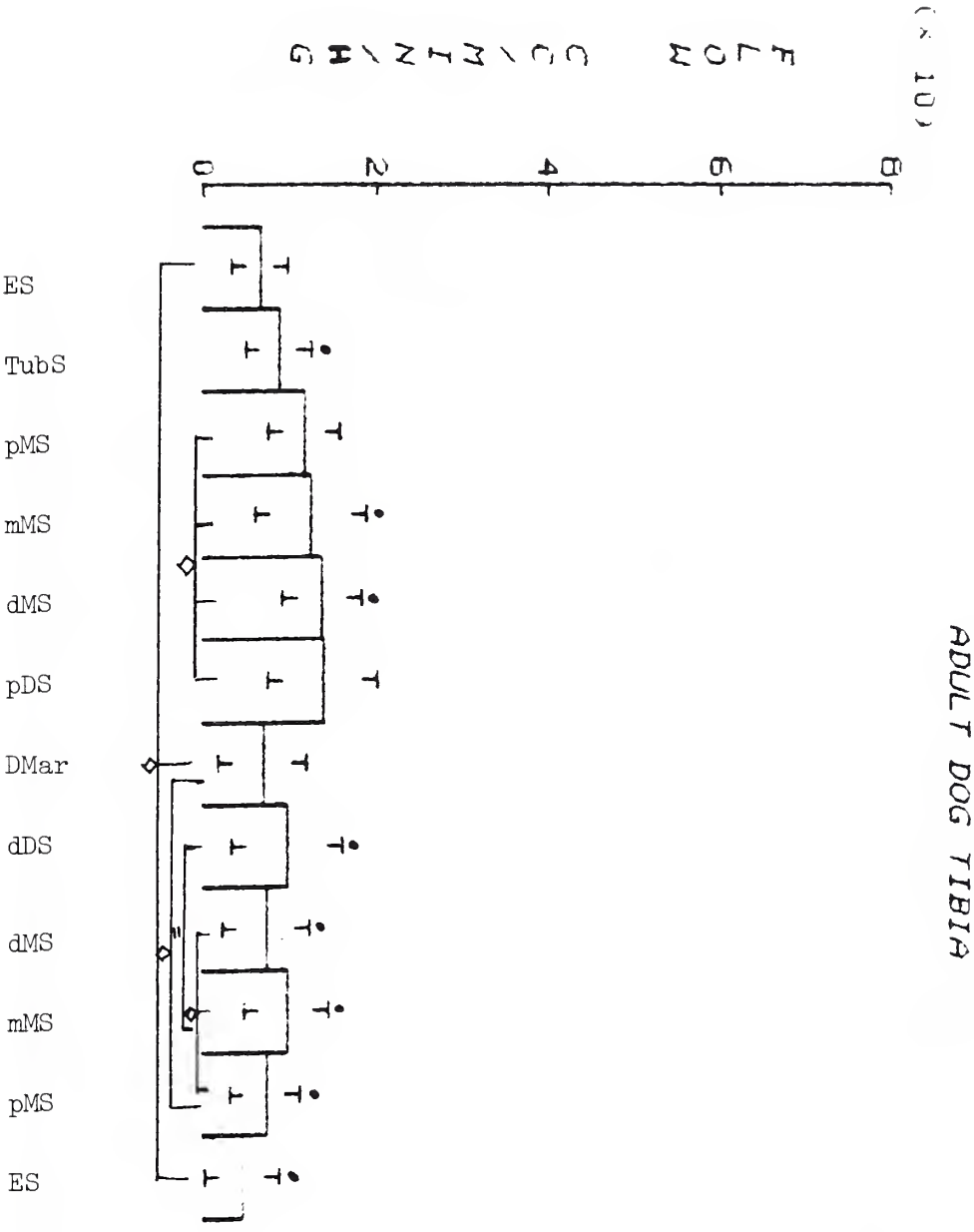

ADULT DOG TIBIA

GRAPH 29B

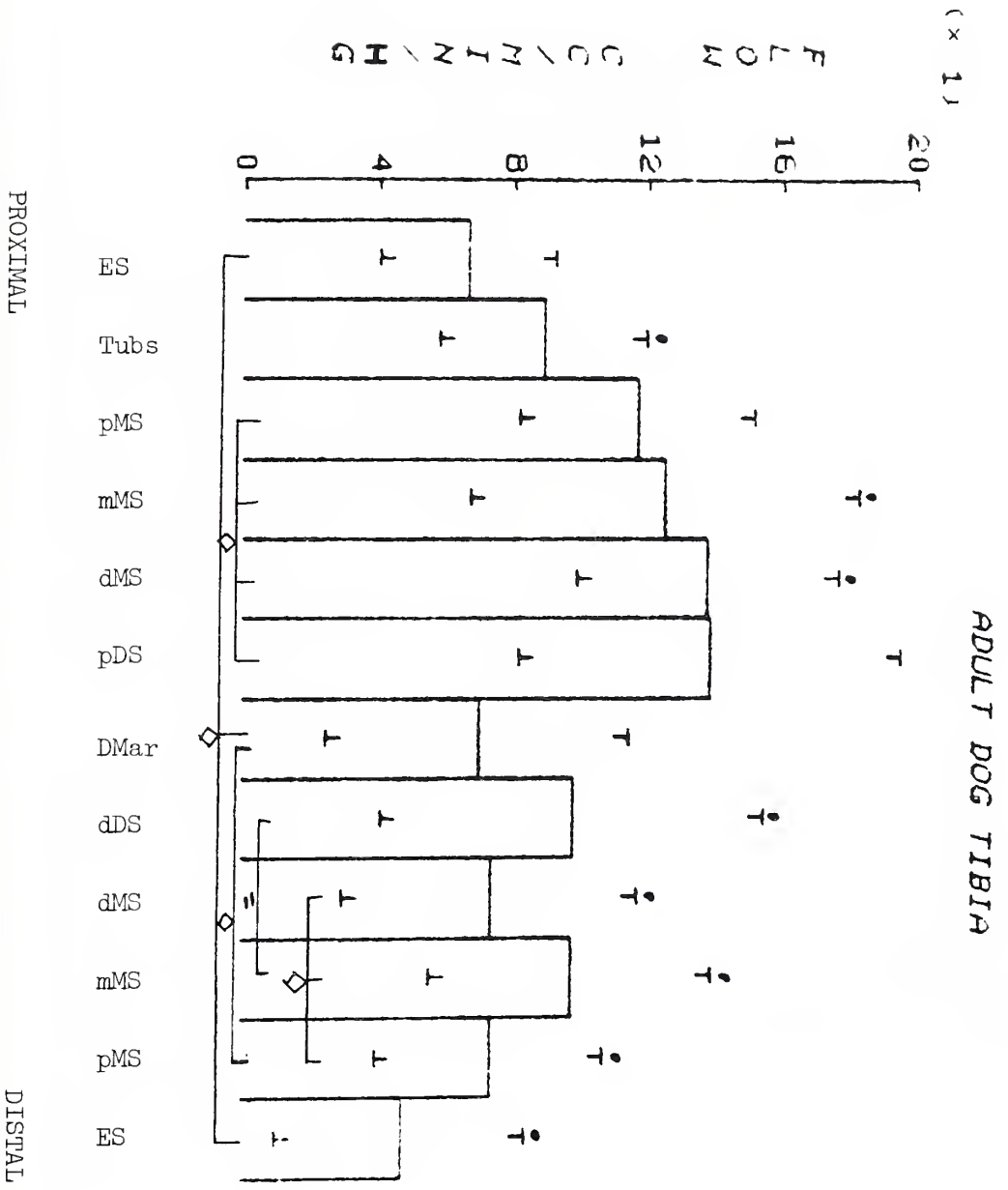
ADULT DOG TIBIA
FREQUENCY COUNTING (× 1)
0
4
8
12
16
20
ES
Tubs
pMS
mMS
dMS
pDS
DMar
dDS
dMS
mMS
pMS
ES
PROXIMAL
DISTAL

GRAPH 30

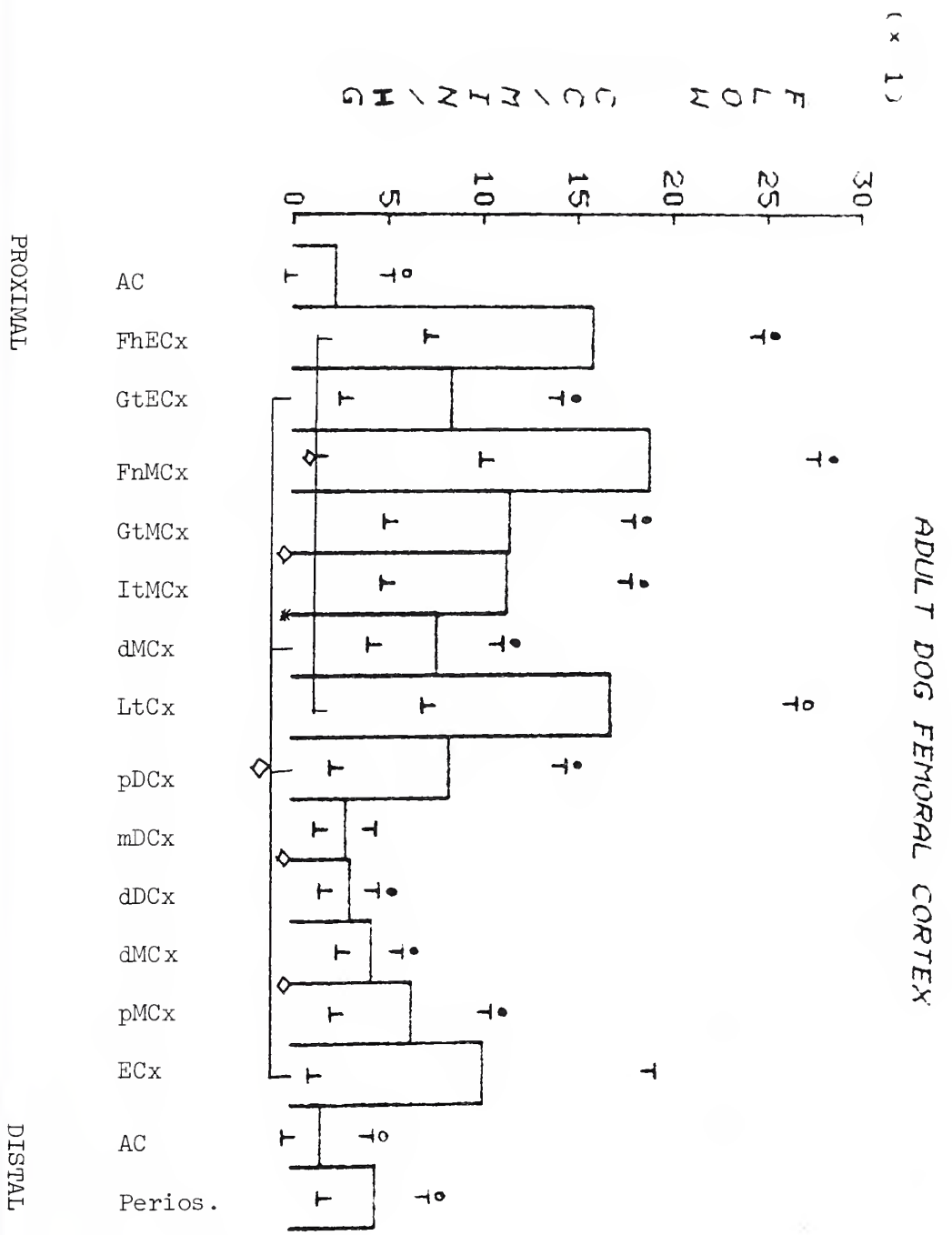
ADULT DOG FEMORAL CORTEX
FLOW
SCINTIMG
(× 1)
0
5
10
15
20
25
30
PROXIMAL
DISTAL
AC
FhECx
GtECx
FnMCx
GtMCx
ItMCx
dMCx
LtCx
pDCx
mDCx
dDCx
dMCx
pMCx
ECx
AC
Perios.

GRAPH 31

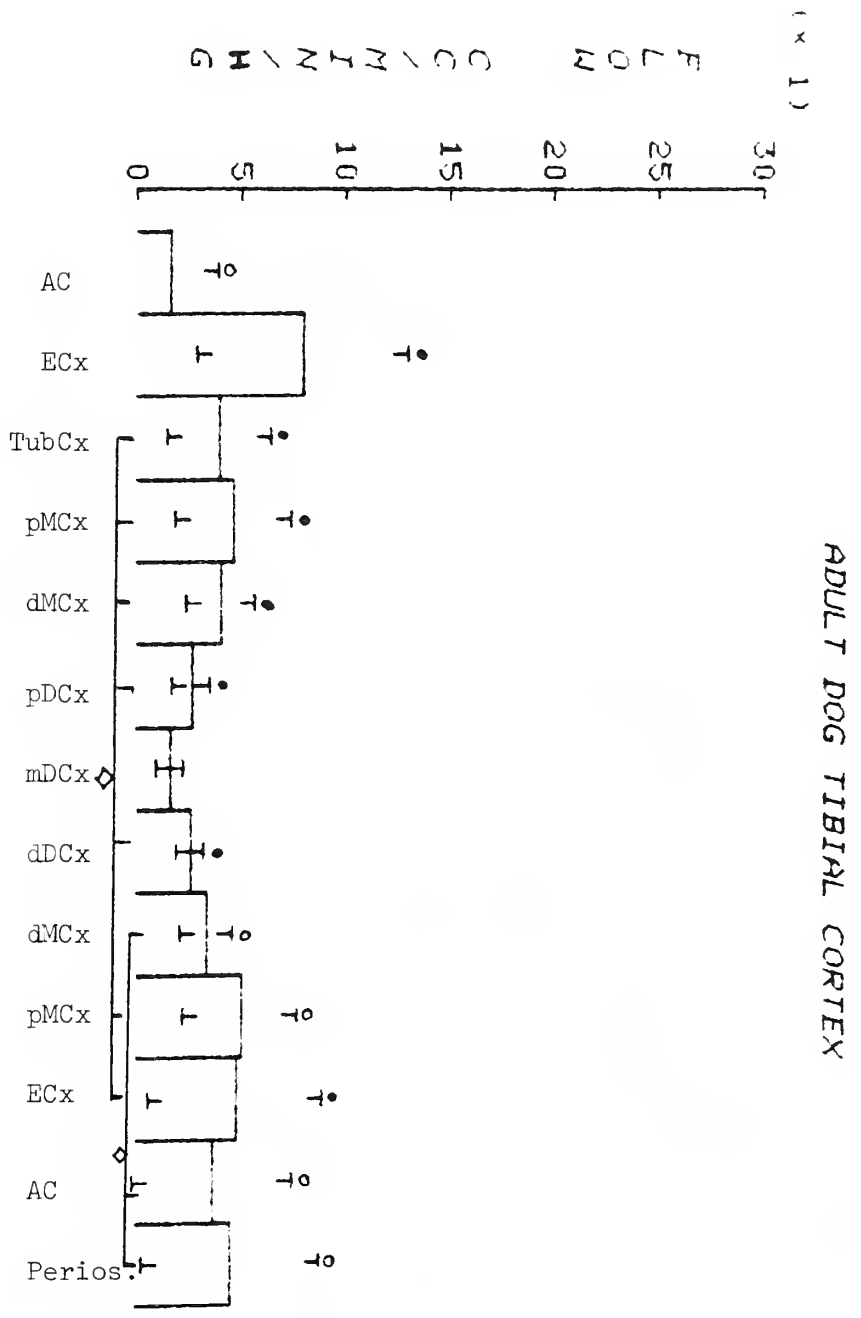

ADULT DOG TIBIAL CORTEX

GRAPH 32

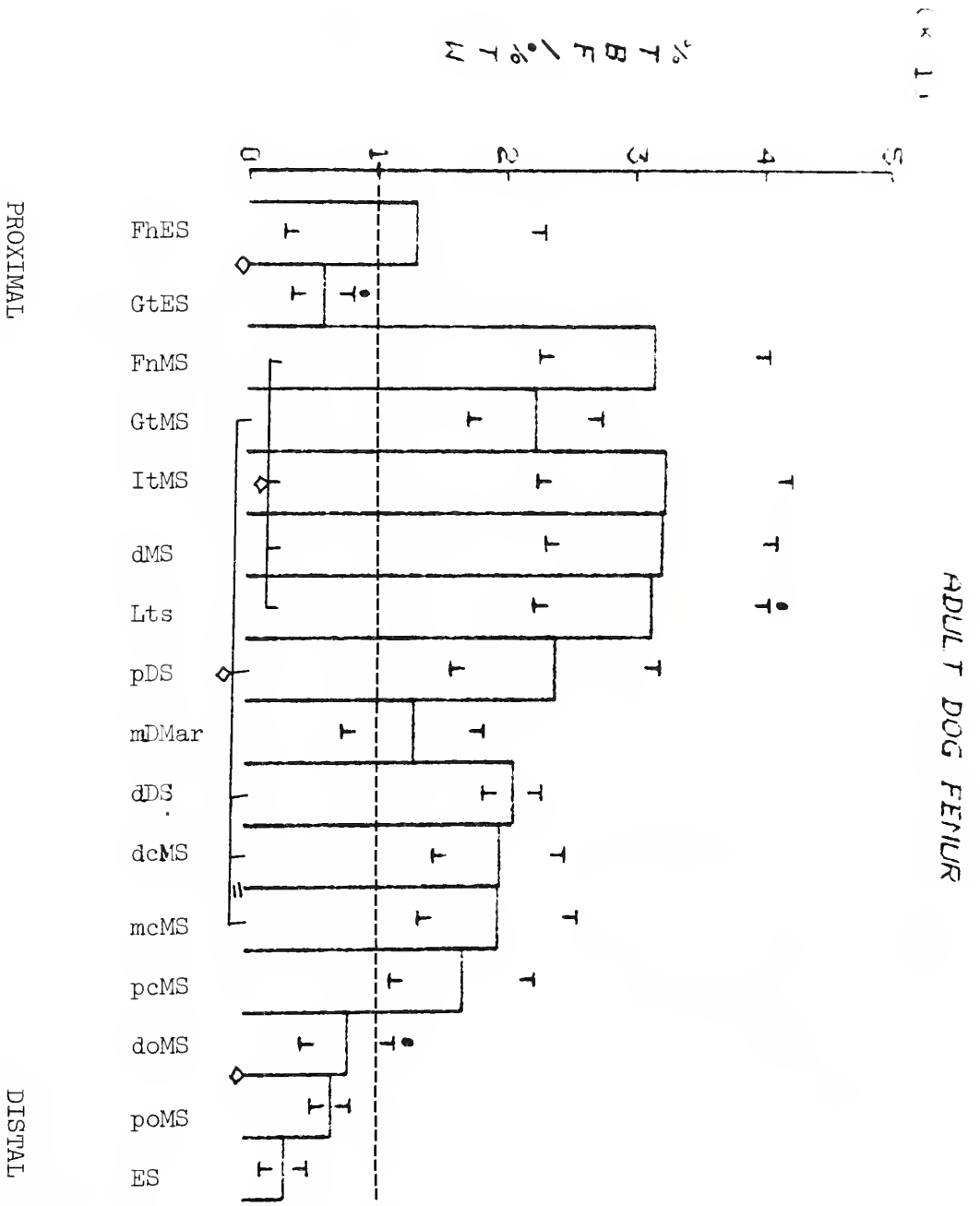
ADULT DOG FEMUR
PROXIMAL
DISTAL
FnES
GtES
FnMS
GtMS
ItMS
dMS
Lts
pDS
mDMar
dDS
dcMS
mcMS
pcMS
doMS
poMS
ES

GRAPH 33

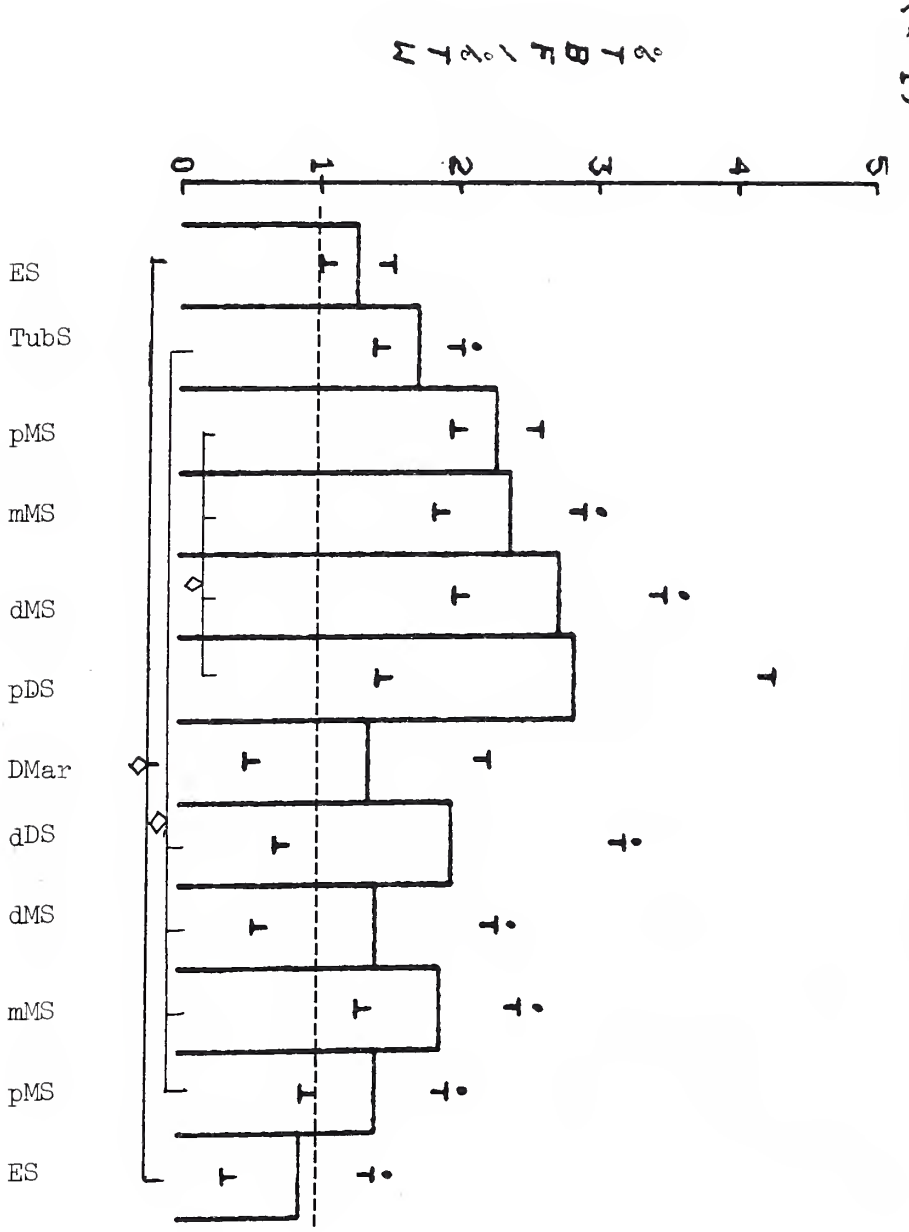
ADULT DOG TIBIA
0
1
2
3
4
5
ES
TubS
pMS
mMS
dMS
pDS
DMar
dDS
dMS
mMS
pMS
ES
PROXIMAL
DISTAL

GRAPH 34

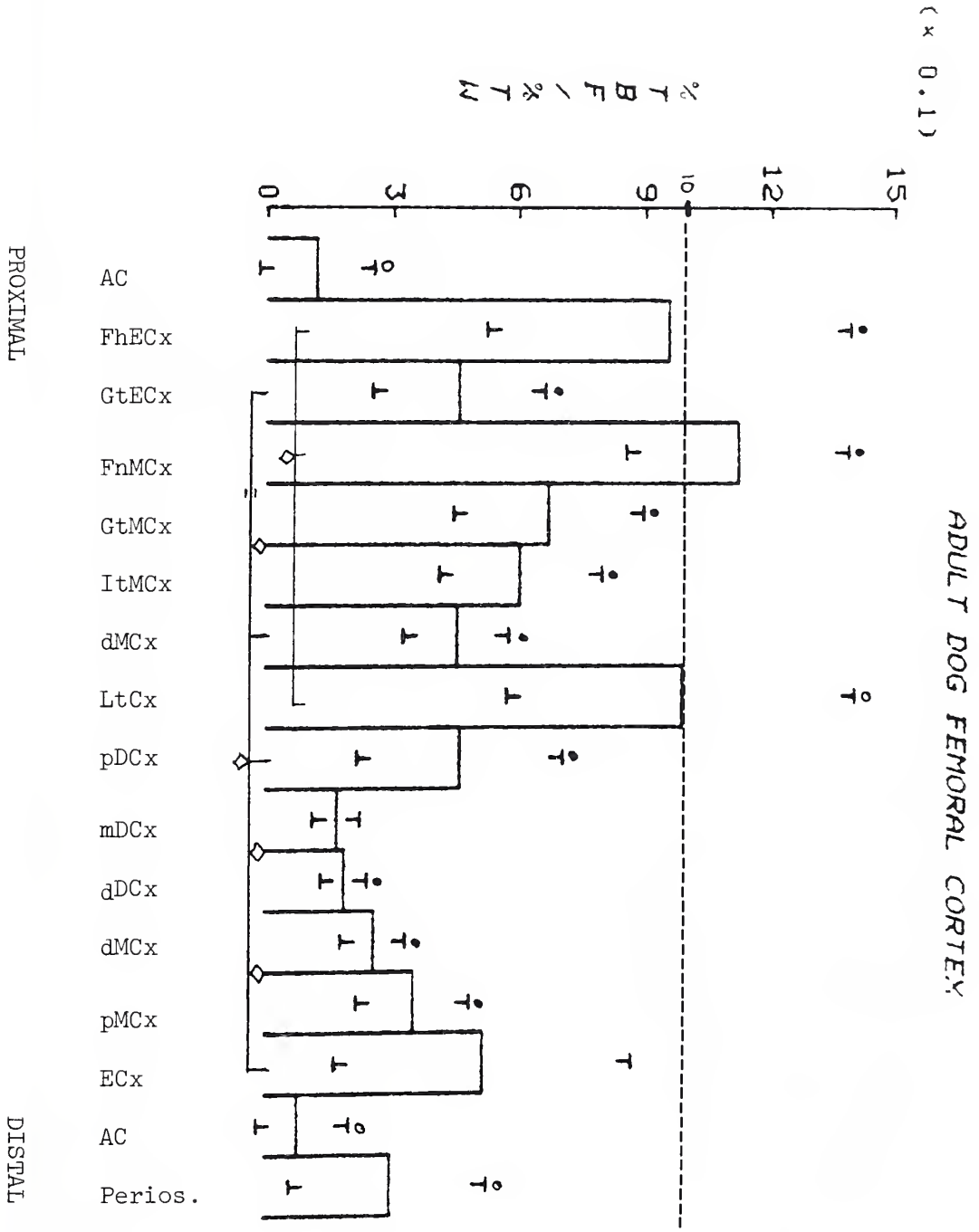
ADULT DOG FEMORAL CORTEX
% TBF / % TN
(× 0.1)
0
3
6
9
10
12
15
PROXIMAL
DISTAL
AC
FhECx
GtECx
FnMCx
GtMCx
ItMCx
dMCx
LtCx
pDCx
mDCx
dDCx
dMCx
pMCx
ECx
AC
Perios.

GRAPH 35

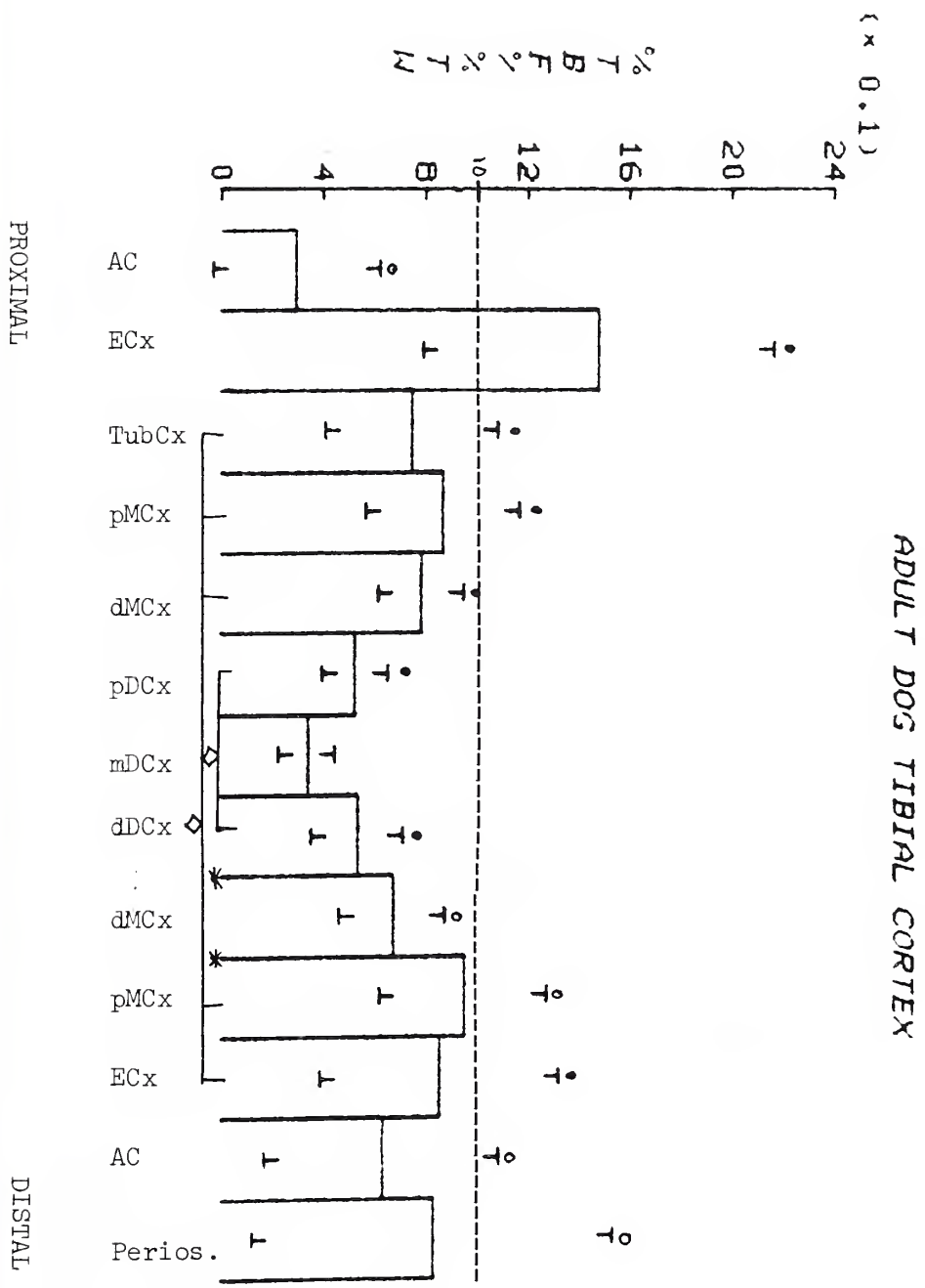
ADULT DOG TIBIAL CORTEX
% TOTAL BONE FREE
(× 0.1)
0
4
8
10
12
16
20
24
AC
ECx
TubCx
pMCx
dMCx
pDCx
mDCx
dDCx
dMCx
pMCx
ECx
AC
Perios.
PROXIMAL
DISTAL

GRAPH 36

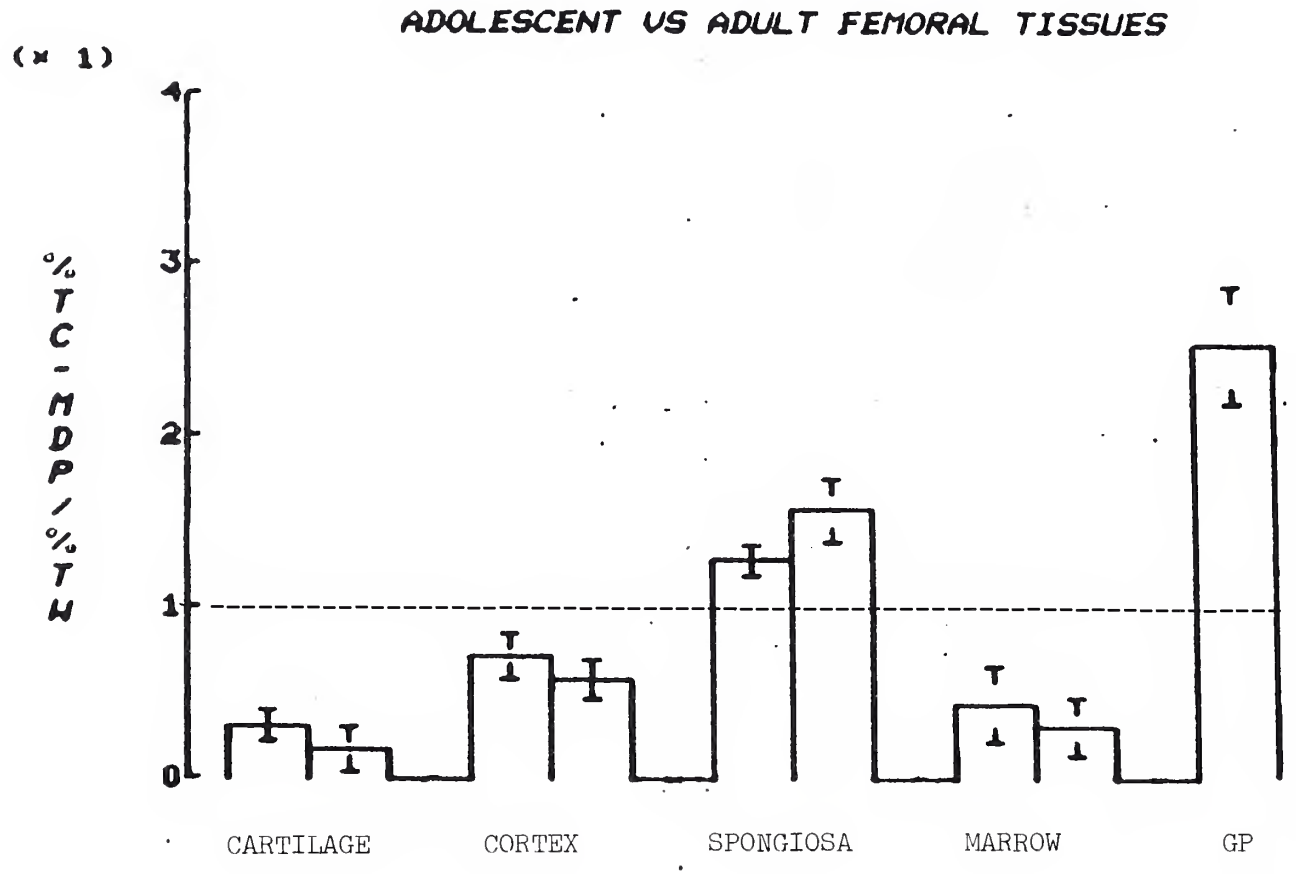
ADOLESCENT VS ADULT FEMORAL TISSUES
(× 1)
% TC - MDP / % TN
4
3
2
1
0
CARTILAGE
CORTEX
SPONGIOSA
MARROW
GP

GRAPH 37

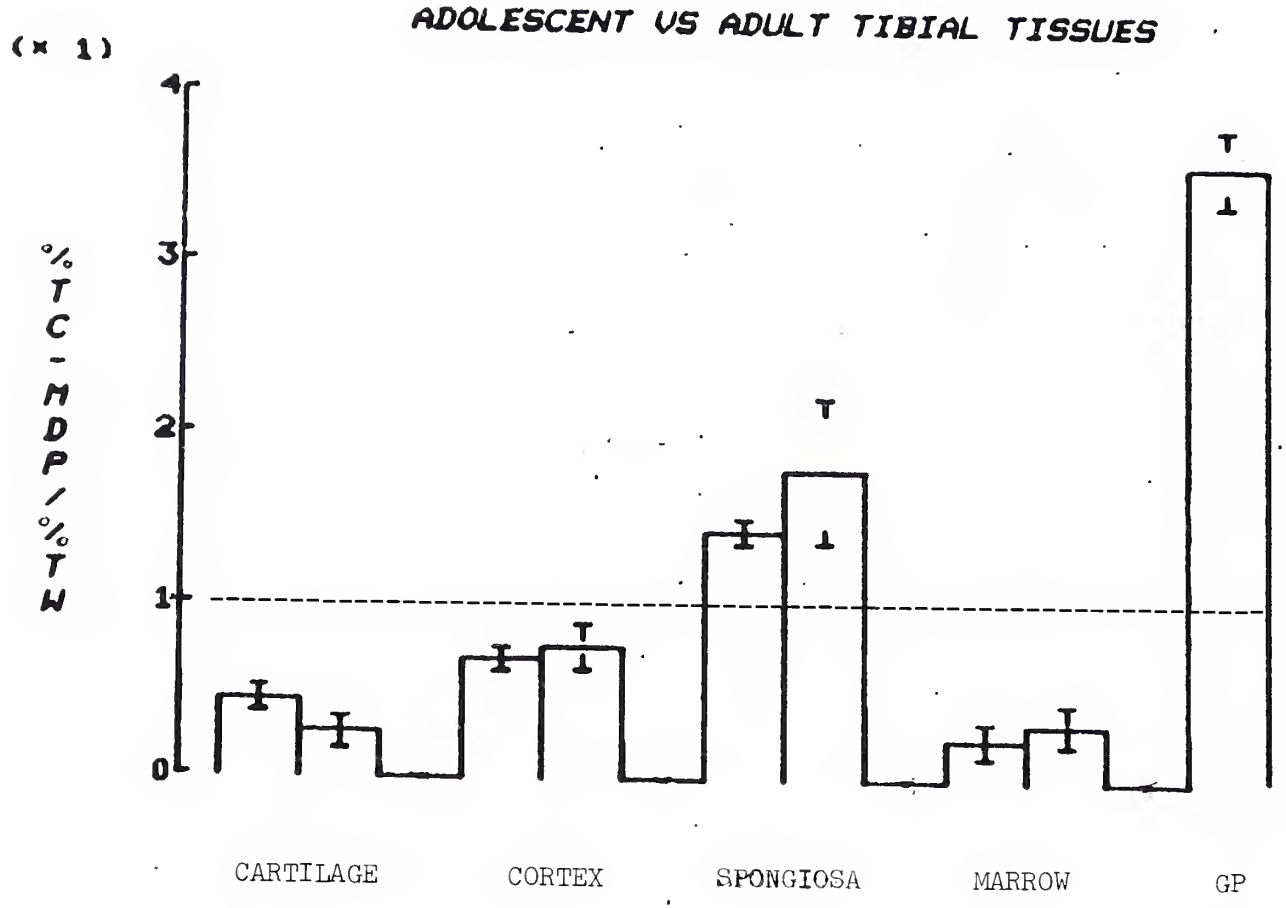
ADOLESCENT VS ADULT TIBIAL TISSUES
(× 1)
% TC-MDP / % TW
4
3
2
1
0
CARTILAGE
CORTEX
SPONGIOSA
MARROW
GP

GRAPH 38

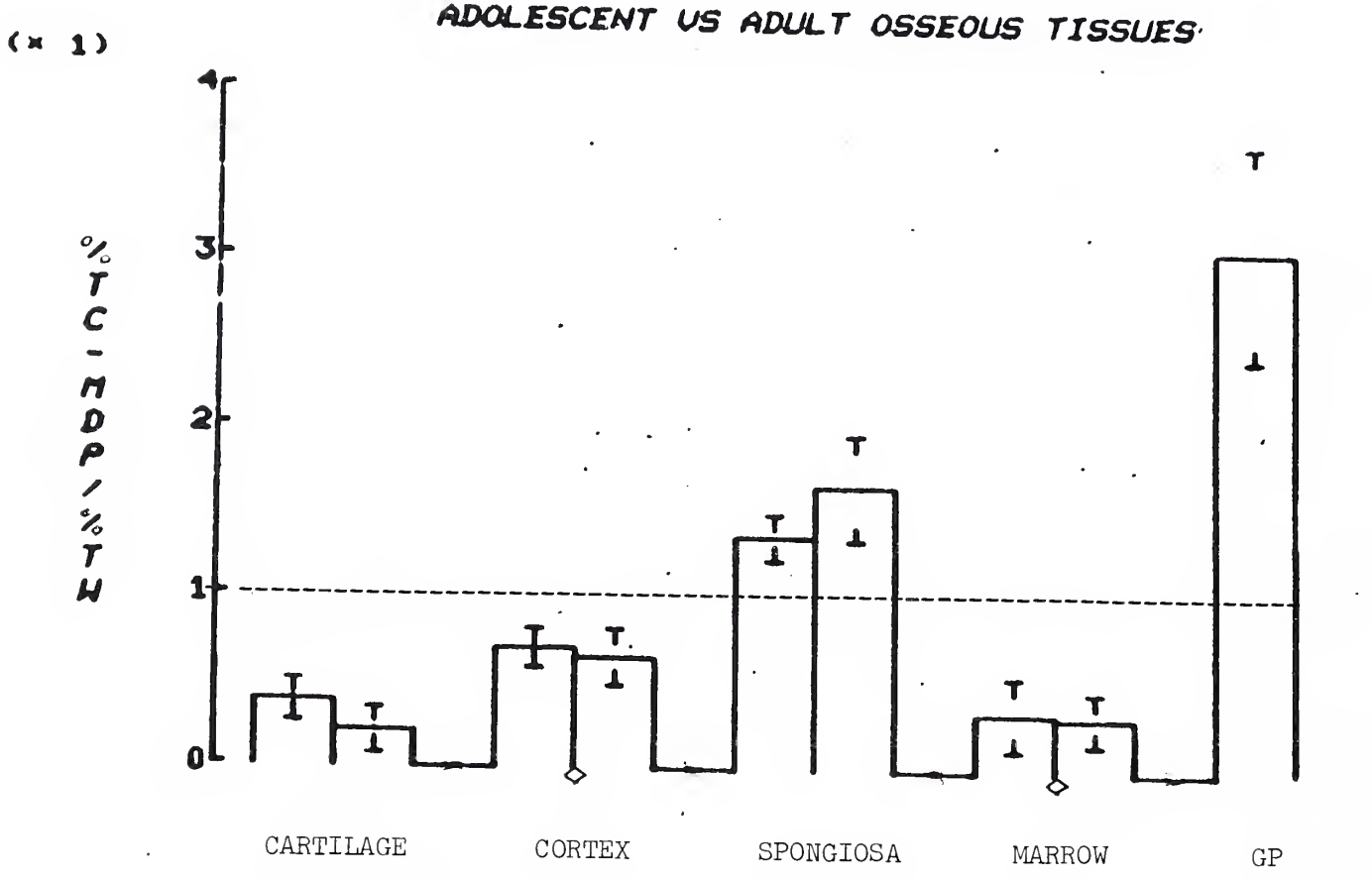
ADOLESCENT VS ADULT OSSEOUS TISSUES
(× 1)
% TC-NDP / % TH
4
3
2
1
0
CARTILAGE
CORTEX
SPONGIOSA
MARROW
GP

GRAPH 39

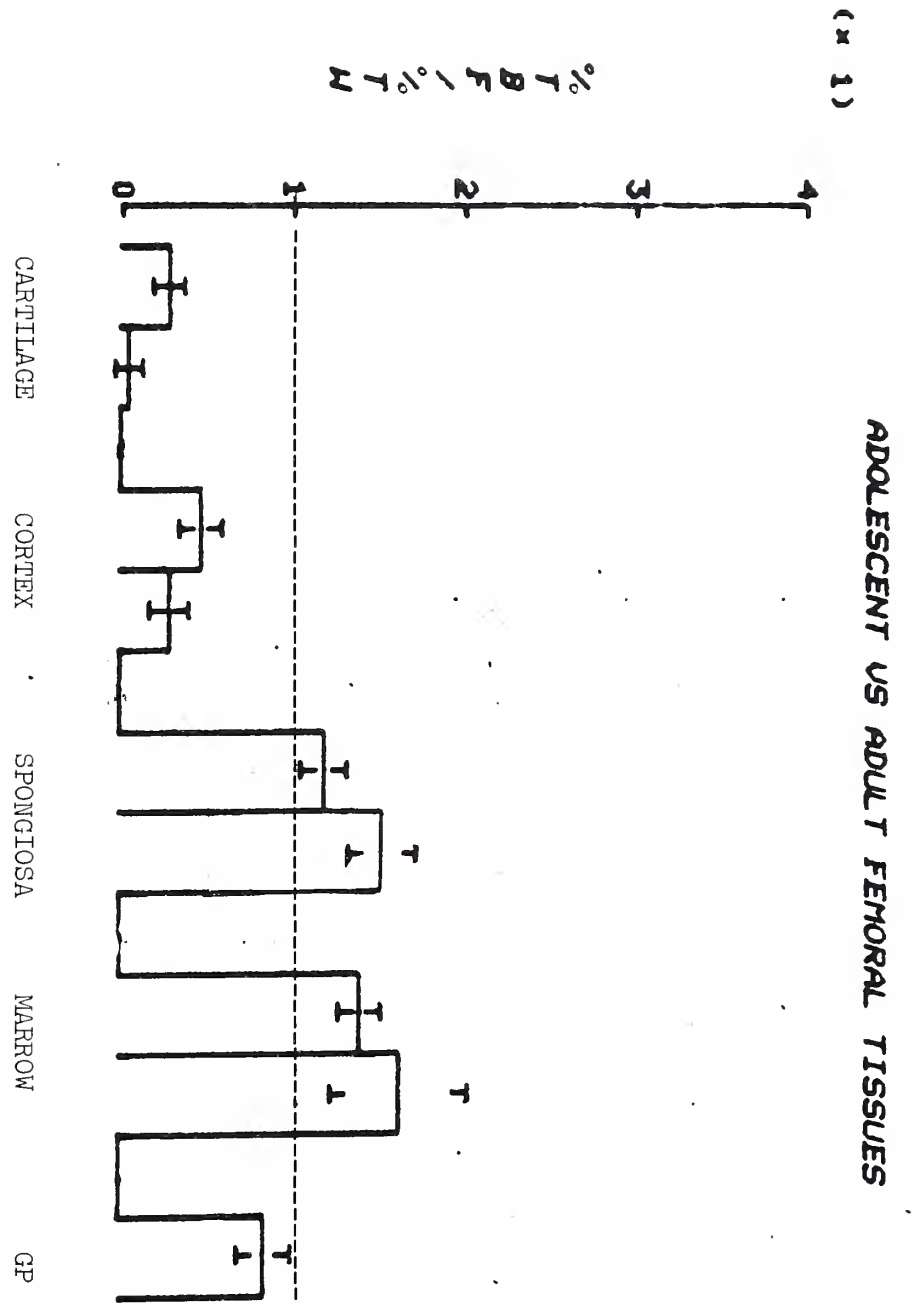
ADOLESCENT VS ADULT FEMORAL TISSUES
(x 1)
% T B F / % T M
4
3
2
1
0
CARTILAGE
CORTEX
SPONGIOSA
MARROW
GP

GRAPH 40

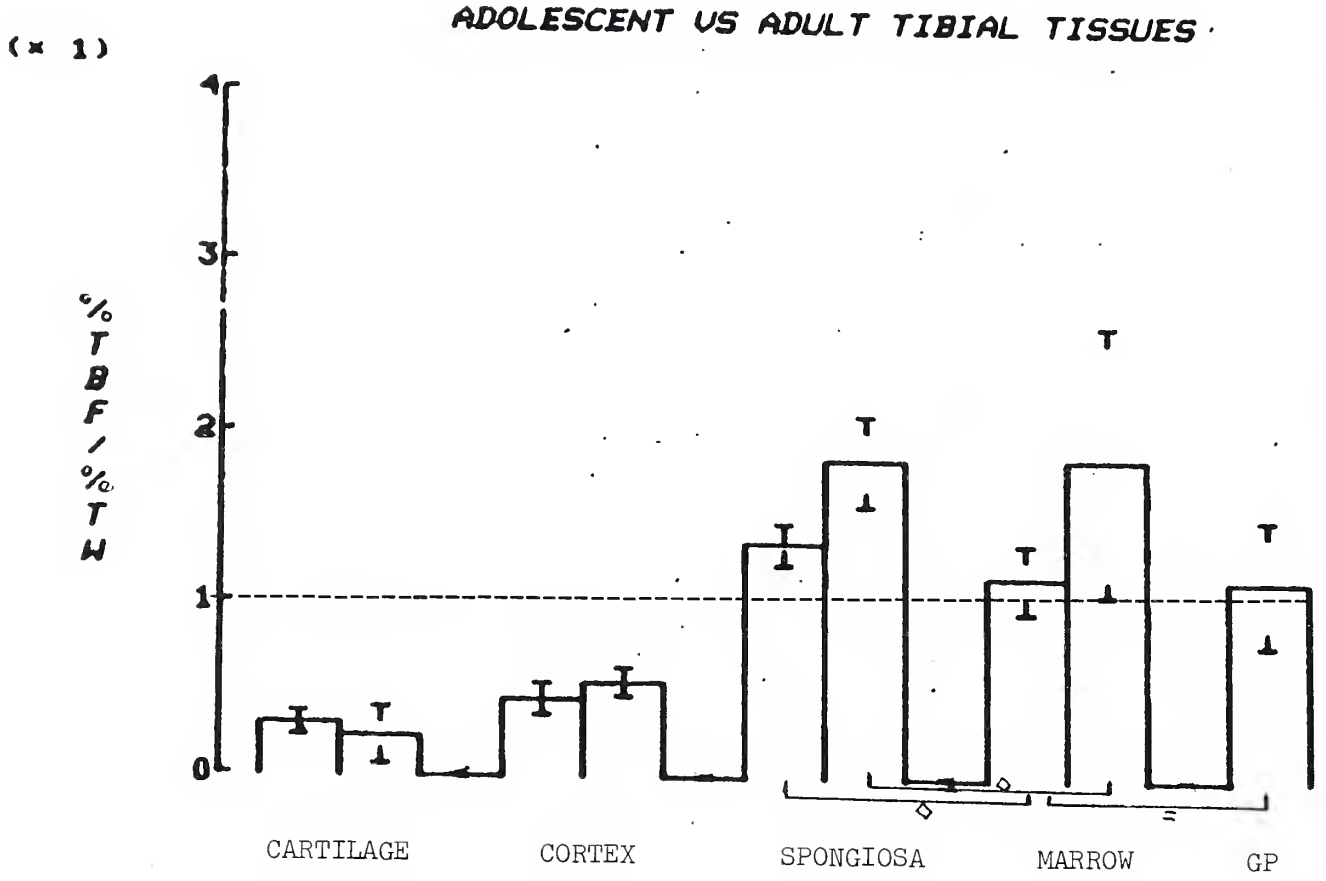
ADOLESCENT VS ADULT TIBIAL TISSUES
(× 1)
% TBF / % TW
4
3
2
1
0
CARTILAGE
CORTEX
SPONGIOSA
MARROW
GP

GRAPH 41

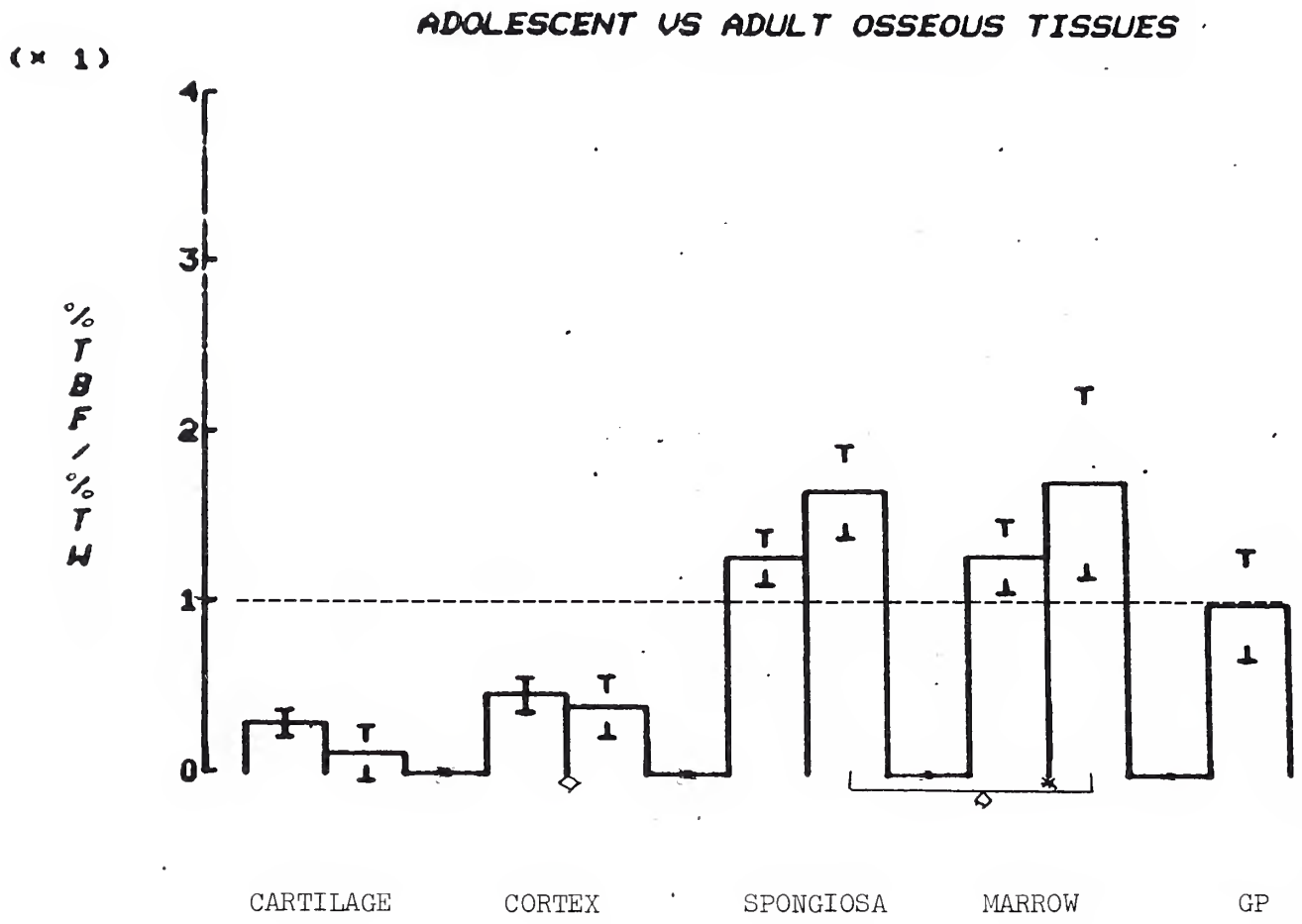
ADOLESCENT VS ADULT OSSEOUS TISSUES
(× 1)
% TBF / % TW
4
3
2
1
0
CARTILAGE
CORTEX
SPONGIOSA
MARROW
GP

GRAPH 42

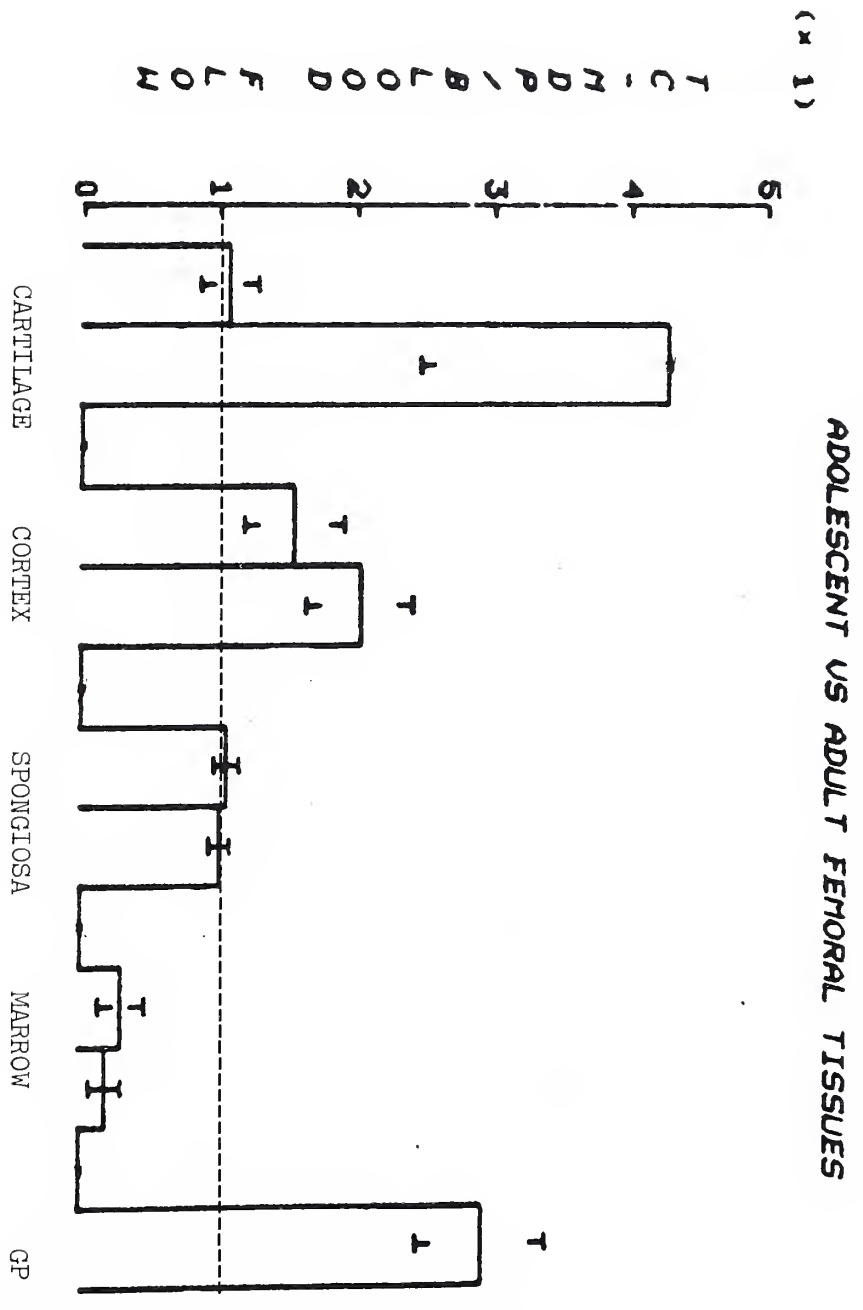
ADOLESCENT VS ADULT FEMORAL TISSUES
T-C-H-D-P-B-L-O-O-D FLOW (× 1)
0
1
2
3
4
5
CARTILAGE
CORTEX
SPONGIOSA
MARROW
GP

GRAPH 43

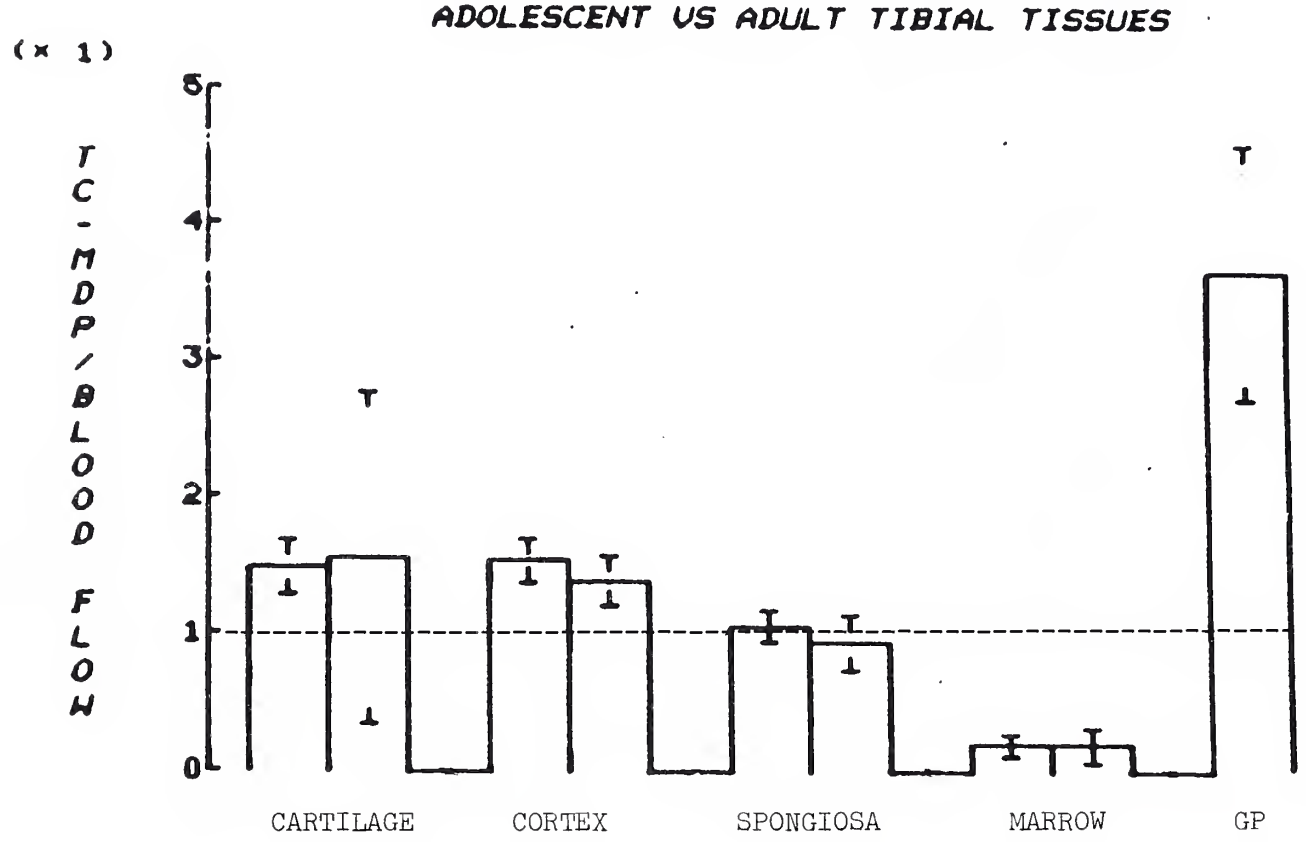
ADOLESCENT VS ADULT TIBIAL TISSUES
(× 1)
TC-MDP/BLOOD FLOW
5
4
3
2
1
0
CARTILAGE
CORTEX
SPONGIOSA
MARROW
GP

GRAPH 44

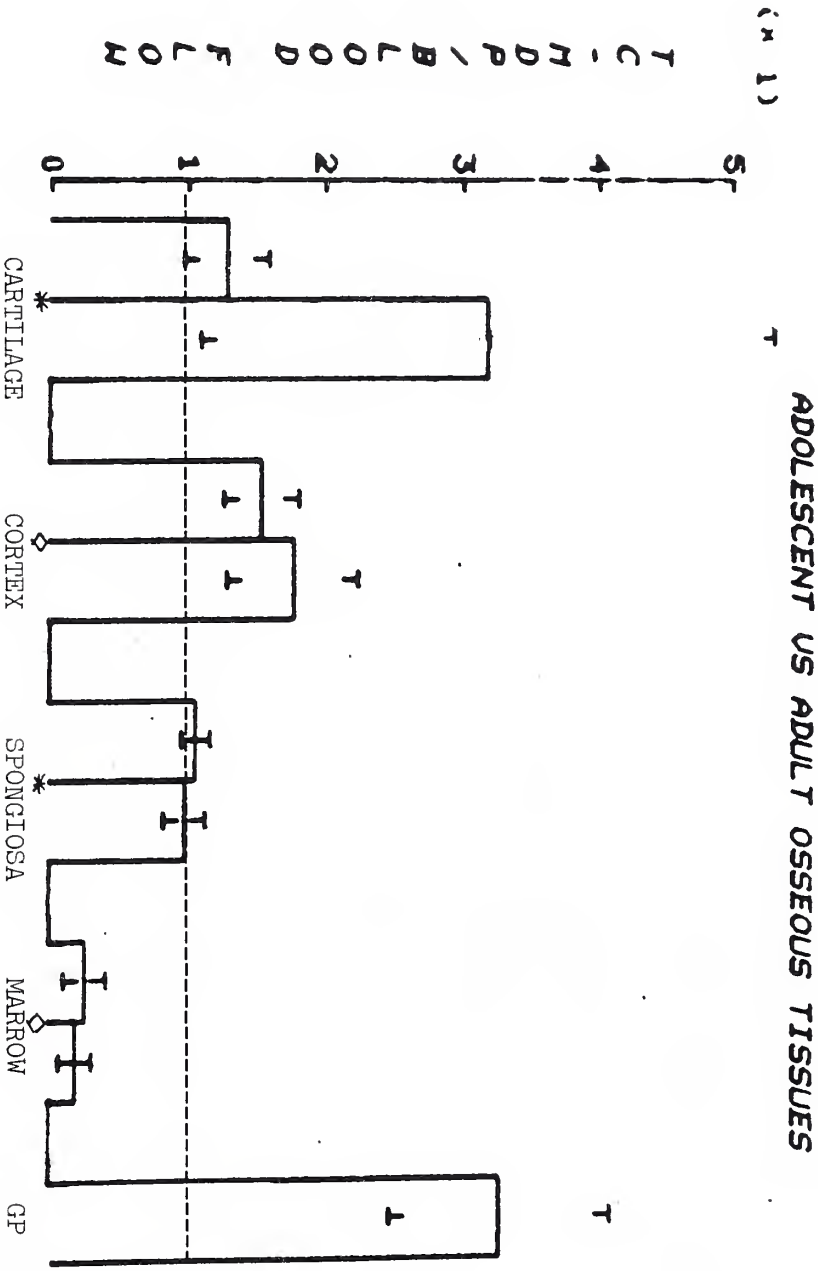
ADOLESCENT VS ADULT OSSEOUS TISSUES
T C - H D P / B L O O D F L O W N
(x 1)
0
1
2
3
4
5
CARTILAGE
CORTEX
SPONGIOSA
MARROW
GP

GRAPH 45

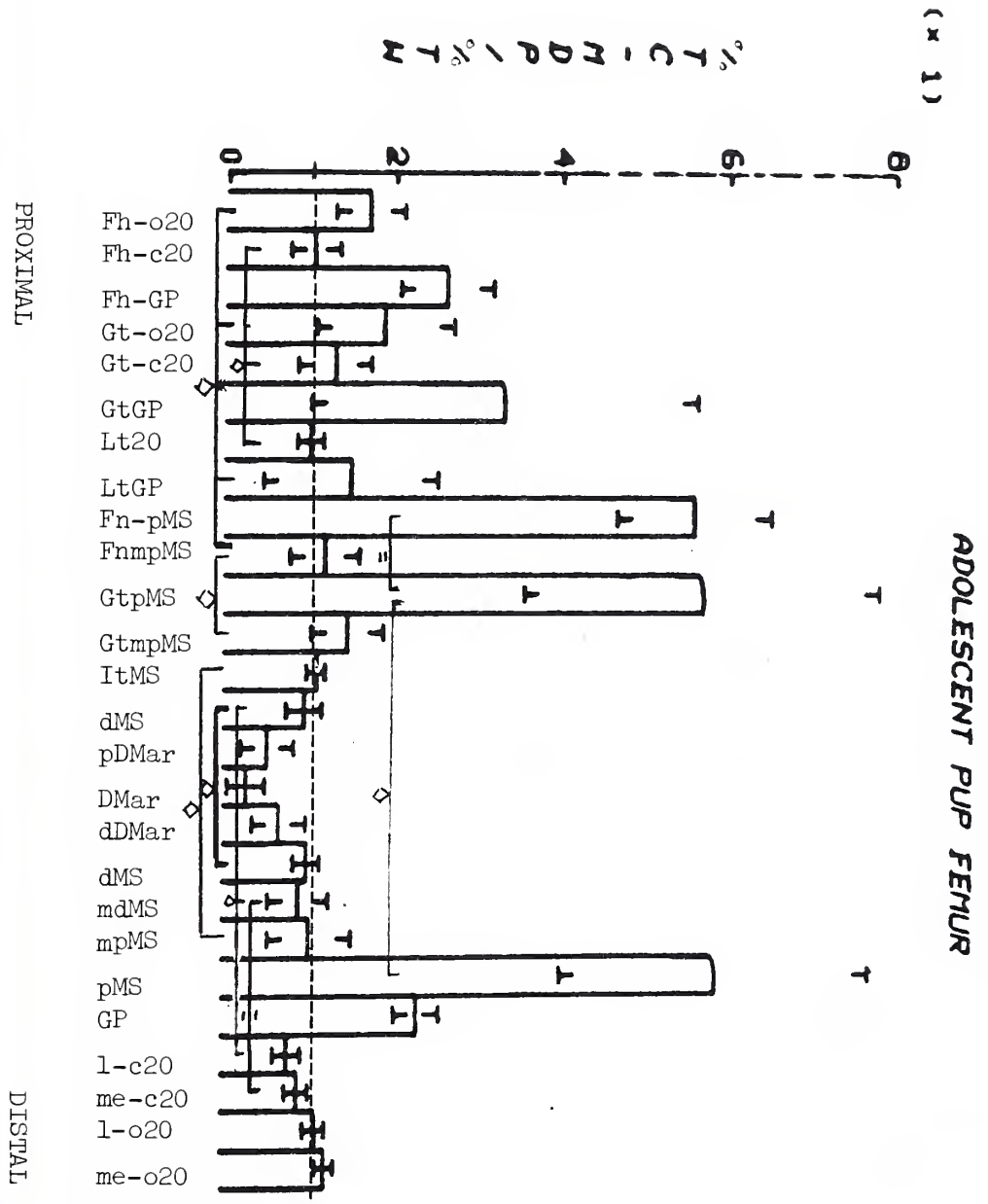
ADOLESCENT PUP FEMUR
PROXIMAL
DISTAL
Fh-o20
Fh-c20
Fh-GP
Gt-o20
Gt-c20
GtGP
Lt20
LtGP
Fn-pMS
FnmpMS
GtpMS
GtmpMS
ItMS
dMS
pDMar
DMar
dDMar
dMS
mdMS
mpMS
pMS
GP
l-c20
me-c20
l-o20
me-o20
0
2
4
6
8

GRAPH 46A

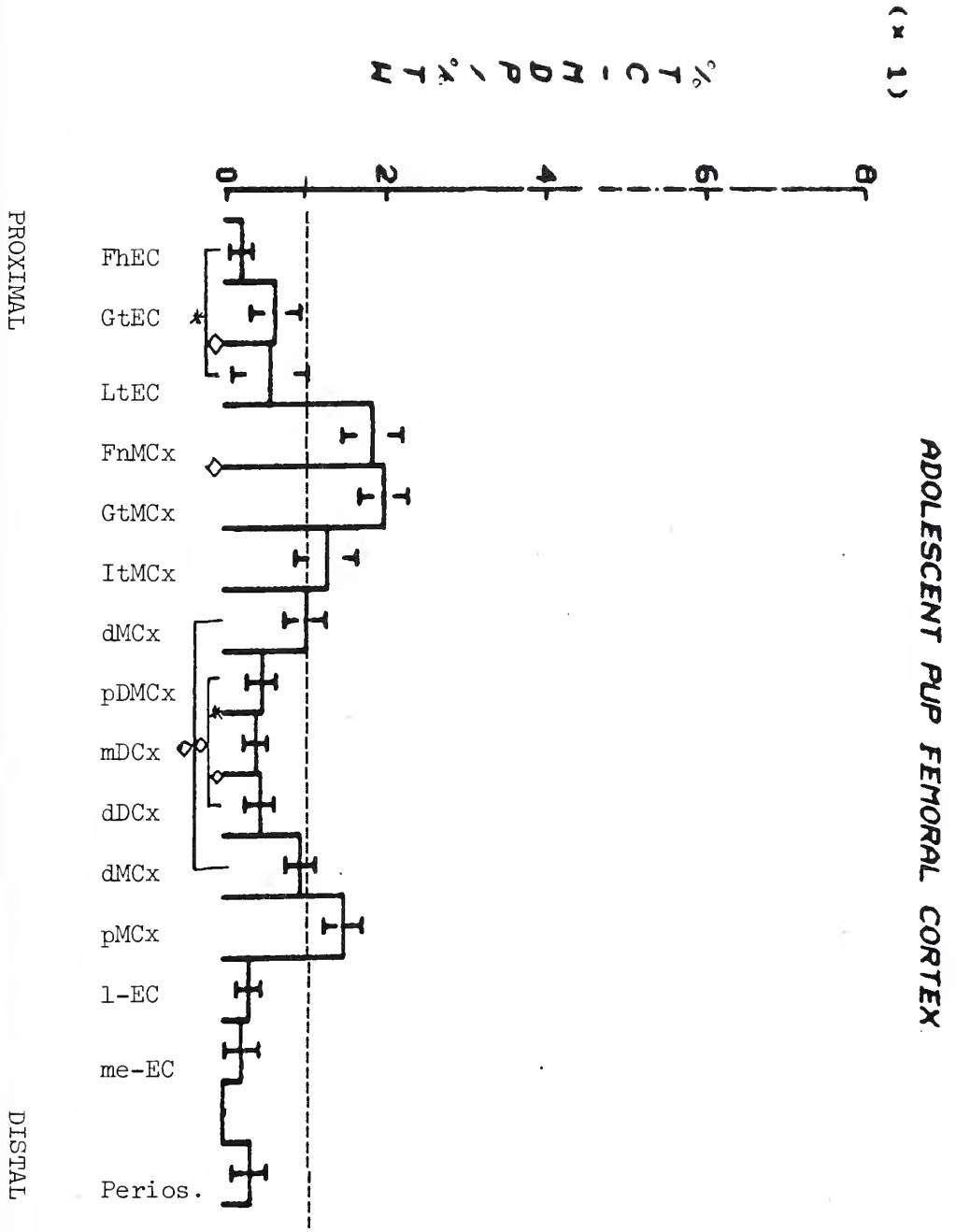
ADOLESCENT PUP FEMORAL CORTEX
% LABELLING INDEX
(× 1)
0
2
4
6
8
FhEC
GtEC
LtEC
FnMCx
GtMCx
ItMCx
dMCx
pDMCx
mDCx
dDCx
dMCx
pMCx
l-EC
me-EC
Perios.
PROXIMAL
DISTAL

GRAPH 46B

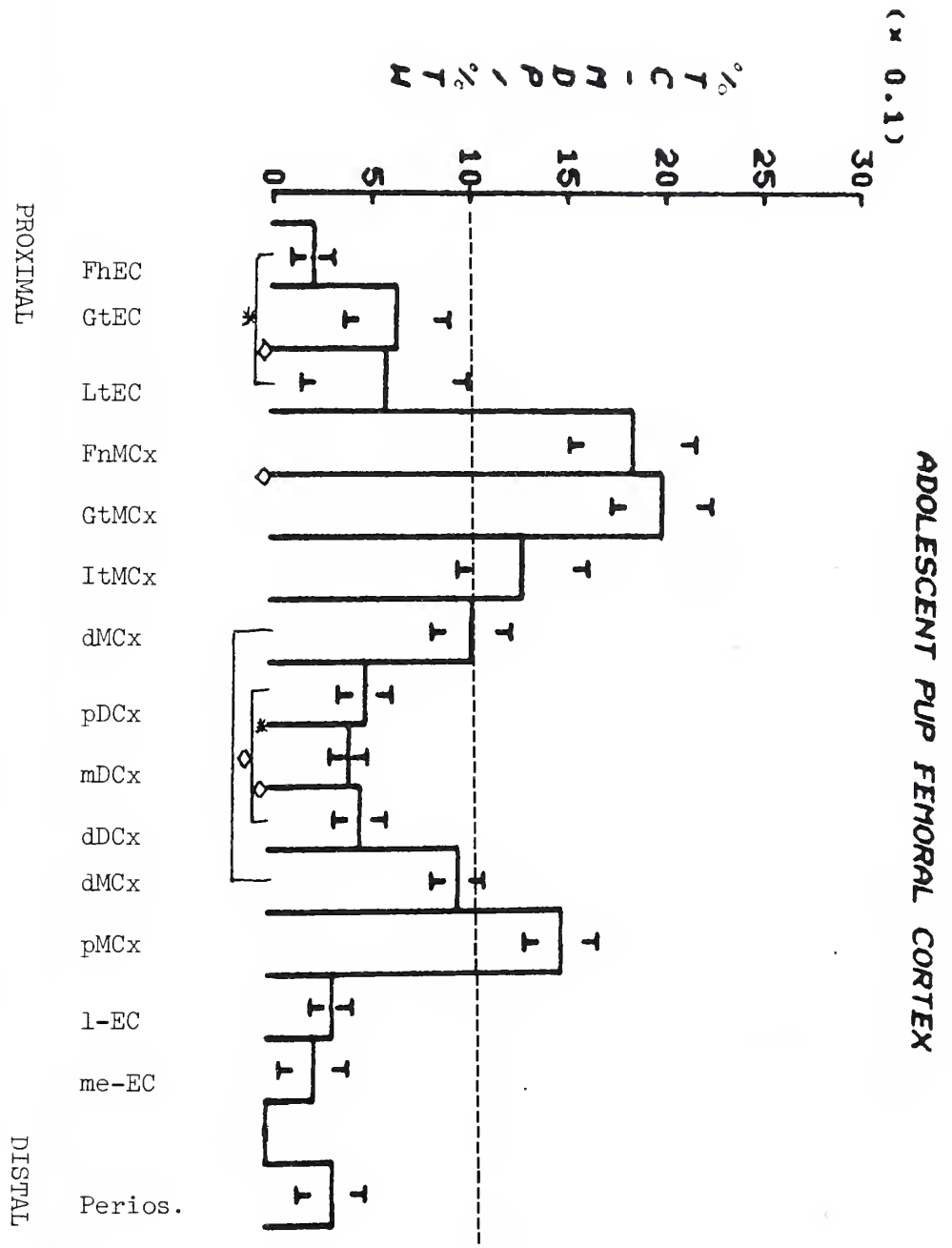
ADOLESCENT PUP FEMORAL CORTEX
% TCA-DPM (× 0.1)
0
5
10
15
20
25
30
PROXIMAL
DISTAL
FhEC
GtEC
LtEC
FnMCx
GtMCx
ItMCx
dMCx
pDCx
mDCx
dDCx
dMCx
pMCx
l-EC
me-EC
Perios.

GRAPH 47

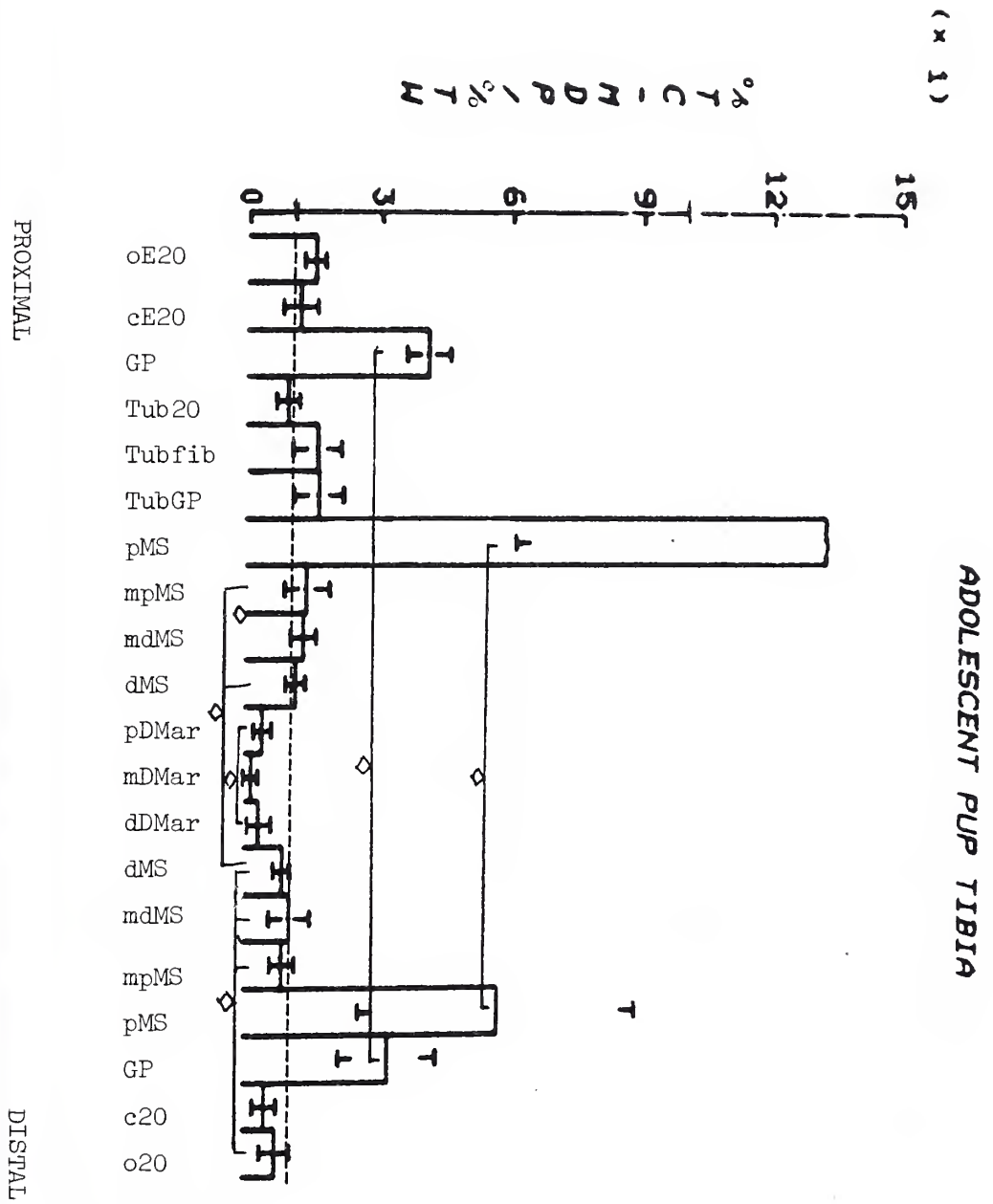
ADOLESCENT PUP TIBIA
% TOTAL - MADP (× 1)
0
3
6
9
12
15
oE20
cE20
GP
Tub20
Tubfib
TubGP
pMS
mpMS
mdMS
dMS
pDMar
mDMar
dDMar
dMS
mdMS
mpMS
pMS
GP
c20
o20
PROXIMAL
DISTAL

GRAPH 48A

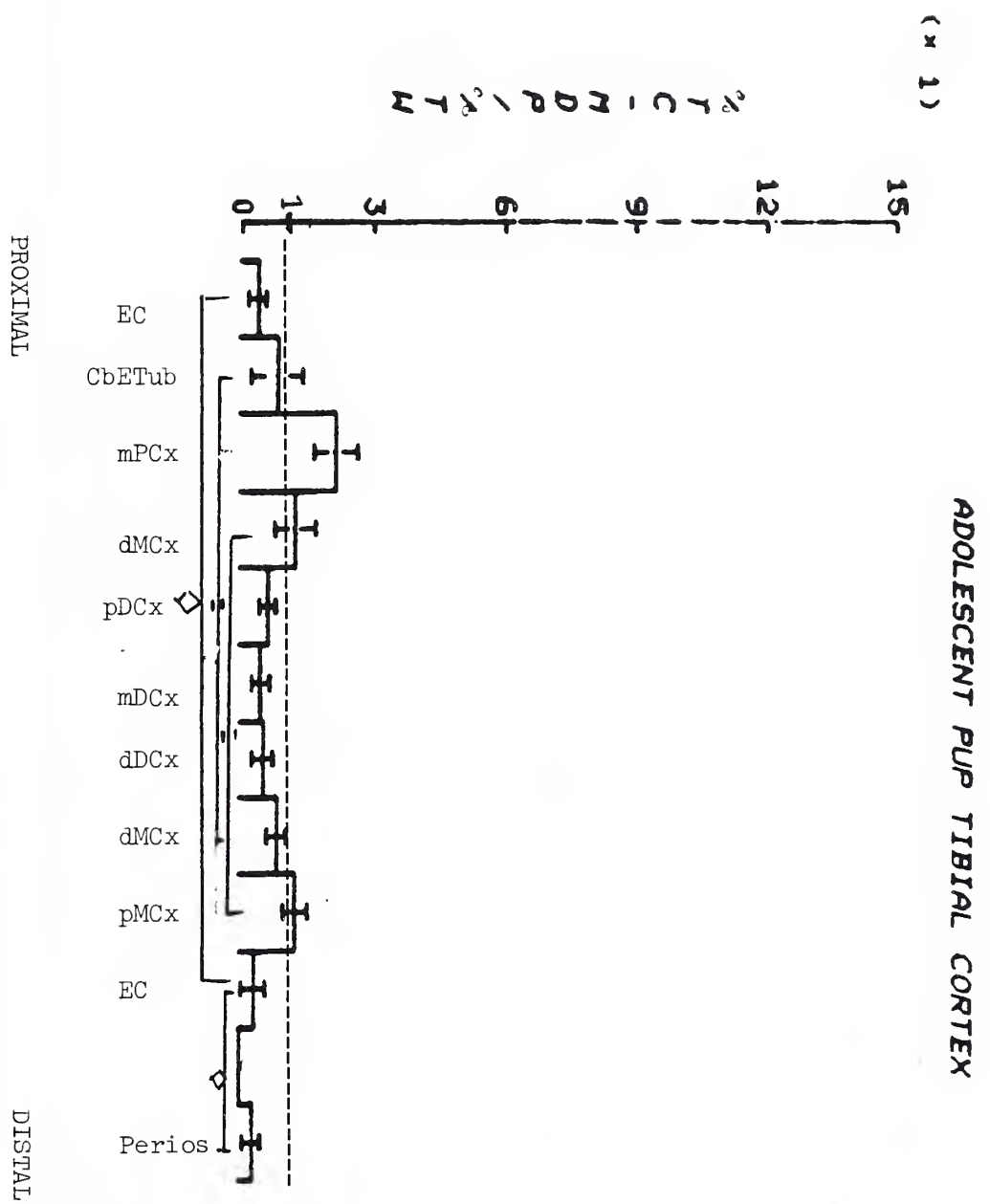
ADOLESCENT PUP TIBIAL CORTEX
% TOTAL CROSS-SECTIONAL AREA
(× 1)
0
1
3
6
9
12
15
PROXIMAL
DISTAL
EC
CbETub
mPCx
dMCx
pDCx
mDCx
dDCx
dMCx
pMCx
EC
Perios

GRAPH 48B

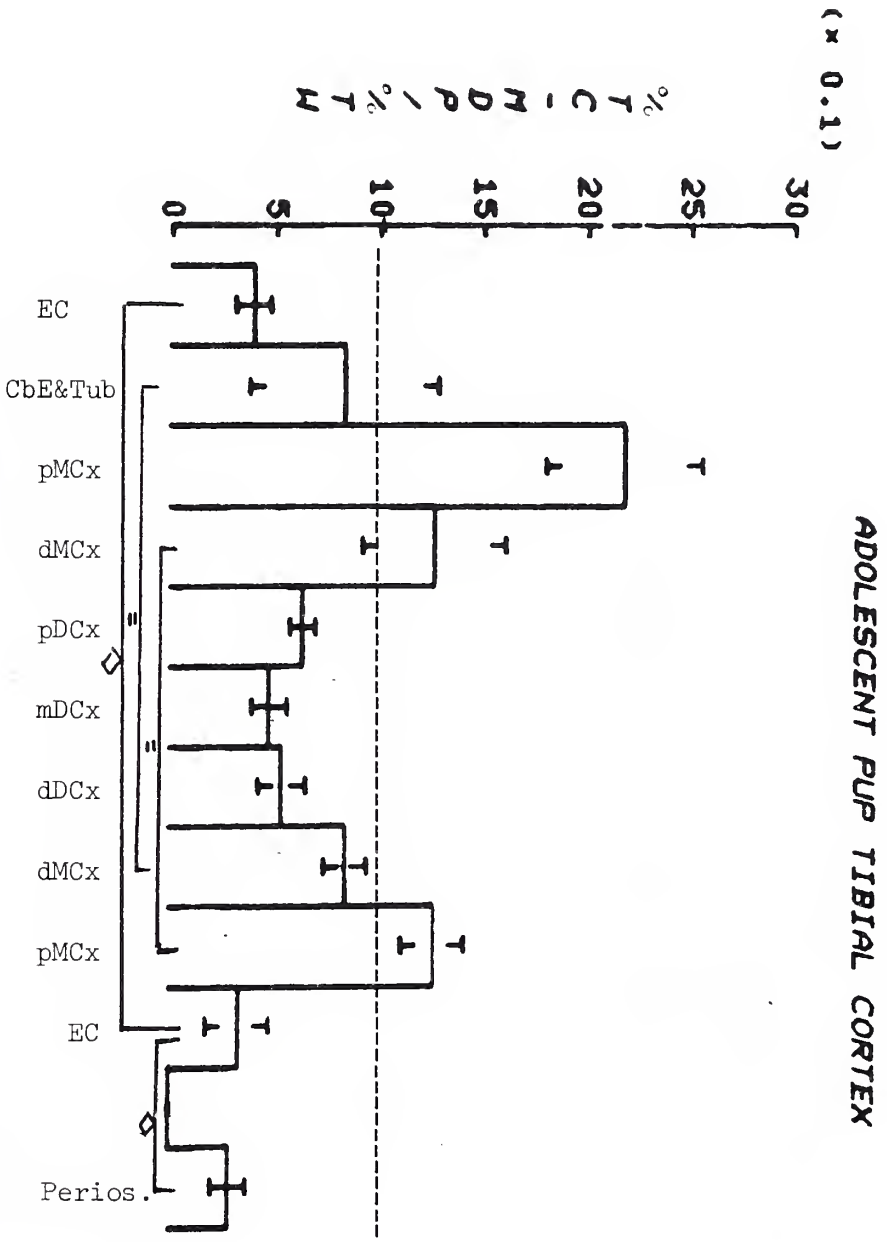
ADOLESCENT PUP TIBIAL CORTEX
% TOTAL RADIOACTIVITY
(× 0.1)
0
5
10
15
20
25
30
EC
CbE&Tub
pMCx
dMCx
pDCx
mDCx
dDCx
dMCx
pMCx
EC
Perios.
PROXIMAL
DISTAL

GRAPH 49

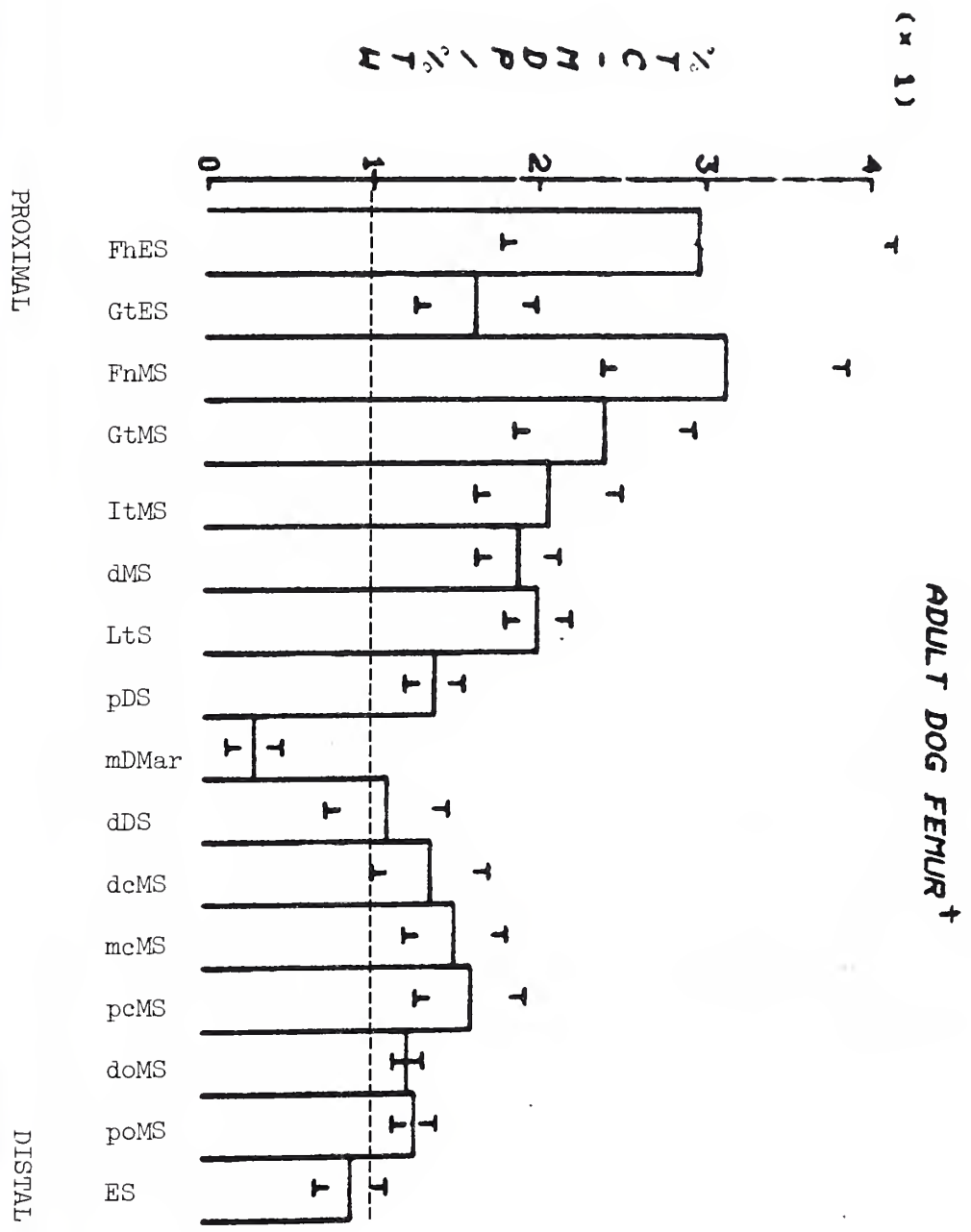
ADULT DOG FEMUR
(× 1)
0
1
2
3
4
FhES
GtES
FnMS
GtMS
ItMS
dMS
LtS
pDS
mDMar
dDS
dcMS
mcMS
pcMS
doMS
poMS
ES
PROXIMAL
DISTAL

GRAPH 50

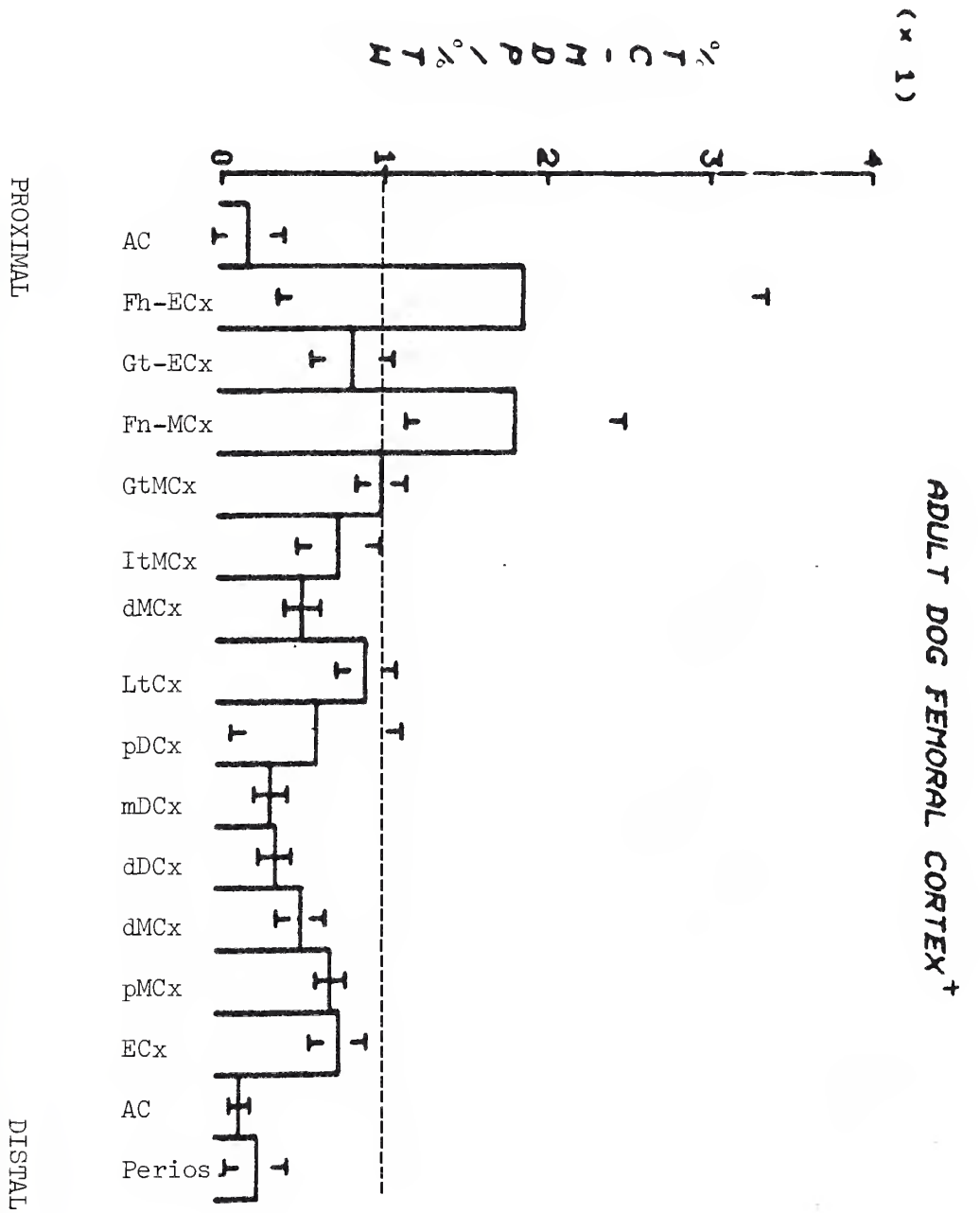
ADULT DOG FEMORAL CORTEX+
% TOTAL - RADIUM
(× 1)
0
1
2
3
4
AC
Fh-ECx
Gt-ECx
Fn-MCx
GtMCx
ItMCx
dMCx
LtCx
pDCx
mDCx
dDCx
dMCx
pMCx
ECx
AC
Perios
PROXIMAL
DISTAL

GRAPH 51

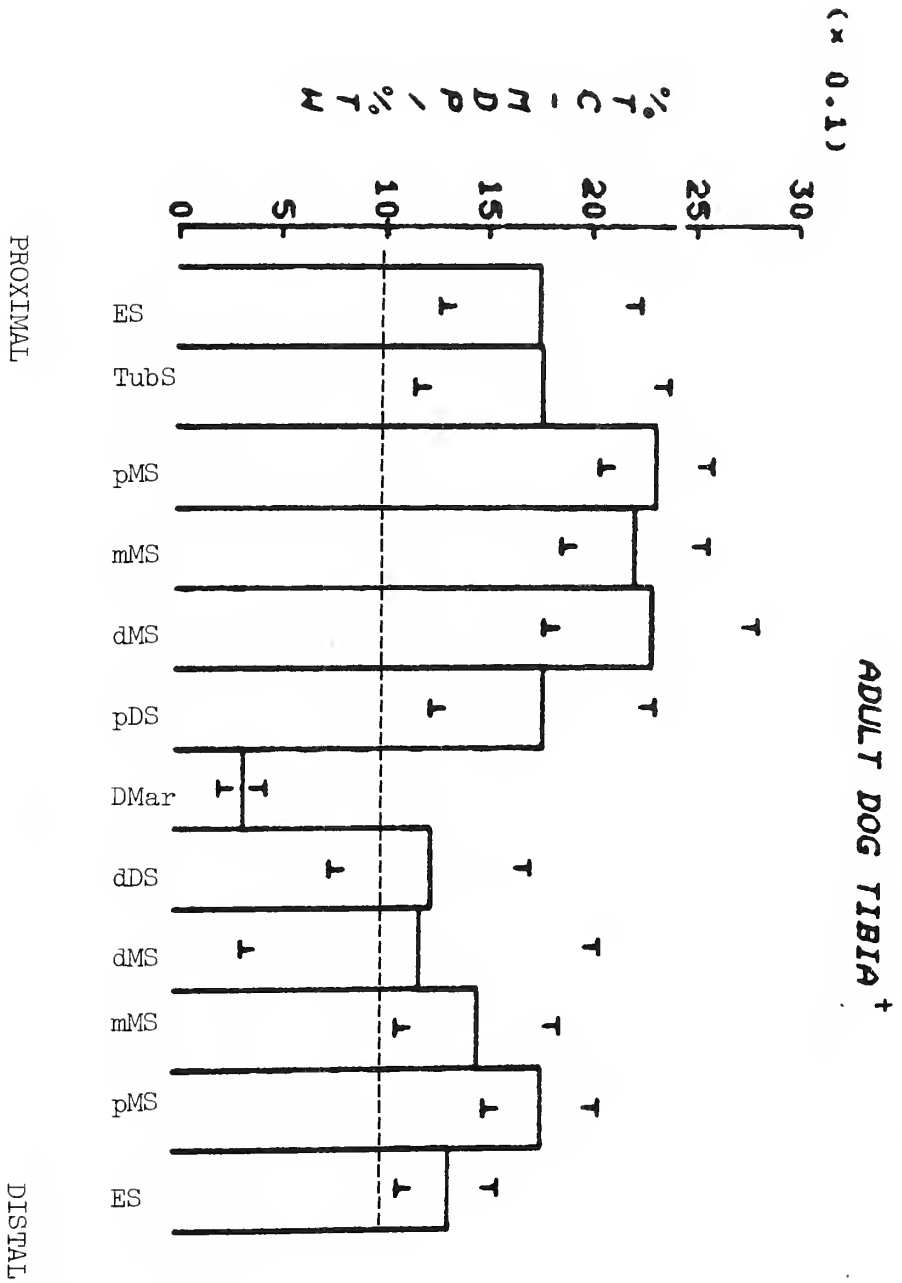
ADULT DOG TIBIA+
% T.C.A. - PADDLE
(× 0.1)
0
5
10
15
20
25
30
ES
TubS
pMS
mMS
dMS
pDS
DMar
dDS
dMS
mMS
pMS
ES
PROXIMAL
DISTAL

GRAPH 52

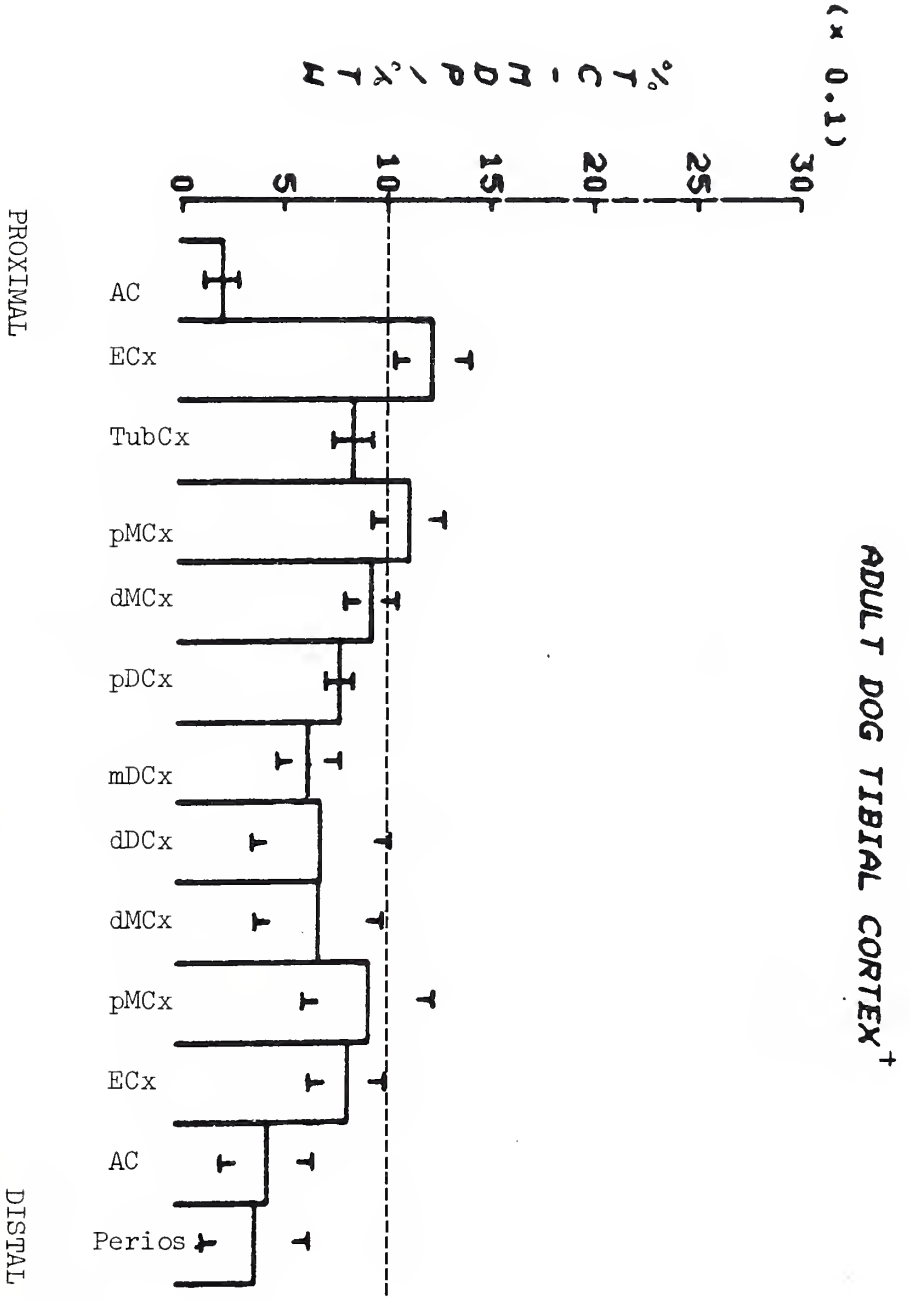
ADULT DOG TIBIAL CORTEX+
% T - RADIOACTIVITY
(× 0.1)
0
5
10
15
20
25
30
AC
ECx
TubCx
pMCx
dMCx
pDCx
mDCx
dDCx
dMCx
pMCx
ECx
AC
Perios
PROXIMAL
DISTAL

GRAPH 53

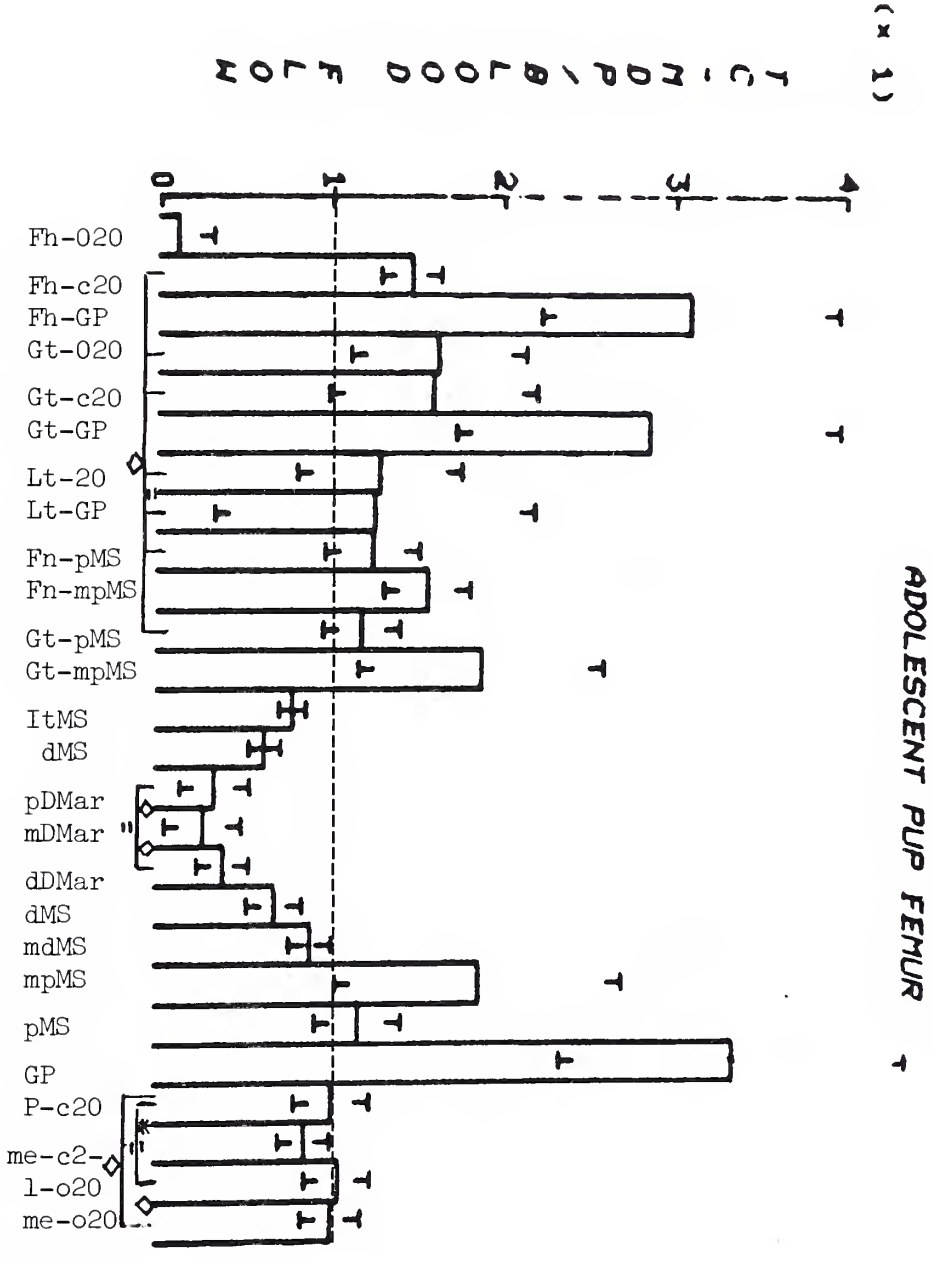
ADOLESCENT PUP FEMUR
(× 1)
0
1
2
3
4
PROXIMAL
DISTAL
Fn-020
Fn-c20
Fn-GP
Gt-020
Gt-c20
Gt-GP
Lt-20
Lt-GP
Fn-pMS
Fn-mpMS
Gt-pMS
Gt-mpMS
ItMS
dMS
pDMar
mDMar
dDMar
dMS
mdMS
mpMS
pMS
GP
P-c20
me-c2-
l-o20
me-o20

GRAPH 54

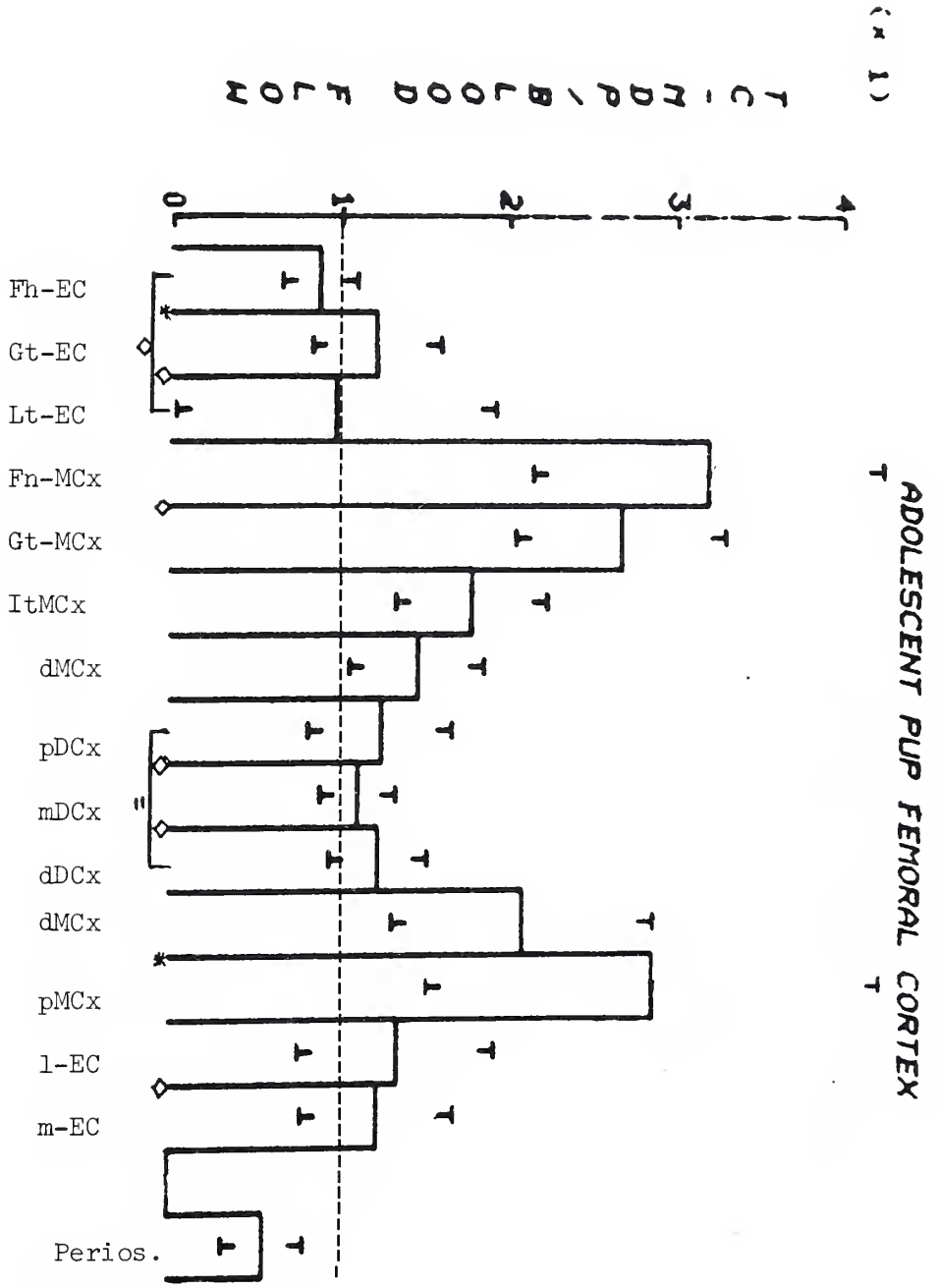
ADOLESCENT PUP FEMORAL CORTEX
PROXIMAL
DISTAL
Fh-EC
Gt-EC
Lt-EC
Fn-MCx
Gt-MCx
ItMCx
dMCx
pDCx
mDCx
dDCx
dMCx
pMCx
l-EC
m-EC
Perios.

GRAPH 55

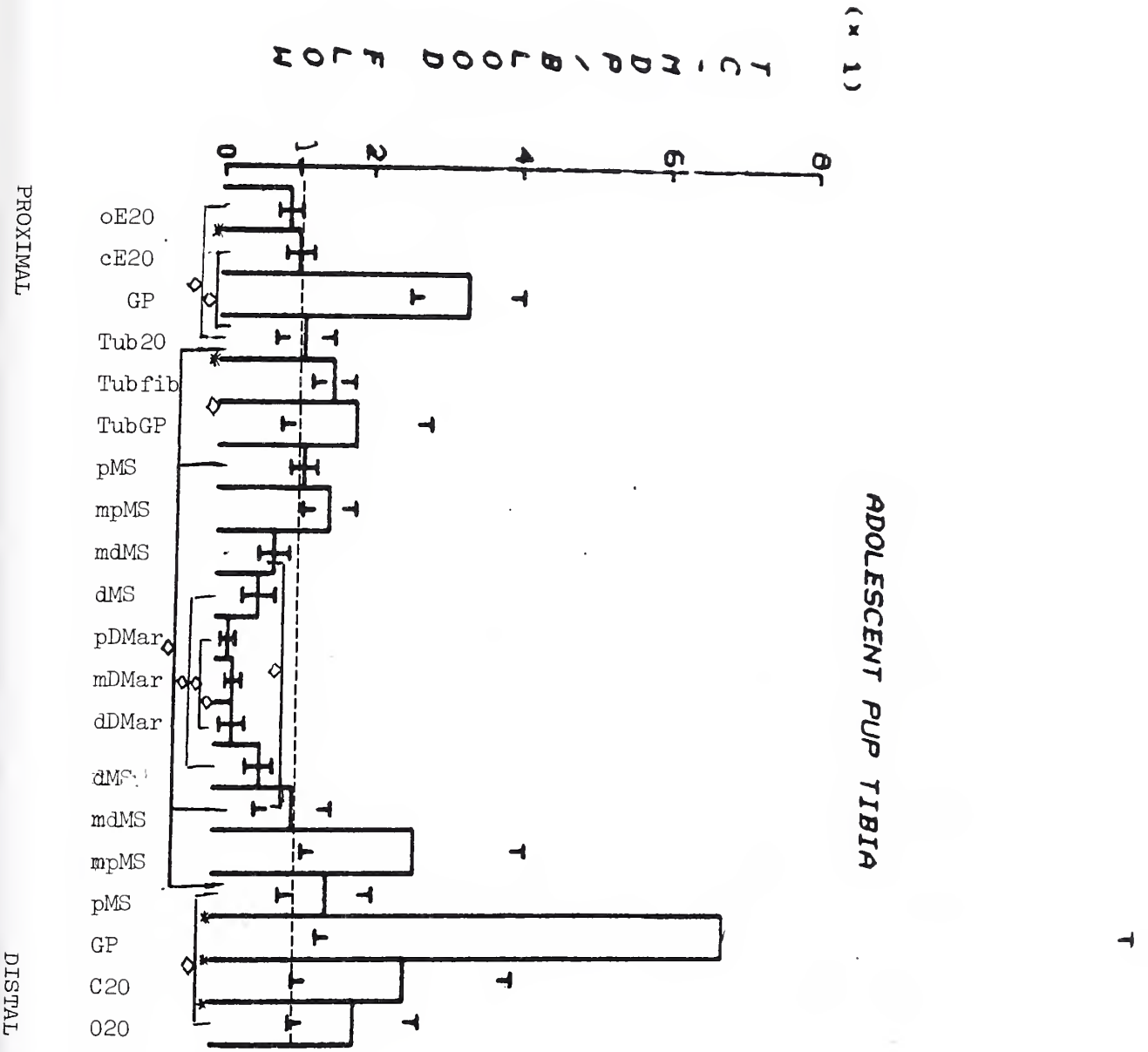
MOT BOOBJOOD
T C - M A P
(× 1)
0
2
4
6
8
oE20
cE20
GP
Tub20
Tubfib
TubGP
pMS
mpMS
mdMS
dMS
pDMar
mDMar
dDMar
dMS
mdMS
mpMS
pMS
GP
C20
020
PROXIMAL
DISTAL
ADOLESCENT PUP TIBIA

GRAPH 56

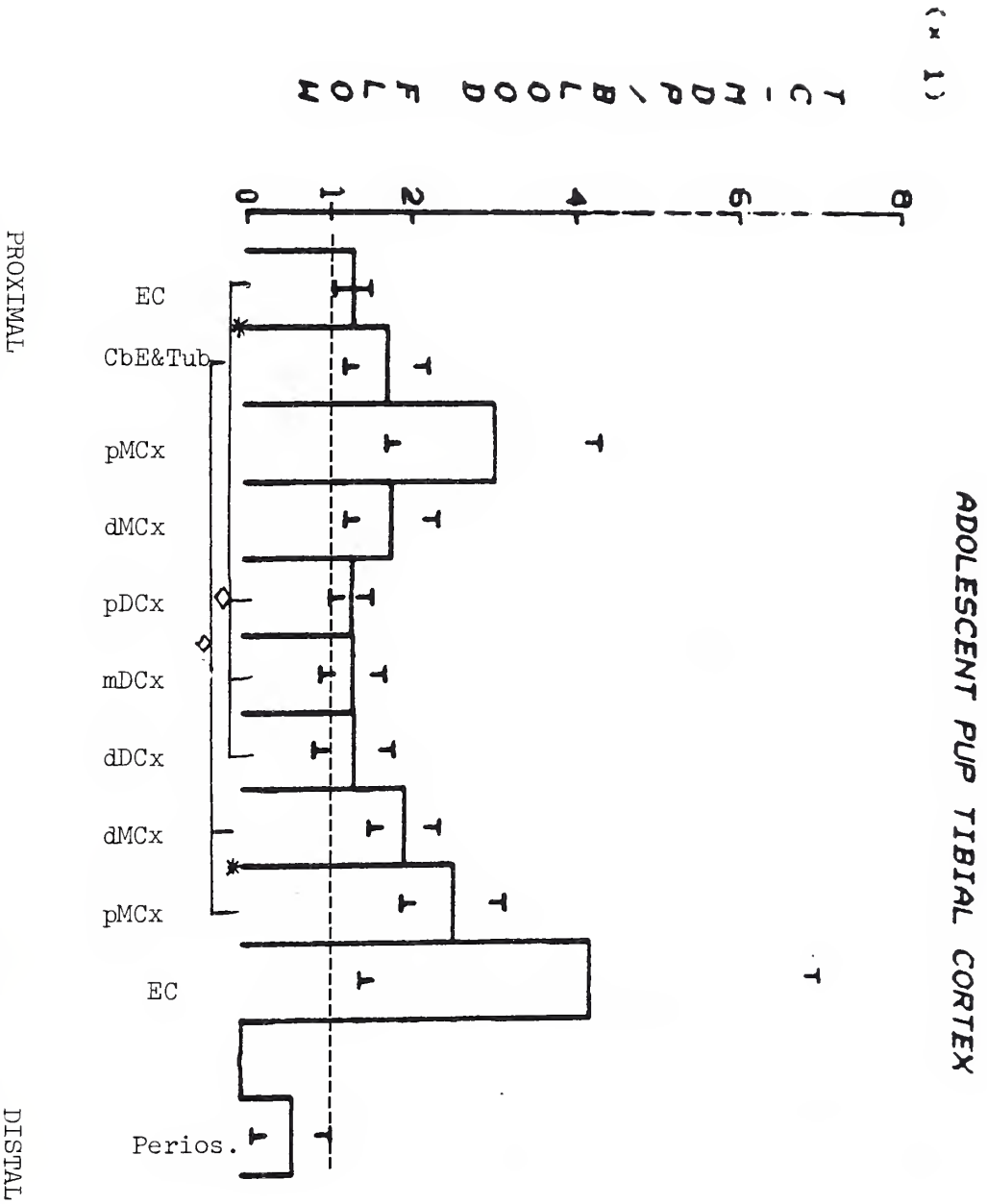
ADOLESCENT PUP TIBIAL CORTEX
MOF BOOB\ADD
(x 1)
0
1
2
4
6
8
EC
CbE&Tub
pMCx
dMCx
pDCx
mDCx
dDCx
dMCx
pMCx
EC
Perios.
PROXIMAL
DISTAL

GRAPH 57

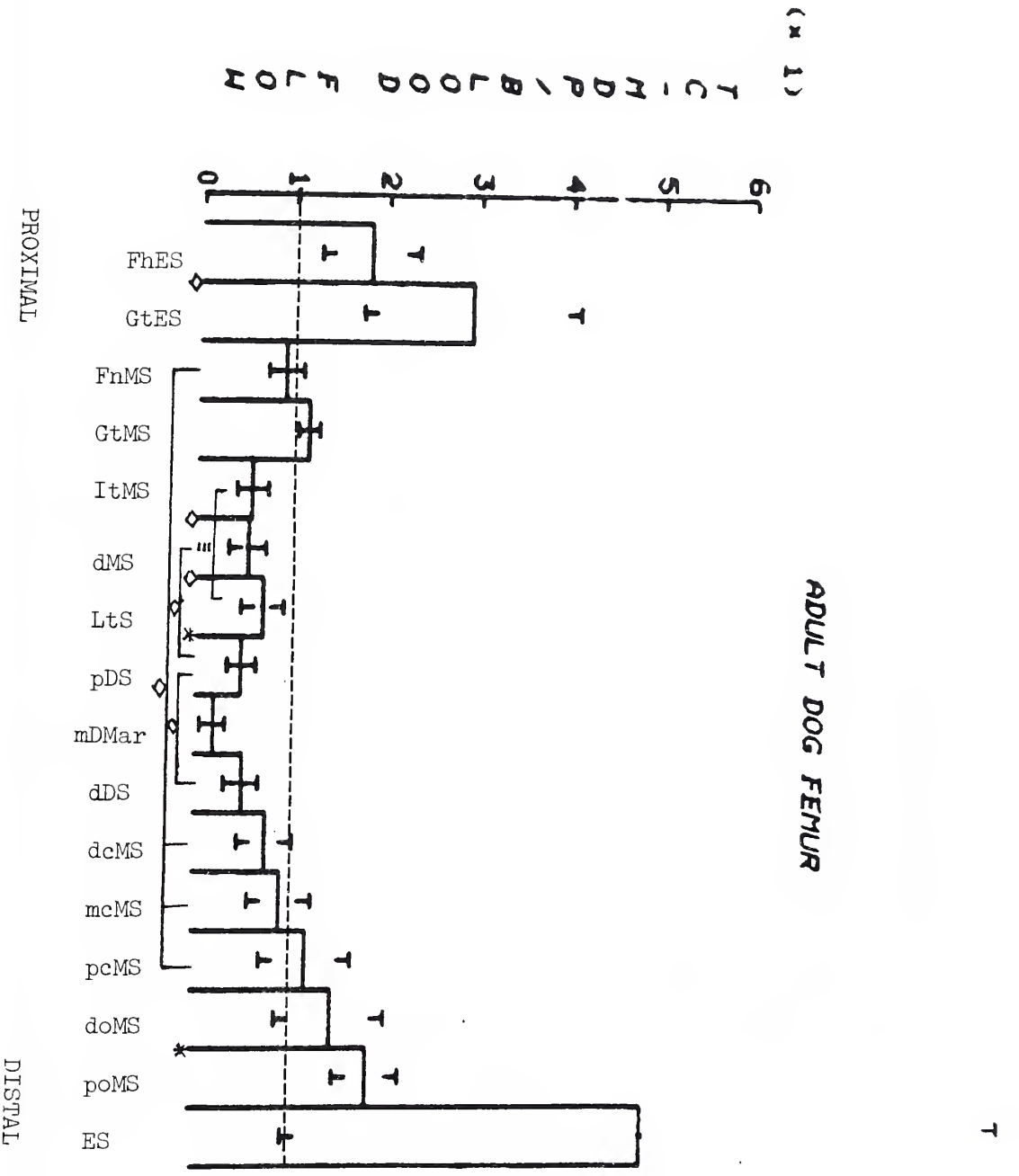
ADULT DOG FEMUR
PROXIMAL
DISTAL
FhES
GtES
FnMS
GtMS
ItMS
dMS
LtS
pDS
mDMar
dDS
dcMS
mcMS
pcMS
doMS
poMS
ES
0
1
2
3
4
5
6

GRAPH 58

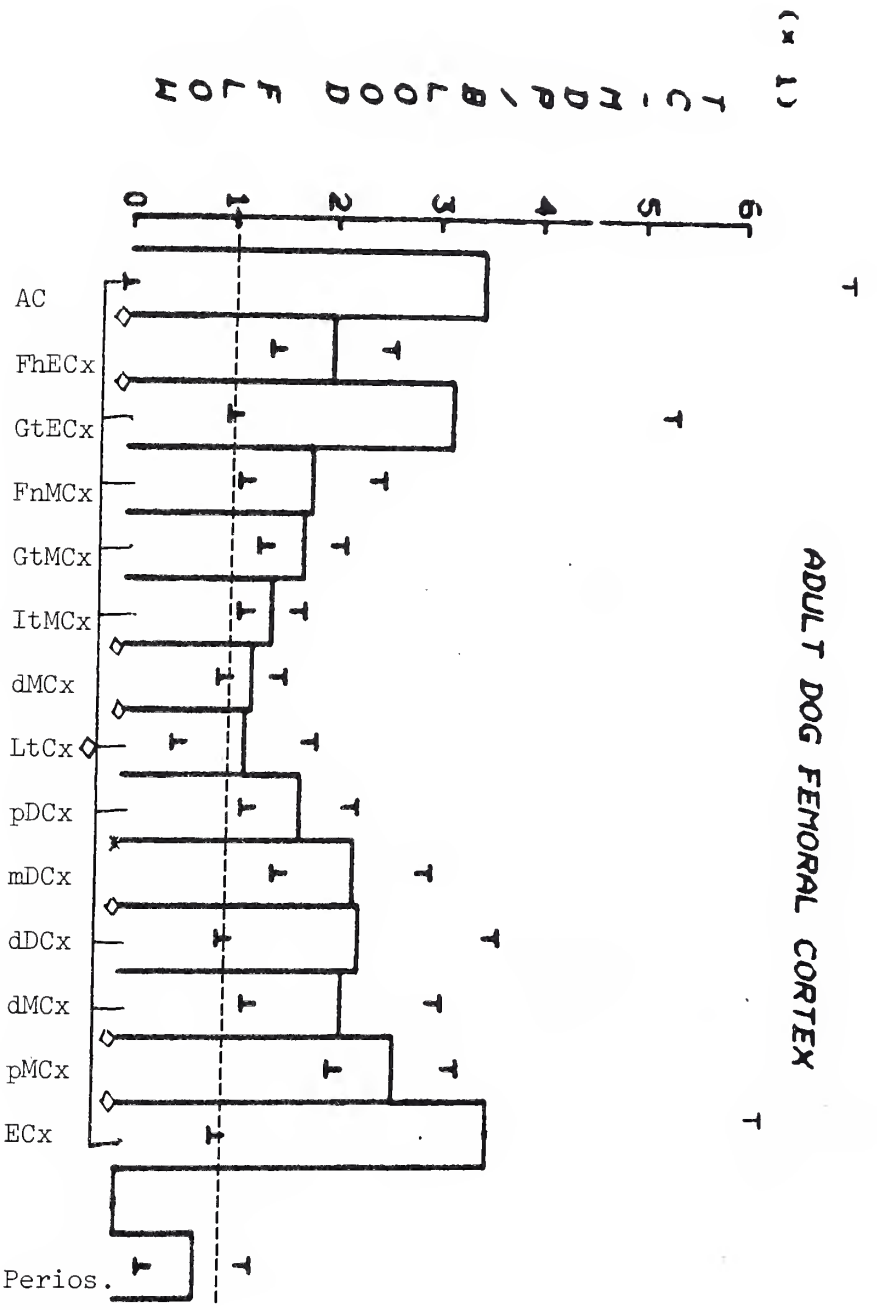

ADULT DOG FEMORAL CORTEX

GRAPH 59

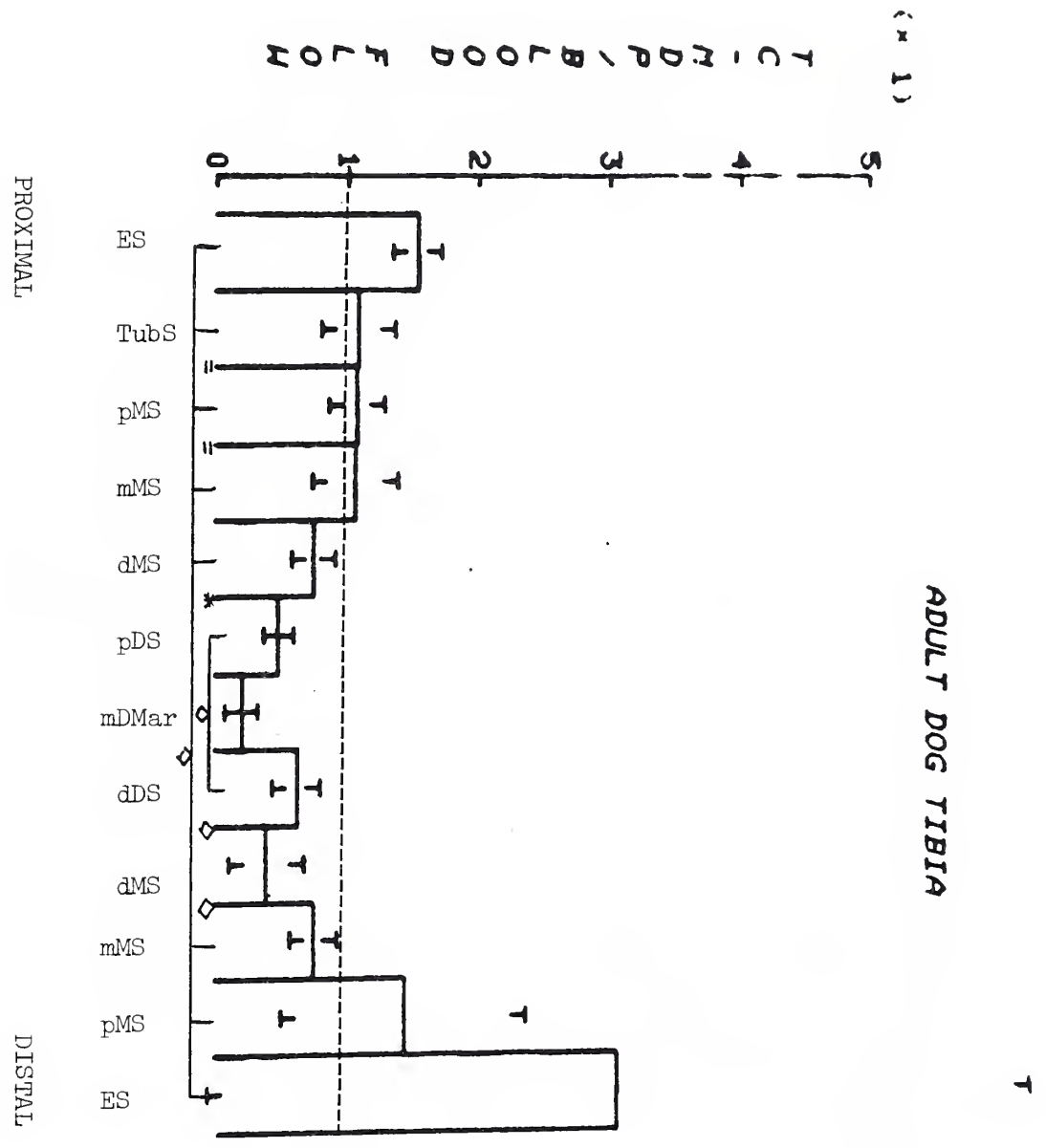
ADULT DOG TIBIA
PROXIMAL
DISTAL
ES
TubS
pMS
mMS
dMS
pDS
mDMar
dDS
dMS
mMS
pMS
ES
0
1
2
3
4
5

GRAPH 60

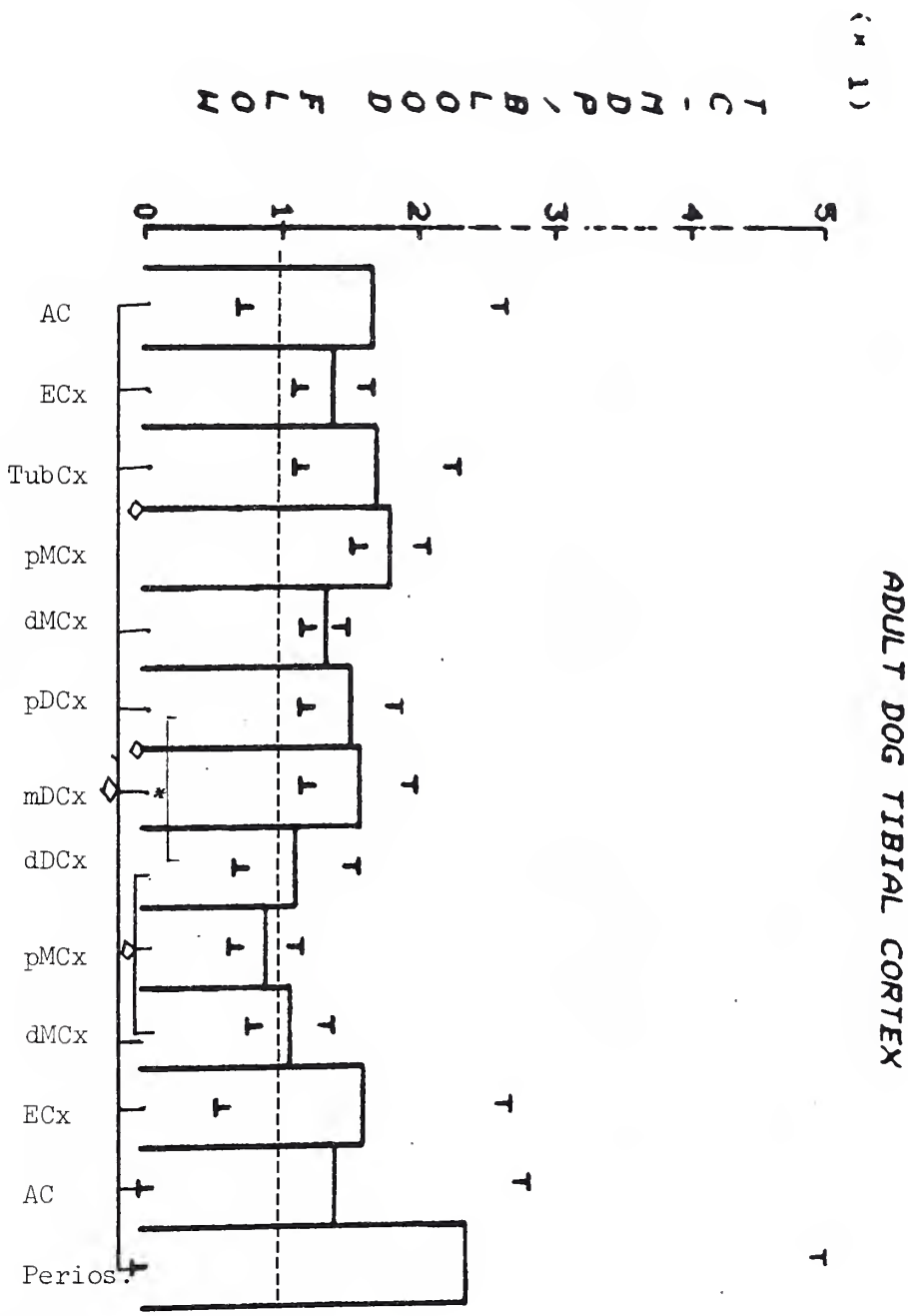
ADULT DOG TIBIAL CORTEX
AC
ECx
TubCx
pMCx
dMCx
pDCx
mDCx
dDCx
pMCx
dMCx
ECx
AC
Perios.
0
1
2
3
4
5

Table 11

OSSEOUS TISSUE FLOW BY AGE CC/MIN./HG

BONE=1 AGE=1

VARIABLE	N	MEAN	STANDARD DEVIATION	C.V.	STD ERROR OF MEAN
CART	8	20.35	6.68	32.829	2.36
CORTEX	8	21.02	8.50	40.425	3.00
SPONG	8	76.57	27.48	35.884	9.71
MARROW	8	17.65	7.50	42.482	2.65
GP	0	.	.	.	.
---------- BONE=1 AGE=2 ----------					
CART	8	6.78	1.27	18.686	0.45
CORTEX	8	11.22	2.64	23.558	0.93
SPONG	8	28.24	2.98	10.554	1.05
MARROW	8	33.19	3.79	11.419	1.34
GP	8	19.34	1.94	10.038	0.69
---------- BONE=1 AGE=3 ----------					
CART	10	1.72	1.93	112.200	0.61
CORTEX	10	5.54	2.60	46.861	0.82
SPONG	10	25.51	8.21	32.177	2.60
MARROW	10	20.01	5.48	27.413	1.73
GP	0	.	.	.	.
---------- BONE=2 AGE=1 ----------					
CART	8	25.22	9.61	38.101	3.40
CORTEX	8	17.92	7.45	41.596	2.64
SPONG	8	82.86	36.01	43.465	12.73
MARROW	8	24.78	7.14	28.816	2.52
GP	0	.	.	.	.
---------- BONE=2 AGE=2 ----------					
CART	8	4.59	0.90	19.599	0.32
CORTEX	8	6.90	1.77	25.611	0.62
SPONG	8	20.58	4.78	23.219	1.69
MARROW	8	17.72	3.17	17.915	1.12
GP	8	16.20	5.99	36.936	2.12
---------- BONE=2 AGE=3 ----------					
CART	8	1.91	2.03	106.218	0.72
CORTEX	8	3.00	0.91	30.430	0.32
SPONG	8	9.39	2.57	27.383	0.91
MARROW	8	7.03	4.28	60.819	1.51
GP	0	.	.	.	.

Table 11
(Cont.)

OSSEOUS TISSUE FLOW BY AGE CC/MIN/HG

AGE=1

VARIABLE	N	MEAN	STANDARD DEVIATION	C.V.	STD ERROR OF MEAN
CART	16	22.79	8.38	36.779	2.10
CORTEX	16	19.47	7.89	40.504	1.97
SPONG	16	79.71	31.12	39.033	7.78
MARROW	16	21.21	7.98	37.595	1.99
GP	0	.	.	.	.
AGE=2					
CART	16	5.69	1.55	27.313	0.39
CORTEX	16	9.06	3.11	34.371	0.78
SPONG	16	24.41	5.52	22.598	1.38
MARROW	16	25.45	8.67	34.079	2.17
GP	16	17.77	4.59	25.845	1.15
AGE=3					
CART	18	1.81	1.92	106.251	0.45
CORTEX	18	4.41	2.37	53.630	0.56
SPONG	18	18.34	10.31	56.218	2.43
MARROW	18	14.24	8.21	57.674	1.94
GP	0	.	.	.	.

Table 12

OSSEOUS TISSUE CIRCULATION %TBF/%TW

VARIABLE	N	MEAN	STANDARD DEVIATION	C.V.	STD ERROR OF MEAN
		AGE=2 BONE=1			
CART	8	0.287	0.051	17.935	0.018
CORTEX	8	0.472	0.078	16.533	0.028
SPONG	8	1.192	0.087	7.320	0.031
MARROW	8	1.397	0.083	5.917	0.029
GP	8	0.845	0.113	13.348	0.040
		AGE=2 BONE=2			
CART	8	0.300	0.030	10.096	0.011
CORTEX	8	0.448	0.048	10.817	0.017
SPONG	8	1.357	0.077	5.703	0.027
MARROW	8	1.169	0.161	13.747	0.057
GP	8	1.155	0.323	27.937	0.114
		AGE=3 BONE=1			
CART	6	0.049	0.038	78.076	0.016
CORTEX	6	0.290	0.067	23.161	0.027
SPONG	6	1.535	0.150	9.760	0.061
MARROW	6	1.630	0.363	22.263	0.148
GP	0	.	.	.	.
		AGE=3 BONE=2			
CART	4	0.228	0.124	54.444	0.062
CORTEX	4	0.547	0.043	7.846	0.021
SPONG	4	1.846	0.222	12.018	0.111
MARROW	4	1.863	0.738	39.611	0.369
GP	0	.	.	.	.

Table 12
(Cont.)

OSSEOUS TISSUE CIRCULATION %TBF/%TW

AGE=2

VARIABLE	N	MEAN	STANDARD DEVIATION	C.V.	STD ERROR OF MEAN
CART	16	0.293	0.041	14.094	0.010
CORTEX	16	0.460	0.064	13.922	0.016
SPONG	16	1.274	0.116	9.132	0.029
MARROW	16	1.283	0.171	13.305	0.043
GP	16	1.000	0.283	28.319	0.071

AGE=3

CART	10	0.121	0.120	99.825	0.038
CORTEX	10	0.393	0.144	36.631	0.046
SPONG	10	1.659	0.234	14.085	0.074
MARROW	10	1.723	0.519	30.113	0.164
GP	0	.	.	.	.

Table 13

DEVELOPMENTAL OSSEOUS REGIONAL FLOW CC/MIN/HG
BONE=1 AGE=1

VARIABLE	N	MEAN	STANDARD DEVIATION	C.V.	STD ERROR OF MEAN
PEPI	8	21.96	8.50	38.686	3.00
GTTUB	6	16.00	9.74	60.852	3.98
PMCX	8	38.22	16.00	41.874	5.66
PMS	8	78.25	25.70	32.841	9.09
DCX	8	16.05	7.18	44.724	2.54
DMAR	8	17.65	7.50	42.482	2.65
DMS	8	74.85	30.66	40.964	10.84
DMCX	8	29.62	13.34	45.032	4.72
DEPI	8	20.63	7.05	34.167	2.49
TOTAL	8	34.38	11.46	33.328	4.05
---------- BONE=1 AGE=2 ----------					
PEPI	8	22.37	2.63	11.745	0.93
GTTUB	8	21.94	2.48	11.294	0.88
PMCX	8	17.05	4.23	24.801	1.49
PMS	8	32.85	3.61	10.997	1.28
DCX	8	9.11	1.81	19.911	0.64
DMAR	8	31.87	4.03	12.660	1.43
DMS	8	29.89	4.63	15.506	1.64
DMCX	8	13.18	5.26	39.934	1.86
DEPI	8	22.67	3.08	13.571	1.09
TOTAL	8	23.73	2.40	10.129	0.85
---------- BONE=1 AGE=3 ----------					
PEPI	10	15.27	5.55	36.369	1.76
GTTUB	10	9.19	4.29	46.686	1.36
PMCX	10	11.41	4.76	41.685	1.50
PMS	10	48.60	12.87	26.471	4.07
DCX	10	3.48	1.79	51.419	0.57
DMAR	10	28.53	7.23	25.324	2.28
DMS	10	25.23	11.83	46.899	3.74
DMCX	10	5.25	2.57	48.984	0.81
DEPI	10	6.41	4.25	66.268	1.34
TOTAL	10	16.63	5.39	32.412	1.70
---------- BONE=2 AGE=1 ----------					
PEPI	8	20.27	8.85	43.650	3.13
GTTUB	8	35.20	17.45	49.580	6.17
PMCX	8	17.20	10.51	61.088	3.72
PMS	8	79.46	36.33	45.723	12.85
DCX	8	18.60	8.05	43.272	2.85
DMAR	8	24.78	7.14	28.816	2.52
DMS	8	89.71	39.68	44.233	14.03
DMCX	8	15.44	7.71	49.904	2.72
DEPI	8	35.13	12.19	34.691	4.31
TOTAL	8	36.92	13.68	37.040	4.84

DEVELOPMENTAL OSSEOUS REGIONAL FLOW CC/MIN/HG
BONE=2 AGE=2

VARIABLE	N	MEAN	STANDARD DEVIATION	C.V.	STD ERROR OF MEAN
PEPI	8	17.98	5.02	27.886	1.77
GTTUB	8	13.43	4.46	33.194	1.58
PMCX	8	11.43	1.34	11.717	0.47
PMS	8	30.10	5.62	18.677	1.99
DCX	8	6.19	1.99	32.172	0.70
DMAR	8	17.72	3.17	17.915	1.12
DMS	8	17.41	4.46	25.601	1.58
DMCX	8	7.30	1.64	22.458	0.58
DEPI	8	4.38	1.56	35.498	0.55
TOTAL	8	15.37	3.20	20.807	1.13
---------- BONE=2 AGE=3 ----------					
PEPI	8	6.70	2.83	42.240	1.00
GTTUB	8	5.39	2.04	37.814	0.72
PMCX	8	4.36	1.85	42.472	0.65
PMS	8	12.56	3.44	27.423	1.22
DCX	8	2.12	0.32	15.260	0.11
DMAR	8	9.85	3.88	39.405	1.37
DMS	8	9.58	3.05	31.899	1.08
DMCX	8	4.17	1.49	35.704	0.53
DEPI	8	4.76	3.65	76.605	1.29
TOTAL	8	5.17	1.44	27.837	0.51

DEVELOPMENTAL OSSEOUS REGIONAL FLOW %TBF/%TW
BONE=1 AGE=1

VARIABLE	N	MEAN	STANDARD DEVIATION	C.V.	STD ERROR OF MEAN
PEPI	8	0.637	0.172	27.055	0.061
GTTUB	6	0.432	0.209	48.248	0.085
PMCX	8	1.094	0.194	17.721	0.069
PMS	8	2.296	0.318	13.842	0.112
DCX	8	0.453	0.066	14.549	0.023
DMAR	8	0.572	0.367	64.101	0.130
DMS	8	2.138	0.249	11.629	0.088
DMCX	8	0.869	0.250	28.725	0.088
DEPI	8	0.602	0.073	12.153	0.026
---------- BONE=1 AGE=2 ----------					
PEPI	8	0.949	0.055	5.783	0.019
GTTUB	8	0.928	0.100	10.812	0.035
PMCX	8	0.728	0.109	15.011	0.039
PMS	8	1.383	0.051	3.712	0.018
DCX	8	0.382	0.053	13.766	0.019
DMAR	8	1.399	0.083	5.935	0.029
DMS	8	1.262	0.146	11.552	0.052
DMCX	8	0.549	0.195	35.422	0.069
DEPI	8	0.977	0.129	13.247	0.046
---------- BONE=1 AGE=3 ----------					
PEPI	10	1.047	0.613	58.549	0.194
GTTUB	10	0.535	0.130	24.266	0.041
PMCX	10	0.682	0.139	20.382	0.044
PMS	10	3.016	0.761	25.237	0.241
DCX	10	0.251	0.117	46.623	0.037
DMAR	10	1.765	0.347	19.629	0.110
DMS	10	1.454	0.287	19.721	0.091
DMCX	10	0.304	0.065	21.310	0.021
DEPI	10	0.348	0.155	44.544	0.049
---------- BONE=2 AGE=1 ----------					
PEPI	8	0.547	0.157	28.737	0.056
GTTUB	8	0.940	0.256	27.196	0.090
PMCX	8	0.450	0.133	29.524	0.047
PMS	8	2.099	0.367	17.487	0.130
DCX	8	0.504	0.146	29.071	0.052
DMAR	8	0.671	0.132	19.607	0.047
DMS	8	2.418	0.628	25.974	0.222
DMCX	8	0.411	0.095	23.004	0.033
DEPI	8	0.988	0.280	28.378	0.099

Table 14
(Cont.)

DEVELOPMENTAL OSSEOUS REGIONAL FLOW %TBF/%TW
BONE=2 AGE=2

VARIABLE	N	MEAN	STANDARD DEVIATION	C.V.	STD ERROR OF MEAN
PEPI	8	1.234	0.121	9.813	0.043
GTTUB	8	0.878	0.142	16.200	0.050
PMCX	8	0.795	0.170	21.397	0.060
PMS	8	1.969	0.118	5.987	0.042
DCX	8	0.397	0.067	16.801	0.024
DMAR	8	1.169	0.161	13.751	0.057
DMS	8	1.130	0.142	12.536	0.050
DMCX	8	0.490	0.083	16.868	0.029
DEPI	8	0.284	0.056	19.712	0.020
---------- BONE=2 AGE=3 ----------					
PEPI	8	1.267	0.303	23.914	0.107
GTTUB	8	1.032	0.226	21.864	0.080
PMCX	8	0.834	0.192	23.060	0.068
PMS	8	2.432	0.199	8.180	0.070
DCX	8	0.422	0.057	13.526	0.020
DMAR	8	1.924	0.842	43.746	0.298
DMS	8	1.864	0.366	19.632	0.129
DMCX	8	0.809	0.211	26.114	0.075
DEPI	8	0.858	0.453	52.750	0.160

INFANT PUP OSSEOUS REGIONAL FLOW CC/MIN/HG

BONE=1

VARIABLE	N	MEAN	STANDARD DEVIATION	C.V.	STD ERROR OF MEAN
POEC	8	12.97	5.15	39.753	1.82
PIEC	8	28.99	11.12	38.369	3.93
GTTUBC	6	16.00	9.74	60.852	3.98
PMCX	8	38.22	16.00	41.874	5.66
PPMS	8	203.42	90.11	44.298	31.86
PDMS	8	13.16	6.03	45.843	2.13
DCX	8	16.05	7.18	44.724	2.54
DMAR	8	17.65	7.50	42.482	2.65
DOEC	8	13.70	4.39	32.027	1.55
DIEC	8	25.30	9.87	39.031	3.49
DMCX	8	29.62	13.34	45.032	4.72
DPMS	8	191.99	84.49	44.007	29.87
DDMS	8	9.59	3.09	32.241	1.09
TOTAL	8	34.38	11.46	33.328	4.05
---------- BONE=2 ----------					
POEC	8	15.06	6.47	42.968	2.29
PIEC	8	25.90	12.83	49.550	4.54
GTTUBC	8	35.20	17.46	49.583	6.17
PMCX	8	17.33	10.63	61.346	3.76
PPMS	8	167.29	78.49	46.918	27.75
PDMS	8	10.04	2.35	23.454	0.83
DCX	8	18.60	8.05	43.272	2.85
DMAR	8	24.78	7.14	28.816	2.52
DOEC	8	26.17	8.57	32.740	3.03
DIEC	8	44.39	17.41	39.213	6.15
DMCX	8	15.45	7.71	49.921	2.73
DPMS	8	184.04	81.51	44.289	28.82
DDMS	8	9.97	3.09	30.978	1.09
TOTAL	8	36.92	13.68	37.040	4.84

Table 16

INFANT PUP OSSEOUS REGIONAL FLOW %TBF/%TW

VARIABLE	N	MEAN	STANDARD DEVIATION	C.V.	STD ERROR OF MEAN
BONE=1					
POEC	8	0.383	0.122	31.902	0.043
PIEC	8	0.847	0.232	27.436	0.082
GTTUBC	6	0.432	0.208	48.158	0.085
PMCX	8	1.093	0.194	17.748	0.069
PPMS	8	5.769	0.870	15.083	0.308
PDMS	8	0.377	0.082	21.803	0.029
DCX	8	0.453	0.066	14.550	0.023
DMAR	8	0.573	0.367	63.976	0.130
DOEC	8	0.409	0.101	25.010	0.035
DIEC	8	0.733	0.134	18.310	0.047
DMCX	8	0.869	0.250	28.725	0.088
DPMS	8	5.444	1.035	19.009	0.366
DDMS	8	0.289	0.082	28.433	0.029
BONE=2					
POEC	8	0.408	0.090	22.057	0.032
PIEC	8	0.692	0.292	42.225	0.103
GTTUBC	8	0.940	0.256	27.204	0.090
PMCX	8	0.450	0.133	29.524	0.047
PPMS	8	4.472	0.839	18.764	0.297
PDMS	8	0.292	0.095	32.448	0.034
DCX	8	0.504	0.146	29.071	0.052
DMAR	8	0.670	0.132	19.684	0.047
DOEC	8	0.740	.228	30.773	0.080
DIEC	8	1.228	0.388	31.568	0.137
DMCX	8	0.411	0.095	23.004	0.033
DPMS	8	4.990	1.324	26.537	0.468
DDMS	8	0.298	0.145	48.629	0.051

Table 17

ADOLESCENT PUP FEMORAL REGIONAL FLOW CC/MIN/HG

VARIABLE	N	MEAN	STANDARD DEVIATION	C.V.	STD ERROR OF MEAN
FHEC	8	5.64	1.73	30.604	0.61
FHO2O	8	36.55	6.36	17.390	2.25
FHC2O	8	17.23	4.04	23.432	1.43
FHGP	8	20.74	4.30	20.724	1.52
GTEC	8	12.86	5.39	41.880	1.90
GTO2O	8	27.03	2.91	10.766	1.03
GTC2O	8	19.80	2.83	14.316	1.00
GTGP	8	26.34	8.92	33.870	3.15
LTEC	8	18.37	9.68	52.700	3.42
LT2O	8	20.57	6.32	30.736	2.24
LTGP	8	29.05	6.93	23.841	2.45
FNMCX	8	15.34	6.09	39.708	2.15
GTMCX	8	18.33	4.25	23.156	1.50
ITMCX	8	17.23	3.59	20.830	1.27
PDMCX	8	17.26	3.80	21.993	1.34
FNPMS	8	107.91	16.34	15.144	5.78
FNMPMS	8	17.87	3.61	20.217	1.28
GTPMS	8	113.13	34.84	30.797	12.32
GTMPMS	8	19.26	4.24	22.021	1.50
ITMS	8	33.16	4.10	12.364	1.45
PDMS	8	36.32	7.37	20.293	2.61
PDCX	8	9.62	1.94	20.147	0.69
MDCX	8	8.90	1.88	21.146	0.67
DDCX	8	8.93	1.52	17.058	0.54
PDMAR	8	36.33	5.04	13.979	1.77
MDMAR	8	26.09	4.95	18.984	1.75
DDMAR	8	39.58	4.89	12.364	1.73
DMEEC	8	4.83	1.98	40.949	0.70
DLEC	8	6.61	3.25	49.097	1.15
DMEO2O	8	28.80	2.77	9.631	0.98
DLO2O	8	25.26	3.56	14.095	1.26
DMEC2O	8	25.12	3.69	14.680	1.30
DLC2O	8	18.62	4.95	26.592	1.75
DGP	8	17.07	2.66	15.566	0.94
DPMCX	8	14.55	5.83	40.090	2.06
DDMCX	8	12.47	5.14	41.206	1.82
DPMS	8	118.59	29.77	25.103	10.53
DMPMS	8	15.15	9.03	59.598	3.19
DMDMS	8	23.82	7.13	29.942	2.52
DDMS	8	35.14	7.45	21.207	2.63
PERIOS	8	14.02	4.34	30.922	1.53
TOTAL	8	23.73	2.40	10.129	0.85

ADOLESCENT PUP TIBIAL REGIONAL FLOW CC/MIN/HG

VARIABLE	N	MEAN	STANDARD DEVIATION	C.V.	STD ERROR OF MEAN
PEC	8	4.76	1.31	27.494	0.46
PO2O	8	25.74	5.23	20.322	1.85
PC2O	8	18.81	8.04	42.740	2.84
PGP	8	20.12	7.49	37.244	2.65
TUBC	7	4.63	2.94	63.625	1.11
TUB2O	8	13.63	5.44	39.894	1.92
TUBFIB	8	15.95	4.79	30.048	1.69
TUBGP	8	14.97	5.75	38.421	2.03
CBETUB	8	7.52	4.06	53.975	1.44
PPMCX	8	11.73	1.57	13.405	0.56
PDMCX	8	10.98	2.21	20.131	0.78
PPMS	8	178.77	105.96	59.268	37.46
PMPMS	8	16.13	9.41	58.357	3.33
PMDMS	8	25.82	5.06	19.606	1.79
PDMS	8	31.26	5.51	17.638	1.95
PDCX	8	7.51	0.86	11.512	0.31
MDCX	8	5.85	2.23	38.163	0.79
DDCX	8	6.53	2.29	35.093	0.81
PDMAR	8	33.97	4.70	13.847	1.66
MDMAR	8	6.94	0.96	13.839	0.34
DDMAR	8	21.73	4.34	19.968	1.53
DEC	8	1.57	1.18	75.097	0.42
DO2O	8	6.16	2.00	32.532	0.71
DC2O	8	3.53	1.69	47.813	0.60
DGP	8	10.63	6.21	58.377	2.19
DPMCX	8	7.75	1.75	22.547	0.62
DDMCX	8	7.05	1.67	23.747	0.59
DPMS	8	54.92	12.85	23.405	4.54
DMPMS	8	7.40	5.40	73.064	1.91
DMDMS	8	16.11	7.35	45.608	2.60
DDMS	8	22.67	7.04	31.044	2.49
PERIOS	8	11.09	7.55	68.138	2.67
TOTAL	8	15.37	3.20	20.807	1.13

Table 19

ADOLESCENT PUP FEMORAL REGIONAL FLOW %TBF/%TW

VARIABLE	N	MEAN	STANDARD DEVIATION	C.V.	STD ERROR OF MEAN
FHEC	8	0.235	0.060	25.417	0.021
FHO2O	8	1.536	0.180	11.699	0.064
FHC2O	8	0.733	0.184	25.139	0.065
FHGP	8	0.881	0.202	22.877	0.071
GTEC	8	0.541	0.220	40.660	0.078
GTO2O	8	1.145	0.138	12.023	0.049
GTC2O	8	0.838	0.115	13.716	0.041
GTGP	8	1.105	0.351	31.771	0.124
LTEC	8	0.782	0.414	52.983	0.146
LT2O	8	0.875	0.293	33.439	0.103
LTGP	8	1.236	0.315	25.495	0.111
FNMCX	8	0.643	0.242	37.725	0.086
GTMCX	8	0.770	0.139	18.053	0.049
ITMCX	8	0.723	0.103	14.254	0.036
PDMCX	8	0.722	0.115	15.986	0.041
FNPMS	8	4.555	0.596	13.083	0.211
FNMPMS	8	0.758	0.156	20.544	0.055
GTPMS	8	4.750	1.365	28.732	0.483
GTMPMS	8	0.819	0.188	22.918	0.066
ITMS	8	1.395	0.068	4.859	0.024
PDMS	8	1.523	0.238	15.607	0.084
PDCX	8	0.404	0.060	14.868	0.021
MDCX	8	0.373	0.054	14.450	0.019
DDCX	8	0.375	0.043	11.474	0.015
PDMAR	8	1.523	0.097	6.372	0.034
MDMAR	8	1.101	0.184	16.697	0.065
DDMAR	8	1.668	0.141	8.445	0.050
DMEEC	8	0.207	0.088	42.554	0.031
DLEC	8	0.281	0.145	51.404	0.051
DMEO2O	8	1.218	0.128	10.471	0.045
DLO2O	8	1.069	0.150	14.045	0.053
DMEC2O	8	1.067	0.175	16.430	0.062
DLC2O	8	0.791	0.221	27.887	0.078
DGP	8	0.727	0.141	19.444	0.050
DPMCX	8	0.608	0.220	36.209	0.078
DDMCX	8	0.519	0.190	36.571	0.067
DPMS	8	4.966	0.997	20.083	0.353
DMPMS	8	0.649	0.384	59.214	0.136
DMDMS	8	1.011	0.300	29.696	0.106
DDMS	8	1.470	0.197	13.410	0.070
PERIOS	8	0.588	0.155	26.440	0.055

Table 20

ADOLESCENT PUP TIBIAL REGIONAL FLOW %TBF/%TW

VARIABLE	N	MEAN	STANDARD DEVIATION	C.V.	STD ERROR OF MEAN
PEC	8	0.307	0.051	16.505	0.018
PO2O	8	1.679	0.120	7.150	0.042
PC2O	8	1.177	0.303	25.728	0.107
PGP	8	1.294	0.299	23.075	0.106
TUBC	8	0.319	0.324	101.492	0.115
TUB2O	8	0.855	0.212	24.840	0.075
TUBFIB	8	1.050	0.299	28.476	0.106
TUBGP	8	0.982	0.309	31.514	0.109
CBETUB	8	0.487	0.204	41.850	0.072
PPMCX	8	0.800	0.231	28.851	0.082
PDMCX	8	0.716	0.052	7.261	0.018
PPMS	8	11.362	5.367	47.238	1.898
PMPMS	8	0.983	0.414	42.164	0.147
PMDMS	8	1.687	0.132	7.816	0.047
PDMS	8	2.087	0.454	21.752	0.160
PDCX	8	0.500	0.071	14.185	0.025
MDCX	8	0.374	0.087	23.242	0.031
DDCX	8	0.418	0.084	20.154	0.030
PDMAR	8	2.287	0.523	22.845	0.185
MDMAR	8	0.465	0.094	20.264	0.033
DDMAR	8	1.421	0.172	12.097	0.061
DEC	8	0.108	0.090	83.247	0.032
DO2O	8	0.394	0.078	19.756	0.028
DC2O	8	0.220	0.070	32.084	0.025
DGP	8	0.671	0.321	47.859	0.113
DPMCX	8	0.509	0.093	18.285	0.033
DDMCX	8	0.599	0.365	60.875	0.129
DPMS	8	3.656	0.965	26.395	0.341
DMPMS	8	0.440	0.273	61.939	0.096
DMDMS	8	0.929	0.417	44.944	0.148
DDMS	8	1.449	0.192	13.251	0.068
PERIOS	8	0.679	0.392	57.724	0.139

Table 21

ADULT VS ADOLESCENT FEMORAL REGIONAL FLOW CC/MIN/HG
AGE=2

VARIABLE	N	MEAN	STANDARD DEVIATION	C.V.	STD ERROR OF MEAN
FHECCX	8	5.64	1.73	30.604	0.61
FHES	8	27.39	3.11	11.351	1.10
GTECCX	8	12.86	5.39	41.880	1.90
GTES	8	24.20	2.25	9.301	0.80
LTCCX	8	18.37	9.68	52.700	3.42
LTS	8	20.57	6.32	30.736	2.24
FNMCX	8	15.34	6.09	39.708	2.15
GTMCX	8	18.33	4.25	23.156	1.50
ITMCX	8	17.23	3.59	20.830	1.27
PDMCX	8	17.23	3.80	22.033	1.34
FNMS	8	30.76	3.60	11.711	1.27
GTMS	8	30.15	3.06	10.154	1.08
ITMS	8	33.16	4.10	12.364	1.45
PDMS	8	36.32	7.37	20.293	2.61
PDCX	8	9.62	1.94	20.147	0.69
MDCX	8	8.90	1.88	21.146	0.67
DDCX	8	8.93	1.52	17.058	0.54
PDSMAR	8	36.23	5.04	13.920	1.78
MDSMAR	8	26.09	4.95	18.984	1.75
DDSMAR	8	39.58	4.89	12.364	1.73
DDMS	8	35.14	7.45	21.207	2.63
DPMS	8	27.78	6.14	22.095	2.17
DDMCX	8	12.47	5.14	41.206	1.82
DPMCX	8	14.55	5.83	40.090	2.06
DES	8	24.46	3.28	13.426	1.16
DECCX	8	5.64	2.48	43.921	0.88
PERIOS	8	14.02	4.34	30.922	1.53

ADULT VS ADOLESCENT FEMORAL REGIONAL FLOW CC/MIN/HG
AGE=3

VARIABLE	N	MEAN	STANDARD DEVIATION	C.V.	STD ERROR OF MEAN
FHECCX	10	10.60	5.26	49.629	1.66
FHES	10	18.29	9.51	51.987	3.01
GTECCX	9	9.23	5.17	56.040	1.72
GTES	10	9.81	4.37	44.537	1.38
LTCCX	10	16.87	9.60	56.876	3.04
LTS	10	53.37	22.95	43.011	7.26
FNMCX	10	18.94	8.66	45.692	2.74
GTMCX	10	11.52	6.31	54.764	2.00
ITMCX	10	10.37	5.54	53.411	1.75
PDMCX	10	7.63	3.18	41.688	1.01
FNMS	10	50.34	12.96	25.752	4.10
GTMS	10	38.72	18.05	46.609	5.71
ITMS	10	48.33	18.86	39.023	5.96
PDMS	10	50.63	11.19	22.106	3.54
PDCX	10	11.46	9.76	85.135	3.09
MDCX	10	3.02	1.29	42.704	0.41
DDCX	10	3.06	1.29	42.240	0.41
PDSMAR	10	36.81	13.43	36.489	4.25
MDSMAR	10	21.36	5.08	23.778	1.61
DDSMAR	10	33.95	12.23	36.030	3.87
DDMS	10	25.51	8.27	32.408	2.61
DPMS	10	25.49	13.77	54.023	4.35
DDMCX	10	5.24	3.32	63.431	1.05
DPMCX	10	6.51	3.72	57.173	1.18
DES	10	5.91	3.28	55.512	1.04
DECCX	10	9.20	8.28	89.968	2.62
PERIOS	10	4.99	3.73	74.611	1.18

Table 22

ADULT VS ADOLESCENT TIBIAL REGIONAL FLOW CC/MIN/HG

AGE=2

VARIABLE	N	MEAN	STANDARD DEVIATION	C.V.	STD ERROR OF MEAN
PECCX	8	4.76	1.31	27.494	0.46
PES	8	20.33	6.25	30.754	2.21
TUBS	8	13.43	4.46	33.194	1.58
PPMCX	8	11.73	1.57	13.405	0.56
PDMCX	8	10.98	2.21	20.131	0.78
PPMS	8	30.99	7.63	24.625	2.70
PMMS	8	25.82	5.06	19.606	1.79
PDMS	8	31.26	5.51	17.638	1.95
PDCX	8	7.51	0.86	11.462	0.30
MDCX	8	5.85	2.23	38.163	0.79
DDCX	8	6.53	2.29	35.093	0.81
PDSMAR	8	33.97	4.70	13.847	1.66
MDSMAR	8	6.94	0.96	13.839	0.34
DDSMAR	8	21.73	4.34	19.968	1.53
DDMS	8	22.67	7.04	31.044	2.49
DMMS	8	16.11	7.35	45.608	2.60
DPMS	8	15.73	3.23	20.519	1.14
DDMCX	8	7.05	1.67	23.747	0.59
DPMCX	8	7.75	1.75	22.547	0.62
DES	8	4.59	1.71	37.127	0.60
DECCX	8	1.58	1.18	75.091	0.42
PERIOS	8	11.09	7.55	68.138	2.67
---------- AGE=3 ----------					
PECCX	8	6.74	3.90	57.934	1.38
PES	8	6.68	2.42	36.180	0.85
TUBS	8	8.94	2.92	32.647	1.03
PPMCX	8	4.70	2.39	50.764	0.84
PDMCX	8	4.07	1.27	31.199	0.45
PPMS	8	11.76	3.27	27.813	1.16
PMMS	8	12.60	5.57	44.178	1.97
PDMS	8	13.77	3.76	27.283	1.33
PDCX	8	2.69	0.64	23.775	0.23
MDCX	8	1.70	0.27	16.140	0.10
DDCX	8	2.65	0.35	13.104	0.12
PDSMAR	8	13.97	5.54	39.625	1.96
MDSMAR	8	7.03	4.28	60.819	1.51
DDSMAR	8	9.87	5.46	55.361	1.93
DDMS	8	11.67	4.21	36.095	1.49
DMMS	8	9.84	4.03	40.970	1.43
DPMS	8	7.41	3.19	43.028	1.13
DDMCX	8	3.39	0.91	26.860	0.32
DPMCX	8	5.05	2.41	47.799	0.85
DES	8	4.77	3.53	74.125	1.25
DECCX	8	4.74	3.77	79.521	1.33
PERIOS	8	4.57	3.97	86.909	1.40

Table 23

ADULT VS ADOLESCENT FEMORAL REGIONAL FLOW %TBF/%TW
AGE=2

VARIABLE	N	MEAN	STANDARD DEVIATION	C.V.	STD ERROR OF MEAN
FHECCX	8	0.235	0.060	25.392	0.021
FHES	8	1.136	0.085	7.439	0.030
GTECCX	8	0.541	0.220	40.616	0.078
GTES	8	1.024	0.093	9.127	0.033
LTCCX	8	0.783	0.409	52.310	0.145
LTS	8	0.873	0.292	33.411	0.103
FNMCX	8	0.642	0.242	37.637	0.085
GTMCX	8	0.770	0.138	17.907	0.049
ITMCX	8	0.722	0.102	14.103	0.036
PDMCX	8	0.722	0.115	15.904	0.041
FNMS	8	1.301	0.131	10.034	0.046
GTMS	8	1.278	0.082	6.427	0.029
ITMS	8	1.439	0.100	6.938	0.035
PDMS	8	1.522	0.237	15.571	0.084
PDCX	8	0.404	0.060	14.783	0.021
MDCX	8	0.372	0.054	14.382	0.019
DDCX	8	0.375	0.043	11.384	0.015
PDSMAR	8	1.522	0.096	6.319	0.034
MDSMAR	8	1.101	0.184	16.740	0.065
DDSMAR	8	1.668	0.141	8.452	0.050
DDMS	8	1.469	0.196	13.336	0.069
DPMS	8	1.175	0.250	21.244	0.088
DDMCX	8	0.519	0.189	36.497	0.067
DPMCX	8	0.608	0.220	36.145	0.078
DES	8	1.037	0.151	14.530	0.053
DECCX	8	0.241	0.110	45.904	0.039
PERIOS	8	0.587	0.154	26.269	0.055

ADULT VS ADOLESCENT FEMORAL REGIONAL FLOW %TBF/%TW
AGE=3

VARIABLE	N	MEAN	STANDARD DEVIATION	C.V.	STD ERROR OF MEAN
FHECCX	10	0.636	0.228	35.791	0.072
FHES	10	1.304	0.966	74.077	0.305
GTECCX	9	0.501	0.157	31.370	0.052
GTES	10	0.586	0.190	32.340	0.060
LTCCX	10	0.994	0.400	40.242	0.126
LTS	10	3.159	0.859	27.197	0.272
FNMCX	10	1.127	0.254	22.572	0.080
GTMCX	10	0.674	0.208	30.847	0.066
ITMCX	10	0.608	0.183	30.156	0.058
PDMCX	10	0.456	0.108	23.578	0.034
FNMS	10	3.173	0.844	26.590	0.267
GTMS	10	2.250	0.474	21.065	0.150
ITMS	10	3.257	0.942	28.913	0.298
PDMS	10	3.237	0.851	26.299	0.269
PDCX	10	0.466	0.228	48.968	0.072
MDCX	10	0.173	0.041	23.448	0.013
DDCX	10	0.190	0.043	22.739	0.014
PDSMAR	10	2.409	0.764	31.719	0.242
MDSMAR	10	1.308	0.503	38.493	0.159
DDSMAR	10	2.089	0.180	8.594	0.057
DDMS	10	1.485	0.186	12.521	0.059
DPMS	10	1.440	0.388	26.971	0.123
DDMCX	10	0.259	0.065	25.090	0.021
DPMCX	10	0.355	0.122	34.437	0.039
DES	10	0.322	0.127	39.351	0.040
DECCX	10	0.462	0.335	72.457	0.106
PERIOS	10	0.299	0.220	73.625	0.070

Table 24

ADULT VS ADOLESCENT TIBIAL REGIONAL FLOW %TBF/%TW

AGE=2

VARIABLE	N	MEAN	STANDARD DEVIATION	C.V.	STD ERROR OF MEAN
PECCX	8	0.307	0.051	16.570	0.018
PES	8	1.398	0.170	12.147	0.060
TUBS	8	0.878	0.142	16.200	0.050
PPMCX	8	0.800	0.231	28.882	0.082
PDMCX	8	0.716	0.052	7.264	0.018
PPMS	8	2.042	0.208	10.171	0.073
PMMS	8	1.687	0.132	7.849	0.047
PDMS	8	2.087	0.455	21.782	0.161
PDCX	8	0.500	0.071	14.187	0.025
MDCX	8	0.374	0.087	23.206	0.031
DDCX	8	0.418	0.084	20.158	0.030
PDSMAR	8	1.958	0.812	41.458	0.287
MDSMAR	8	0.465	0.094	20.273	0.033
DDSMAR	8	1.421	0.172	12.123	0.061
DDMS	8	1.449	0.192	13.232	0.068
DMMS	8	1.009	0.301	29.875	0.107
DPMS	8	1.139	0.364	31.963	0.129
DDMCX	8	0.459	0.057	12.335	0.020
DPMCX	8	0.509	0.094	18.370	0.033
DES	8	0.298	0.064	21.410	0.023
DECCX	8	0.108	0.089	82.856	0.032
PERIOS	8	0.679	0.392	57.689	0.138
----------		AGE=3	----------		
PECCX	8	1.248	0.555	44.441	0.196
PES	8	1.273	0.214	16.807	0.076
TUBS	8	1.719	0.269	15.657	0.095
PPMCX	8	0.872	0.276	31.616	0.098
PDMCX	8	0.786	0.144	18.262	0.051
PPMS	8	2.283	0.271	11.877	0.096
PMMS	8	2.381	0.493	20.713	0.174
PDMS	8	2.724	0.706	25.914	0.250
PDCX	8	0.530	0.099	18.745	0.035
MDCX	8	0.342	0.077	22.375	0.027
DDCX	8	0.541	0.148	27.253	0.052
PDSMAR	8	2.857	1.382	48.367	0.489
MDSMAR	8	1.363	0.835	61.282	0.295
DDSMAR	8	1.962	1.209	61.637	0.428
DDMS	8	2.307	0.834	36.148	0.295
DMMS	8	1.883	0.542	28.794	0.192
DPMS	8	1.421	0.478	33.594	0.169
DDMCX	8	0.677	0.184	27.254	0.065
DPMCX	8	0.956	0.304	31.765	0.107
DES	8	0.871	0.491	56.398	0.174
DECCX	8	0.845	0.442	52.365	0.156
PERIOS	8	1.279	1.260	98.457	0.445

ADULT DOG FEMORAL REGIONAL FLOW CC/ MIN/HG

VARIABLE	N	MEAN	STANDARD DEVIATION	C.V.	STD ERROR OF MEAN
PAC	10	2.29	2.72	118.868	0.86
FHECX	10	15.93	8.58	53.865	2.71
FHES	10	18.29	9.51	51.992	3.01
GTECX	9	9.23	5.17	56.024	1.72
GTES	10	9.80	4.37	44.532	1.38
FNMCX	10	18.94	8.65	45.667	2.74
GTMCX	10	11.53	6.31	54.768	2.00
ITMCX	10	10.37	5.54	53.389	1.75
PDMCX	10	7.63	3.18	41.645	1.01
FNMS	10	50.34	12.97	25.759	4.10
GTMS	10	38.72	18.05	46.608	5.71
ITMS	10	51.21	12.18	23.792	3.85
PDMS	10	50.87	10.77	21.165	3.40
LTCX	10	16.87	9.59	56.851	3.03
LTS	10	53.37	22.95	43.013	7.26
PDCX	10	8.34	5.92	71.000	1.87
MDCX	10	2.89	1.36	46.908	0.43
DDCX	10	3.12	1.23	39.495	0.39
PDS	10	39.18	7.41	18.909	2.34
DMAR	10	20.01	5.48	27.413	1.73
DDS	10	34.64	11.01	31.783	3.48
DAC	10	1.61	2.49	154.834	0.79
DECX	10	10.18	8.78	86.209	2.78
DES	10	5.81	3.42	58.932	1.08
DPMCX	10	6.37	3.87	60.832	1.22
DDMCX	10	4.22	1.46	34.533	0.46
DPOMS	10	11.21	3.73	33.269	1.18
DDOMS	10	12.72	3.78	29.686	1.19
DPCMS	10	30.06	15.90	52.897	5.03
DMCMS	10	34.50	17.50	50.732	5.53
DDCMS	10	34.16	15.27	44.706	4.83
PERIOS	10	4.48	2.62	58.479	0.83
TOTAL	10	16.63	5.39	32.406	1.70

Table 26

ADULT DOG TIBIAL REGIONAL FLOW CC/MIN/HG

VARIABLE	N	MEAN	STANDARD DEVIATION	C.V.	STD ERROR OF MEAN
PAC	8	1.65	2.02	122.518	0.71
PECX	8	8.03	4.73	58.951	1.67
PES	8	6.68	2.42	36.210	0.86
TUBCX	8	4.01	2.18	54.321	0.77
TUBS	8	8.94	2.92	32.647	1.03
PPMCX	8	4.70	2.39	50.764	0.84
PDMCX	8	4.07	1.27	31.199	0.45
PPMS	8	11.76	3.27	27.813	1.16
PMMS	8	12.60	5.57	44.178	1.97
PDMS	8	13.77	3.76	27.283	1.33
PDCX	8	2.69	0.64	23.775	0.23
MDCX	8	1.70	0.27	16.140	0.10
PDS	8	13.97	5.54	39.625	1.96
DMAR	8	7.03	4.28	60.819	1.51
DDS	8	9.87	5.46	55.361	1.93
DAC	8	3.68	3.46	93.894	1.22
DECX	8	4.82	3.76	78.034	1.33
DES	8	4.77	3.53	74.125	1.25
DPMCX	8	5.05	2.41	47.799	0.85
DDMCX	8	3.39	0.91	26.860	0.32
DPMS	8	7.41	3.19	43.023	1.13
DMMS	8	9.84	4.03	40.970	1.43
DDMS	8	11.67	4.21	36.095	1.49
PERIOS	8	4.57	3.97	86.909	1.40
TOTAL	8	5.17	1.44	27.837	0.51
DDCX	8	2.65	0.35	13.208	0.12

ADULT DOG FEMORAL REGIONAL FLOW %TBF/%TW

VARIABLE	N	MEAN	STANDARD DEVIATION	C.V.	STD ERROR OF MEAN
PAC	10	0.121	0.117	96.800	0.037
FHECX	10	0.961	0.417	43.425	0.132
FHES	10	1.304	0.965	73.968	0.305
GTECX	10	0.461	0.195	42.335	0.062
GTES	10	0.587	0.190	32.289	0.060
FNMCX	10	1.127	0.254	22.581	0.080
GTMCX	10	0.675	0.207	30.715	0.066
ITMCX	10	0.608	0.183	30.104	0.058
PDMCX	10	0.456	0.108	23.717	0.034
FNMS	10	3.179	0.839	26.407	0.265
GTMS	10	2.248	0.475	21.122	0.150
ITMS	10	3.257	0.941	28.905	0.298
PDMS	10	3.234	0.851	26.321	0.269
LTCX	10	0.994	0.399	40.156	0.126
LTS	10	3.156	0.862	27.301	0.272
PDCX	10	0.465	0.228	48.958	0.072
MDCX	10	0.171	0.041	24.075	0.013
DDCX	10	0.189	0.044	23.133	0.014
PDS	10	2.508	0.699	27.859	0.221
DMAR	10	1.307	0.504	38.590	0.159
DDS	10	2.086	0.180	8.633	0.057
DAC	10	0.078	0.106	136.380	0.033
DECX	10	0.523	0.340	64.911	0.107
DES	10	0.322	0.127	39.408	0.040
DPMCX	10	0.355	0.122	34.362	0.039
DDMCX	10	0.259	0.065	25.107	0.021
DPOMS	10	0.679	0.097	14.340	0.031
DDOMS	10	0.811	0.309	38.118	0.098
DPCMS	10	1.706	0.514	30.159	0.163
DMCMS	10	1.975	0.565	28.603	0.179
DDCMS	10	1.986	0.462	23.276	0.146
PERIOS	10	0.299	0.220	73.767	0.070

Table 28

ADULT DOG TIBIAL REGIONAL FLOW %TBF/%IW

VARIABLE	N	MEAN	STANDARD DEVIATION	C.V.	STD ERROR OF MEAN
PAC	8	0.299	0.299	100.112	0.10
PECX	8	1.483	0.661	44.586	0.23
PES	8	1.274	0.214	16.837	0.07
TUBCX	8	0.754	0.309	40.992	0.10
TUBS	8	1.719	0.269	15.654	0.09
PPMCX	8	0.872	0.276	31.604	0.09
PDMCX	8	0.786	0.143	18.250	0.05
PPMS	8	2.282	0.269	11.794	0.09
PMMS	8	2.381	0.493	20.700	0.17
PDMS	8	2.724	0.706	25.928	0.25
PDCX	8	0.530	0.099	18.726	0.03
MDCX	8	0.342	0.076	22.322	0.02
DDCX	8	0.541	0.148	27.270	0.05
PDS	8	2.858	1.382	48.350	0.48
DMAR	8	1.363	0.835	61.275	0.29
DDS	8	1.963	1.210	61.668	0.42
DAC	8	0.638	0.434	68.002	0.15
DECX	8	0.862	0.442	51.239	0.15
DES	8	0.871	0.491	56.395	0.17
DPMCX	8	0.956	0.304	31.780	0.10
DDMCX	8	0.677	0.185	27.273	0.06
DPMS	8	1.422	0.478	33.613	0.16
DMMS	8	1.883	0.543	28.812	0.19
DDMS	8	2.307	0.834	36.128	0.29
PERIOS	8	0.836	0.680	81.370	0.24

Table29

99M TC-MDP UPTAKE IN BONE TISSUES %TC/%TW
AGE=2 BONE=1

VARIABLE	N	MEAN	STANDARD DEVIATION	C.V.	STD ERROR OF MEAN
CART	8	0.306	0.049	16.098	0.017
CORTEX	8	0.721	0.095	13.108	0.033
SPONG	8	1.275	0.051	3.978	0.018
MARROW	8	0.435	0.184	42.274	0.065
GP	8	2.538	0.305	12.035	0.108
----------	AGE=2	BONE=2	----------		
CART	8	0.445	0.027	6.104	0.010
CORTEX	8	0.685	0.035	5.134	0.012
SPONG	8	1.440	0.035	2.441	0.012
MARROW	8	0.236	0.057	24.153	0.020
GP	8	3.591	0.177	4.936	0.063
----------	AGE=3	BONE=1	----------		
CART	6	0.167	0.089	53.449	0.037
CORTEX	6	0.576	0.068	11.814	0.028
SPONG	6	1.566	0.137	8.754	0.056
MARROW	6	0.310	0.134	43.319	0.055
GP	0	.	.	.	.
----------	AGE=3	BONE=2	----------		
CART	4	0.263	0.051	19.298	0.025
CORTEX	4	0.759	0.094	12.350	0.047
SPONG	4	1.801	0.382	21.181	0.191
MARROW	4	0.332	0.077	23.284	0.039
GP	0	.	.	.	.

Table 29
(Cont.)

99M TC-MDP UPTAKE IN BONE TISSUES %TC/%TW
AGE=2

VARIABLE	N	MEAN	STANDARD DEVIATION	C.V.	STD ERROR OF MEAN
CART	16	0.375	0.081	21.630	0.020
CORTEX	16	0.703	0.071	10.153	0.018
SPONG	16	1.357	0.095	7.004	0.024
MARROW	16	0.336	0.167	49.750	0.042
GP	16	3.065	0.595	19.414	0.149
AGE=3					
CART	10	0.205	0.088	42.780	0.028
CORTEX	10	0.649	0.120	18.531	0.038
SPONG	10	1.660	0.271	16.352	0.086
MARROW	10	0.319	0.110	34.557	0.035
GP	0	.	.	.	.

Table 30

99M TC-MDP UPTAKE/BLOOD FLOW IN BONE TISSUES
AGE=2 BONE=1

VARIABLE	N	MEAN	STANDARD DEVIATION	C.V.	STD ERROR OF MEAN
CART	8	1.08	0.16	15.13	0.06
CORTEX	8	1.56	0.31	19.80	0.11
SPONG	8	1.07	0.04	3.92	0.01
MARROW	8	0.31	0.12	39.89	0.04
GP	8	2.94	0.42	14.22	0.15
---------- AGE=2 BONE=2 ----------					
CART	8	1.49	0.15	10.17	0.05
CORTEX	8	1.54	0.11	7.20	0.04
SPONG	8	1.06	0.06	5.22	0.02
MARROW	8	0.20	0.03	14.64	0.01
GP	8	3.65	0.88	24.19	0.31
---------- AGE=3 BONE=1 ----------					
CART	6	4.28	1.75	40.93	0.72
CORTEX	6	2.04	0.34	16.56	0.14
SPONG	6	1.02	0.02	2.43	0.01
MARROW	6	0.19	0.07	38.06	0.03
GP	0	.	.	.	.
---------- AGE=3 BONE=2 ----------					
CART	4	1.56	1.16	74.40	0.58
CORTEX	4	1.39	0.13	9.23	0.06
SPONG	4	0.94	0.15	16.35	0.08
MARROW	4	0.20	0.07	36.37	0.04
GP	0	.	.	.	.

Table 30
(Cont.)

99M TC-MDP UPTAKE/BLOOD FLOW IN BONE TISSUES
AGE=2

VARIABLE	N	MEAN	STANDARD DEVIATION	C.V.	STD ERROR OF MEAN
CART	16	1.29	0.26	20.41	0.07
CORTEX	16	1.55	0.22	14.47	0.06
SPONG	16	1.07	0.05	4.48	0.01
MARROW	16	0.26	0.10	40.83	0.03
GP	16	3.30	0.76	23.08	0.19
AGE=3					
CART	10	3.19	2.03	63.70	0.64
CORTEX	10	1.78	0.43	24.03	0.14
SPONG	10	0.99	0.10	10.15	0.03
MARROW	10	0.19	0.07	35.31	0.02
GP	0	.	.	.	.

Table 31

ADOLESCENT FEMORAL REGIONAL UPTAKE OF 99M TC-MDP %TC/%TW

VARIABLE	N	MEAN	STANDARD DEVIATION	C.V.	STD ERROR OF MEAN
FHEC	8	0.206	0.068	32.960	0.024
FHO2O	8	1.709	0.324	18.935	0.114
FHC2O	8	1.063	0.213	20.073	0.075
FHGP	8	2.634	0.474	18.006	0.168
GIEC	8	0.641	0.232	36.185	0.082
GIO2O	8	1.898	0.731	38.537	0.259
GIC2O	8	1.309	0.357	27.277	0.126
GIGP	8	3.331	2.227	66.841	0.787
LIEC	8	0.577	0.394	68.308	0.139
LI2O	8	1.024	0.073	7.082	0.026
LIGP	8	1.499	0.963	64.230	0.340
FNMCX	8	1.847	0.290	15.708	0.103
GIMCX	8	1.997	0.218	10.895	0.077
ITMCX	8	1.289	0.298	23.083	0.105
PDMCX	8	1.034	0.168	16.234	0.059
FNPMS	8	5.620	0.837	14.891	0.296
FNMPMS	8	1.200	0.329	27.392	0.116
GIPMS	8	5.722	2.038	35.618	0.721
GIMPMS	8	1.474	0.344	23.342	0.122
IIMS	8	1.102	0.031	2.791	0.011
PDMS	8	0.957	0.133	13.933	0.047
PDCX	8	0.489	0.101	20.659	0.036
MDCX	8	0.412	0.064	15.647	0.023
DDCX	8	0.465	0.104	22.300	0.037
PDMAR	8	0.525	0.242	46.138	0.086
MDMAR	8	0.272	0.138	50.813	0.049
DDMAR	8	0.670	0.245	36.529	0.087
DMEEC	8	0.237	0.075	31.594	0.027
DLEC	8	0.334	0.143	42.724	0.051
DMEO2O	8	1.239	0.033	2.680	0.012
DLO2O	8	1.121	0.039	3.495	0.014
DMEC2O	8	0.911	0.051	5.607	0.018
DLC2O	8	0.786	0.093	11.778	0.033
DGP	8	2.331	0.180	7.726	0.064
DPMCX	8	1.502	0.148	9.840	0.052
DDMCX	8	0.971	0.101	10.360	0.036
DPMS	8	5.894	1.772	30.066	0.627
DMPMS	8	1.039	0.410	39.466	0.145
DMDMS	8	0.911	0.270	29.664	0.096
DDMS	8	0.996	0.069	6.896	0.024
PERIOS	8	0.335	0.145	43.279	0.051

ADOLESCENT TIBIAL REGIONAL UPTAKE OF 99M TC-MDP %TC/%TW

VARIABLE	N	MEAN	STANDARD DEVIATION	C.V.	STD ERROR OF MEAN
PEC	8	0.395	0.048	12.167	0.017
PO2O	8	1.519	0.089	5.848	0.031
PC2O	8	1.203	0.235	19.497	0.083
PGP	8	4.109	0.337	8.207	0.119
TUBC	8	0.263	0.216	82.236	0.077
TUB2O	8	0.921	0.100	10.810	0.035
TUBFIB	8	1.585	0.388	24.453	0.137
TUBGP	8	1.637	0.418	25.531	0.148
CBETUB	8	0.841	0.424	50.446	0.150
PPMCX	8	2.190	0.342	15.613	0.121
PDMCX	8	1.273	0.306	24.035	0.108
PPMS	8	13.267	6.960	52.453	2.461
PMPMS	8	1.375	0.366	26.601	0.129
PMDMS	8	1.286	0.139	10.837	0.049
PDMS	8	1.132	0.071	6.251	0.025
PDCX	8	0.638	0.026	4.025	0.009
MDCX	8	0.477	0.054	11.398	0.019
DDCX	8	0.536	0.082	15.229	0.029
PDMAR	8	0.384	0.055	14.215	0.019
MDMAR	8	0.115	0.034	29.681	0.012
DDMAR	8	0.323	0.135	41.788	0.048
DEC	8	0.327	0.119	36.248	0.042
DO2O	8	0.716	0.193	26.947	0.068
DC2O	8	0.481	0.122	25.432	0.043
DGP	8	3.274	0.959	29.304	0.339
DPMCX	8	1.269	0.122	9.586	0.043
DDMCX	8	0.854	0.071	8.295	0.025
DPMS	8	5.766	3.004	52.099	1.062
DMPMS	8	0.857	0.119	13.911	0.042
DMDMS	8	1.020	0.322	31.580	0.114
DDMS	8	0.864	0.030	3.454	0.011
PERIOS	8	0.292	0.050	17.194	0.018

Table 33

ADULT FEMORAL REGIONAL UPTAKE OF 99M TC-MDP %TC/%TW

VARIABLE	N	MEAN	STANDARD DEVIATION	C.V.	STD ERROR OF MEAN
PAC	6	0.167	0.182	108.746	0.074
FHECX	6	1.858	1.461	78.622	0.596
FHES	6	2.966	1.142	38.509	0.466
GTECX	6	0.864	0.207	23.930	0.084
GTES	6	1.629	0.317	19.486	0.130
FNMCX	6	1.823	0.635	34.834	0.259
GTMCX	6	1.000	0.107	10.678	0.044
ITMCX	6	0.739	0.208	28.192	0.085
PDMCX	6	0.515	0.072	14.044	0.030
FNMS	6	3.139	0.703	22.399	0.287
GTMS	6	2.408	0.496	20.592	0.202
ITMS	6	2.072	0.400	19.304	0.163
PDMS	6	1.891	0.209	11.070	0.085
LTCX	6	0.908	0.140	15.405	0.057
LTS	6	2.010	0.158	7.875	0.065
PDCX	6	0.610	0.479	78.573	0.196
MDCX	6	0.326	0.063	19.253	0.026
DDCX	6	0.361	0.062	17.101	0.025
PDS	6	1.389	0.142	10.200	0.058
DMAR	6	0.310	0.134	43.319	0.055
DDS	6	1.109	0.334	30.144	0.136
DAC	6	0.145	0.019	13.081	0.008
DECX	6	0.749	0.134	17.825	0.055
DES	6	0.902	0.169	18.742	0.069
DPMCX	6	0.699	0.056	7.968	0.023
DDMCX	6	0.516	0.106	20.592	0.043
DPOMS	6	1.282	0.089	6.922	0.036
DDOMS	6	1.238	0.047	3.829	0.019
DPCMS	6	1.622	0.295	18.201	0.121
DMCMS	6	1.517	0.271	17.843	0.111
DDCMS	6	1.369	0.310	22.678	0.127
PERIOS	6	0.245	0.152	61.803	0.062

Table 34

ADULT TIBIAL REGIONAL UPTAKE OF 99M TC-MDP %TC/%TW

VARIABLE	N	MEAN	STANDARD DEVIATION	C.V.	STD ERROR OF MEAN
PAC	4	0.203	0.049	24.187	0.025
PECX	4	1.234	0.150	12.178	0.075
PES	4	1.758	0.448	25.471	0.224
TUBCX	4	0.848	0.057	6.745	0.029
TUBS	4	1.770	0.579	32.689	0.289
PPMCX	4	1.120	0.140	12.529	0.070
PDMCX	4	0.935	0.092	9.830	0.046
PPMS	4	2.319	0.244	10.507	0.122
PMMS	4	2.220	0.323	14.563	0.162
PDMS	4	2.297	0.480	20.897	0.240
PDCX	4	0.785	0.026	3.255	0.013
MDCX	4	0.643	0.116	18.094	0.058
DDCX	4	0.697	0.292	41.873	0.146
PDS	4	1.777	0.508	28.580	0.254
DMAR	4	0.332	0.077	23.284	0.039
DDS	4	1.237	0.449	36.338	0.225
DAC	4	0.450	0.190	42.072	0.095
DECX	4	0.825	0.153	18.595	0.077
DES	4	1.329	0.210	15.820	0.105
DPMCX	4	0.926	0.278	29.979	0.139
DDMCX	4	0.690	0.272	39.379	0.136
DPMS	4	1.777	0.239	13.452	0.120
DMMS	4	1.470	0.361	24.566	0.181
DDMS	4	1.189	0.833	70.017	0.416
PERIOS	4	0.394	0.222	56.259	0.111

Table 35

ADOLESCENT FEMORAL REGIONAL 99M TC-MDP UPTAKE/BLOOD FLOW

VARIABLE	N	MEAN	STANDARD DEVIATION	C.V.	STD ERROR OF MEAN
FHEC	8	0.88	0.18	20.00	0.06
FHO2O	8	1.11	0.16	14.80	0.06
FHC2O	8	1.47	0.13	8.73	0.05
FHGP	8	3.10	0.83	26.93	0.29
GTEC	6	1.22	0.34	28.17	0.12
GTO2O	8	1.63	0.47	28.96	0.17
GTC2O	8	1.60	0.56	34.82	0.20
GTGP	8	2.86	1.08	37.67	0.38
LTEC	8	0.98	0.91	92.50	0.32
LT2O	8	1.29	0.44	34.07	0.16
LTGP	8	1.26	0.89	70.81	0.32
FNMCX	8	3.20	1.00	31.34	0.35
GTMCX	8	2.68	0.58	21.80	0.21
ITMCX	8	1.79	0.41	22.70	0.14
PDMCX	8	1.47	0.36	24.44	0.13
FNPMS	8	1.25	0.23	18.42	0.08
FNMPMS	8	1.57	0.21	13.57	0.08
GTPMS	8	1.19	0.18	15.48	0.07
GTMPMS	8	1.89	0.67	35.51	0.24
ITMS	8	0.79	0.04	4.65	0.01
PDMS	8	0.63	0.05	7.73	0.02
PDCX	8	1.25	0.39	31.18	0.14
MDCX	8	1.12	0.18	15.98	0.06
DDCX	8	1.24	0.25	20.28	0.09
PDMAR	8	0.34	0.16	45.93	0.06
MDMAR	8	0.27	0.18	67.90	0.07
DDMAR	8	0.39	0.11	28.55	0.04
DMEEC	8	1.24	0.41	32.82	0.14
DLEC	8	1.35	0.54	39.62	0.19
DMEO2O	8	1.03	0.13	12.58	0.05
DLO2O	8	1.07	0.15	13.85	0.05
DMEC2O	8	0.87	0.11	12.96	0.04
DLC2O	8	1.03	0.18	17.50	0.06
DGP	8	3.36	0.96	28.60	0.34
DPMCX	8	2.87	1.30	45.48	0.46
DDMCX	8	2.10	0.74	35.13	0.26
DPMS	8	1.16	0.21	17.78	0.07
DMPMS	8	1.88	0.79	41.79	0.28
DMDMS	8	0.90	0.08	8.75	0.03
DDMS	8	0.89	0.12	16.69	0.04
PERIOS	8	0.56	0.20	34.78	0.07

Table 36

ADOLESCENT TIBIAL REGIONAL 99M TC-MLP UPTAKE/BLOOD FLOW

VARIABLE	N	MEAN	STANDARD DEVIATION	C.V.	STD ERROR OF MEAN
PEC	8	1.30	0.13	9.69	0.04
PC2O	8	0.91	0.07	7.28	0.02
PC2O	8	1.04	0.10	9.17	0.03
PGP	8	3.30	0.69	20.76	0.24
TUBC	8	1.20	1.31	109.35	0.46
TUB2O	8	1.13	0.30	26.84	0.11
TUBFIB	8	1.53	0.20	13.26	0.07
TUBGP	8	1.84	0.92	50.11	0.33
CBETUB	8	1.72	0.43	24.89	0.15
PPMCX	8	3.03	1.23	40.64	0.44
PDMCX	8	1.79	0.48	26.86	0.17
PPMS	8	1.15	0.09	8.04	0.03
PMPMS	8	1.49	0.27	17.80	0.09
PMDMS	8	0.77	0.12	15.53	0.04
PDMS	8	0.57	0.14	24.32	0.05
PDCX	8	1.30	0.18	13.64	0.06
MDCX	8	1.33	0.31	23.30	0.11
DDCX	8	1.35	0.40	30.03	0.14
PDMAR	8	0.17	0.02	11.44	0.01
MDMAR	8	0.24	0.03	13.68	0.01
DDMAR	8	0.23	0.09	41.46	0.03
DEC	8	4.24	2.73	64.34	0.97
DO2O	8	1.93	0.78	40.49	0.28
DC2O	8	2.58	1.39	54.10	0.49
DGP	8	6.87	5.38	78.35	1.90
DPMCX	8	2.56	0.54	21.06	0.19
DDMCX	8	1.96	0.35	18.02	0.12
DPMS	8	1.52	0.53	34.70	0.19
DMPMS	8	2.69	1.42	52.79	0.50
DMDMS	8	1.06	0.43	40.96	0.15
DDMS	8	0.61	0.10	15.72	0.03
PERIOS	8	0.61	0.39	63.10	0.14

Table 37

ADULT FEMORAL REGIONAL 99M TC-MDP UPTAKE/BLOOD FLOW

VARIABLE	N	MEAN	STANDARD DEVIATION	C.V.	STD ERROR OF MEAN
PAC	6	3.46	3.74	108.05	1.53
FHECX	6	1.99	0.54	26.85	0.22
FHES	6	1.83	0.46	25.01	0.19
GTECX	6	3.17	2.13	67.18	0.87
GTES	6	2.94	1.10	37.34	0.45
FNMCX	6	1.80	0.64	35.30	0.26
GTMCX	6	1.72	0.35	20.63	0.14
ITMCX	6	1.43	0.25	17.75	0.10
PDMCX	6	1.24	0.26	20.92	0.11
FNMS	6	0.93	0.12	13.43	0.05
GTMS	6	1.18	0.05	4.09	0.02
ITMS	6	0.58	0.10	17.52	0.04
PDMS	6	0.54	0.13	23.76	0.05
LTCX	6	1.18	0.64	54.35	0.26
LTS	6	0.71	0.16	22.44	0.07
PDCX	6	1.72	0.50	28.91	0.20
MDCX	6	2.25	0.70	31.28	0.29
DDCX	6	2.32	1.30	56.21	0.53
PDS	6	0.49	0.08	16.39	0.03
DMAR	6	0.19	0.07	38.06	0.03
DDS	6	0.51	0.11	22.09	0.05
DAC	6	9.71	10.26	105.68	4.19
DECX	6	3.61	2.62	72.53	1.07
DES	6	4.91	3.83	77.98	1.56
DPMCX	6	2.68	0.56	20.77	0.23
DDMCX	6	2.17	0.90	41.36	0.37
DPOMS	6	1.91	0.29	15.34	0.12
DDOMS	6	1.51	0.52	34.27	0.21
DPCMS	6	1.23	0.43	34.76	0.17
DMCMS	6	0.94	0.27	28.30	0.11
DDCMS	6	0.77	0.23	29.16	0.09
PERIOS	6	0.78	0.47	59.88	0.19

Table 38

ADULT TIBIAL REGIONAL 99M TC-MDP UPTAKE/BLOOD FLOW

VARIABLE	N	MEAN	STANDARD DEVIATION	C.V.	STD ERROR OF MEAN
PAC	4	1.670	0.933	55.880	0.467
PECX	4	1.385	0.237	17.132	0.119
PES	4	1.542	0.126	8.155	0.063
TUBCX	4	1.707	0.551	32.274	0.276
TUBS	4	1.085	0.227	20.889	0.113
PPMCX	4	1.805	0.232	12.838	0.116
PDMCX	4	1.335	0.117	8.768	0.059
PPMS	4	1.082	0.165	15.205	0.082
PMMS	4	1.072	0.270	25.139	0.135
PDMS	4	0.747	0.107	14.299	0.053
PDCX	4	1.515	0.323	21.297	0.161
MDCX	4	1.590	0.367	23.097	0.184
DDCX	4	1.132	0.396	34.998	0.198
PDS	4	0.477	0.062	12.952	0.031
DMAR	4	0.197	0.072	36.365	0.036
DDS	4	0.522	0.129	24.628	0.064
DAC	4	1.420	1.383	97.409	0.692
DECX	4	1.627	1.028	63.186	0.514
DES	4	3.072	3.271	106.463	1.636
DPMCX	4	1.092	0.264	24.129	0.132
DDMCX	4	0.907	0.219	24.132	0.109
DPMS	4	1.442	0.884	61.284	0.442
DMMS	4	0.752	0.123	16.397	0.062
DDMS	4	0.392	0.231	58.815	0.115
PERIOS	4	2.392	2.701	112.893	1.350

DISCUSSION

A. Microscphere Technique and Comparison to Previous Studies for Quantification of Regional Osseous Blood Flow

In summary, microspheres were used to quantitate regional osseous blood flow in three age groups of dogs: five day old (neonatal), four month old (immature), and dogs more than two years old (mature). Microspheres are the simpliest and most accurate method of quantitating osseous flow under physiological conditions in experimental animals. It is essential though to adhere to proper experimental technique. Fifteen μm microspheres were employed since previous experiments have shown that this is the smallest size appropriate for entrapment in bone with minimal shunting. A left artrial injection over a thirty second period assured even mixing and minimized temporal heterogenecity. Injections of 8.6×10^6 microspheres in the immature and mature dogs, and 2.15×10^6 microspheres in the neonate resulted in > 400 microspheres in the majority of bone regions, despite the fact that the bones were cut into numerous small regions.

Past experiments and methods of quantitating osseous flow were reviewed in the Background section. Table 2 summarizes the combined results of each technique in various species. The total bone blood flow in ml/min/100g for the tibia and femur combined are 20.2 and 11.8 for the immature and mature dogs, respectively. These results agree quite closely with the average of flow values obtained by measuring ^{85}Sr clearance (corrected for the extraction ratio not equal one) and by measuring ^{42}K or ^{86}Rb clearance. Although, as the data in Table 1 shows, other investigators have studied regional osseous flow or flow in different tissue types, no

prior experiments that have attempted to measure blood flow to regions as small as those in this study. This experiment provides the most detailed and precise quantification of regional osseous circulation to date. It also provides the first available data documenting flow in neonatal animals.

B. The Association Between Chondro-osseous Blood Flow and Osteogenesis

Our results, like those of previous studies (Niv and Hungerford, 1979; Pasternak et al, 1966; Whiteside et al, 1977), indicate that relative blood flow is greater in growing than mature bones. In the past, investigators have attempted to relate bone blood flow and osteogenesis. During the growth spurt, increased vascularity has been noted on both the E-side (epiphyseal) and M-side (metaphyseal) of the growth plate (Stockwell, 1979; Trueta, 1968). If flow to the physis is limited, either by compressing the vasculature with excessive unremitting pressure at the ends of the bone (Trueta and Trias, 1961) or by totally ablating the E-side vasculature (Trueta and Amato, 1960), growth ceases. Clinical conditions associated with overgrowth, such as fracture, chronic infection and tumor, are experimentally accompanied by increased total bone blood flow (Table 4). Ferguson (1933) proposes that these conditions divert flow from the nutrient arterial system to the epiphyseo-metaphyseal arteries on either side of the physis. If his proposition is true, it would indicate that chondro-osseous growth is, in part, regulated by vascular dynamics.

Blood flow is normally mediated by metabolic needs. Flow through bone tissue appears to be autoregulated, as is flow through other organs of the body (except the lungs). Vascular dilation occurs in response to the by-products of increased metabolism: low pH, excess carbon dioxide, and insufficient oxygen (Shim, 1968). Hence, intravascular administration

of lactic acid or a small amount of hydrochloric acid causes increased osseous blood flow (Shim, 1968).

Although blood flow is greater in immature bone than mature bone and greater in fractured bone than uninjured bone, the arteriovenous oxygen and carbon dioxide differences remain constant; this may indicate that increased chondro-osseous flow is an autoregulatory response to the increased metabolic needs of bone growth or repair. Flow is locally augmented in the osseous regions that contain a greater concentration of osteoblasts and presumably a heightened metabolic rate (Whiteside et al, 1977). It is thus understandable that flow rate is proportional to bone deposition, shown with tetracycline labelling (Sim and Kelly, 1970; Stadalnik et al, 1975). Blood flow may also respond to the metabolic demands of osteoclasts which carry out resorption. This relationship has been documented by the enhancement of flow, oxygen consumption and bone resorption that follow administration of parathyroid hormone, a substance known to stimulate osteoclast formation and activity (Boelkins et al, 1976; Sim and Kelly, 1970).

Growth does not proceed at a constant rate, the relative contribution of each physis to lower extremity elongation probably varies at different points in development and is species dependent (Ogden, 1979). In the human, for example, growth occurs at opposite ends of the fetal tibia and femur at equal rates (Brookes, 1972). After birth, however, the physes adjacent to the knee grow faster than the physes at opposite ends of the tibia and femur. The relative contribution of each physis to total growth in the human leg is as follows: proximal femur, 15%; distal femur, 35%; proximal tibia, 30%; distal tibia, 20% (Digby, 1916; Tachdjian, 1972).

Although growth rates of the physes in dog bones at various ages are unavailable, it may be that the relative rate of growth at each physis is proportional to the rate of blood flow in the adjacent pMS. All pMS flows in the neonatal tibia and femur were equivalent. It is quite possible that the rates of growth in the four ossification centers were equivalent or 25% apiece at five days. This is analogous to the situation in human fetal bones. The relative flow rates in the pMSs of our immature dogs were as follows: proximal femur, 23%; distal femur, 27%; proximal tibia, 39%; distal tibia, 12%. Based on this blood flow data, the most rapid growth in the lower extremity of four month old dogs may occur in the proximal tibia.

Another region whose blood flow may demonstrate a close correspondence to growth is the 1.5 mm of the spongiosa on the E-side of the growth plate. Past histological studies have demonstrated that the amount of vascularity in the region varies directly with growth rate (Stockwell, 1979), possibly more closely than the amount of M-side vascularity varies with growth rate. The present study did not speficically isolate this tissue for separate quantitative analysis.

C. Neonatal Regional Chondro-osseous Flow

Graphs 6 and 7 show that in the neonatal bone, flow to the pMS (1.5 mm of spongiosa on the M-side of the growth plate) greatly exceeds that to the remainder of the bone. For example, the proximal femoral MS constitutes approximately 7% of the total femoral weight, yet it receives more than 30% of the total blood flow to the bone. This bone region receives more flow than any other region sampled in the three age groups with an average of 187 ml/min/100g.

At birth there is no medullary hematopoiesis; thus, the metabolic demands of the neonatal bone are principally for growth and maintenance. During the postnatal period when the growth rate is highest substantial blood flow is required by the growth centers. This blood flow carries minerals for calcification and provides nutrients to support high level osteoblastic and osteoclastic activity. The substantial numbers of microspheres which localize in the juxtaphyseal region probably embolize the lodge in the M-side capillary loops. From the pMS capillaries, oxygen, minerals, and other nutrients diffuse to the growth plate (Stockwell, 1979; Trueta and Amato, 1960). The dMS region has less osteogenic activity so that a much lower flow rate than in the pMS is expected.

The neonatal age group is unique in that it is the only age group with a substantial documented flow in the cartilage. With their low sample weights, the mature and immature cartilage regions contain too few microspheres for accurate quantification of blood flow. The infant cartilage, however, receives approximately the same amount of blood flow as the cortex and marrow, an average of 23 cc/min/100g in both bones. Moreover, within each of the epiphyseal cartilage areas, flow to the inner central area is greater than flow to the outer area. The infant epiphyseal cartilage contains blood vessels in cartilage canals which are a few millimeters apart (Wilsman and Van Sickle, 1970). The vessels of these canals have glomerular-type endings in the central cartilage which coalesce at four days of age in the dog and come to resemble the dilated capillary loops of the metaphysis by six days (Wilsman and Van Sickle, 1970). As osteoid appears the following day, this is the site of incipient secondary ossification (Wilsman and Van Sickle, 1970). One would thus predict

that the five day old pups must have greater flow to the coalescing capillaries in the inner epiphyseal cartilage than to the more peripherally located outer epiphyseal cartilage.

It is possible that the flow values obtained for the neonatal bone studied may be somewhat above physiological values. Unlike the animals in the mature and immature groups, which were injected while conscious and standing, the neonatal animals were anesthetized with pentobarbitol at the time of injection. MacPherson and Tothill (1977) report that bone blood flow in rats was not affected by ether anesthesia. In an effort to determine the effect of anesthesia, we ran a pilot study in which we performed two injections of microspheres in adult dogs, the first while they were anesthetized with Suritol, a short-acting barbituate, and the second while they were awake and standing. With the exception of two regions, the diaphyseal marrow and proximal ES in the tibia of one dog, in which flow was reduced during anesthesia, there was no significant difference between the first and second injections. Our findings suggest that anesthesia did not affect bone blood flow, but they are not conclusive for they only involve two mature animals and only eight bones were studied.

D. Immature Regional Chondro-osseous Circulation

The immature animals are similar to the neonatal animals in that the pMSs have the highest amount of blood flow. The pMS is the same width in the immature animal, 1.5 mm, but flows are lower than in the same region in the neonatal animals with an average flow of 116 cc/min/100g. This is consistent with the greater growth rate at five days in the pup compared to that at four months of age.

While there is no significant difference in blood flow among the four pMS regions in the neonate, in the immature animal the rank order is significant and is as follows: proximal tibia > distal femur $\geq$ proximal femur > distal tibia. If the growth rate is proportional to blood flow, then at four months growth at the various growth plates would be expected to be unequal. As expected, the known greater osteogenic activity of the two growth centers near the knee seems to have led to greater blood flow rates.

As in the neonate, there is significantly less flow to the region of metaphyseal spongiosa adjacent to the pMS (mpMS). The pMS is a region of high growth while the mpMS is a relatively quiescent region.

High flow is associated not only with regions with high growth, but also regions with significant hematopoietic activity. Bone marrow becomes hematopoietic after three months of age in the human and probably much earlier in the dog. Hematopoiesis increases the metabolic demands of the marrow and local blood flow simultaneously increases (Van Dyke, 1967). Hematopoietic activity is pronounced in the femur (Van Dyke, 1967). Among the immature animal femoral tissues, the hematopoietic marrow receives the highest blood flow, exceeding even the effect of the rapidly growing pMS on total spongiosa flow. Thus, increased hematopoiesis will result in greater flow to those areas predominant in marrow tissue (Van Dyke, 1967).

Within each metaphysis, flow is lowest in the mpMS and increases as one approaches the diaphysis so that mpMS < mdMS < dMS. The ratio of soft hematopoietic marrow tissue to trabeculae also increases in this manner. Of the three metaphyseal regions analyzed, the dMS has the least

dense cancellous bone, resulting in the highest ratio of soft marrow tissue to bony trabeculae. Because marrow tissue receives more blood flow than mineralized bone, the flow to the dMS also must be highest. Conversely, the mpMS has the lowest soft marrow to trabeculae ratio, and accordingly, the lowest flow. The mdMS is intermediate in both.

Within each diaphysis in the immature tibia and femur, the peripheral red marrow (pDMar and dDMar) receives higher flow than in the central fatty marrow (mDMar), presumably due to greater hematopoietic activity in the red marrow. Hematopoiesis is much less active in the immature tibia than femur; accordingly, the mean flow to the diaphyseal marrow in the tibia is 17.7 as compared to 33.2 ml/min/100g in the femur. Nevertheless, hematopoiesis does seem to have an influence on regional circulation in the immature tibia, for blood flow to the marrow is not significantly less than flow to the spongiosa and is greater than the flow to the cortex.

Within each secondary ossification center, the peripheral areas receive more flow than the inner areas. Although this is the opposite of the neonatal pattern, this variation is an understandable result of growth dynamics. In the neonate, the secondary ossification center is on the verge of forming in the inner cartilage. At four months the secondary ossification center has developed to the extent that nearly all the epiphyseal cartilage has been replaced by bone. The secondary center of ossification expands outward towards the periphery of the epiphysis, with the spongiosa-cartilage junction being analogous to the M-side spongiosa-growth cartilage junctions in the primary ossification centers. Thus, in the immature group one would expect the o20, the epiphyseal

spongiosa adjacent to the cartilage, to have a higher blood flow rate than the c20, just as the pMS has higher flow than mpMS distal to the growth plate. The pMS and o20 are analogous areas in their respective ossification centers since each was 1.5 mm wide. The substantially higher flow to the pMS may reflect the higher rate of growth in the primary ossification centers, which provide bone elongation, as opposed to the secondary ossification centers, which are concerned with hemispherization.

The immature distal tibial epiphysis received less flow than any other epiphysis of the immature lower extremity. Almost all of the cartilage on the periphery of the spongiosa has been replaced by bone. Perhaps by four months of age, this secondary ossification center is approaching the limits of its growth so that its rate of growth is now slowed relative to both its former growth rate and the growth rate in the other secondary ossification centers of the lower extremity at four months. This might explain why blood flow to the distal tibial secondary ossification center is so low. Nevertheless, based on the above growth-circulation correlation theory, one may surmise that some growth is still occurring in the distal tibial epiphysis, for it too has o20 > c20. All of the lower extremity epiphyses undergo epiphyseodesis after eight months of age in the dog (Chapman, 1965; Hare, 1960).

There is a controversy over the existence of transphyseal blood vessels in the immature bone. A number of authors feel that these vessels do not exist (Bassett et al, 1969; Irving, 1964). On the other hand, Brookes (1972) finds them whenever the secondary ossification centers are expanding. Wang et al (1975) published some beautiful photographs of transphyseal vessels in immature bones and Ogden et al. (1975) reported

the presence of these vessels in the tibial tuberosity physis. Our experiments reveal significant blood flow in the immature growth plate with values ranging from 11 to 26 ml/min/100g. This flow could have been due to vessels within the growth plate or to contamination with the spongiosa on either side of the growth plate, the o2O and pMS.

We feel that contamination was minimal. A shearing force was applied to fracture the physis through the zone of hypertrophy which is above the level of the M-side vascular loops. When the growth cartilage was peeled away from the epiphyseal spongiosa, meticulous care was taken to avoid including any spongiosa or "red" cartilage in the "growth plate" tissue; the cleaned growth plates were all completely white or translucent. Moreover, the rank order of blood flow in the various growth plates does not mimic the order in either the adjacent pMSs or o2Os, making it more unlikely that the "physeal flow" was due to excess microsphere from one of the adjacent spongiosa regions.

Hence, there is an excellent likelihood that there is significant flow through discreet vessels within the well-developed growth plate of a four month old pup. These vessels could be transphyseal vessels as well as unusually long vascular loops extending into the physis from the adjacent epiphysis and metaphysis. This does not imply that the physis is solely nourished by these "intra-physeal" vessels. The microsphere data only reflects blood flow within blood vessels. The physis may receive nutrients that diffuse out of other nearby capillaries of the pMS or o2O regions.

In immature bone, cortical flow is less than physeal flow. In each bone, blood flow is highest to the proximal metaphyseal cortex, followed

by the distal metaphyseal cortex with the diaphyseal cortex receiving the least flow. The circulatory rate to each of the four major metaphyseal cortices the tibia and femur decreases with distal progression in the extremity, following the same trend as the four major metaphyseal spongiosa regions. One would expect the spongiosa and cortex to vary together since their circulation is intimately interconnected. In addition, the metaphyseal cortical vessels are, for the most part, former spongiosa vessels with bone laid down around them. In each metaphyseal cortical region, the part nearer the growth plate receives higher blood flow than the region further down the shaft. Ultimately, the diaphyseal cortex in the middle of the bone receives the least flow. This is consistent with the hypothesis that the cortex near the growth plate receives blood from the metaphyseal arteries that penetrate it. Previous experiments indicate that the metaphyseal arteries can only maintain the metaphyseal cortex, while the nutrient artery system supplies blood to both metaphyseal and diaphyseal cortices (Trueta, 1968).

One might try to attribute the higher flow in the adolescent pMCx to increased metabolic demands of remodeling and funnelization. However, there is remodeling throughout the cortex. The relative differences in flow between various regions of the immature cortex are not dissimilar to the relative differences in the mature cortex where funnelization is not occurring.

Flow to the periosteum in the immature animals varied directly with, though exceeding, blood flow to the cortex it surrounded. Since the capillary circulations of the two tissues are continuous, one would expect the cortex with a higher flow to be surrounded by a periosteum with a higher flow as in the femur.

E. Mature Regional Chondro-osseous Circulation

In the mature animal there is a much greater disparity between the femoral and tibial blood flow than in the younger age groups. The mature bones have reached their full size and apparently no longer require high blood flow to satisfy the high metabolic demands of osteogenesis. Although some bone remodeling continues throughout life, the principle metabolic activity of the lower extremity is hematapoiesis. The center of hematopoiesis in the dog is the femoral marrow, mostly in the proximal metaphyseal spongiosa which receives about 51 ml/min/100g of blood flow. Flows in the proximal diaphyseal spongiosa and GtMS are about 39 ml/min/100g and the spongiosa in the femoral diaphysis and central distal metaphysis receive blood flows of about 34 cc/min/100g. The blood flow rates correlate with the gross anatomical findings; all of these areas contain red marrow.

In contrast, the peripheral distal femoral metaphyseal spongiosa regions, poMS and doMS, are yellow-white with blood flows of only approximately 12 ml/min/100g. The metaphyseal and diaphyseal spongiosa of the tibia are of the same appearance and also have similar blood flows. The femoral mDMar appears fatty, but receives higher flow (20 ml/min/100g) than the neonatal femoral marrow and over twice as much flow as the mature tibial marrow, both known to have little hematopoietic activity. Blood flow throughout tibial spongiosa and marrow is relatively constant and low.

The proximal femoral epiphysis receives significantly higher flow than any other epiphyseal region in the mature animal and receives more flow than any region in the tibia. This same area also receives relatively

high flow in the other age groups. It has the highest flow of any adolescent secondary ossification center, and even as epiphyseal cartilage in the neonate it has the second highest flow among the neonatal epiphyses. Interestingly, it is the same region in the human which is so susceptible to aseptic necrosis.

Flows to the two mature epiphyses on either side of the knee joint are not significantly different. This is interesting since past experiments have shown that starch particles injected in the distal femoral epiphyses diffuse across the articular cartilage and into the joint faster than when the particles are injected into the proximal tibial epiphysis (Brookes, 1972). On the basis of our data, one cannot attribute this to the higher flow rates in the distal femur delivering the solute to the articular cartilage more quickly. Other factors beyond blood flow alone must be operant in modulating this diffusion process.

With the questionable exception of articular cartilage, the mature cortex receives less blood flow than any other tissue in the three age groups, including the immature epiphyseal cartilage. Since none of the mature epiphyseal cortices had significantly different flow from that of their enclosed epiphyseal spongiosas, the two regions need not be separated in future experiments of this type. The proximal femoral metaphyseal cortex has the highest cortical flow with flow to its adjoining spongiosa being highest of the medullary flow. In both bones, similar to the adolescent pup cortices, flow to the cortical shaft is highest at the extremities, the pMCx region. Blood flow decreases as the middle of the bone is approached with the mDCx having the lowest flow. Since the upper metaphysis probably receives more flow due to the penetrating metaphyseal

arteries, the higher flow in the proximal femoral cortex also may result from the continuous medullary and cortical circulations.

The mature cortex receives much lower flow than in the younger animals since it does not have significant growth requirements. It still needs circulation of blood for slow remodeling of the Haversian systems, for maintenance of blood-bone mineral equilibrium, and for fracture healing. Blood flow to the mature tibial diaphyseal cortex is extremely low, averaging 2.1 cc/min/100g. This is contrasted to the 3.5 value in the mature femur, or 6.2 and 18.6 cc/min/100g in the tibial diaphyseal cortices of immature and neonatal bone, respectively. Not surprisingly, the circulation in the middle and distal mature tibial cortex is sometimes not sufficient to adequately carry out fracture repair (Trueta, 1974). Thus, this bone section is more likely to be affected by delayed union or non-union. Healing also involves the medullary and periosteal circulatory systems and low blood flow through these two areas may also contribute to the vulnerability of the distal tibia to non-union. Experiments (Rhinelander, 1974) indicate that medullary circulation is the more important of the two since healing is slowed to a greater extent if medullary blood flow is compromised; the mature distal flow of 5-11 cc/min/100g is lower than in any other medullary area studied in this experiment. We did not find blood flow to the tibial periosteum to be significantly different than that to the femoral periosteum. However, both mature animal periostea receive about half as much flow as the immature animal periostea. The latter, with its higher rate of blood flow, is much more reactive, thereby contributing to faster fracture healing in youth.

F. Blood Supply and Age

Experiments concerned with the changes of osseous circulation with age consistently prove that flow to mature bone is lower than that to immature bone (Brookes, 1975; Hruza and Wachtlova, 1969, MacPherson and Tothill, 1977). Immature bone has greater bone turnover, greater number of osteoblasts, and greater oxygen consumption. Injured bone heals faster and more completely in the immature animals. Osseous flow in adult rats of 11 months is half of that in immature 10 week old rats, and flow rates are halved again in senescense (MacPherson and Tothill, 1977). Flow steadily drops from 20 ml/min/100g in 8 week old rats to only 2 ml/min/100g in senescent animals (Brookes, 1975). The decrease in flow in rat bones with aging is associated with a decrease in cortical capillary density (Hruza and Wachtlova, 1969). No prior studies have documented regional developmental changes in blood supply.

In our study, the neonatal bones have the highest blood flow rates followed by the immature bones, and then the mature bones. Just after birth, bone growth rate or doubling time is maximal. The rate of growth is still high but not quite so great in the immature stage. This high neonatal growth rate mostly affects the spongiosa (Graphs 1-3) or the metaphyseal spongiosa (Graphs 4-7) flow since all the neonatal spongiosa is metaphyseal.

The differences in blood flow to the cortex tissue among the three ages is also probably primarily a result of growth activity. All cortices are involved in mineral storage and homeostasis. All cortical regions undergo some remodeling, though growth and remodeling activities are maximal in the neonate. In the neonate, sequential layers of bone are laid inside the cylinders or the tunnels of the peripheral metaphyseal

spongiosa to create cortical haversial canals. Secondly, the metaphyseal cortex is converted into diaphyseal cortex by the process of resorptive funnelization. In addition, the whole diaphyseal cortex undergoes periosteal addition and endosteal resorption so that the diameter and thickness of the bone are increasing. This high bone turnover is logically associated with considerable blood flow. With age, the rate of bone turnover decreases until adulthood where a baseline remodeling function is maintained. Hence, less blood to the cortical tissue is required in the immature followed by the mature animal.

Neonatal cartilage receives much higher blood flow than both the immature and mature cartilage. This is probably because the neonatal cartilage has numerous cartilage canals containing blood vessels. The number of canals, and thus cartilage blood flow, decreases with age. They have disappeared by adulthood (Stockwell, 1979). Only a few long vascular loops stemming from the subchondral vessels extend up into the uncalcified layer of articular cartilage in the adult (Trueta, 1968). These loops probably trap the miniscule number of microspheres that we found in the adult articular cartilage.

The one neonatal region which does not have the highest blood flow amongst the three age groups is the soft femoral diaphyseal marrow. This is not surprising since the neonatal marrow is not hematopoietic. The immature and mature circulations undergo an autoregulatory response to meet the nutritional demands of hematopoiesis (Trueta, 1968). There is less hematopoiesis in the marrow of the tibia, perhaps none in the adult tibia; thus, interestingly, the normal order of blood flow (infant >

adolescent > adult) persists in the tibial diaphyseal marrow.

Since hematopoiesis in the lower extremity of the adult is concentrated in the proximal femoral metaphyseal spongiosa and pDS while it is more widely dispersed in the adolescent (Root, 1963), flow to the proximal femoral metaphyseal spongiosa is greater in the adult than the adolescent. Apparently the hematopoietic metabolic needs of the adult proximal femur supercede the combined osteogenic and hematopoietic flow demands in this same area of immature femur. Hence, in Graph 4 the flows to the mature DMar and immature DMar are not significantly different. On the other hand, the very rapid growth rate in neonatal bone boosts the required blood flow giving the neonatal age the highest flow in the proximal femoral metaphysis.

In the nine region graphs comparing the three age groups, there are four other areas in addition to the femoral marrow where the neonate does not have significantly greater flow than the immature animal. These are the three most proximal epiphyses and the greater trochanteric region. In these regions, the neonatal epiphyseal cartilage is compared to the immature expanding secondary ossification centers plus a small amount of cartilage. The anaerobic metabolism of resting cartilage has much lower nutritional demands than resting bone (Fitzgerald, 1961); thus, one might surmise that the neonatal epiphyseal growth rate is relatively higher than that of the immature animal since flow to neonatal cartilage and immature spongiosa are nearly the same.

G. Osseous Blood Flow Related to Acute Hematogenous Osteomyelitis

The various factors affecting the localization of infection in acute hematogenous osteomyelitis, as discussed earlier are (1) delivery determined by blood flow; (2) colonization, favored by local slowing of blood

in the sinusoids; and (3) clearance determined by the local activity of the immunological defense system. Our flow data demonstrates that one would most expect hematogenously disseminated infection to start in the metaphysis just under the growth plate, the pMS, in the neonate and the immature animal, for the highest rate of delivery would be to this region.

Previous studies in this lab on experimental hematogenous osteomyelitis in the immature animal demonstrate that the bacteria tend to localize first in the metaphyseal region immediately adjacent to the growth plate; later the injection spread towards the diaphysis. The M-side vascular loops have an anatomical configuration which should favor colonization. However, there are also vascular loops or tufts in the growing epiphysis, and the epiphyseal sinusoids are wider than in the metaphysis, perhaps making flow dynamics more favorable for colonization in the epiphysis than in the metaphysis. If one considers this contention and the fact that the amount of blood delivery to the epiphysis versus metaphysis is not very different, one wonders why there would not be more frequent primary injection in the epiphysis. The ratio of epiphyseal-to-metaphyseal blood flow is about 1:1.5 in the immature distal femur and proximal tibia, the most common sites of infection. Although total epiphyseal and metaphyseal spongiosa blood flows are not very different, there is a vast difference in the flow to the pMSs and o2Os. Both regions favor colonization due to abrupt increases in vessel diameter and consequent slowing of blood flow. Of these two areas, the pMS with its higher flow rate has the greater bacterial delivery. The various pMSs, going from proximal femur to distal tibia, receive 4.2, 4.4, 6.9, and 9.2 times as much blood flow as the o2Os on the opposite side of the growth plate. Hence, blood flow may become the rate limiting

step allowing greater bacterial accumulation in the metaphyseal spongiosa.

Hobo (1921) noted that early in the development of experimental osteomyelitis, bacteria located in the diaphysis are cleared while bacteria in the metaphysis under the growth plate are not cleared (Hobo, 1921). In our preliminary experiments, the bacteria in the central epiphysis are cleared within one-half hour. However, the bacteria stays in the metaphysis. Hobo attributed the clearance in the diaphysis to a relatively more active immune system. There also may be a more effective immune system in the epiphysis. On the other hand, localization of the disease can be explained even if there is no regional difference in the competance of the immune system. Bacteria are delivered to all areas of the immature bone in proportion to blood flow, the highest delivery being to the pMS, then the dMS and diaphyseal marrow, and finally the o2Os. Of these areas, the pMS and o2O have the most favorable vascular hemodynamics for colonization. But since there are 4.4 to 9 times as many bacteria initially delivered to the pMS, the pMS is much more likely to reach the threshold concentration of 10^5 bacteria needed for sustained infection if the immune systems are equivalent. Obviously, studies are needed to define the immunologic capabilities of various regions of bone.

H. Skeletal Metastases

Most skeletal metastases are found in the red marrow (Fitzgerald, 1961). It has been proposed that perhaps hematopoietic marrow is a more favorable environment for tumor growth than other bone tissues (Van Dyke, 1967). Alternatively, the proximal femur may receive a relatively

high number of metastases because the metastases travel through the vertebral venous plexus. While either of these proposals may be operant, our studies suggest that in the adult the osseous area in the lower limb receiving the most blood flow is the hematopoietic marrow of the proximal femoral metaphysis and diaphysis. Thus, the localization of skeletal metastases in the proximal femur could be solely attributed to the high rate of delivery of tumor emboli in the blood stream to that area with arteriolar entrapment and a favorable environment for localization and growth. Studies correlating regional bone localization of metastases to the regional bone blood flow may be profitable in the future.

I. Effects of Illness on One Immature Pup

As noted in the Materials and Methods section, prior to surgery one of the immature animals was ill and was not eating. Although he was apparently well by the time of surgery, his bones were excluded from the composite results. The data is included in the Appendix as "Adolescent Pup #4". It is interesting to note that the distribution pattern of osseous blood flow to this pup's bones is different from that in the other immature bones. In all four bones, this adolescent pup had much higher than the mean flow in all regions of the bone medulla except the growth plates and pMSs. These two regions received less than average flow. Blood flow to the cortical and cartilaginous regions were consistent with those of the other animals. Although it is impossible to draw any conclusions from a single animal, two possible implications of these findings are interesting. The first is that marrow flow apparently increased secondary to increased marrow activity in response to the

illness. The area with the most dramatic increase in blood flow compared to that in the other animals is in the femoral diaphyseal marrow, the most hematopoietically active region of the lower extremity. Thus, when the body responds to infection with increased hematopoiesis, blood flow increases to all areas of the marrow, especially the femoral diaphyseal marrow. Secondly, with the exception of the left distal tibia, flow to each growth plate and adjacent metaphyseal spongiosa decreases; this occurred despite an increase in flow beyond the mean value in the remainder of metaphysis including the mpMS. It is possible that this pup's illness caused a temporary arrest in growth. "In children during periods of illness or starvation there is a failure of cartilaginous growth and longitudinal columns are not formed; osteoblasts, however, continue to manufacture osseous tissue and the newly formed bone accumulates, depicted as radiopaque transverse striations in the roentgenogram" (Tachdjain, 1979).

J. Factors Determining Uptake of ^{99m}Technetium-Methylene Diphosphate

The second part of this study examines the regional osseous distribution of ^{99m}Technetium-methylene diphosphate, the most ideal clinical agent for bone scanning of those presently known. The animals were sacrificed three hours after intravenous ^{99m}Tc-MDP injection, so that the results are equivalent to late phase scans which depict tracer uptake rather than blood flow. The dot densiograms of %Tc-MDP/%TW (Figures 24 and 25) closely resemble negatives of the actual bone scans.

The distribution of regional osseous %Tc-MDP uptake/%TW and %TBF/%TW are fairly similar. Thus, in the adolescent bones the highest %Tc-MDP/%TW is in the pMS. In the adult lower extremity, the most %Tc-MDP/%TW goes

to the proximal femur. However, the ^{99m}Tc-MDP has greater affinity for certain regions of bone than for others. Dividing %^{99m}Tc-MDP by % blood flow tends to cancel out the role that blood flow plays in distributing the tracer to the tissue, thereby showing the relative affinity of Tc-MDP for that particular region or tissue.

Osseous Tissues. The order of %Tc-MDP/%TW and %TBF/%TW for the three of the five tissue types is the same with spongiosa, cortex, and cartilage appearing in the same decreasing order. Thus, the ratio of Tc-MDP-to-flow is near unity for these three tissues, with the exception of the adult articular cartilage. The adult cartilage values, however, are unreliable since these specimens contained too few microspheres to be statistically significant.

The growth plate region clearly has the highest affinity for Tc-MDP of all the tissues studied. The growth plate cartilage is undergoing calcification and ossification, and thus has a high adsorption of PO_4^{--}, or its analogue, ^{99m}Tc-MDP. This uptake maintains the diffusion gradient necessary for substantial accumulation.

The rate of delivery of Tc-99m MDP to the physis is probably augmented by the high flow of the adjacent metaphysis. The metaphyseal tracer may diffuse to the calcifying cartilage of the growth plate. It has been shown that calcification of physeal cartilage is dependent upon intact metaphyseal vessels (Trueta and Amato, 1960).

The cortex, cartilage, and spongiosa have somewhat less affinity than the growth plate. The adolescent cartilage has only slightly lower affinity for Tc-99m MPD than the cortex. This is surprising since the cortex has so much more hydroxyapatite crystal and PO_4^{--} available for

exchange. But the differentiating hyaline cartilage of the immature animal is undergoing extensive calcification preparatory to expansion of the ossification center, thereby accumulating calcium, phosphate, and phosphate analogues.

Cortical bone has higher Tc-MDP affinity than spongiosa, apparently because there is a higher amount of bone mineral surface in contact with the capillaries. The diphosphate binds sites on the hydroxapatite crystal in exchange for inorganic phosphate. Spongiosa might be considered a mixture of bone and marrow. There is almost no uptake of Tc-MDP in marrow because there is no hydroxapatite crystal for the tracer to bind. Hence, affinity of Tc-MDP is high for the cortex, low for marrow, and intermediate for spongiosa. Within the spongiosa, as the proportion of marrow relative to osseous trabeculae increases, affinity of Tc-MDP decreases.

Mature Animals. Among the various regions of the adult bones, the rank order for %Tc-99m MDP uptake/%blood flow is ES, Cortex (ECx $\geq$ MCx $\geq$ DCx) > MS(pMS $\geq$ mMS $\geq$ dMS) > DS > Periosteum > DMar. The marrow and periosteum, both being soft tissues containing little hydroxyapatite, have the lowest affinity for Tc-MDP. Tracer affinity for the spongiosa regions is highest in the proximal and distal ends of the bone and decreases as one approaches the central marrow. This is quite reasonable since the ratio of bony trabeculae to marrow decreases towards the center of the bone. In other words, within the bone medulla, the PS product at the blood-bone interface is highest at the ends of the bone and lowest in the middle. The gross anatomy correlated well with this. The diaphyseal spongiosa contained relatively little trabecular bone,

and thus smaller amounts of bone mineral. The affinity of metaphyseal bone was intermediate between diaphyseal and epiphyseal affinity. The central portion of the distal femoral metaphyseal spongiosa was of softer tissue and had higher Tc-MDP/flow than the outer or peripheral portion. The epiphyses were extremely hard and dense and contained a high proportion of trabecular bone. Indeed, the affinity of the tracers for this cancellous bone was not statistically different from cortical bone. There was almost no significant difference in tracer affinity among any of the cortical regions in each adult bone.

Skeletally Immature Animals. The relative affinity of Tc-99m MDP for various bone regions in the skeletally immature animals were generally similar to equivalent regions in the mature animals. However, the skeletally immature bones were divided into a greater number of regions than the adult bones. The skeletally immature animal has a growth plate; the very high affinity of tracer for the physeal region is discussed above.

The mature animal's metaphyseal spongiosa region closest to the epiphysis was equivalent to two of the various subdivisions in the skeletally immature metaphysis. The smaller of these two subdivisions, the 1.5 mm of spongiosa abutting on the physis (pMS), contained the capillary loops of the nutrient arterial system. The pMS regions have higher blood flow and higher Tc-99m MDP uptake than any other area in the bone. Here, osteoblasts are forming osteoid on the remnants of the already calcified cartilage matrix, a process requiring a great deal of metabolic energy. Osteoid becomes mineralized with Ca^{++} and PO_4^{--} or ^{99m}Tc-MDP. The constant formation of hydroxyapatite crystals using

^{99m}Tc-MDP from the bone interstitial fluid maintains a concentration gradient between the blood and interstitial fluid that allows continuous ^{99m}Tc-MDP uptake.

The second of the two skeletally immature metaphyseal subdivisions, the mpMS, has higher affinity for Tc-99m MDP than any of the other cancellous bone regions. There is also active mineralization in this region of metaphysis, but ratio of mineralization-to-osteoid formation is probably higher than in the 1.5 mm pMS abutting on the physis, and thus the ratio of ^{99m}Tc-MDP uptake/blood flow is higher. The rest of the metaphyseal spongiosa, where primary ossification and mineralization has already occurred, has a lower rate of extraction of ^{99m}Tc-MDP. As in each adult metaphysis, tracer affinity is lowest in the subdivision adjacent to the diaphysis (dMS) which contains a high ratio of marrow-to-bony trabeculae.

The secondary ossification centers in skeletally immature animals were divided into a 1.5 mm thick outer sphere abutting on cartilage (o20) and a central core (c20). The outer and central epiphyseal spongiosa regions are analogous respectively to the 1.5 mm of metaphysis abutting on the physis (pMS) and the adjacent metaphyseal subdivision (mpMS). The Tc-MDP extraction is higher in the central region than the outer epiphyseal regions for probably the same reasons as in the analogous metaphyseal regions.

Although there is little difference in affinity of Tc-99m MDP among the various cortical regions in the mature animal, in the immature animals cortical affinity is highest in the metaphyseal cortex nearest the growth plate, where there is the most remodeling. The metaphyseal cortex

is being formed as concentric layers of bone are laid down inside each tunnel or cylinder housing a vertical vascular loop. The cortex so formed is remodelled into a narrower cylinder as it undergoes funnelization. Remodelling and growth cause an increase in blood flow, but the ^{99m}Tc-MDP uptake increases to an even greater extent. This is probably because the newly formed bone has smaller hydroxyapatite crystals than older bone and thus new bone has a greater surface area and a number of available phosphate binding sites (Termine and Posner, 1967).

In summary, in the mature animal bones, affinity of Tc-99m MDP is highest in the cortex, which has the most bone mineral for exchange, and lowest in soft marrow where there is little hydroxyapatite crystal. Tracer affinity is intermediate in the adult spongiosa, within which the affinity generally increases as the ratio of bony trabeculae-to-marrow increases. The skeletally immature bone is similar to the mature, but uptake of Tc-99m MPD is further increased in areas of active mineralization, which presumably have increased availability of phosphate binding sites (Brookes, 1967). The area of greatest affinity is the calcifying cartilage of the adolescent growth plate. Cortical affinity is highest in the areas with the most remodelling. The region of metaphyseal spongiosa with the highest affinity is that removed from the physis by at least 1.5 mm, where newly formed osteoid is undergoing mineralization.

K. Clinical Applicability

In this series of investigations each bone has been divided into many regions. For each of these regions we have measured absolute blood flow in cc/min/100g and %^{99m}Tc-MDP uptake/%total weight. The normal regional distribution of ^{99m}Tc-MDP uptake throughout the whole bone has been measured as well. This might be useful clinically. If a gamma camera were coupled to an appropriate computer it might be possible to compare the relative regional distribution in a patient's bones to normal ^{99m}Tc-MDP distribution data. The computer could provide a more sensitive indicator of variations from the norm than the human eye. "Hot spots" that are now missed might be more easily detected if the computer were able to distinguish cortical and cancellous representation.

It might then be possible to reconstruct regional blood flow projections on the basis of the documented extent of local correlation between Tc distribution, and blood flow. Such estimates might prove helpful in the management of a child with synovitis or a caisson with equivocal hip symptoms.

A more direct quantitative representation of osseous blood flow might also affect the management of many fracture situations in which flow is critical to healing.

REFERENCES

1. Azuma, H. (1964): Intraosseous Pressure as a Measure of Hemodynamic Changes in Bone Marrow. Angiology, 12:230.

2. Barnes, D.W.H., Bishop, M., Harrison, G.E. and Sutton, A. (1961): Comparison of the Plasma Concentration and Urinary Excretion of Strontium and Calcium in Man. Internat. J. Rad. Bio., 3:637.

3. Bassett, F.H., Wilson, J.W., Allen, B.L. and Azuma, H. (1969): Normal Vascular Anatomy of the Head of the Femur in Puppies with Emphasis on the Inferior Retinacular Vessels. J. Bone Joint Surg., 51-A:1139.

4. Bateson, Q.V. (1940). Function of Vertebral Veins and Their Role in the Spread of Metastases. Ann. Surg., 112:138.

5. Beekman, F. (1928): Acute Hematogenous Osteomyelitis, the Relationship of Its Pathology to Prognosis and Treatment. Annals of Surgery, August, p. 270.

6. Bell, E.G. (1972): Nuclear Medicine and Skeletal Disease. Hosp. Practice, August, p. 49.

7. Bell, E.G. and Subramanian, G. (1979): The Skeleton, Chapter 3 in Textbook of Nuclear Medicine: Clinical Applications, Ed. by Rocha, A.F.G. and Harbert, J.C., Lea & Febiger, Philadelphia.

8. Belliveau, R.E. and Spencer, R.P. (1975): Incidence and Sites of Bone Lesions Detected by ^{99m}Tc-Polyphosphate Scans in Patients with Tumors. Cancer, 36:359.

9. Bertino, J.R. (1977): Principles of Neoplasia, in Harrison's Principles of Internal Medicine, 8th Edition, Ed. Thorn, G.W., Adams, R.D., Braunwald, E., Isselbacherk, J. and Petersdorf, R.G., McGraw-Hill Book Co., New York, p. 1731.

10. Bloom, W. and Fawcett, D.W. (1962): A Textbook of Histology, 10th Edition, W.B. Saunders Co., Philadelphia.

11. Bloomthal, E.D., Olsen, W.H. and Necheles, H. (1952): Studies on Bone Marrow Cavity of the Dog. Fat Embolism and Marrow Pressure. Surg. Gyn. Obs., 94:215.

12. Boelkins, J.N., Mazurkiewicz, M., Mazur, P.E. and Mueller, W.J. (1976): Changes in Blood Flow to Bones During the Hypocalcemic and Hypercalcemic Phases of the Response to Parathyroid Hormone. Endocin., 98:403.

13. Borgsmiller, W.K., Whiteside, L.A., Goldsand, E.M. and Lange, D.R. (1980): Effect of Hydrostatic Pressure in the Hip Joint on Proximal Femoral Epiphyseal and Metaphyseal Blood Flow. Abstract, 26th Annual Orthopaedic Research Society Meeting, Atlanta, Georgia, p. 23.

14. Bouch, W.J. (1969): Plasma ^{45}Ca Clearance by the Tibia in the Immature Dog. Am. J. Physiol., 216:1150.

15. Branemark, P.J. (1959): Vital Microscopy of the Bone Marrow in the Rabbit. Scand. J. Clin. Lab. Inves., 38:1.

16. Brookes, M. (1967): Blood Flow Rates in Compact and Cancellous Bone and Bone Marrow. J. Anat., 101:553.

17. Brookes, M. (1968): A Measurement of the Rates of Blood Flow Circulating Red Cell Volume and Velocity in Bone Marrow and Cortex. Acta Anat., 69:201.

18. Brookes, M. (1970): Arteriolar Blockade: A Method of Measuring Blood Flow Rates in the Skeleton. J. Anat., 106:557.

19. Brookes, M. (1972): Venous Shunt in Bone After Ligation of the Femoral Vein. Surg. Gyn. and Obs., 135:85.

20. Brookes, M. (1972): The Blood Supply of Bone. An Approach to Bone Biology, Butterworths, London.

21. Brookes, M. (1974): Approaches to Non-invasive Blood Flow Measurement in Bone. Biomed. Eng., August, p. 342.

22. Brookes, M. (1975): Bone Growth and Circulation. Br. J. Rad., 48:71.

23. Brookes, M., et al (1961): A New Concept of Capillary Circulation in Bone Cortex. Lancet, May, p. 1078.

24. Buckberg, G.D., Luck, J.C., Payne, B., Hoffman, J.I.E., Archie, J.P. and Fixler, D.E. (1971): Some Sources of Error in Measuring Regional Blood Flow with Radioactive Microspheres. J. Appl. Physiol., 31:598.

25. Brookes, M. and Harrison, R.C. (1957): The Vascularization of the Rabbit Femur and Tibiofibula. J. of Anatomy, 91:61.

26. Chapman, W.L. (1965): Appearance of Ossification Centers and Epiphyseal Closures as Determined by Radiographic Techniques. J.A.V.M.A., 147:138.

27. Chung, S.M.K. (1976): The Arterial Supply of the Developing Proximal End of the Human Femur. J. Bone Joint Surg., 58-A:961.

28. Copp, D.H. and Shim, S.S. (1964): Quantitative Studies of Bone Blood Flow in Dogs and Rabbits. J. Bone Joint Surg., 46-B:781.

29. Copp, D.H. (1957): Seminar on Bone Disease: Calcium and Phosphorus Metabolism. Am. J. Med., 22:275.

30. Copp, D.H. and Shim, S.S. (1965): Extraction Ratio and Bone Clearance of Sr^{85} as a Measure of Effective Bone Blood Flow. Circ. Res., 16:461.

31. Cofield, R.H., Bassingthweighte, J.B. and Kelly, P.J. (1970): Sr^{85} Extraction and Clearance and Bone Blood Flow. Surg. Forum, 21:481.

32. Crelin, E.D. and Koch, W.E. (1967): An Autoradiographic Study of Chondrocyte Transformation Into Chondroclasts and Osteocytes During Bone Formation In Vitro. Anat. Rec., 158:473.

33. Cumming, J.D. (1962): A Study of Blood Flow Through Bone Marrow by a Method of Venous Effluent Collection. J. Physiol., 162:13.

34. D'Ambrosia, R.D., Riggans, R.S., Stadalnik, R.C. and DeNardo, G.L. (1976): Vascularity of the Femoral Head - ^{99m}Tc Diphosphonate Scintigraphy Validated with Tetracycline Labeling. Clin. Orthop. Rel. Res., 121:143.

35. Dale, C.G. and Harris, W.R. (1958): Prognosis of Epiphyseal Separation: An Experimental Study. J. Bone Joint Surg., 40-B:116.

36. Davies, D.R., Bassingthwaighte, J.B. and Kelly, P.J. (1976): Transcapillary Exchange of Strontium and Sucrose in Canine Tibia. J. Appl. Physiol., 40:17.

37. Delaney, J.P. and Grim, E. (1964): Canine Gastric Blood Flow and Its Distribution. Am. J. Physiol., 207:1195.

38. Deysine, M., Rafkin, H., Russel, R., Teider, I. and Aufses, A.H. (1975): The Detection of Acute Experimental Osteomyelitis with ^{67}Ga Citrate Scannings. Surg., Gyn. and Obs., 141:40.

39. Deysine, M., Robinson, R., Rafkin, H., Teicher, I., Silver, L. and Sufses, A.H. (1974): Clinical Infections Detected by ^{67}Ga Scanning. Ann. Surg., 180:897.

40. Dickerson, R.C. (1966): The Diversion of Arterial Blood to Growing Bone. Surg., Gyn. and Obs., July, p. 103.

41. Digby, K.H. (1916): The Measurement of Diaphyseal Growth in Proximal and Distal Directions. J. Anat. Physiol., 50:187.

42. Drinker, C.K., Drinker, K.R. and Lund, C.C. (1922): Circulation in the Mammalian Bone Marrow. Am. J. Physiol., 62:1.

43. Eisenstein, R., Sorgente, N., Soble, L.W. et al (1973): The Resistance of Certain Tissues to Invasion: Penetrability of Explanted Tissues by Vascularized Mesenchymes. Am. J. Pathology, 73:765.

44a. Edholm, O.G., Howarth, S. and McMichael, J. (1945): Heart Failure and Bone Blood Flow in Osteitis Deformans. Clin. Sci., 5:249.

44b. Falsetti, H.L., Carroll, R.J. and Marcus, M.L. (1975): Temporal Heterogeneity of Myocardial Blood Flow in Anesthetized Dogs. Circulation 52:848.

45. Feigin, D.S., Strauss, H.W., and James, A.E. (1976): The Bone Marrow Scan in Experimental Osteomyelitis. Skeletal Radiol., 1:103.

46. Felix, R. and Fleish, H. (1976): The Role of Matrix Vesicles in Calcification. Calc. Tiss. Res., Suppl. 21:344.

47. Ferguson, A.B. (1933): Surgical Stimulation of Bone Growth by a New Procedure. J.A.M.A., 100:26.

48. Fitzgerald, T.C. (1961): Blood Supply of the Head of the Canine Femur. Vet. Med., 56:389.

49. Folkow, B. (1952): A Critical Study of Some Methods Used in Investigations on the Blood Circulation. Acta Physiol. Scand., 27:118.

50. Frederickson, J.M., Honour, A.J. and Copp, D.H. (1955): Measurement of Initial Bone Clearance of Ca^{45} From Blood in the Rat. Fed. Proc., 14:19.

51. Galasko, C.S.B. (1975): The Pathological Basis for Skeletal Scintigraphy. J. Bone Joint Surg., 57-B:353.

52. Garnett, E.S., Bowen, B.M., Coates, G. and Nahmics, C. (1975): An Analysis of Factors Which Influence the Local Accumulation of Bone-Seeking Radiopharmaceuticals. Inves. Radiology, 10:564.

53. Genant, H.K., Bautovich, G.J., Singh, M., Lathrop, K.A. and Harper, P.V. (1974). Bone Seeking Radionucleotides: An In Vivo Study of Factors Affecting Skeletal Uptake. Radiology, 113:373.

54. Ginsburg, J. (1965): Clubbing of the Fingers, in Handbook of Physiology, Vol. III, Circulation, Eds. Hamilton, W.F. and Dow, P., Am. Physiol. Soc., Washington, D.C., p. 2377.

55. Guyton, A.C. (1976): Textbook of Medical Physiology, Fifth Edition, W.B. Saunders Co., Philadelpia.

56. Hall, B.K. (1978): Developmental and Cellular Skeletal Biology, Academic Press, New York.

57. Ham, A. (1974): Histology, J. B. Lippincott Co., Philadelphia, p. 378.

58. Helal, B. (1965): The Pain in Primary Osteoarthritis of the Knee: Its Causes and Treatment by Osteotomy. Postgrag. Med. J., 41:172.

59. Hammel, C.F., DeNardo, S.J. and Lewis, J.P. (1973): Bone Marrow and Bone Mineral Scintigraphic Studies in Sickle Cell Disease. Br. J. Haematol., 25:593.

60. Hare, W.C.D. (1961): The Ages at Which the Centers of Ossification Appear Roentgenographically in the Limb Bones of Dog. Am. J. Vet. Res., 22:825.

61. Hare, W.C.D. (1960): Radiography of the Canine Pelvic Limb. J.A.V.M.A., 136:603.

62. Harrelson, J.M. and Hills, B.A. (1970): Changes in Bone Marrow Pressure in Response to Hyperbaric Exposure. Aerospace Med., 41:1018.

63. Hart, V.L. (1937): Acute Hematogenous Osteomyelitis in Children. J.A.M.A., 188:524.

64. Hawk and Shim, S. (1970): The Nature of the Intramedullary Pressure of Bone. Surgical Forum, 21:475.

65. Herzig, E. and Root, W.S. (1959): Relation of Sympathetic Nervous System to Blood Pressure of Bone Marrow. Am. J. Physiol., 196:1053.

66. Hills, B.A. and Straley, R. (1972): Aseptic Osteonecrosis: A Study of Tibial Blood Flow Under Various Environmental Conditions. Aerospace Med., 43:724.

67. Heyman, M.A., Payne, B.D., Hoffman, J.I.E. and Rudolf, A.M. (1977): Blood Flow Measurements with Radionucleotide-Labelled Particles. Progress in Cardiovascular Diseases, 20:55.

68. Hobo, T. (1921): Zur Pathogenese der Akuten haemstogenen Osteomyelitis, mit Beruckisichtigan der Vitalfar bungslehre. Acta Scholae Medicinclis Universitalis Imperialials. Kioto, 4:1.

69. Holdsworth, F.W. (1966): Epiphyseal Growth: Speculation on the Nature of Perthes' Disease. Ann. R. Coll. Surg., 39:1.

70. Holling, E., Brodey, R.S. and Boland, H.C. (1961): Pulmonary Hypertrophic Osteoarthropathy. Lancet, 2:1269.

71. Hopkins, G.B., Kristensen, K.A.B. and Campbell, C.G. (1974): Skeletal Scintigraphy - The Use of Technitium 99m-Labelled Complexes in the Detection of Early Osseous Involvement by Metastatic Tumors. West. J. Med., 120:448.

72. Hruza, Z. and Wachtlova, M. (1969): Diminution of Bone Blood Flow and Capillary Network in Rats During Aging. J. Geron., 24:315.

73. Hughes, S.P.F., Jeyasingh, K. and Lavender, J.P. (1975): Bone Uptake of Certain Radioactive Phosphate Compounds. Br. J. Rad., 48:73.

74. Hughes, S., Khan, R., Davies, R. and Lavender, P. (1978): The Uptake by the Canine Tibia of the Bone Scanning Agent Before and After Osteotomy. J. Bone Joint Surg., 60-B:579.

75. Irving, M.H. (1964): The Blood Supply of the Growth Cartilage in Young Rats. J. Anat., 98:631.

76. Johnson, R.W. (1927): A Physiological Study of the Blood Supply of the Diaphysis. J. Bone Joint Surg., 9:153.

77. Jung, A., Bisaz, S., Fleish, H. (1972): The Binding of Pyrophosphate and Two Diphosphonates by Hydroxyapatite Crystals. Calc. Tis. Res., 11:269.

78. Kalser, M.H., Ivy, H.K., Prevsner, L., Morbarger, J.B. and Evy, A.C. (1951): Changes in Bone Marrow Pressure During Exposure to Simulated Altitudes. J. Aviat. Med., 22:286.

79. Kane, W.J. (1968): Fundamental Concepts of Bone Blood Flow Studies. J. Bone Joint Surg., 50-A:801.

80. Kane, W.F. (1968b): The Determination of Blood Flow to Tissues of the Human Leg. Abstract, J. Bone Joint Surg., 50-A:1070.

81. Kane, W.F. and Grim, E. (1965): Quantification of Bone Blood Flow in Dogs. Surg. Forum, 16:447.

82. Kane, W. and Grim, E. (1969): Blood Flow to Canine Hind Limb, Bone, Muscle and Skin. J. Bone Joint Surg., 51-A:309.

83. Kato, F., Bassett, F., and Silver, D. (1970): Arterography of the Nutrient Artery and Blood Flow of the Canine Tibia. J. Bone Joint Surg., 52-A:1373.

84. Kelly, P.J. (1968): Anatomy, Physiology and Pathology of the Blood Supply of Bones. J. Bone Joint Surg., 50-A:766.

85. Kelly, P.J. (1973): Comparison of Marrow and Cortical Bone Blood Flow by ^{125}I-Labeled 4 Iodoantipyrine (I-AP) Washout. J. Lab. Clin. Med., 81, 497.

86. Kelly, P.J. and Bassingthwaighte, J.B. (1977): Studies on Bone Ion Exchanges Using Multiple-Tracer Indicator-Dilution Techniques. Fed. Proc., 36:2634.

87. Kelly, P.J. and Janes, J.M. (1968): Microangiographic and Histologic Studies of Vascular Anatomy of the Femur and Tibia Distal to Femoral and Iliac Arteriovenous Fistulas in Dogs. Anat. Rec., 162:255.

88. Kelly, P., Yipintsoi and Bassingthwaighte, J.B. (1971): Blood Flow in Canine Tibial Diaphysis Estimated by Iodoantipyrine - ^{125}I Washout. J. Appl. Physiol., 31:38.

89. Khan, R.A., Best, J.K. and Lavender, J.P. (1978): A Technique for Measuring the Accumulation of ^{99}Tc^{m} Stannous-Ethane-1-hydroxy-1, 1-Diphosphonate in the Canine Tibia. Br. J. Radiol., 51:51.

90. Khan, R.A., Hughes, S., Lavender, P., Leon, M. and Spyrou, N. (1979): Autoradiography of Technetium-labelled Diphosphonate in the Rat Bone. J. Bone Joint Surg., 61-B:221.

91. King, M.A., Kilpper, R.W. and Weber, D.A. (1977): A Model for Local Accumulation of Bone Imaging Radiopharmaceuticals. J. Nuc. Med., 18:1106.

92. Krane, S.M. (1977a): Hyperostosis, Neoplasms and Other Disorders of Bone and Cartilage, in Harrison's Principles of Internal Medicine, 8th Edition, Eds. Thorn, G.W., et al, McGraw-Hill Book Co., New York, p. 2041.

93. Krane, S.M. (1977b): Metabolic Bone Disease, in Harrison's Principles of Internal Medicine, 8th Edition, Eds., Thorn, G.W., et al, McGraw-Hill Book Co., New York, p. 2028.

94. Krane, S.M. (1977c): Paget's Disease of Bone, in Harrison's Diseases of Internal Medicine, 8th Edition, Eds., Thorn, G.W., et al, McGraw-Hill Book Co., New York, p. 2038.

95. Laing, P.G. and Ferguson, A.B. (1959): Iodine 131 Clearance Rates as an Indication of the Blood Supply of Bone. Nature, 183:1595.

96. Lange, D.R., Whiteside, L.A. and Lesker, P.A. (1979): Abstract, Femoral Head Circulation: Blood Q Measurement in Normal and Arthritic Canine Femoral Heads. 25th Annual Orthopaedic Research Society Meeting, San Francisco, California.

97. Lamas, A., Amado, D. and DaCosta, J.C. (1946): La Circulation du Sang dans l'os Presse med., 54:862.

98. Laurnen, E.L. and Kelly, P.G. (1969): Blood Flow, Oxygen Consumption, Carbon Dioxide Production and Blood-Calcium and pH Changes in Tibial Fractures in Dogs. J. Bone Joint Surg., 51-A:298.

99. Lavender, J.P., Khan, R.A.A., Hughes, S.P.F. (1979): Blood Flow and Tracer Uptake in Normal and Abnormal Canine Bone: Comparisons with Sr-85 Microspheres, Kr-81m, and Tc-99m MDP. J. Nuc. Med., 20:413.

100. Lemoine, A. (1957): Vascular Changes After Interference with Blood Flow of the Femoral Head of the Rabbit. J. Bone Joint Surg., 39-B:763.

101. Lockwood, R. and Latta, L.L. (1980): Bone Blood Flow Changes with Diaphyseal Fracture. Abstract, 26th Annual Orthopaedic Research Society Meeting, Atlanta, Georgia, p. 158.

102. Luben, R.A., Chen, M.C., Rosen, D.M. and Mohler, M.A. (1979): Effects of Osteoclast Activating Factor from Human Lymphocytes on Cyclic AMP Concentrations in Isolated Mouse Bone and Bone Cells. Calc. Tis., 28:23.

103. Lunde, P. and Michelsen, K. (1970): Determination of Cortical Blood Flow in Rabbit Femur by Radioactive Microspheres. Acta Physiol. Scand., 80:39.

104. McAlfee, J.F. and Subramanian, G. (1966): Radioactive Agents for the Delineation of Body Organs by External Imaging Devices: A Review. ISA Transactions, 5:349.

105. McElfresh, E.C. and Kelly, P.G. (1970): Effect of Sympathectomy and Sciatic Nerve Stimulation on Bone Blood Flow. Surg. Forum, 21:483.

106. McElfresh, E.C. and Kelly, P.J. (1974): Simultaneous Determination of Blood Flow in Cortical Bone, Marrow and Muscle in Canine Hind Leg gy Femoral Artery Catheterization. Calc. Tis. Res., 14:301.

107. McLean, F.C. (1958): The Ultrastructure and Function of Bone. Science, 127:451.

108. McPherson, A. (1967): Hemodynamics of Bone in the Cat. Proc. R. Soc. Med., 60:7.

109. MacPherson, J.N. and Tothill, P. (1977): Blood Flow and Age in the Rat. Clin. Sci. Mol. Med., 54:111.

110. Mannik, M. and Gilliland, B.C. (1977): Hypertrophic Osteoarthropathy, in Harrison's Principles of Internal Medicine, 8th Edition, Eds. Thorn, G.W., et al, McGraw-Hill Book Co., New York, p. 2077.

111. Matumoto, Y. and Mizuno, S. (1966): Rate of the Blood Flow in the Femoral Head. Med. J. Osaka Univ., 16:431.

112. Mendlowitz, M. and Leslie, A. (1942): The Experimental Stimulation in the Dog of the Cyanosis and Hypertrophic Osteoarthroplasty Which Are Associated with Congenital Heart Disease. Am. Heart J., 24:141.

113. Michelsen, K. (1967): Hemodynamics of the Bone Marrow Circulation. Acta Physiol. Scand., 73:264.

114. Miller, D.S. and de Takata, G. (1942): Posttraumatic Dystrophy of the Extremities: Sudecks Atrophy. Surg. Gyn. and Obs., 75:55.

115. Mizuno, S. and Matumoto, Y. (1969): Fallacy of Phlebography for Estimating the Blood Flow of the Femoral Heal. Internat. Surg., 52:22.

116. Morgan, J.D. (1959): Blood Supply of Growing Rabbit's Tibia. J. Bone Joint Surg., 41-B:185.

117. Morris, M.A. and Kelly, P.J. (1979): Use of Tracer Microspheres to Measure Bone Blood Flow. Abstract, Annual Meeting of the Orthopaedic Research Society.

118. Nelson, G.E., Kelly, P.J., Peterson, F. and Janes, J. (1960): Blood Supply of the Human Tibia. J. Bone Joint Surg., 42-A:625.

119. Neuman, W.F. and Neuman, M.W. (1958): The Chemical Dynamics of Bone Mineral, Chicago Univ. Press, Chicago.

120. Nicholson, J.T., Kopell, H.P. and Mattei, R.A. (1954): Regional Stress Angiography of the Hip. A Preliminary Report. J. Bone Boint Surg., 36-A:503.

121. Niv, A.F. and Hungerford, D.S. (1979): Bone Blood Flow in Anesthetized and Conscious Dogs. Annual Meeting of the Orthopaedic Research Society, p. 17.

122. Niv, A.J., Hungerford, D.S. and Jones, L.C. (1980): Simultaneous Bone Blood Flow Measurement in Dogs Utilizing Radioactive Tracer Microspheres

and Hydrogen Washout. Abstract, Annual Meeting of the Orthopaedic Research Society, Atlanta, Georgia, p. 156.

123. Noback, C.R. (1944): The Developmental Anatomy of the Human Osseous Skeleton During the Embryonic Fetal and Circumnatal Periods. Anat. Rec., 88:91.

124. Ogden, J.A. (1974): Changing Patterns of Proximal Femoral Vascularity. J. Bone Joint Surg., 56-A:941.

125. Ogden, J.A. (1975): Development of Epiphysis and Growth Plate in Orthopaedic Surgery in Infancy and Childhood, Ed. Ferguson, Jr., A.B., Williams and Wilkins, Baltimore, p. 4.

126. Ogden, J. (1976): Pediatric Osteomyelitis, the Pathology of Neonatal Osteomyelitis and Septic Arthritis. Abstract, 22nd Annual Meeting of the Orthopaedic Research Society, New Orleans, Louisiana.

127. Ogden, J.A., Hempton, R.F. and Southwick, W.O. (1975): Development of the Tibial Tuberosity. Anat. Rec., 182:431.

128. Ogden, J.A. and Lister, G. (1975): The Pathology of Neonatal Osteomyelitis. Pediatrics, 55:474.

129. Ogden, J.A. and Southwick, W.O. (1976): Cartilage Canals and Epiphyseal Osteogenesis. 22nd Annual Meeting of the Orthopaedic Research Society, New Orleans, Louisiana, p. 85.

130. O'Mara, R.E. (1974): Bone Scanning in Osseous Metastatic Disease. J.A.M.A., 229:1915.

131. Osmond and Evrett (1965): Bone Marrow Blood Volume and Total Red Cell Mass of the Guinea Pig as Determined by Fe^{59} - Erythrocyte Dilution and Liquid Nitrogen Freezing. Q.J. Expt. Physiol., 50:1.

132. Paridis, G.R. and Kelly, P.G. (1975): Blood Flow and Mineral Deposition in Canine Tibial Fractures. J. Bone Joint Surg., 57-A:220.

133. Pasternak, H.S., Kelly, P.J., and Owen, C.A. (1966): Estimation of Oxygen Consumption and Cardon Dioxide Production and Blood Flow of Bone in Growing and Mature Dogs. Mayo Clinic Proc., 41:831.

134. Petrakis, N.L., Masocredis, S.P. and Miller, P. (1953): The Local Blood Flow in Human Bone Marrow in Leukemia and Neoplastic Diseases as Determined by the Clearance Rate of Radiodide (I^{131}). J. Clin. Invest., 32: 952.

135. Potter, C.M.C. (1954): Osteomyelitis in the Newborn. J. Bone Joint Surg., 36-B:578.

136. Prives, M.G., Funstein, L.V. and Scherban, E.I. (1959): Method of Labelled Atoms in In Vivo Investigations of Arterial Systems of Bone. Ark. Anat. Gistol. Embriol., 37:56.

137. Putschar, W.G.S. (1972): Circulation in Paget's Disease of Bone. New Eng. J. Med., 287:717.

138. Ray, R.D. (1964): Discussion on Quantitative Studies of Bone Blood Flow in Dogs and Rabbits. J. Bone Joint Surg., 46-B:781.

139. Ray, R. (1972): Circulation and Bone, in The Biochemistry and Physiology of Bone, Vol. III, Ed. Bourne, Academic Press, New York, p. 386.

140. Ray, R., Aouad, R. and Kawaba, M. (1967): Experimental Study of Peripheral Circulation and Bone Growth. Clin. Orthop. Rel. Res., 52:221.

141. Ray, R., Kawabata, Galante (1967): Experimental Study of Peripheral Circulation and Bone Growth. Clin. Orthop. Rel. Res., 54:175.

142. Reeve, J., Swain, and Wootton (1977): The Acute Effect of Moderate Exercise on Blood Flow to the Skeleton in Man. Proc. Physiol. Soc., January, p. 31.

143. Regato, J.A. (1977): Pathways of Metastatic Spread of Malignant Tumors. Sem. Oncology, 4:33.

144. Rhinelander, F.W. (1968): The Normal Microcirculation of Diaphyseal Cortex and Its Response to Fracture. J. Bone Joint Surg., 50-A:784.

145. Rhinelander, F.W. (1974): Tibial Blood Supply in Relation to Fracture Healing. Clin. Orthop. Rel. Res., 105:34.

146. Rhinelander, F. (1976): Circulation in Bone, Chapter 9, in The Biochemistry and Physiology of Bone, Vol. IV, Ed. Bourne, Academic Press, New York, p. 1.

147. Rhinelander, F.W. (1979): Amer. Academy Orthop. Surg. Instructional Course Lecture, October, Philadelphia.

148. Rhinelander. F.W. and Baragry, R.A. (1962): Microangiography in Bone Healing. J. Bone Joint Surg., 44-A:1273.

149. Rhodes, B.A., Greyson, N.D., Hamilton, C.R., White R.I., Giargiana, F.A. and Wagner, H.N. (1972): Absence of Anatomic Arteriovenous Shunts in Paget's Disease of Bone. New Eng. J. Med., 287:686.

150. Rhodin, J.A.G. (1974): Histology: A Text and Atlas, Oxford Univ. Press, New York, p. 198.

151. Robertson, D.E. (1927): Acute Haematogenous Osteomyelitis. J. Bone Joint Surg., 9:8.

152. Robbins, S.L. and Angell, M., Eds. (1976): Basic Pathology, W. B. Saunders Co., Philadelphia.

153. Rockoff, S.D., Kaye, H., Armstrong, J.D. and Stansel, H.C. (1969): Effect of Increased Bone Blood Flow on Bone Metabolism. Inves. Rad., 4:230.

154. Root, W.S. (1963): The Flow of Blood Through Bones and Joints, in The Handbook of Physiology, Section 2: Circulation, Vol. II, Ed. Hamilton, W.F. and Dow, P., Am. Physiol. Soc., Washington, D.C., p. 1651.

155. Rosenthal, O., Bowie, M.A. and Wagoner, G. (1941): Studies in the Metabolism of Articular Cartilage. I. Respiration and Glycolysis of Cartilage in Relation to Its Age. J. Cell Comp. Physiol., 17:221.

156. Ross, J.M., Fairchild, H.M., Weldy, J. and Guyton, A.C. (1962): Autoregulation of Blood Flow by Oxygen Lack. Am. J. Physiol., 202:21.

157. Russell, R.G.G. (1975): Background to the Use of Diphosphonates as Bone Scanning Agents. Br. J. Rad., 48:73.

158. Russell, C.D., Cash, A.G. (1979): Complexes of Technetium With Pyrophosphate, Etidronate and Medronate. J. Nuc. Med., 20:532.

159. Salter, R.B., Kostuik, J. and Dallas, S. (1969): Avascular Necrosis of the Femoral Head as a Complication of Treatment for Congenital Dislocation of the Hip in Young Children: A Clinical and Experimental Investigation. Canad. J. Surg., 12:44.

160. Sapirstein, L.A. (1958): Regional Blood Flow by Fractional Distribution of Indicators. Am. J. Physiol., 193:161.

161. Sasaki, Y. and Wagner, H.N., Jr. (1971): Measurement of the Distribution of Cardiac Output in Unanesthetized Rats. J. Appl. Physiol., 30:879.

162. Schiess, F.A. et al (1975): Radionucleotide Investigation of Bone Metabolism in Fractures of the Tibia. Br. J. Rad., 48:73.

163. Schnitzer, J.E. (1979): Personal Communication.

164. Schoenecker, P.L., Bitz, D.M. and Whiteside, L.A. (1978): The Acute Effect of Position of Immobilization on Capital Femoral Epiphyseal Blood Flow. J. Bone Joint Surg., 60-A:899.

165. Schoutens, A., Bergmann, P. and Veras, M. (1979): Bone Blood Flow Measured by ^{85}Sr Microspheres and Bone Seeker Clearances in the Rat. Am. J. Physiol., 236:H1.

166. Semb (1966): Plasma Clearance of Sr^{85} by Bone: An Attempt to Study the Rate of Blood Flow Through Normal and Immobilized Bone in Dog. Acta Soc. Med. Upsal., 71:227.

167. Semb, H. (1968): Effect of Immobilization on Bone Blood Flow Estimated by Initial Uptake of Radioactive Strontium. Surg. Gyn and Obs., August, p. 279.

168. Semb, H. (1969): Experimental Limb Disuse and Bone Blood Flow. Acta Orthop. Scand., 40:552.

169. Shaw, N.E. (1965): The Influence of Muscle Blood Flow on Circulation in Bones. Proc. Roy. Soc. Med., 58:877.

170. Shim, S.S. (1968): Physiology of Blood Circulation of Bone. J. Bone Joint Surg., 50-A:812.

171. Shim, S.S., Copp, D.H. and Patterson, F. (1967): An Indirect Method of Bone Blood Flow Measurement Based on Bone Clearance of a Circulating Bone Seeking Radioisotope. J. Bone Joint Surg., 49-A:693.

172. Shim, S.S., Copp, D.H. and Patterson, F.P. (1968): Measurement of the Rate and Distribution of the Nutrient and Other Arterial Blood Supply in Long Bones of the Rabbit. J. Bone Joint Surg., 50-B:178.

173. Shim, S.S. and Patterson, F.P. (1967): A Direct Method of Qualitative Study of Bone Blood Circulation. Surg. Gyn. and Obs., 125:261.

174. Shim, S.S., Patterson, F.P. and Copp, D.H. (1971): Blood Flow Through Different Regions of Long Bone Measured by a Bone Seeking Radioisotopic Method. Surg., Gyn. and Obs., 132:58.

175. Shim, S.S., Mokkhavesa, S., McPherson and Schweigle (1970): Bone and Skeletal Blood Flow in Man Measured by a Radioisotopic Method. Canad. J. Surg., 14:38.

176. Siegel, B.A., Donovan, R.L., Alderson, P.O. and Mack, G.R. (1976): Skeletal Uptake of ^{99m}Tc-Diphosphonate in Relation to Local Bone Blood Flow. Radiology, 120:121.

177. Sim, F.H. and Kelly, P.J. (1970): Relationship of Bone Remodeling, Oxygen Consumption and Blood Flow in Bone. J. Bone Joint Surg., 52-A:1377.

178. Singh, M. and Brookes, M. (1971): Bone Growth After Experimental Venous Ligation. J. Anat., 108:315.

179. Stadalnik, R., Riggins, D'Ambrosia and DeNardo (1975): Vascularity of the Femoral Head: ^{18}F Scintigraphy Validated with Tetracycline Labeling. Radiology, 114:663.

180. Stem, A.H., Morgan, H.C. and Reynolds, F.C. (1957): Variations in Normal Marrow Pressures. J. Bone Joint Surg., 39-A:1129.

181. Stein, A.H. and White, N.B. (1966): The Effect of Adrenalin on the Blood Flow to a Long Bone. Surg., Gyn. and Ob., 123:55.

182. Stockwell, R.A. (1979): Biology of Cartilage Cells, Cambridge Univ. Press, Cambridge.

183. Subramanian, G., McAfee, J.G., O'Mara, R.E., Rosenstreich, M. and Mehter, A. (1971): ^{99m}Tc-Polyphosphate PP46: A New Radiopharmaceutical for Skeletal Imaging. J. Nuc. Med., 12:399.

184. Sunden, G. (1968): Studies of Intraosseous Flow for Rabbit Tibia. Calc. Tis. Res., Suppl. 2:100.

185. Tachdjian, M.O. (1972): Pediatric Orthopedics, W.B. Saunders Co., Philadelphia.

186. Tachdjian, M.O. and Grana, L. (1968): Response of the Hip to Increased Intra-articular Hydrostatic Pressure. Clin. Orthop., 61:199.

187. Termine, J.D. and Posner, A.S. (1967): Amorphous/Crystalline Interrelationships in Bone Mineral. Cal. Tis. Res., 1:83.

188. Tilden, R.L., Jackson, J., Enneking, W.F., DeLand, F.H. and McVey, J.T. (1973): ^{99m}Tc-Polyphosphate: Histological Localization in Human Femurs by Autoradiography. J. Nuc. Med., 14:576.

189. Tothill, P. and McCormick, J. (1975): Bone Blood Flow in the Rat Determined by the Uptake of Bone Seeking Radionucleotides and Radioactive Particles. Br. J. Radiol., 48:70.

190. Tothill, P. and McCormick, J. (1976): Bone Blood Flow in the Rat Determined by the Uptake of Radioactive Particles. Clin. Sci. Mol. Med., 51:403.

191. Treves, S., Khettry, J., Broker, F.H. and Wilkinson, R.H. (1976): Osteomyelitis: Early Scintigraphic Detection in Children. Pediatrics, 57: 173.

192. Trotmon, N.M. and Kelly, W.D. (1963): The Effect of Sympathectomy on Blood Flow to Bone. J.A.M.A., 183:121.

193. Trueta, J. (1957): The Normal Vascular Anatomy of the Human Femoral Head During Growth. J. Bone Joint Surg., 39-B:358.

194. Trueta, J. (1959): The Three Types of Acute Hematogenous Osteomyelitis. A Clinical and Vascular Study. J. Bone Joint Surg., 41-B:671.

195. Trueta, J. (1963): The Role of the Vessels in Osteogenesis. J. Bone Joint Surg., 45-B:402.

196. Trueta, J. (1968): Studies of the Development and Decay of the Human Frame, William Heinemann Med. Books, Ltd., Ondon.

197. Trueta, J. (1974): Blood Supply and the Rate of Healing of Tibial Fractures. Clin. Orthop. Rel. Res., 105:11.

198. Trueta, J. and Cavadias, A.X. (1955): Vascular Changes Caused by the Kuntscher Type of Nailing. J. Bone Joint Surg., 37-B:492.

199a Trueta, J. and Cavadias, A.X. (1964): A Study of the Blood Supply of the Long Bones. Surg., Gyn. and Obs., 118:485.

199b. Trueta, J. and Amato, V.P. (1960): The Vascular Contribution to Osteogenesis. 3. Changes in the Growth Cartilage Caused by Experimentally Induced Ischaemia. J. Bone Joint Surg. 42-B:571.

200. Trueta, J. and Trias (1961): The Vascular Contribution to Osteogenesis. IV. The Effect of Pressure Upon the Epiphyseal Cartilage of the Rabbit. J. Bone Joint Surg., 43-B:800.

201. Tucker, F.R. (1949): Arterial Supply to the Femoral Head and Its Clinical Importance. J. Bone Joint Surg., 31-B:82.

202. Tucker, F.R. (1950): The Use of Radioactive Phosphorus in the Diagnosis of Avascular Necrosis of the Femoral Head. J. Bone Joint Surg., 32-B:100.

203. Vanderhoft, P.J. and Kelly, P.J. (1964): Selective Angiography of Collateral Vessels in Limbs With an Experimental Arteriovenous Fistula, Acta Orthop. Scand., 34:123.

204. Van Dyke, D. (1967): Similarity in Distribution of Skeletal Blood Flow and Erythropoetic Marrow. Clin. Orthop. Rel. Res., 52:37.

205. Van Dyke, D. et al (1965): Bone Blood Flow Shown With F^{18} and the Positron Camera. Am. J. Physiol., 209:65.

206. Van Dyke, D., Anger, H.O., Parker, H., McRae, J. Dobson, E.L., Yano, Y, Naets, J.P., and Linfoot, J. (1971): Markedly Increased Bone Blood Flow in Myelofibrosis. J. Nuc. Med., 12:506.

207. Veall, N. (1975): Review: Measurement of Bone Blood Flow. Br. J. Rad., 48:70.

208. Walker, W.G. and Wilde, W.S. (1952): Kinetics of Radiopotassium in the Circulation. Am. J. Physiol., 170:401.

209. Wang, Y.C., et al (1975): Intrachondral Microcirculation and Cartilage Growth. Chinese Med. J., 1:449.

210. Waterman, R. (1961): Dite Gefasskanale der Kniegelenksnahen Wachstumszonen, Koln: Universitatsverlag (based on translation by Brookes, 1972).

211. Weinman, D.T., Kelly, P.J., Owen, C.A. and Orvis, A.L. (1963): Skeletal Clearance of Ca^{47} and Sr^{85} and Skeletal Blood Flow in Dogs. Proc. Staff Mtg. Mayo Clinic, 38:559.

212. Weinman, D.T., Kelly, P.J. and Owen, C.A. (1964): Bone Flow Distal to a Femoral Arteriovenous Fistula in Dogs. J. Bone Joint Surg., 46-A:1676.

213. Weiss, L. and Greep, R. (1977): Histology, McGraw-Hill Book Co., New York, p. 375.

214. Wertheimer, L.G. and Lopes, S. (1971): Arterial Supply of the Femoral Head. J. Bone Joint Surg., 53-A:545.

215. White, N.B., Terpogossian, M.M. and Stein, A.H. (1964): A Method to Determine the Rate of Blood Flow in Long Bone and Selected Soft Tissues. Surg., Gyn. and Obs., 119:535.

216. Whiteside, L.A., Ogata, K., Lesker, P. and Reynolds, F.C. (1978): The Acute Effects of Periosteal Stripping and Medullary Reaming on Regional Bone Blood Flow. Clin. Orthop. Rel Res., 131:266.

217. Whiteside, L.A., Lesker, P.A. and Simmons, D.J. (1977a): Measurement of Regional Bone and Bone Marrow Blood Flow in the Rabbit Using the Hydrogen Washout Technique. Clin. Orthop. Rel. Res., 122:340.

218. Whiteside, L.A., Simmons, D.J. and Lesker, P.A. (1977b): Comparison of Regional Bone Blood Flow in Areas with Differing Osteoblastic Activity in the Rabbit Tibia. Clin. Orthop. Rel. Res., 124:267.

219. Whittich, W.G. (1974): Canine Orthopaedics, Lea & Febiger, Philadelphia.

220. Wilsman, N.J. and Van Sickle, D.C. (1970): The Relationship of Cartilage Canals to the Initial Osteogenesis of Secondary Centers of Ossification. Anat. Rec., 168:381.

221. Wooton (1975): ^{18}F As An Indicator for Bone Blood Flow Measurement. Br. J. Rad., 48:70.

222. Wooton, Reeve, J. and Veall, N. (1976): The Clinical Measurement of Skeletal Blood Flow. Clin. Sci. Mol. Med., 50:261.

223. Yano, Y., McRae, J., Van Dyke, D.C. et al (1973): Technetium-99m-Labeled Stannous Ethane-1-Hydroxyl-1 1-Diphosphonate: A New Bone Scanning Agent. J. Nuc. Med., 14:73.

224. Willis, R.A. (1960): Pathology of Tumours, Third Edition, Butterworths, London.

225. Yu, W., Shim, S. and Hawk, H.E. (1972): Bone Circulation in Hemorrhagic Shock. J. Bone Joint Surg., 54-A:1157.

226. Zimmer, A.M., Isitman, A.T. and Holmes, R.A. (1975): Enzymatic Inhibition of Diphosphonate: A Proposed Mechanism of Tissue Uptake. J. Nuc. Med., 16:352.

227. Ogden, J.A. (1979): The Development and Growth of the Musculoskeletal System. Chapter 3, In: The Scientific Basis of Orthopaedics, Albert, J.A. and Brand, R.A., eds. Appleton-Century-Crofts, New York, pp. 41-104.

YALE MEDICAL LIBRARY

Manuscript Theses

Unpublished theses submitted for the Master's and Doctor's degrees and deposited in the Yale Medical Library are to be used only with due regard to the rights of the authors. Bibliographical references may be noted, but passages must not be copied without permission of the authors, and without proper credit being given in subsequent written or published work.

This thesis by has been used by the following persons, whose signatures attest their acceptance of the above restrictions.

NAME AND ADDRESS	DATE
Whiteside, Julia A., 1 South St., New Haven, CT	Feb. 17, 1982